INFORMATION TO USERS

This manuscript has been reproduced from the microfilm master. UMI films the text directly from the original or copy submitted. Thus, some thesis and dissertation copies are in typewriter face, while others may be from any type of computer printer.

The quality of this reproduction is dependent upon the quality of the copy submitted. Broken or indistinct print, colored or poor quality illustrations and photographs, print bleedthrough, substandard margins, and improper alignment can adversely affect reproduction.

In the unlikely event that the author did not send UMI a complete manuscript and there are missing pages, these will be noted. Also, if unauthorized copyright material had to be removed, a note will indicate the deletion.

Oversize materials (e.g., maps, drawings, charts) are reproduced by sectioning the original, beginning at the upper left-hand corner and continuing from left to right in equal sections with small overlaps. Each original is also photographed in one exposure and is included in reduced form at the back of the book.

Photographs included in the original manuscript have been reproduced xerographically in this copy. Higher quality 6" x 9" black and white photographic prints are available for any photographs or illustrations appearing in this copy for an additional charge. Contact UMI directly to order.

UMI

A Bell & Howell Information Company
300 North Zeeb Road, Ann Arbor MI 48106-1346 USA
313/761-4700 800/521-0600

Regulation of the Flagellar Specific Sigma Factor, Sigma28,

of *Salmonella typhimurium* by the Anti-Sigma Factor FlgM

by

Meggen Shepherd Chadsey

A dissertation submitted in partial fulfillment of
the requirements for the degree of

Doctor of Philosophy

University of Washington

1998

Approved by _____
Chairperson of Supervisory Committee

Program Authorized to Offer Degree Department of Microbiology

Date September 21, 1998

Doctoral Dissertation

In presenting this dissertation in partial fulfillment of the requirements for the Doctoral degree at the University of Washington, I agree that the Library shall make its copies freely available for inspection. I further agree that extensive copying of this dissertation is allowable only for scholarly purposes, consistent with "fair use" as prescribed in the U.S. Copyright Law. Requests for copying or reproduction of this dissertation may be referred to University Microfilms, 1490 Eisenhower Place, P.O. Box 975, Ann Arbor, MI 48106, to whom the author has granted "the right to reproduce and sell (a) copies of the manuscript in microform and/or (b) printed copies of the manuscript made from microform."

Signature _____

Date 7/21/98

University of Washington

Abstract

Regulation of the Flagellar Specific Sigma Factor, Sigma28,
of *Salmonella typhimurium* by the Anti-Sigma Factor FlgM

by Meggen Shepherd Chadsey

Chairperson of the Supervisory Committee
Professor Kelly T. Hughes
Department of Microbiology

Expression of the flagellar genes of *Salmonella typhimurium* occurs in an ordered heirarchy that is coupled to the morphogenesis of the flagellar organelle. Transcription of the late (Class 3) flagellar genes is dependent upon a positive transcriptional regulatory protein, the flagellar specific sigma factor, σ^{28}, encoded by the *fliA* gene. σ^{28} activity is inhibited by an anti-sigma factor, FlgM, encoded by the *flgM* gene. Inhibition of σ^{28} is accomplished through a direct interaction between σ^{28} and FlgM that interferes with the association of σ^{28} with core RNA polymerase (RNAP) to form a transcriptionally active holoenzyme complex ($E\sigma^{28}$). The mechanism of FlgM-mediated inhibition of $E\sigma^{28}$ formation became the subject of my thesis research.

A genetic analysis of *fliA* mutants defective for negative regulation by FlgM identified potential FlgM binding domains in conserved sigma factor regions 2.1, 3.1 and 4.1/4.2 of σ^{28}. It was proposed that FlgM could interfere directly with holoenzyme formation by masking potential core RNAP binding determinants in these regions. Alternatively, FlgM could inhibit the core binding activity of σ^{28} allosterically.

Previous biochemical analyses of the σ^{28}/FlgM interaction had suggested that FlgM might be capable of binding to $E\sigma^{28}$ in addition to free σ^{28}. A surface plasmon resonance (SPR) based assay suggested that FlgM was able to interact transiently with $E\sigma^{28}$ to increase the rate of holoenzyme dissociation. FlgM mutants defective for σ^{28}

binding (FlgM* mutants) were also defective for this activity, termed "holoenzyme destabilization."

SPR measurements of the affinities of the FlgM/σ^{28}* complexes revealed that most of the σ^{28}* mutants were defective for FlgM binding. These defects were reflected by the decreased sensitivity of these mutants to FlgM in *in vitro* transcription assays.

We propose that FlgM inhibits σ^{28} activity on two levels during flagellar biogenesis. Our model predicts that FlgM sequesters free σ^{28} from core RNAP by binding to regions 2.1, 3.1 and 4.1/4.2. In addition, FlgM may also interact with σ^{28} bound to core RNAP, at the subset of FlgM binding determinants that are accessible in the Eσ^{28} complex, to effect destabilization of that complex.

TABLE OF CONTENTS

LIST OF FIGURES

LIST OF TABLES

Page

ACKNOWLEDGMENTS

I owe everything to the family and friends who have stuck with me through the highs and lows of these past six and a half (!) years, my husband chief among them. Without his support, patience, and (most importantly) his sense of perspective, I would never have seen this day.

There are a number of colleagues and mentors whom I have had the honor to know, who have served as examples of the kind of scientist and person that I wish to be. Clem Furlong, Richard Burgess, Joyce Karlinsey, Kathy Stephens, and Veronique Robigou, thank you!

I would like to recognize my graduate committee for their time and effort on my behalf, especially Jim Champoux and Beth Traxler, who, besides serving on my reading committee, advised and encouraged me as if I were their own student.

Finally, though I don't doubt that my name will live on in infamy in the Hughes lab, I would like to leave a little something that I know I will be remembered for favorably--my recipe for banana bread:

2 cups all-purpose flour
1 tsp baking powder
1/2 tsp *each* baking soda and salt
1/2 to 3/4 cup sugar
1/2 cup *each* chopped walnuts and chopped dried apricots (optional)
3 to 4 really overripe bananas (these can accumulate in the freezer)
1/2 cup nonfat sour cream
1 egg
1/8 to 1/4 cup canola oil

In a bowl, stir together flour, baking powder and soda, salt, sugar, apricots and nuts. In a separate bowl, combine bananas, sour cream, egg and oil; stir into dry ingredients until just well blended. Pour batter into a greased and floured loaf pan, and bake in a preheated oven for 1 to 1 1/4 hours until a knife inserted in the center comes out clean. Cool, and take to lab meeting.

DEDICATION

This dissertation is dedicated to my grandfather, Dr. William G. Shepherd.

It has been a privilege to follow in his footsteps.

CHAPTER 1

Introduction to sigma factor function, structure and regulation

Eubacterial core RNA polymerase (RNAP or E) is a multisubunit enzyme with a molecular composition of $\alpha_2\beta\beta'$. It has the ability to transcribe RNA processively from a nick or bubble in double stranded DNA (dsDNA), but is unable to initiate transcription specifically from a promoter. Promoter specificity is conferred by a dissociable sigma subunit (σ), that contains the determinants necessary for promoter recognition and local denaturization (melting) of the dsDNA. Eubacteria express multiple species of sigma factors; each is specific for a different class of promoter DNA sequence. The sigma subunit, or sigma factor, is therefore a key element in the flow of information from the genome to the translational machinery.

This chapter will review the sigma factor literature, beginning with an introduction of the various types of sigma factors in the σ^{70} family, and their evolutionarily conserved regions. This will be followed by a discussion of the transcription cycle and the roles played by sigma factor during this process. The next section will summarize what is known about the structure of the σ^{70} family members, and how that structure may relate to domain function. Finally, some examples of regulatory mechanisms that influence sigma factor activity will be presented, with a particular emphasis on negative regulation by anti-sigma factors.

THE σ^{70} FAMILY OF SIGMA FACTORS

Soon after RNAP was isolated from *E. coli* and shown to be capable of promoter-specific transcription of RNA from a dsDNA template, it was noticed that RNAP purified by chromatography over a phosphocellulose column lacked the high activity and promoter specificity of RNAP purified by other means (12). This activity could be restored by adding back an earlier fraction from the phosphocellulose column,

which suggested that the chromatography step had dissociated some stimulating factor from the fundamental "core" RNAP complex.

Characterization of the promoter specificity factor revealed it to be a protein of approximately 70 kilodaltons (kDa). Although not required for nonspecific transcription from the ends of linear dsDNA, the presence of this factor, designated sigma factor, greatly stimulated both the level and specificity of transcription from circular dsDNA. It was proposed that sigma factor acted at the level of transcript initiation by facilitating promoter recognition and perhaps by catalyzing some early step in the transcription cycle. It was known that certain phages also expressed sigma-like factors, and that these appeared to stimulate transcription from different promoters than the ones recognized by RNAP isolated from *E. coli* (175, 180). This led to the hypothesis that multiple sigma factors might exist to regulate the transcription of different classes of genes (11). This prediction has since been upheld; alternative sigma factors have been identified in many species of bacteria and somephages. These sigma factors direct the transcription of genes whose products are required only in certain environments or during cell development. The use of alternative sigma factors has emerged as a major regulatory strategy that allows cells (and phage) to rapidly and coordinately shift the focus of transcription.

σ^{70} homologues and at least 18 different types of alternative sigma factors have been identified in a variety of bacterial species. The seven sigma factors expressed by *E. coli* are: the primary sigma factor, σ^{70}, which is essential and directs the majority of transcription during exponential growth, and six alternative sigma factors, σ^{38}, σ^{32}, σ^{24}, σ^{28}, FecI, and σ^{54} (recently reviewed by 78). σ^{38} (or σ^{S}) becomes active after the cell has entered stationary phase, and redirects the transcription machinery away from σ^{70}-dependent genes towards a smaller set of stationary phase genes. σ^{32} and σ^{24} (or σ^{E}) help the cell cope with increased temperature and other forms of stress by upregulating

the heat shock genes. The signal that induces the expression of these two heat shock sigma factors is an increase in the level of denatured proteins caused by exposure to heat or stress. σ^{24} responds specifically to the appearance of denatured proteins in the periplasm; its discovery defined a new subfamily of alternative sigma factors that are activated by extracytoplasmic signals. FecI is the most recently discovered member of this subfamily in *E. coli*. It regulates transcription of the ferric citrate transport system in response to extracellular substrate under iron-limiting conditions. σ^{28} coordinates the transcription of the genes for flagellar biogenesis and chemotaxis, and is found in many flagellated bacteria. σ^{54} (or σ^{N}) is the only *E. coli* sigma factor that is not a member of the σ^{70} family; it shares no overall homology with the other sigma factors, and its activity differs in many important ways. For example, unlike other sigma factors, σ^{54} is able to bind to promoters in the absence of core enzyme (136). σ^{54} was originally identified as the factor required for expression of genes involved in nitrogen metabolism in *E. coli*. It now defines the other major class of sigma factors (136). In *Caulobacter*, σ^{54}, not σ^{28}, is responsible for transcription of some of the genes of the flagellar regulon (9).

There are ten sigma factors in *B. subtilis* (reviewed by 59). Four, σ^{E}, σ^{F}, σ^{G}, and σ^{K}, are required specifically for expression of sporulation genes. Some other examples of alternative sigma factors that are required for specialized functions are AlgT in *P. aeruginosa*, involved in alginate production, CarQ in *M. xanthus*, which regulates carotenoid biogenesis, and σ^{E} of *Photobacterium* SS9, a barosensitive regulator of outer membrane protein (OMP) expression (reviewed in 75).

CONSERVED REGIONS OF THE σ^{70} FAMILY OF SIGMA FACTORS

In keeping with their many conserved functions (core RNAP binding, promoter recognition and dsDNA strand separation), the members of the σ^{70} family of sigma

factors share significant sequence homology. Alignments of primary and alternative sigma factors from diverse bacterial species has defined four conserved regions, which were further divided into subregions based on their putative functions (54, 118). Figure 1.1 depicts the conserved regions of the primary sigma factors. The flagellar-specific alternative sigma factor, σ^{28}, and the phage T4 sigma factor, gp55, are also represented. All three of these proteins are capable of carrying out the basic functions of a sigma factor (though gp55 requires an accessory factor to stabilize the holoenzyme/promoter interaction (63).

Region 1. Region 1.1 is present only in the primary sigma factors, but several residues of region 1.2 are highly conserved among most primary and alternative sigma factors. An analysis of the DNA binding activity of N-terminally truncated σ^{70} molecules in the absence of core RNAP demonstrated that regions 1.1 and 1.2 interfered with the nonspecific and specific interactions of sigma factor with DNA, respectively (38). Further experiments suggested that region 1.2 might fold back on the C-terminal DNA binding domain in free sigma factor; it was proposed association of the sigma factor with core RNAP displaces region 1.2 and unmasks the C-terminal DNA binding domain (36). σ^{70} mutants lacking regions 1.1 and 1.2 were arrested at the earliest point of promoter recognition, suggesting that these domains may also facilitate transcription initiation (187).

Region 2. Region 2, the most conserved of all the sigma factor regions, consists of four subdomains, 2.1 through 2.4. There is substantial evidence, both genetic and biochemical, that conserved regions 2.1 and 2.2 comprise the minimal core RNAP binding domain. An *in vitro* analysis of the core RNAP binding activity of σ^{70} deletion mutants and σ^{70} peptides demonstrated that residues 361 through 390 within region 2.1, were both necessary and sufficient for holoenzyme formation (109). Point mutations in region 2.1 of σ^{E} of *B. subtilis*, and region 2.2 of σ^{32} of *E. coli* cause defects in core

binding (84, 164). Region 2.1 contains a seven residue motif, VEANLRL, that resembles a region of σ^{54} demonstrated to be important for core binding (178). Although this motif is not present in phage T4 gp55, mutation of analogous residues impair the ability of this sigma factor to bind core RNAP, suggesting that the secondary structure of this region may be conserved despite the sequence divergence (108). Similar results obtained from an analysis of the interaction between a mitochondrial sigma-like factor, Mtf1p, and mitochondrial core RNAP support this conclusion. Though the homology between the Mtf1p and σ^{70} is weak, residues in the region 2.1 and 2.2-like sequence appear to contribute to core binding (23).

A role for region 2.3 in promoter melting was proposed on the basis of similarity between this region and eukaryotic single stranded DNA binding proteins, particularly in regard to the high content of aromatic residues characteristic of these proteins (62). It is thought that DNA strand separation at the promoter occurs through intercalation of the aromatic side chains between the nucleotide bases. Studies of mutants in σ^{A}, the primary sigma factor of *B. subtilis*, have confirmed that the conserved aromatic residues in region 2.3 are important to the process of promoter melting(86, 87).

There is strong genetic evidence that region 2.4 is responsible for recognition of the -10 promoter sequence. Mutations in this region of σ^{70} were found to compensate for base pair changes at -12, within the -10 hexamer (165, 183). Similar contacts have been demonstrated between region 2.4 of the *B. subtilis* sigma factors and the -10 motif (27, 176, 195). Although intact free σ^{70} does not bind specifically to DNA, σ^{70} peptides containing regions 2 and 3 selectively recognized the -10 region of the promoter (38, 159). Recently, specific binding of -10 region nontemplate strand DNA oligos by $E\sigma^{70}$ and $E\sigma^{A}$ has been demonstrated (73, 131, 154). Binding was shown to depend on residues in region 2.4. At some promoters, additional bases upstream of the -10 hexamer (referred to an "extended -10 element") were also important for transcription

initiation. Residues immediately downstream of region 2.4 in σ^{70} (termed region 2.5) have been shown to contact this element (4).

Region 3. A possible role for region 3 in sigma factor/core RNAP interaction was suggested by the *in vivo* core binding defect exhibited by a σ^{32} mutant carrying a deletion of 34 residues in region 3.2 (193). Amino acid substitutions in regions 3.1 and 3.2 of σ^{32} have also been shown to destabilize the $E\sigma^{32}$ complex (85). That these mutations also appeared to be defective in steps following promoter binding suggests that region 3 may serve several functions. Point mutations in region 3.1 of σ^{70} altered the pattern of abortive transcripts synthesized by RNAP suggesting that this region may influence the events that occur between transcription initiation and promoter clearance (65).

Region 4. Genetic studies similar to those used to characterize the promoter binding activity of region 2.4 have implicated region 4.2 in recognition of the -35 promoter sequence (44, 165, 183). Specific recognition of -35 promoter DNA by σ^{70} peptides containing only region 4 has also been demonstrated (38, 159). It has been proposed that masking of this domain by region 1.1 is responsible for the lack of DNA binding activity exhibited by free σ^{70} (36, 38). Region 4 may also make contacts with core RNAP. Mutations in both 4.1 and 4.2 in σ^{32} weakened the affinity of purified sigma factor for core (85).

THE ROLES OF THE SIGMA FACTOR SUBUNIT IN THE TRANSCRIPTION CYCLE

Transcription is a multistep process, and the sigma factor subunit plays important roles at many points in the transcription cycle. The cycle begins with the association of core RNAP with a free sigma factor molecule to form transcriptionally active holoenzyme ($E\sigma$). By making contacts with the promoter sequence determinants, sigma factor positions the catalytic center of core RNAP over the transcription start site

(defined as +1) on the DNA. The initial Eσ/promoter complex is referred to as "closed complex," in reference to the fact that the DNA remains double-stranded at this stage. Following closed complex formation, Eσ undergoes a series of conformational changes that culminate in the melting of a 10 to 15 base pair (bp) region overlapping the transcription start site. Sigma factor is required for this process of isomerization from closed to "open" complex. In the open complex, the catalytic center of core RNAP is able to access the single stranded template DNA strand. RNAP synthesizes and releases many short RNA transcripts up to 12 nucleotides (NTPs) in length without leaving the promoter region, in a process called abortive transcription. Although sigma factor is not thought to participate directly in RNA polymerization, it remains associated with core RNAP through this stage. Sigma factor is released only when the cycle of abortive transcript synthesis is broken, and core RNAP transcribes beyond the promoter region. This process is summarized in Figure 1.2. The involvement of sigma factor in each of the steps I through V, and some of the techniques used to assay sigma factor activity at these stages, are considered below.

Step I: Holoenzyme formation. The high degree of conservation in σ^{70} family regions 2.1 and 2.2 (118), which are believed to comprise the minimum core binding domain, suggested that the sigma factor/core RNAP interaction may be fundamentally similar for all members of this family. Competition between sigma factor species for core RNAP binding has been observed (85, 99, 144, 186, 193), supporting the idea that different sigma factors may recognize the same domains on core RNAP (or at least a common subset of those domains). Competition for core RNAP predicts that the focus of the transcription machinery should be influenced by the relative levels or availability of the various sigma factor species. In fact, expression of genes dependent upon alternative sigma factors for transcription, such as the heat shock and stationary phase genes, has

been shown to be accompanied by increases in the steady state levels of their respective sigma factors (56, 83, 169). Although the total amount of core RNAP in an *E. coli* cell, which ranges between 1000 and 3000 molecules (77), is in excess over the various sigma factor species (78), only ~1% of that pool is believed to be available to bind sigma factors at any given time (the remainder was sequestered as holoenzyme, bound non-specifically to DNA, or is actively transcribing) (134). Thus, the ability of different sigma factors to compete for core RNAP would be expected to play a major role in determining the focus of cellular transcription.

The interaction between sigma factor and core RNAP has been studied by a variety of methods. Fluorescence spectroscopy was used to measure the binding of fluorescently tagged σ^{70} to core RNAP in solution; the binding constant (K_a) of $E\sigma^{70}$ calculated from these data was greater than 10^9 M^{-1} (49). Glycerol gradient sedimentation analysis and gel filtration HPLC have been used to compare the relative affinities of different sigma factors for core RNAP (99), and to evaluate the effect of sigma factor mutations on core binding activity (84, 85, 99, 164, 193). Crosslinking and σ-conjugated chemical probes have been employed to map core subunit domains adjacent to sigma factor in the holoenzyme complex (24, 66, 82, 135, 147). FeEDTA protein footprinting of core RNAP and holoenzyme has identified regions of core that become buried upon holoenzyme formation (53, 108). The mapping of subunit interaction domains suggests that sigma factor makes multiple contacts with both β and β' (but not α). The highest affinity interaction may be on the N-terminal half of the β' subunit, between residues 200 and 330 [R. Burgess, personal communication; Vishage, 1998 #100]

Step II: Closed complex formation. Formation of the initial closed holoenzyme/promoter complex is reversible, and is described by a binding constant K_B

(see Figure 1.2). Direct measurements of K_B are difficult, since in general, closed complex rapidly isomerizes to form a stable open complex above 15°C. The kinetic parameters governing closed complex formation (and the subsequent isomerization to open complex) were separately determined using τ plot analysis of abortive initiation transcription assays (134). When excess holoenzyme was added to a transcription reaction, transcription reached a maximum after a lagtime (τ), which represented the time required for polymerase to bind, isomerize, and initiate transcription. Plotting τ as a function of 1/[RNAP] allowed for the determination of K_B and k_f (the isomerization rate constant; see Figure 1.2). In general, structural characterization of closed complexes requires that they be trapped at low temperatures (typically ~0 to 10°C) to prevent isomerization (153). Footprinting studies have indicated that the closed complex undergoes major structural changes prior to melting of the dsDNA. The initial footprint, centered upstream of the +1 site from approximately -55 to -5 bp, expanded downstream as the temperature was increased above 10°C (153). This expansion is presumed to be a prerequisite for the nucleation of melting around the start site.

Step III: Open complex formation. The isomerization of unstable closed complex to stable open complex is characterized by the formation of a "transcription bubble," a region of denatured DNA approximately 1.5 helix turns in length, extending from the -10 motif across the transcriptional start site(153). This process requires no input of energy; melting of the dsDNA is thought to be driven by the binding free energy of contacts between holoenzyme and the single-stranded DNA (ssDNA). Evidence for the close association of core subunits with the unpaired bases in the transcription bubble came from the observation that both sigma factor and the β subunit could be crosslinked to the ssDNA within the open complex by u.v. irradiation (10, 168). Melting of the

DNA is thought to make the template strand available to the catalytic center of core, which is formed by the β and β' subunits of core RNAP (98).

Base-specific contacts between holoenzyme and the -10 nontemplate strand were demonstrated *in vitro* (154). Formation of these contacts was subsequently shown to require region 2 residues in both σ^{70} (131) and σ^{E} of *B. subtilis* (73). Recently, a direct interaction between two region 2.3 tryptophan residues in σ^{70} and the -10 nontemplate strand was demonstrated using fluorescent spectroscopy (15). Specific binding of the oligo required that σ^{70} be associated with core RNAP, implying that the DNA binding activity of region 2.3 is regulated allosterically by the σ^{70}/core RNAP interaction. The purpose of a tight specific association between sigma factor and the nontemplate strand is probably to prevent reannealing of the transcription bubble during initiation of RNA synthesis (34).

Techniques for the detection of RNAP/promoter complexes, such as filter binding and gel shift assays, have been used to measure the rate of open complex formation and steady state levels of open complex. Abortive initiation reactions performed in the presence of excess RNAP can also provide this information, since the steady state reaction rate is proportional to the concentration of open complex (134). DNA footprinting assays have generated qualitative information about contacts between RNAP and the promoter DNA sequence. RNAP that has been incubated with promoter DNA can be challenged with the polyanion heparin or with high salt to disrupt closed complexes; the fraction of RNAP that remains bound to DNA is assumed to be involved in a stable open complex (20, 134).

Step IV: Ternary initiated complex formation. Polymerization of the first pair of nucleotides defines the transition from open complex to ternary initiation complex. Following each polymerization step, the complex has a finite chance of advancing by

binding the next nucleotide; alternatively, it may release the nascent RNA chain and revert to open complex (153). It is this recycling process that results in approximately 90% of initiated transcripts being prematurely released as abortive products (72). The amount of time spent by RNAP in this stage, before it breaks free of the promoter and synthesizes a mature transcript, may be an important determinant of the overall rate of transcription for some promoters (153). There is some evidence for an indirect role of sigma factor in retention of RNAP at the promoter (154). The contacts that form between sigma factor and the nontemplate strand of the -10 promoter region during open complex formation persist in the ternary initiated complex; a strong RNAP/promoter association mediated by these contacts may favor abortive initiation at the expense of promoter clearance.

Step V: Transition to elongating complex. Once transcript synthesis proceeds beyond the 7th to 12th nucleotide, contacts between RNAP and the promoter region are broken, and the sigma factor is released. Footprinting studies indicate that the transition to elongating complex is accompanied by loss of protection upstream of the -35 region (94), perhaps reflecting the loss of the sigma factor subunit.

STRUCTURE/FUNCTION RELATIONSHIPS OF THE SIGMA FACTOR SUBUNIT

There is strong genetic and biochemical evidence that the sigma factor subunit plays an important role at multiple steps of the transcription cycle. Much less is known, however, about the mechanisms for these sigma factor-mediated functions. Speculation has been hampered by an almost complete lack of structural information. Ideas about sigma factor structure have been based on secondary structure predictions based on the primary sequence, and by analogy to homologous proteins for which a crystal structure is known (118). Recently, the crystal structure of a σ^{70} fragment (residues 114 through

448) encompassing part of region 1.2 and all but the last eight residues of region 2 was solved at a resolution of 2.6 Angstroms (128). Much of what was previously speculated about the functions of conserved sigma factor regions 2.1 through 2.4 has been confirmed by this analysis.

Intact σ^{70} has proven recalcitrant to crystallization. Proteolytic digestion of sigma factors has suggested that the overall structure is one of independently folded domains connected by flexible linkers (22, 159). While the full-length molecule may be too flexible to permit crystallization, proteolytic digestion of σ^{70} was able to generate a stable fragment that could be crystallized (159). The fact that this fragment, which contained the regions implicated in core RNAP binding (2.1 and 2.2), -10 promoter sequence recognition (2.4) and promoter melting (2.3), retained the ability to bind core and specifically recognize the -10 nontemplate strand, suggested that important structural motifs had not been disrupted by digestion (159). Thus, structural information derived from a crystallographic analysis of this fragment was expected to be biologically relevant.

The structure of this fragment was found to consist entirely of helices and connecting loops (Figure 1.3). The helices of region 2 (helices 12a through 14) are clustered together in the tertiary structure. Helix 13 (essentially region 2.2), which contains several conserved hydrophobic residues, lies sandwiched between helices 12 and 14, and constitutes the hydrophobic core of this domain. The importance of region 2.2 to stabilization of the tertiary structure is consistent with its being the most highly conserved region among σ^{70} family sigma factors (118). Helices 12a and 12b, which contain residues demonstrated to be important for core RNAP binding, constitutes one of the solvent exposed faces of this domain (Figure 1.4). Helix 14, which contains both regions 2.3 and 2.4, forms the opposite face of this domain. Thus, region 2 forms a

stable domain that presents a surface for core binding on one side, and promoter recognition and melting on the other.

Core RNAP binding. A heptad motif important for core RNAP binding, first identified in σ^{54}, but also well conserved among the primary sigma factors (178), lies centered on the kink between helices 12a and 12b (Figure 1.4, residues 381 to 387, shown in green). Site-directed mutagenesis of this motif yielded sigma factor mutants with decreased transcriptional activity, though the transcription defects are not exclusively due to a decreased affinity of the mutant sigma factors for core RNAP (L. Rao and R. Burgess, personal communication). Thus, these residues may also function at a later step in transcription. Adjacent to the heptad motif are several solvent exposed conserved hydrophobic residues (L384, I388, F401, L402, and I405, shown in yellow) that form a hydrophobic patch that may contribute to the sigma factor/core RNAP interface (128). Several charged residues in this domain are also conserved (shown in blue), suggesting that ionic interactions may also participate in core RNAP binding.

Promoter recognition and melting. The spacing of region 2.4 residues important for promoter binding, and of hydrophobic residues, led to the proposal that this region formed an amphipathic helix (183). The crystal structure data has upheld this prediction (128). Residues Q437, T440 and R441, believed to contact the -12 and -13 positions, align on the solvent exposed face of helix 14, while the conserved hydrophobic residues face inward to pack against helix 13. Furthermore, several of the conserved aromatic residues in adjacent region 2.3 proposed to mediate promoter melting (Y425, Y430, W433, and Y434) (87), are also located on the charged face of helix 14, just N-terminal to the three residues in region 2.4 implicated in promoter binding. This location is consistent with the observation that nucleation of promoter melting occurs within the -10 sequence, at -10 and -11 (86). Thus, helix 14 appears to form specific contacts with the promoter throughout its length, and may make important contributions to the stability of

closed and open complexes. Conserved basic residues in this helix could stabilize this interaction by neutralizing the negatively charged DNA phosphate backbone.

Inhibition of DNA binding. The residues of helix 14 implicated in DNA binding all face into a cleft formed by the helices 12 and 13 (Figure 1.3) (128). Recognition and melting of -10 promoter sequence may require the DNA to align along this cleft. In the crystal structure, this cleft is potentially occupied by a nearby disordered loop that is highly negatively charged (residues 188 to 209 of the linker region between regions 1.2 and 2.1), leading to the proposal that inhibition of DNA binding by free sigma factor may in part be due to steric or electrostatic exclusion of DNA from this cleft (128). Association with core RNAP may displace this loop, perhaps by providing an alternative positively charged binding surface. This model is consistent with the proposed role for the residues N-terminal of region 2 in masking promoter binding determinants (36, 38). It is not supported, however, by studies of σ^{70} fluorescently labeled at residues W433 and W434 which showed that association of σ^{70} with core RNAP led to a decrease in the solvent accessibility of these region 2.3 residues (15).

No definitive structural information exists for regions 3 or 4. Sequence based structure predictions suggest that region 3.1 of the primary sigma factor may contain a helix-turn-helix (HTH) motif (this motif is only weakly conserved or absent among the alternative sigma factors). This region of σ^{70} has been crosslinked to nucleotide analogues bound in the initiating site of the catalytic center of core RNAP (158), suggesting that region 3.1 is proximal to the transcription start site in open complex. This implies that regions 2 and 3 are aligned "parallel" to the promoter in open complex. Evidence for an "antiparallel" orientation also exists, however. Residues immediately downstream of region 2.4 are involved in the recognition of bases immediately upstream of the -10 motif in "extended -10" promoters (4), and region 4.2 contacts the -35 promoter sequence. It has been proposed that region 4 could fold back to form

upstream contacts with the promoter (158). Perhaps extended -10 promoters are bound by holoenzyme in a different manner than classical -35/-10 promoters; it would be interesting to know whether the region 3.1 crosslinking result could be repeated at one of the extended -10 promoters.

The similarity of regions 4.1 and 4.2 to the family of HTH DNA binding proteins (118) implied region 4 might interact with the -35 promoter sequence in a analogous manner. The model for DNA binding by HTH proteins (reviewed by 148) proposes that the second helix lies along the major groove of the DNA, where it can interact with nucleotide bases. It is stabilized in this position by the first helix, which lays across it. Region 4 is most similar to λ cro and the homeodomain proteins, which are characterized by the presence of an amphipathic helix upstream of the HTH motif. In these proteins, the amphipathic helix packs against the HTH domain, further stabilizing the interaction with DNA. Region 4.1, which can be modeled as an amphipathic helix, is likely to serve this purpose in the interaction with the -35 promoter DNA (118).

Much of what is known about structure/function relationships of sigma factor is based on studies of primary sigma factors. Can models for the mechanism of sigma factor activity be extended to the alternative sigma factors, whose sequences are often significantly diverged from that of the primary sigma factors? In general, the phenotypes of alternative sigma factor mutants are consistent with studies of σ^{70} mutants. Highly conserved residues, even when the overall homology between an alternative sigma factor and σ^{70} is poor, appear to fulfill similar functions among the members of the σ^{70} family (23, 37, 84, 97, 108, 164, 176). It seems reasonable to expect that the fundamental processes carried out by all sigma factors should be carried out by similar mechanisms. Models based on our understanding of σ^{70}

structure/function relationships can at the very least serve as a starting point for the analysis of alternative sigma factor activities.

REGULATION OF SIGMA FACTOR ACTIVITY

The central importance of the sigma subunit in the transcription cycle makes it a logical target for regulatory proteins. Binding of Eσ to the promoter (described by K_B) and the rate of isomerization of closed complex to open complex (described by k_f), both sigma factor-mediated processes, are key determinants of the rate of transcription (134). Transcriptional regulatory proteins that interact with sigma factor have been shown to influence both of these kinetic variables. This section will include a brief discussion of some examples of positive regulatory proteins that act on sigma factor activity, and a more in-depth look at negative regulation of sigma factor activity by a family of proteins known as anti-sigma factors.

Positive activators. The class of DNA binding regulatory proteins that influence RNAP activity at the promoter via interactions with the sigma factor subunit have been termed Class II activators (79). This class is distinct from those proteins that regulate RNAP activity through contacts with the α subunit of RNAP (the Class I activators). Class II activators are also defined by the location of their binding site at the promoter; these proteins typically recognize sequence elements centered ~42 bp upstream of the +1 transcription start site, overlapping the -35 motif (79). Although Class II activators have not exhibited a high specific affinity for sigma factors in solution (estimates place the KD of solution interactions around ~10-6 M; 3, 149), these weak protein/protein interactions are thought to have a significant effect on the stability of the RNAP/DNA complex when the activator is tethered to the promoter. Presumably, at the promoter the activator is optimally positioned to interact with sigma factor. It has been proposed that one advantage of requiring that activators be bound to promoters in order to interact with

a sigma factor is that promiscuous activation at promoters lacking the activator binding site is avoided (70).

The proximity of Class II activator binding sites to the -35 element would be predicted to place the activator in a position to make contacts with region 4 of sigma factor. In fact, the target sites of a number of Class II activators have been identified, and they all mapped to this region (79). The binding domain for one such activator, PhoB, has been genetically mapped to the predicted amphipathic helix of region 4.1 (127). A PhoB-dependent promoter was transcribed by holoenzyme containing a mutant σ^{70} deleted for all of region 4.2, as long as PhoB was present (95). This result demonstrated that contacts between PhoB and σ^{70} can functionally substitute for the interaction between σ^{70} and the -35 element. The binding site of another Class II activator, λcI, was mapped to region 4.2, just downstream of the DNA binding helix (helix 2) of the HTH motif (110). Thus, it appears that even when RNAP is bound to the promoter, residues flanking the -35 binding domain in region 4.2 are available for interaction with accessory proteins.

An early model for promoter function proposed that the -35 element was responsible for mediating initial contacts between RNAP and the promoter, and that the -10 element controlled the subsequent isomerization step (47). Subsequent analyses of the effects of base pair mutations on K_B and k_f indicated that this model was overly simplistic. It now appears that both the -35 and -10 sequence elements influence the binding and isomerization steps (134). In keeping with these observations, Class II activators that contact the -35 promoter sequence binding domain of sigma factor were able to enhance both of these processes (153). An analysis of the effect of catabolite gene activator protein, CAP, on the kinetics of open complex formation at a synthetic Class II promoter revealed that both K_B and k_f were increased by the presence of this activator (45). λcI repressor at the λP_{RM} promoter had a similar effect (61). The basis

for an increased affinity of RNAP for the promoter in the presence of an activator may simply be due to stabilization of a suboptimal contact by supplementary protein/protein contacts. The mechanism for an increased k_f is still unclear. One possibility is that RNAP achieves a conformation that is optimally aligned for an interaction between the activator and region 4 of sigma factor only after it isomerizes to form open complex (70). Alternatively, contact between the activator and region 4 could induce an allosteric change in region 2.3/2.4 that facilitates open complex formation. More structural information about the C-terminal regions of sigma factor should provide insight into this process.

Negative Regulation. The classic mechanism for negative regulation of transcription is occlusion of RNAP from the promoter by the presence of a repressor protein bound to an overlapping operator sequence (81, 151). A second class of negative regulators that specifically target the sigma factor subunit for inhibition has recently been recognized. These proteins, called anti-sigma factors, negatively regulate transcription by competing with core RNAP for sigma factor. A sigma factor that is bound by an anti-sigma factor appears to be unable to interact with core RNAP. The details of the mechanism for anti-sigma factor activity are still unclear, but it could involve steric interference with the core RNAP binding determinants on sigma factor, or induction of an alternative sigma factor conformation that is incompatible with core RNAP binding. Since the first anti-sigma factor was reported (142), members of this class of negative regulatory proteins have been described in a wide variety of bacteria and in phage T4 (reviewed in 8, 75). Generally, anti-sigma factors regulate the activity of alternative sigma factors, although σ^{70} is subject to regulation by at least one member of this family, encoded by phage T4 (143), and possibly by a bacterially encoded protein expressed during stationary phase (82). Anti-sigma factors may have evolved to allow the cell to maintain pools of alternative sigma factors during normal exponential

growth without compromising σ^{70}-dependent transcription. This strategy would be advantageous, since it would enable the cell to respond rapidly to environmental or developmental changes that necessitated a shift in the focus of transcription. Anti-sigma factors are themselves negatively regulated by a variety of mechanisms that are tied to the cells ability to sense its environmental or developmental status (75).

As stated above, the general mechanism for anti-sigma factor activity is competition with core RNAP for sigma factor binding. Differences among the various sigma factor/anti-sigma factor systems do exist, however, both in the manner in which the anti-sigma factors interact with their targets, and in the nature of those targets (free sigma factor vs. sigma factor bound to core RNAP). Several sigma factor/anti-sigma factor pairs that illustrate the diversity found in these systems are discussed below (the flagellar specific sigma factor σ^{28} and its anti-sigma factor FlgM are not considered here, as these proteins are the subject of the research described in this thesis, and are introduced in a later chapter). This section will focus on genetic and biochemical studies that have led to models for sigma factor/anti-sigma factor interactions, and the effects of those interactions on sigma factor activity. For a more comprehensive review of these and other sigma factor/anti-sigma factor systems, the reader is directed to the review by Hughes and Mathee (75).

σ^F/SpoIIAB of B. subtilis. Sporulation in *B. subtilis* is governed by a cascade of alternative sigma factors that are expressed sequentially (121, 174). The second of these, σ^F, is synthesized in the predivisional cell, but only becomes active in the forespore following septation (42). An anti-sigma factor, SpoIIAB, is responsible for the inhibition of σ^F activity prior to septation and in the mother cell following septation (40). SpoIIAB-mediated inhibition in the forespore is lifted by the action of a third regulatory protein, SpoIIAA (an anti-anti-sigma factor)(35). Interaction of SpoIIAA with the σ^F/SpoIIAB complex results in the release of the sigma factor (39), and the

formation of a SpoIIAB/SpoIIAA complex. This partner switching process is influenced *in vitro* by the nucleotides ATP and ADP, though the biological relevance of this process is controversial. In the presence of ADP, SpoIIAB formed a stable complex with SpoIIAA (2), but in the presence of ATP, SpoIIAB, which is also a kinase, phosphorylated SpoIIAA (35, 137). SpoIIAA-PO_4 was shown to adopt an altered conformation that prevents it from binding to SpoIIAB (125). Studies have suggested that the ATP/ADP ratio in the cell might be the determining factor in the choice of binding partner by SpoIIAB (120). This model is consistent with the observation that starvation (which would be expected to cause an ATP deficit) induced sporulation (42). However, a recent kinetic analysis of SpoIIAB-dependent phosphorylation of SpoIIAA suggests that the relative levels of ATP and ADP do not regulate partner switching. These data suggest that it is the slow dissociation of ADP or SpoIIAA-PO_4 from SpoIIAB following phosphorylation that determines the availability of SpoIIAB to sequester σ^F (126).

Genetic studies of the interaction between σ^F and SpoIIAB suggest that SpoIIAB makes multiple contacts with σ^F at conserved regions 2.1, 3.1 and 4.1 (33). A multipartite interaction could account for the stability of the σ^F/SpoIIAB complex (surface plasmon resonance assays estimate the KD to be on the order of 10-8 M; 126). Alanine substitution analysis has suggested that hydrophobic residues make important contributions to this interaction. A hydrophobic interface would be consistent with the stability of the complex in 1M NaCl (39). Binding of SpoIIAB to σ^F regions 2.1 and 3.1, both of which may participate in core RNAP binding by σ^F, was proposed to sterically interfere with holoenzyme formation (33). *In vitro* transcription analyses of the effect of SpoIIAB on σ^F-dependent transcription were consistent with this model (2, 40), though they did not rule out an alternative model for direct inhibition of $E\sigma^F$ by SpoIIAB bound at exposed region 4.

AsiA of phage T4. Transcriptional regulation plays an important role in the temporal control of gene expression during phage T4 development. The phage encodes a number of factors that modify or interact with the host *E. coli* RNAP. These factors help to redirect the host RNAP away from bacterial promoters and early phage genes, and recruit it to middle and late phage promoters. One of these proteins is the anti-sigma factor AsiA, which interacts directly with σ^{70}. This interaction affects transcription in three ways: 1) it inhibits transcription from the host and early phage promoters, 2) it facilitates transcription from the middle phage promoters, and 3) it weakens the affinity of σ^{70} for core RNAP, presumably to enable the phage-encoded late gene specific sigma factor, gp55, to compete more efficiently with σ^{70}.

A possible mechanism for AsiA-mediated inhibition of host and early phage promoters has been proposed (1, 25). Protease and hydroxyl radical protein footprinting of the AsiA/σ^{70} complex have mapped the AsiA binding domain to conserved sigma factor region 4.2 (159), between residues 554 and 597 (25). *In vitro*, AsiA bound to σ^{70} with a 1:1 stoichiometry, and inhibited closed complex formation at a σ^{70}-dependent promoter (1). The location of the AsiA binding site on σ^{70}, and the effect of AsiA on promoter recognition, led to the model that AsiA may interfere with transcription by sterically masking the -35 promoter binding determinants in region 4.2. Consistent with this model was the observation that extended -10 promoters lacking an identifiable -35 motif were insensitive to AsiA-mediated inhibition (25).

Middle phage promoters are distinguished from early promoters by their lack of a σ^{70} -35 consensus sequence. Instead, these promoters contain a sequence motif centered at -30 bp that is recognized by a phage encoded transcriptional activator protein, MotA (68). Both MotA and AsiA were required *in vivo* for transcription from phage middle promoters (69, 145). Thus AsiA appears to function as a coactivator as well as an anti-sigma factor. *In vitro* footprinting analyses of middle promoters showed that

both of these proteins were required in order for modified RNAP to interact with the promoter upstream of -20 bp, and for the transition to open complex (69). The model suggested by these experiments was that an interaction between AsiA bound to sigma factor region 4.2 and MotA bound at the -30 region of the promoter functioned to substitute for a direct interaction between region 4.2 and the missing -35 element.

Late phage promoters are recognized by the phage encoded sigma factor, gp55 (46). During infection, this sigma factor must compete with σ^{70} for core RNAP; evidence pointed to an indirect role for AsiA in facilitating gp55 holoenzyme formation. Though AsiA was known to form a stable complex with $E\sigma^{70}$, the observation that σ^{70} was more readily dissociated from core RNAP in the presence of AsiA implied that the anti-sigma factor weakened the interaction between core RNAP and σ^{70} (143, 173). The increased sensitivity of σ^{70} regions 1, 2 and 3.1 to hydroxyl radical cleavage in the presence of AsiA suggested that AsiA binding at region 4.2 induces a conformational change in the σ^{70} (25). Such a change might have been responsible for the decreased stability of holoenzyme in the presence of AsiA.

σ^{32}/DnaK/DnaJ. The heat shock response of *E. coli* is regulated at the transcriptional level by the activity of the heat shock sigma factor σ^{32} (reviewed by 56). σ^{32} is in turn post-translationally regulated by the heat shock chaperones DnaK, DnaJ and GrpE (56), which normally target σ^{32} for degradation by the FtsH protease (64, 179), but under conditions that induce stress are titrated away from σ^{32} by the presence of misfolded proteins in the cytoplasm (26, 56). These manner in which these proteins regulated σ^{32} activity was reminiscent of their activity as chaperones (43, 112, 113); an ATP-mediated cycle of substrate binding and release has been proposed to regulate the level of free σ^{32} available to associate with core RNAP (111, 114) and (43). σ^{32} could be liberated from an inactive complex with DnaK-ADP and DnaJ by GrpE-stimulated nucleotide exchange (43).

An analysis of σ^{32} binding by a nested set of DnaK peptides identified seven regions in σ^{32} that were recognized by DnaK (McCarty et al, 1995). The dominant DnaK binding domain, termed region C (140), is highly conserved among σ^{32} homologues, but is absent in other σ^{70} family members (133), making it an appropriate target for specific negative regulation by the heat shock chaperones. Region C extends from the C-terminal end of conserved sigma factor region 2.4 to the N-terminal end of region 3.1 (140). The σ^{32}-binding domain of DnaK is located in the C-terminal 250 amino acids (13, 194). Interestingly, this region shares homology with a flagellar specific anti-sigma factor, FlgM, of several enteric bacteria and of two *Bacillus* species (8).

On the basis of glycerol gradient centrifugation, gel filtration and native PAGE experiments, DnaK was proposed to interact with σ^{32} holoenzyme to effect the release of the sigma factor subunit (170). It was subsequently shown that DnaK, DnaJ, and GrpE were able to inhibit σ^{32}-dependent transcription, even when σ^{32} was preincubated with core RNAP (111). These observations led to the proposal that the heat shock chaperones mediated σ^{32} activity by "stripping" the sigma factor away from core RNAP. Other gel filtration assays failed to demonstrate a stable Eσ^{32}/DnaK/DnaJ complex (43). However, a transient complex that rapidly resolved to a σ^{32}/DnaK/DnaJ complex and free core RNAP could not be ruled out by these experiments.

σ^E/RseA. σ^E, also known as the extreme heat shock sigma factor, responds to the presence of misfolded outer membrane proteins in the periplasm by upregulating expression of σ^{32} and a periplasmic protease, among other proteins (152). σ^E is the founding member of a subfamily of σ^{70}-related sigma factors that activate the expression of extracytoplasmic functions (the ECF family) (119). Information about the state of the periplasmic space is communicated to σ^E by the products of genes cotranscribed with *rpoE*, the gene encoding σ^E (31, 138).

rseA, the second gene in the *rpoE* operon, encodes an anti-sigma factor. RseA spans the inner membrane. The current model is that the periplasmic C-terminal domain of RseA receives signals about the status of the periplasmic proteins, and its N-terminal cytoplasmic domain relays that information to the transcription machinery by regulating the activity of σ^E (31, 138). A direct interaction between σ^E and RseA has been demonstrated by coimmuneprecipitation, crosslinking and native gel analysis (31, 138). σ^E-dependent transcription was efficiently inhibited *in vivo* and *in vitro* by RseA polypeptides containing just the N-terminal 97 to 100 amino acids (*in vitro* inhibition requires a 1:1 ratio of the RseA peptide to σ^E) (31, 138). Null mutations in the third gene in the *rpoE* operon, *rseB*, enhanced RseA activity, suggesting that RseB negatively regulates (31, 138). RseB has been shown to localize to the periplasm, and to interact with the C-terminal domain of RseA (31, 138). The model proposed to explain the sensory and regulatory activities of RseA and RseB is that in the absence of a periplasmic signal, an RseB/RseA complex sequesters σ^E to the cytoplasmic face of the inner membrane. Misfolding of periplasmic proteins caused by extracytoplasmic stress titrates RseB away from RseA. In the absence of RseB, RseA may adopt an altered conformation that is unable to interact with σ^E. The actual mechanism of σ^E inhibition by RseA has not been determined. A genetic analysis of σ^E mutants defective for the interaction with RseB would provide clues about the σ^E domain(s) targeted for inhibition.

Figure 1.1 Conserved regions of the σ^{70} family of sigma factors. The bar at top represents the *E. coli* σ^{70} primary sequence (613 amino acids). Evolutionarily conserved regions (shaded in grey) are indicated above the bar. Putative domain functions are indicated. The bars beneath σ^{70} represent the alternative sigma factor σ^{28} from *S. typhimurium* (239 amino acids), and the T4 phage sigma factor gp55 (185 amino acids). The degree of homology between the conserved sigma regions present in σ^{28} and gp55, and σ^{70} is indicated as follows: hatching indicates >50% homology; stippled regions are between 25 and 50% homologous; blank regions show <25% homology. Groups of residues considered homologous are: ST, RK, DE, NQ, FYW, and ILVM.

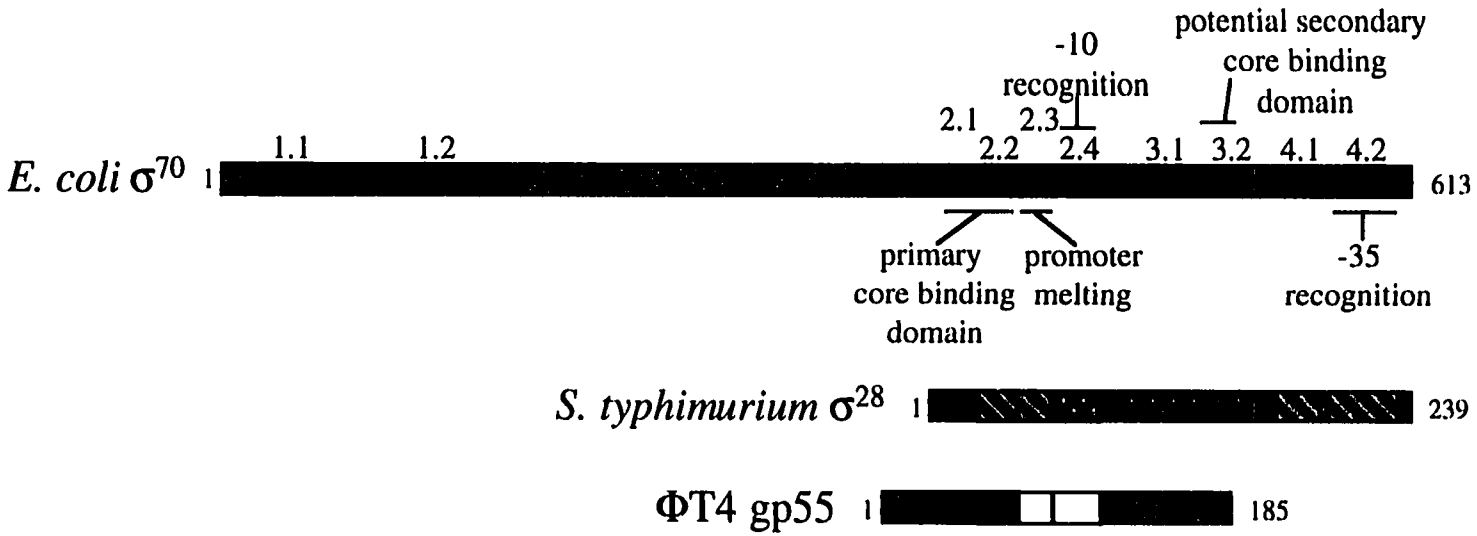
potential secondary
core binding
domain
-10
recognition
1.1
1.2
2.1
2.3
2.2
2.4
3.1
3.2
4.1
4.2
E. coli σ70
1
613
primary
core binding
domain
promoter
melting
-35
recognition
S. typhimurium σ28
1
239
ΦT4 gp55
1
185

Figure 1.2 Steps of the transcription cycle. Step I. Core RNAP (E) associates with a molecule of σ to form holoenzyme. Step II. Holoenzyme binds to the promoter (P) to form closed complex with an affinity dictated by the dissociation constant K_B. Step III. Closed complex ($E\sigma/P_{closed}$) isomerizes to form open complex ($E\sigma/P_{open}$). The rate of isomerization, k_f is essentially equal to the forward rate of the reation (k_{III}). Step IV. Binding of initiating ribonucleotides (NTP) leads to the formation of a series of ternary initiating complexes ($E\sigma/P_{init}$). Premature release of abortive transcripts reverts $E\sigma/P_{init}$ to open complex. Step V. Synthesis of a nascent transcript greater than 7 to 12 nucleotides in length is accompanied by the release of the σ subunit, and the formation of the elongating complex (E_{elong}), capable of processive synthesis of a mature length transcript.

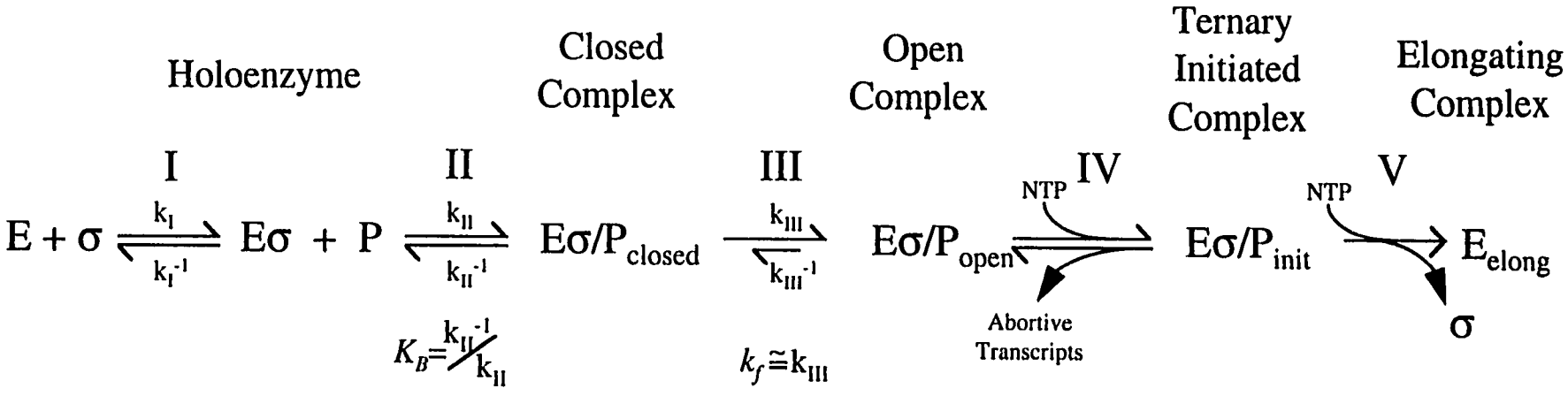
Holoenzyme
Closed Complex
Open Complex
Ternary Initiated Complex
Elongating Complex
I
II
III
IV
V
E + σ
Eσ + P
Eσ/P closed
Eσ/P open
Eσ/P init
E elong
σ
NTP
NTP
Abortive Transcripts
K_B = k_II^-1 / k_II
k_f ≅ k_III

Figure 1.3 [A] Secondary structure of region 2 of σ^{70} (residues 371 to 456). Conserved subregions 2.1, 2.2, 2.3, and 2.4 are indicated by shading. The location and extent of helices 12a through 14 (identified by X-ray crystalographic analysis of a σ^{70} peptide (128) are indicated above the protein sequence.

[B] Tertiary structure of regions 1.2 through 2.4 of σ^{70} (residues 114 through 448). Helices are shown as cylinders. Three disordered regions that were not modeled are indicated (not to scale) as dotted lines. These are residues 168-172, 192-211, and 238-241. Conserved regions are color coded as follows: region 2.1 (green), region 2.2 (yellow), region 2.3 (cyan), and region 2.4 (orange). The nonconserved region inserted between conserved regions 1.2 and 2.1 is colored gray. Figure 1.3A reproduced with permission from (128).

A

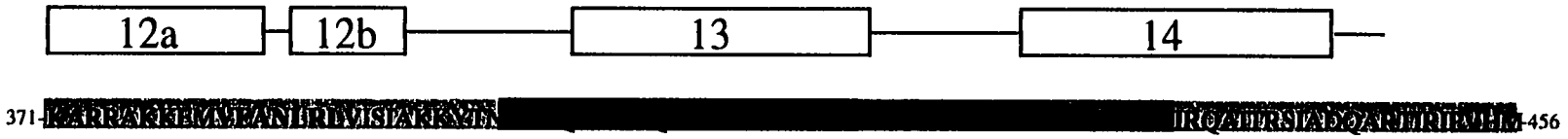

B

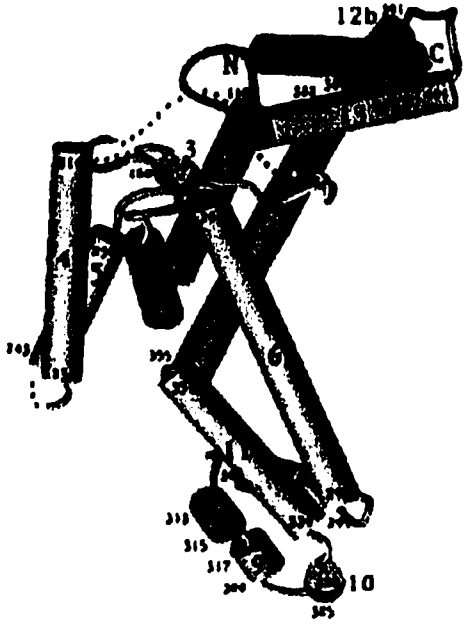

Figure 1.4 Core RNAP binding surface of σ^{70}. The backbone trace is displayed as a white tube, showing the cluster of four helices comprising the conserved regions. A partially transparent, solvent-accessible surface encloses the structure. The large black labels denote the helices. The view is directly at the face containing helices 12a and 12b, comprising conserved regions 2.1. The kink between these helices is centered aboutn Asn-383. Helices 1 and 12a form an intramolecular, antiparallel coiled-coil dimer, only part of which is shown. Some selected, conserved hydrophobic residues are shown in yellow. The green backbone and side chains (residues 380-385) denote a region known from mutagenesis studies to be important for core RNAP binding (178). Shown also are other highly conserved residues that are speculated to be involved in core RNAP binding (128). These are, first, an adjacent patch of conserved solvent-exposed hydrophobic residues (Leu-386, Ile-388, Phe-401,Leu-402, and Ile-405, shown in yellow) that are suggestive of a protein interaction surface and, second, three other highly conserved, exposed residues (shown in blue). Figure reproduced with permission from (128).

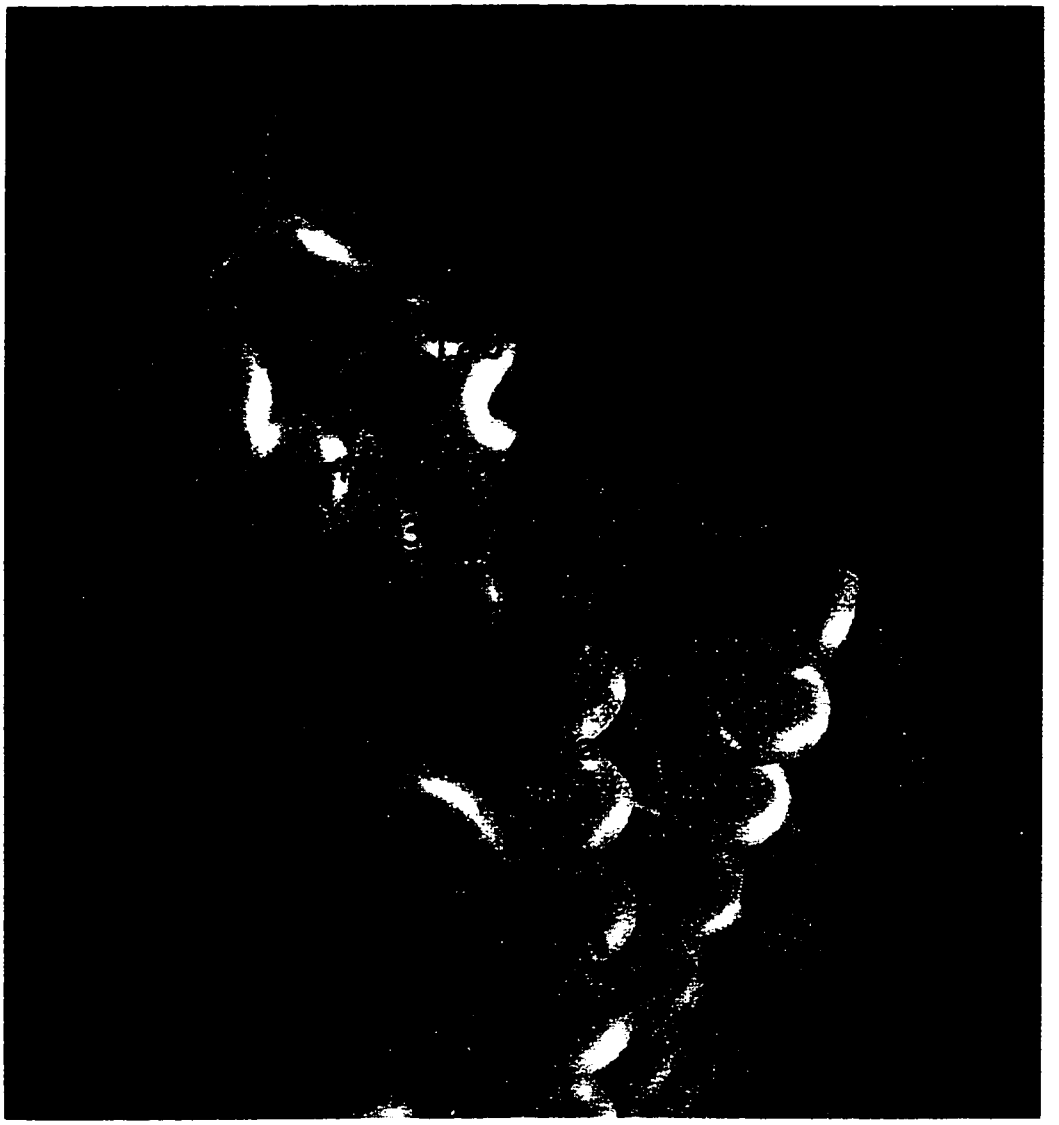

CHAPTER 2

Materials and Methods

Media . Cells were normally grown in Luria-Bertani (LB) medium (30). Minimal E salts medium (182), supplemented with 0.2% glucose, was used as a minimal medium. No-citrate E medium (NCE) (130) was used in minimal media supplemented with carbon sources other than glucose. Bacto-Agar was added to a final concentration of 1.5% for solid medium. Motility medium contained tryptone (Difco; 10g/liter), NaCl (5g/liter), and 0.35% Bacto-Agar. Medium for the propagation of P22 phage lysates was LB supplemented with 1x E salts and glucose to 0.2% final concentration. λ Top agar contained tryptone (Difco; 10g/liter), NaCl (8g/liter), and 0.7% Bacto-Agar.

Indicator plates included MacConkey-lactose (Difco), 2,3,5-triphenyltetrazolium chloride (TTC)-lactose (107, 188), and media containing 5-bromo-4-chloro-3-idolyl-β-D-galacotside (X-gal). TTC-lactose indicator plates (in which TTC was used as an acid or base indicator) contained tryptone (10g/liter), yeast extract (1g/liter), NaCl (5g/liter), lactose (10g/liter) and Bacto-Agar (15g/liter). TTC (1 mg/ml; 200x) was dissolved in water, filter sterilized, and added at 1x strength before the plates were poured. On TTC-lactose indicator plates, Lac+ colonies are white while Lac- colonies are red. A 2% stock solution of X-gal dissolved in dimethylsulfoxide (DMSO) or dimethylformamide (DMF), and added before plates were poured. On X-gal indicator plates, Lac+ colonies are blue while Lac- colonies are white. Green indicator media was prepared as described (21).

Auxotrophic supplements were included in media at final concentrations suggested by Davis et al (30). The following additives were included in media as needed (final concentrations given): X-gal, 100 μg/ml in rich media, 25 μg/ml in minimal media; tetracycline hydrochloride (15 μg/ml in rich media, 10 μg/ml in minimal

media); kanamycin sulfate (50 μg/ml in rich media, 125 μg/ml in minimal media); ampicillin (100 μg/ml in rich media for selection of high-copy plasmids, 30 μg/ml for selection for chromosomal Mu*d*A elements), and chloramphenicol (12.5 μg/ml in rich media, 5 μg/ml in minimal media).

Bacterial strains, phage and transduction methods. Strains used or constructed in the course of this work are listed in Table 2.1. Strains carrying the derivatives of the transposition-defective phage Mu*d*(lac) transposons Mu*d*1 (17) and Mu*d*2 (16) were used in this work. The kanamycin resistant transposons Mu*d*J and Mu*d*K (19) integrate into the chromosome to form *lac* operon and gene fusions, respectively. The larger ampicillin resistant transposons Mu*d*A and Mu*d*B (76), also integrate into the chromosome to form *lac* operon and gene fusions, respectively. Mu*d*-Cm (41) is a small derivative of phage Mu that contains a gene for chloramphenicol resistance. Strains containing Mu*d*-Cm were constructed by conversion of existing Mu*d*J insertions as described (41). Tn10*d*Tc refers to a 3-kb transposition-defective derivative of Tn10 (184). *S. typhimurium* strains defective in flagellar assembly due to a defect in flagellar genes are collectively termed *fla*. Merodiploid strains were constructed by standard genetic procedures (30). LT2 was used for the overexpression of native σ^{28}/FlgM complex. TH3656 was used for the expression of His-core RNAP. BL21(DE3) (Novagen), lysogenic for bacteriophage λ DE3, was used for the expression of His-σ^{28}, His-σ^{70} and His-FlgM proteins. *E. coli* strain DH5α was used for cloning.

Challenge phage in which *ant* expression was being driven by the *fliC* promoter (P_{fliC}-*ant* phage) were constructed by recombination between derivatives of the P22 integration vector pMS284 (192) and the prophage P22 (Ap521). P22 (Ap521) is unable to propagate lytically because the size of its chromosome exceeds that which can be packaged in a single phage capsid (due to the presence of an ampicillin resistant

transposon in the *mnt* locus). Recombinant challenge phage were obtained by electroporating strain TH1901 with phage integration vectors pMC16, pMC66 and pMC74. The transformants were grown to mid-log phase, and mitomycin was added to a 1% final concentration to stimulate recombination. Mitomycin-treated cells were incubated at 37° C with shaking for 4 to 12 hours, or until culture lysed. The culture was vortexed vigorously with chloroform to insure complete lysis, and culture supernatant, which contained recombinant challenge phage, was harvested following centrifugation to pellet cell debris. 0.1 ml of supernatant was mixed with 0.1 ml of a late-log culture of LT2 and 3 mls of λ Top Agar, poured onto LB Agar, and incubated at 37° C until plaques arose. Turbid plaques were streaked for purification three times on a lawn of LT2, and lysogens were checked for kanamycin resistance and ampicillin sensitivity to verify that recombination between the phage and plasmid had occurred and were not due to spontaneous deletions of P22 (Ap521). Replacement of the *ant* gene with the gene for chloramphenicol resistance (CAT) to generate P22 P_{fliC}-CAT phage was performed as follows. A *Salmonella* strain containing plasmid pMS357 (CAT-fusion plasmid; M. Susskind) was infected by P_{fliC}-*ant* phage. Recombination between phage sequence on the plasmid and the P_{fliC}-*ant* phage yields two types of recombinant phage: P_{fliC}-*cat tpfr*$^-$ phage and P_{fliC}-*cat tpfr*$^+$ phage; only the later can be propagated in the absence of exogenously supplied P22 tail protein. Recombinant P_{fliC}-*cat tpfr*$^+$ phage were purified from the resulting lysate by streaking for single plaques on a Cm^{sens} *Salmonella* host, and purifying Cm^r lysogens from the center of turbid plaques on LB agar containing 12.5 μg/ml chloramphenicol.

Transductions in *S. typhimurium* were carried out using the generalized transducing phage P22 (HT105/1 *int-201*)(156). Transductants were purified on green indicator media (21). Challenge phage plaque assays were performed on LB agar media

overlaid with a lawn of host cells in λ Top agar. Phage were either streaked out directly onto a fresh lawn of cells, or 0.1 ml of diluted phage was mixed with 0.1 ml of cells and 3 mls of λ Top agar, then poured onto LB agar media.

Plasmids and transformation methods. Plasmids used or constructed in the course of this work are listed in Table 2.2. Plasmids were purified using a miniprep procedure (71) for small-scale purification, or by the cesium chloride procedure (Promega) for large-scale purification. Plasmids were transformed into *E. coli* and *S. typhimurium* using by electroporation using a Gene Pulser (Biorad) according to manufacturers instructions. P22-mediated transduction was also used to mobilize plasmids between *S. typhimurium* strains.

The P22 integration plasmids pMC16, pMC17, pMC66 and pMC74 were constructed as follows: an ~500 bp *Eco*RI-*Bam*HI fragment from pPY190 (P. Youderian) containing 160 bp from the 5' end of the P22 *arc ant* operon was cloned into pBSIISK$^+$ digested with the same restriction enzymes to create pMC3. A *Pst*I-*Kpn*I-*Pst*I linker was cloned into the *Pst*I site of pMS361 (M. Susskind; identical to pMS284 except that the orientation of the gene for kanamycin resistance is in the opposite orientation) immediately upstream of the *arc ant* promoter to create pMC7. pMC3 was digested with BamHI, treated with Klenow, and digested with KpnI to release a fragment containing the *arc*' sequence preceded by sequence from the vector multiple cloning site. This fragment was cloned into pMC7 digested with SphI, treated with Klenow, and digested with BamHI to create pMC11. pMC11 was linearized by partially digestion with EcoRI, treated with Klenow, and religated to destroy one of two *Eco*RI sites (the *Eco*RI site preceding the P22 *sieA* sequence), creating pMC16. A *Kpn*I-*Eco*RI fragment from pJK127 containing the minimal *fliC* promoter (-36 to +6 bp relative to the start of transcription; H. Bonifield, personal communication) was cloned

into pMC16 digested with the same enzymes to create pMC17. pMC66 was created by inserting a Klenow-treated *BssH*II fragment from pMS531 (172), containing the *fliA* promoter and coding sequence into the unique *Stu*I site of pMC17 downstream of the gene for kanamycin resistance. pMC74 is identical to pMC66, except that the *fliA* allele contains the *fliA*5244* mutation (E203D).

The collection of plasmids used to overexpress truncated FlgM peptides, pJK238, and pMC135-pMC138 were constructed as follows: a 212 bp fragment containing codons 42 through 97 of *flgM* preceded by an in-frame *Nco*I site was amplified using PCR from the *S. typhimurium* chromosome. The primers used were "FlgM45" (ACAGACCATGGCAACGTTAAGCGACGCGCA) and "FlgMend" (GTATTTCTGACAAACGAGTC). The fragment was treated with Klenow and digested with NcoI, then cloned into the IPTG inducible expression vector pTrc99A (Pharmacia) digested with NcoI and SmaI to create pJK238. pJK238 was digested with *Hph*I, treated with Mung Bean exonuclease, and digested with *Nco*I to release a fragment containing codons 42 through 77 of *flgM*. This fragment was cloned into pTrc99A digested with *NcoI* and *Sma*I to create pMC135. pJK238 was digested with *Ple*I, treated with Klenow, and digested with *Nco*I to release a fragment containing codons 42 through 81 of *flgM*. This fragment was cloned into pTrc99A digested with *NcoI* and *Sma*I to create pMC136. pJK238 was digested with *Taq*I, treated with Klenow, and digested with *Nco*I to release a fragment containing codons 42 through 63 of *flgM*. This fragment was cloned into pTrc99A digested with *NcoI* and *Sma*I to create pMC137. pJK238 was digested with *Nru*I and *Pst*I to release a 30 bp fragment containing the last 10 codons of *flgM*, treated with Klenow, and religated to create pMC138.

The His-σ^{28} fusion expression vector pKH445 was derived as follows: a 764 bp *Eco*RI fragment from pMS531 was cloned into the *Bam*HI site of the vector pET15b

(Novagen) to create pKH441 (both insert and vector were treated with Klenow prior to ligation). pKH441 was linearized with XhoI, partially filled in with Klenow using dTTP, dCTP, and dGTP, blunted with mung bean nuclease and religated to create pKH445. The GST-σ^{28} fusion expression vector pKH486 was made by ligating the *Eco*RI fragment from pMS531 into the *Eco*RI site of pGEX-3X (Pharmacia).

The FlgM expression vector pMC64 was derived as follows: a 326 bp fragment containing the *flgM* gene was amplified from the LT2 chromosome by PCR, using primers "*Eco*RI-*Bsp*HI-FlgM" (GAATTCATGAGCATTGACCGTACC) and "FlgMend" such that a *Bsp*HI site was introduced at the start codon of the *flgM* gene. This fragment was cloned into the *Sma*I site of BluescriptII vector KS$^+$ (Stratagene) to create pMC56. A *Bsp*HI(Klenow-treated)-*Hind*III fragment from pMC56 was cloned into pTrc99A digested with NcoI, blunted with mung bean nuclease, and digested with HindIII.

pMC96 is a derivative of pMC64 designed to coexpress FlgM and σ^{28}, and was derived as follows: the 764 bp *Eco*RI fragment from pMS531 was cloned into pTrc99A digested with NcoI to create the σ^{28} expression vector pMC61 (both insert and vector were treated with Klenow prior to ligation). An *Ssp*I fragment carrying the σ^{28} expression cassette from pMC61 was cloned into the unique *Nsi*I site of pMC64 to create pMC96.

The His-FlgM$^+$ expression vector pJK302 was constructed by cloning a *Bsp*HI(Klenow-treated)-*Hind*III fragment from pMC56 into pET28c (Novagen) digested with NheI, treated with Klenow, and digested with HindIII. The His-FlgM*I82T expression vector pJK306 was constructed as follows: *flgM*5436*(I82T) was PCR-amplified from the chromosome of TH3472 using primers *Eco*RI-*Bsp*HI-FlgM and FlgMend. The PCR fragment was treated with Klenow, digested with EcoRI, and ligated into BluescriptII vector SK- digested with EcoRI and EcoRV to

create pJK300. A *Bsp*HI(Klenow-treated)-*Hind*III fragment from pJK300 was cloned into pET28c as in the construction of pJK302 to create pJK306. The His-FlgM*L66S expression vector pJK314 was constructed as follows: *flgM*5224*(L66S) was cloned by overlap extension mutagenesis as described (185). The first round of PCR used pMC56 as a template for two sets of reactions. Set A primers: "M5'sense" (GGAATTCCATATGAGCATTGACCGT) and "L66Santisense" (GCCGTTTTGCTTGCTTCGAC); set B primers "L66Ssense" (GTCGAAGCAAGCAAAACGGC) and FlgMend. PCR fragments generated from sets A and B were gel purified, pooled, and used as templates for a second round of PCR using primers M5'sense and FlgMend, generating a 340 bp fragment containing the *flgM*5224* allele with an *Nde*I site at the start codon. This fragment was treated with Klenow and cloned into BluescriptII vector SK- digested with SmaI to create pJK310. An *Nde*I-*Bam*HI fragment from pJK310 was cloned into pET28c digested with the same enzymes to create pJK314.

The His-σ^{28+} and His-σ^{28*} expression vectors pMC204, and 208 through 219 were constructed as follows: a 119 bp *Xba*I-*Bam*HI fragment from pET15b (Novagen) containing the hexahistidine (His_6) fusion cassette followed by an in-frame *Nde*I site was cloned into the T7 RNAP-dependent His-fusion expression vector paii17 (gift of B. Jack, NEB) digested with the same restriction enzymes to create pMC180. An *Ssp*I fragment from pMC64 containing the P_{tac}*flgM* expression cassette was cloned into the unique *Nru*I site of pMC180 to create pMC195. The presence of an IPTG-inducible copy of the *flgM* gene on this expression vector was intended to mitigate the toxicity of some of the *fliA** alleles that were subsequently cloned under the control of the T7 RNAP-dependent promoter in pMC195 (see below). Thirteen *fliA* genes (*fliA*$^+$ and twelve *fliA** alleles) were cloned into pMC195 to create the His-σ^{28} expression vectors pMC204, and pMC208 through pM219. The *fliA* alleles were PCR amplified from the

chromosomes of LT2 and 12 *fliA** mutants (TH2965, TH2967, TH2971, TH2973, TH2975, TH2981, TH2995, TH2997, TH3003, TH3005, TH3009 and TH3017) using the primers "FliANE" (GGCAGCCATATGCTGGAGAATTCACTGTATACCGCTG) and "FliA4Bam" (GGGGATCCTGGTAGTCTATACGTTG), which introduce an in-frame *Nde*I site followed by two codons (CTG GAG) upstream of the second codon of *fliA*, and a *Bam*HI site downstream of the *fliA* stop codon. PCR products were digested with NdeI and BamHI, and cloned into pMC195 digested with the same restriction enzymes. All *fliA* alleles were sequenced to confirm that PCR had not introduced any secondary mutations.

pJK127 was made by cloning a 56 bp *Hin*dIII-*Eco*RI *fliC* promoter fragment from M13mp19-P_{fliC} (A. Dombroski) into pBSIISK- digested with the same enzymes. A 211 bp *Bss*HII fragment from pJK127 served as the DNA fragment for the DNA filter binding assays. pJK128 was made by cloning a 141 bp *Hin*dIII-*Bss*HII fragment from pJK127 into pKK233-2 (Pharmacia) digested with EcoRI and HindIII (both insert and vector were treated with Klenow prior to ligation).

Selections for fliA mutants.* To isolate spontaneous Lac$^+$ revertants of *fla fliC*::Mu*dJ* strains, independent cultures were grown to mid-log phase and plated on NCE lactose media (~10^8 cells/plate). In the experiment summarized in Table 3.3, the parent strain (MC2) also carried additional copies of the *flgM* gene on a plasmid to bias the selection against *flgM* mutants. Linkage data for the spontaneous Lac$^+$ revertants obtained by Keith Compton are summarized in the Appendix. Spontaneous Lac$^+$ revertants obtained by Kelly Hughes were isolated using a two-step selection process: revertants arising from 40 independent cultures of TH2892 [*fla-2157 fliC5050*::Mu*dA vh2*$^-$ *fljB*^{e,n,x}] were pooled separately and used to prepare transduction lysates. These lysates were used to transduce TH2893 [*fliA5059*::Tn10*d*Tc *fla-2157 fliC5050*::Mu*dA*

vh2⁻ fljB^{on}] to Lac$^+$, selecting for replacement of the *fliA5059*::Tn10*d*Tc allele by a *fliA**. Two Lac$^+$ colonies from each transduction were saved for sequence analysis. Hydroxylamine and diethylsulfate mutagenesis experiments were carried out as described (129). Screens for mutagen-induced Lac$^+$ revertants were carried out on LB X-gal media. The isolation of Lac$^+$ motile revertants of TH2510 and TH2780 were described previously (28, 181).

Sequence analysis of fliA mutants.* The *fliA* locus from the set of 64 potential *fliA** mutants was PCR amplified using the primers "FliA3" (GGCGCTACAGGTTACATAAG) and "FliA4" (TAGTCTATACGTTGTGCGGC) (Starnbach et al, 1992). Template DNA was prepared by diluting a fresh overnight culture of cells 1:10 in distilled water, aliquoting 0.5 ml to an eppendorf tube, and alternately freezing the cells in a dry ice/ethanol bath (3 minutes) and boiling them (5 minutes) (2x), transferring to wet ice for 10 minutes, then centrifuging for 5 minutes to pellet cell debris. 40 µl of the supernatant containing chromosomal DNA was used per PCR reaction. 100 µl reactions contained 1x ULTma PCR buffer (Perkin Elmer), 1.5 mM $MgCl_2$, 40 µM dNTPs, 0.5 µM each primer, and 0.5 µl ULTma polymerase (Perkin Elmer). Reactions were initiated using the HotStart technique (Molecular Bio-Products, Inc.); reactions were performed in a Perkin Elmer thermocycler. The following conditions were used: 2 minutes at 95° C; 31 cycles, 1 minute at 95° C, 1 minute at 50° C, and 1 minute at 72° C (the extension step was extended to 7 minutes during the final cycle). PCR products were purified over Sepharose CL-6B columns (Sigma) equilibrated with STE (10 mM Tris-HCl pH 8.0; 1 mM EDTA; 100 mM NaCl). The amplified fragment was 884 bp, and extended from -117 (relative to the first base of the coding sequence) beyond the stop codon.

PCR products were sequenced directly using the Sequenase 2.0 kit (USB) according to manufacturers instructions except that annealing of sequencing primers were carried out as described by Casanova (18) and extensions were carried out for 45 to 60 seconds at 25° C. ^{35}S-labeled α-dATP was obtained from NEN. Reactions contained a 20:1 molar ratio of primer to template. Primers used to sequence *fliA* were "FliA6" (CCGCTTGTAGCAGATCG), "FliA2" (TGCGATTGCCGGCGAGC), "FliA1" (CGATGGGACAACTGGAG), and "FliA5" (AGCGGGTAATGGATGCG).

In vivo assays of fliA mutants.* β-galactosidase assays were performed in triplicate on mid-log phase cells as described (129). β-galactosidase activities are expressed as nMol/minute/unit of optical density at 650 nm/ml. To evaluate the levels of σ^{28}-dependent expression of β-galactosidase in the collection of *fliA** mutants, the *fliA** alleles were mobilized into an isogenic *fla* background, *fla-2157* (Δ*flgG-L*) *fliC5050*::Mu*dA vh2*$^{-}$ *fljB*^{e,n,x}. Table 3.8 summarizes the results of β-galactosidase assays performed on strains TH2965 through TH3018. Table 3.9 summarizes the results of β-galactosidase assays performed on strains MC1038 through MC1066.

In vivo characterization of truncated FlgM peptides. Motility assays were employed to evaluate the ability of the collection of truncated FlgM peptides to inhibit σ^{28}-dependent transcription *in vivo*. Plasmids pMC64, pJK238, pMC135, pMC136, pMC137 and pMC138 were electroporated into LT2 to generate strains MC65, pTH818, MC973, MC974, MC975 and MC971, respectively. Cells were grown to mid-log phase, stabbed into motility media containing ampicillin and 1 mM IPTG to induce protein expression, and incubated at 37° C. The motility of strains expressing FlgM peptides was compared with that of a control strain containing the vector (pTrc99A) alone. Non motile strains were scored as "+" to indicate full anti-sigma factor activity;

motile strains were scored as "-" to indicate a lack of anti-sigma factor activity. Western blot analysis was used to assay for the presence of the FlgM peptides. Strains containing plasmids were grown to late log phase in LB broth containing 100 μg/ml ampicillin, and induced for 2 hours with 1 mM IPTG (TH2780 was simply grown to late log phase in LB). Samples for Western analysis were prepared from 50 μl aliquots of cells. The level of FlgM expressed by MC65 was scored as "+," less abundant but detectable FlgM peptide levels were scored as "+/-," and the absence of detectable protein was scored as "-."

CAT assay. The chloramphenicol acetyl transferase (CAT) activity assay was adapted from a protocol published by (161). P22 (P_{fliC}-CAT) phage lysogens of strains MC1252, MC1253, MC1254 and MC1255 were obtained by streaking the supernatant from a chloroform-lysed culture of TH3225 onto lawns of the host strains, and streaking out lysogens from the centers of plaques. The presence of the P_{fliC}-CAT phage in the lysogens was verified by testing for resistance to superinfection by P22, and by resistance to chloramphenicol (12.5 μg/ml) in the absence of IPTG. Crude cell extracts of the lysogens were prepared as follows: 3 mls of early-log-phase cultures (A_{450} = 1.1 to 1.4) grown in LB broth + 100 μg/ml of ampicillin were spun down and resuspended in 1 ml of chilled TDTT buffer (50 mM Tris-HCl pH 7.8, 30 μM DTT), and sonicated on ice until cell lysis was complete (two 10 second pulses generally sufficient). Lysed cells were spun 15 minutes in a microcentrifuge to pellet cell debris; supernatants were reserved on ice, and were stable for at least 12 hours. To assay CAT activity, 28 μl of cell extract was added to 823 μl of fresh CAT assay buffer (100 mM Tris-HCl pH 7.8, 1.0 μM DTNB (5,5'-Dithio-bis(2-Nitrobenzoic acid)), 100 μM Acetyl-CoA) prewarmed to 37° C in a 1 cm spectrophotometric cuvette, then inverted to mix contents. 20 seconds prior to initiating spectrophotometric measurement, 16.8 μl of substrate (5 mM

chloramphenicol in distilled water) was mixed with contents of the cuvette. Samples were scanned at A_{412} in a Hitachi Spectrophotometer Model U2000 at 37°C. The increase in OD was recorded for the first 3 minutes of the reaction to derive the slope (ΔA_{412}/min) (reaction rate was linear during this period). CAT activity was calculated using the following equation: ΔOD/minute x (1/molar extinction coefficient$_{A412}$ = 0.0136) x (868λ/16.8λ) = nMol chloramphenicol acetylated/min/ml crude cell extract. The concentration of soluble protein in crude cell extracts was determined the standard Bradford procedure (6) to derive the units of CAT activity/μg total soluble protein.

Overexpression of proteins. His-σ^{28} was overexpressed from pKH445 in *E. coli* strain BL21(DE3). Cells were grown at 37°C in 1 liter batches in LB broth + 50 μg/ml carbenicillin to A_{600} of 0.8; the fusion protein was induced by the addition of 1 mM IPTG for 1 hour. Native FlgM and σ^{28}/FlgM complex were overexpressed from pMC64 and pMC96, respectively, in *S. typhimurium* strain LT2. Cells were grown and induced as described above except that IPTG induction was continued for 2 hours. His-FlgM proteins were overexpressed from pJK302, pJK306 and pJK314 in BL21(DE3). Cells were grown at 37°C in 1 liter batches in LB broth + 50 μg/ml kanamycin to A_{600} of 0.8; fusion proteins were induced by the addition of 1 mM IPTG for 2 hours. His-σ^{70} was overexpressed from pQETσ^{70} in BL21(DE3) (A. Dombroski) as described (187). His-core RNA polymerase was overexpressed from pT7his6flα (R. Gourse) in TH3656. Cells were grown at 37°C in 1 liter batches in LB broth + 50 μg/ml carbenicillin + 0.1 mM IPTG to A_{600} of 0.8.

Purification of native σ^{28} and derivatives. All steps were carried out at 4°C. σ^{28}/FlgM complex was purified as described (28), and dissociated by the addition of Guanidine-HCl to 6 M. Denatured proteins were separated at room temperature over a

Pharmacia Superdex 75 HR 10/30 FPLC column equilibrated with Denaturing FPLC buffer (6 M Guanidine-HCl, 50 mM Tris-HCl pH 7.9, 150 mM NaCl, 0.1 mM EDTA, 1 mM DTT). σ^{28} eluted close to the void volume, while FlgM did not elute from the column. Fractions containing FlgM-free σ^{28} were pooled, concentrated, then renatured by a rapid 50x dilution into Dilution buffer (20% glycerol, 50 mM Tris-HCl pH 7.9, 150 mM NaCl, 0.1 mM EDTA, 1 mM DTT) (58) + 0.01% Triton X-100 at room temperature. Renatured pure σ^{28} was run a second time over the Superdex 75 column equilibrated with TGED (10 mM Tris-HCl pH 7.9, 0.1 mM EDTA, 0.1 mM DTT, 5% glycerol) (122) containing 500 mM NaCl (TGED-500) + 0.01% Triton X-100 to isolate monomeric σ^{28}.

The His-σ^{28} fusion protein was purified according to Novagen's pET-His protocols with 6 M Guanidine HCl in all buffers. Proteins were stored in storage TGED-500 (containing 50% glycerol instead of 5%) + 0.01% Triton X-100 at -20°C or -80°C.

Purification of FlgM and derivatives. All steps were carried out at 4°C. For native FlgM purification, cell pellets were resuspended in AMK buffer (142) and lysed by French Press at 20,000 psi. Total soluble protein was dialyzed into Buffer A (10 mM NaOAc pH 5.2, 0.1 mM EDTA), bound to a CM-52 (Whatman) column, and eluted with a 0 to 500 mM linear NaCl gradient in Buffer A. FlgM-containing fractions were loaded onto a Pharmacia FPLC Mono S column in Buffer A, and eluted with a 0 to 250 mM linear NaCl gradient in Buffer A. FlgM-containing fractions were pooled and loaded onto a FPLC phenyl-Sepharose column in Buffer B (1 M $(NH_4)_2SO_4$, 20 mM Tris-HCl pH 7.2, 1 mM EDTA), and eluted with a 0-100% linear gradient of Buffer C (20 mM Tris-HCl pH 7.2, 1 mM EDTA). FlgM fractions were pooled and dialyzed into TGED storage buffer containing 100 mM NaCl (TGED-100). FlgM was homogeneous

as determined by Coomassie-stained SDS-PAGE analysis. His-FlgM proteins were purified according to Novagen's pET-His protocols. The binding buffer and initial washes contained 6 M Guanidine HCl; subsequent steps were performed with non-denaturing buffers. Proteins were stored in TGED-100 at 4°C or storage TGED-100 at -20°C.

Purification of His-σ^{70} . His-σ^{70} was purified as described (187), and stored in storage TGED-500 + 0.01% Triton X-100 at -80°C.

Purification of core RNA polymerase. Core RNAP was purified from 50 g of *S. typhimurium* strain LT2 as described (177). His-core RNAP from 28 g of *S. typhimurium* TH3656 was purified by the same protocol with an extra passage over the Biorex 70 column to completely separate His-core RNAP from contaminating σ subunits. His-core RNAP was separated from native core RNAP by passage over a HisBind (Novagen) column under non-denaturing conditions according to Novagen's pET-His protocols. Proteins were stored in storage TGED-100 at-20°C.

Protein concentration determination. The concentration of purified proteins was measured using the standard Bradford procedure (6) or determined by absorptance readings at 280 nm corrected for light scattering. Molar extinction coefficients were calculated based on the method of Gill and von Hippel (48), and are reported in units of M^{-1} cm^{-1}: σ^{28} and His-σ^{28}, 27310; FlgM and His-FlgM, 1280; core RNAP, 198500; His-σ^{70}, 39400.

Antibody production and purification . Native σ^{28} and FlgM proteins were isolated as described above. The FlgM protein alone was not immunogenic, so it was

coupled to keyhole limpet hemocyanin (KLH) as described by Pierce Biochemicals to increase its antigenicity. Polyclonal rabbit antibodies against FlgM-KLH and σ^{28} were obtained from the Pocono Rabbit Farm and Laboratory Inc., Canadensis, PA. Anti-FlgM antibodies were purified as follows. The immune sera was fractionated with 50% ammonium sulfate pH 7.0 with stirring overnight at 4°C. The material was centrifuged at 3000xg for 30 minutes and the pellet resuspended in 0.3-0.5 volumes of 100 mM Tris-HCl pH 8.0 and dialyzed overnight in several changes of the resuspension buffer. Total rabbit IgGs were isolated with Protein A beads (Pharmacia) as described by (60). The purified IgG fractions were pooled and dialyzed against TBSa (10 mM Tris-HCl pH 7.5, 170 mM NaCl, 0.02% sodium) overnight at 4°C. Non-specific antibodies were removed by passing the pooled IgG fractions over a bacterial lysate column (32). The eluant and wash were collected and concentrated with Centriprep-30 concentrators (Amicon). Using a 1:10,000 dilution of anti-FlgM, 1 ng of FlgM could be detected by Western blot hybridization as described (74). An affinity purification protocol based on a method described by Masson and Tschopp (132) was developed for the purification of anti-σ^{28} antibodies. Crude immune sera was diluted 10x in Saturation buffer (20 mM Tris-HCl pH 8.4, 150 mM NaCl, 5 mM EDTA, 1% gelatin, 0.1% fetal calf serum), and absorbed at 25°C to purified native σ^{28} bound to Westran PVDF membrane (Schliecher & Schuell) blocked in TBS (10 mM Tris-HCl pH 7.5, 150 mM NaCl) + 0.05% Tween 20 and 5% nonfat milk. Following overnight absorption, the membrane was washed 2x in TBS, and the σ^{28}-specific antibodies eluted with 0.2 M glycine-HCl pH 2.5 for 5 minutes at 4°C. Eluted antibodies were immediately neutralized with 2 M Tris-HCl pH 9.0, then dialyzed at 4°C overnight into TBSa. Using a 1:100 dilution of affinity purified anti-σ^{28}, 2.5 ng of σ^{28} could be detected by Western blot hybridization as described (74).

Western analysis . Western blot analyses were performed as described (74). Blots were either immunostained by an alkaline phosphatase based reaction (89), or using an ECL Western detection kit (Amersham) and Horseradish peroxidase conjugated goat anti-rabbit IgG secondary antibodies (Biorad).

In vitro transcription assays. Spot transcription assays were performed essentially as described (177) except that the reaction buffer contained 150 mM NaCl, 0.05% BSA, and 0.01% Triton X-100, and the final wash of the DEAE cellulose disks in ether was omitted. 100 µl reactions contained 0.3 pmol linear DNA promoter template, and 3 pmol native or His-core RNA polymerase. Linear templates were PCR-amplified from pJK128 with primers "128/233" (CTCATCCGCCAAAACAGCC) and "128" (GATCTTCCCCATCGGTGATGT) to generate a 271 bp *fliC* promoter fragment, and from pKK233-2 with primers 128/233 and "233" (GCGCCGACATATAAACGG) to generate a 158 bp *tac* promoter fragment. Proteins were added to the transcription assay buffer containing NTPs on ice, allowed to equilibrate at 37°C for 10 minutes, and initiated by the addition of template.

Copurification of GST-σ^{28} and σ^{28}-associated proteins. pKH486 or pGEX-3X plasmid DNA (Pharmacia) was electroporated into LT2, TH2822, and TH2825 cells. Cells were grown in LB + 100 µg/ml ampicillin at 37°C to A_{600} of 0.4 to 0.6, then allowed to grow for an additional hour without induction. The cells were lysed by passage through a French Press twice at 20,000 psi. The GST-σ^{28} fusion protein and other complexed proteins were affinity-purified over a Sepharose-glutathione column (Sigma) as described (171). Column eluants were electrophoresed on 10% Tricine SDS-PAGE gels (157). Protein bands were identified by Western analysis or by comparison with purified protein standards.

Filter binding assays . DNA filter binding assays were performed as described (67). The DNA template, a 211 bp *Bss*HII fragment from pJK127 containing the *fliC* promoter was end-labeled with α-^{32}P dCTP (NEN) in a Klenow reaction. DNA binding reactions were carried out in 50 µl TXN buffer (50 mM Tris-HCl pH 7.8, 50 mM NaCl, 0.1 mM EDTA, 0.1 mM DTT, 3 mM MgOAc, 25 µg/ml BSA) at 37°C. The concentration of core RNAP was 30 nM. The concentrations of σ^{28} and FlgM were both 60 nM. Proteins were incubated together for 10 or 15 minutes, followed by the addition of 5 µl pre-warmed radiolabeled *fliC* promoter DNA to a final concentration of 6 nM, and incubated for 5 minutes (samples chased with 1 µg sheared salmon sperm DNA were incubated an additional 5 minutes after the addition of non-specific competitor DNA). Samples were diluted to 1 ml in TXN buffer and filtered through a 13 mm BA83 nitrocellulose filter (Schleicher and Schuell) pre-wetted with 1 ml TXN buffer on a Millipore sampling manifold. The filters were dried and counted by liquid scintillation.

Native PAGE analysis of σ^{28}-holoenzyme associated proteins . 10 µl reactions containing (where indicated) 5 µg σ^{28}, 5 µg FlgM and/or 1 µg core RNAP in modified TXN buffer containing 100 mM NaCl and lacking BSA, were incubated for 15 minutes at 37°C. Native sample buffer (Novex) was added to 1x, and samples were electrophoresed on a 4-12% Native Tris-glycine gel (Novex) according to manufacturer's protocol. Excised gel fragments were equilibrated in 1x Laemmli sample (106) for 15 minutes prior to electrophoresis over a 16.5% Tricine SDS-PAGE gel (157).

SPR assays . Surface Plasmon Resonance (SPR) experiments were carried out with a Biacore 2000 (Biacore Inc.). Kinetic constants k_a and k_d were calculated using

the BIAevaluation software version 2.1 (Biacore Inc.); models assumed a 1:1 interaction.

Eσ dissociation: Measurements of the k_d of $E\sigma^{28}$ and $E\sigma^{70}$ in the presence and absence of FlgM proteins were carried out in HBS buffer (Biacore Inc.) at a flow rate of 10 µl/min. Native σ^{28} or His-σ^{70} (25 µg/ml in 10 mM Acetate pH 4.0 and pH 4.2, respectively) were coupled to the CM5 sensor chip via standard NHS/EDC activation chemistry (Biacore Inc.). Core RNAP in HBS buffer was injected over the ligand surface at 10 µl/minute for 2.5 minutes, followed by injection of HBS buffer, or HBS buffer containing His-FlgM protein. As a control for non-specific binding, analyte was injected over an adjacent flowcell lacking immobilized ligand; the signal from blank runs was subtracted to correct for noise. The σ surface was cleaned of non-covalently bound protein by a 1 minute injection of Denaturing FPLC buffer, followed by a 3 minute injection of Dilution buffer (see *Purification of native* σ^{28}). The immobilized σ factor could be repeatedly regenerated by this procedure, recovering an identical level of analyte binding capacity for over 20 regeneration cycles.

Controls were performed to optimize the level of immobilized ligand (ligand density) and the analyte concentration. This was necessary to eliminate the possibility of analyte rebinding during the dissociation phase of our experiments. If rebinding were allowed to occur, then the observed k_d of $E\sigma^{28}$ would be slower than the true k_d. In addition, an increase in the apparent k_d in the presence of FlgM might then be attributed to the competitive binding of FlgM to ligand sites as they became available, rather than to active dissociation of $E\sigma^{28}$ by FlgM.

Different ligand densities were tested to identify one that could generate a significant binding response curve upon analyte injection, but was not so high that the rates of binding and dissociation were influenced by mass-transport limited kinetics instead of by interaction-limited kinetics. A 50 nM solution of core RNAP was injected

over three different levels of ligand (900, 300 and 100 RU of immobilized σ^{28}). While the 900 RU ligand surface was somewhat limited by mass-transport as judged by the shape of the binding curve during the initial phase of analyte injection (and was therefore excluded from subsequent experiments), the two lower-density ligand surfaces were not. The finding that dissociation of analyte from the 300 and 100 RU ligand surfaces occurred at nearly the same rate (data not shown) was another indication that our measurements were not skewed by mass-transport effects at these ligand densities. The flow rate was increased from the standard 10 µl/minute to 50 µl/minute in order to evaluate the effect of flow rate on analyte dissociation. The k_d of $E\sigma^{28}$ was not altered by an increase in flow rate confirming that dissociation at 10 µl/minute was not mass transport-limited. Various concentrations of analyte were tested to determine the concentration at which the ligand surface would quickly become saturated. It was important that the ligand surface be saturated for our experiments so that during the early phase of analyte dissociation a molecule of core RNAP dissociating from the ligand surface would be unlikely to rebind to an unoccupied molecule of σ^{28} before flowing out of the sensor chamber. Analyte binding reached a maximum at concentrations of 50 nM and above (data not shown), and therefore 50 nM core RNAP was used in all experiments.

As a final test of the experimental conditions, the dissociation of core RNAP was measured in the presence of soluble σ^{28} (50 nM in HBS buffer) as a competitor for rebinding of core RNAP to immobilized σ^{28}. The presence of competitor did not increase in the rate of dissociation of $E\sigma^{28}$ (data not shown), therefore we concluded that rebinding of core RNAP during the dissociation phase was not occurring under our conditions. These controls allowed us to exclude the possibility that the effect of FlgM on the k_d of $E\sigma^{28}$ could be due to inhibition of core rebinding (through competitive binding of the σ^{28} ligand layer). All of the $E\sigma^{28}$ dissociation experiments described in

the Results were performed with both the 300 and 100 RU ligand surfaces; the data depicted in Figure 4.6A are from the 100 RU experiments only. To obtain the k_d values reported in Figure 4.6A, we analyzed the dissociation curves from 210 seconds to 330 seconds.

Kinetic analysis of FlgM/σ^{28} and core RNAP/σ^{28}interactions: To prepare the sensor chip for the measurements of the interaction between His-FlgM proteins (ligand) and native σ^{28} (analyte), 20 µl of a 500 µM $NiCl_2$ solution was passed through the flowcell of a Sensor NTA chip at 20 µl/minute to prime the surface for capture of the His-tagged ligand. Ligand was applied to the primed flowcell surface by injecting 15 µl of a 50 nM solution of the His-FlgM protein ($FlgM^+$, FlgM*L66S, or FlgM* I82T) in Eluent buffer (Biacore Inc.) at 10 µl/min. Typically, 60-80 RU of ligand were captured during these injections. A fresh ligand surface was applied to the chip before each analyte injection. Analyte was serially diluted into Eluent buffer to prepare 100 µl samples ranging in concentration from 0.625 to 40 nM, and injected at 20 µl/min. Rate constants for each σ^{28}/His-FlgM protein pair were derived by analyzing the data from 6 or 7 analyte injections. As a control for non-specific binding, analyte was injected over an adjacent Ni^{2+}-primed flowcell lacking immobilized ligand; the signal from these blank runs was subtracted to correct for noise. After each experiment, the NTA chip surface was regenerated by injection of 60 µl of Regeneration solution (Biacore Inc.), followed by 20 µl of 50 mM NaOH at 20 µl/min. This treatment stripped the flowcell of Ni^{2+} and any nonspecifically bound protein.

For measurement of the His-σ^{28}/His-FlgM and His-σ^{28}/core RNAP interactions, ligand was covalently coupled to flowcells 2, 3 and 4 of CM5 chips (flowcell 1 served as a blank control for non-specific analyte binding). ~200 RU of each His-σ^{28} protein was covalently coupled as described above (see *Eσ^{28} dissociation*) for analyses in which the His-σ^{28} proteins served as the ligands. ~100

RU of His-FlgM$^+$ was covalently coupled (soluble His-FlgM$^+$ was applied to the activated chip surface in 5 mM maleate buffer pH 6.2) for analyses of the interaction of His-FlgM$^+$ with the His-σ^{28} proteins. The ligand surfaces were regenerated prior to each analyte injection with Denaturing FPLC buffer as described above. 50 µl analyte samples were prepared by serial dilution of protein into HBS buffer. Concentration range for His-FlgM$^+$ was from 500 to 15.6 nM; for core RNAP, from 80 to 1.25 nM; for His-σ^{28}, from 80 to 2.5 nM (except in the case of His-σ^{28}*(L199R), where analyte concentrations ranged from 500 nM to 1 nM). Analytes were injected at 10 µl/min. Data were corrected for noise and analyzed as above. K_d values were calculated from the equation $K_d = k_d / k_a$.

Table 2.1. List of strains used or constructed in the course of this work

E. coli strains

TH strain	Original strain	Genotype	Source
TH1275	DH5α	*endA1 hsdR17* ($r_K^- m_K^-$) *supE44 thi-1 recA1 gyrA* (Nal^r) *relA1* Δ(*lacZYA-argF*) *U169* (Φ80d*lac*Δ(*lacZ*) M15)	New England Biolabs
TH2426	BL21(DE3)	F^- *ompT* (*lon*) *hsdS*$_B$ ($r_B^- m_B^-$) with DE3, a λ prophage carrying the T7 RNA polymerase gene	Novagen

S. typhimurium strains

TH strain	Original strain	Genotype	Source[a]
TH437	LT2	wild type	J. Roth
	MC2	pMH71 (*flgM*$^+$)/ *fla-2157* (Δ*flgG-L*) *fliC5050*::MudJ *vh2*$^-$ *fljB*^{e,n,x,off}	*
TH2430		*fla-2157* (Δ*flgG-L*) *fliC5050*::MudJ *vh2*$^-$ *fljB*^{e,n,x,off}	K. Hughes
TH1077		*fliC5050*::MudJ	K. Hughes
TH1722	SJW1518	*fla-2157* (Δ*flgG-L*) *vh2*$^-$ *fljB*^{e,n,x,off}	S.Yamaguchi
TH2111		*fla-958* (Δ*flgHI*) *fliC5050*::MudJ *vh2*$^-$ *fljB*^{e,n,x,off}	K. Hughes
TH2431		*fla-2039* (Δ*tar-flhD*) *fliC5050*::MudJ *vh2*$^-$ *fljB*^{e,n,x,off}	K. Hughes
TH2432		*fla-2018* (Δ*flhA-cheA*) *fliC5050*::MudJ *vh2*$^-$ *fljB*^{e,n,x,off}	K. Hughes
TH2433		*fla-2211* (Δ*fliE-K*) *fliC5050*::MudJ *vh2*$^-$ *fljB*^{e,n,x,off}	K. Hughes
TH2434		*fla-2195* (Δ*fliJ-R*) *fliC5050*::MudJ *vh2*$^-$ *fljB*^{e,n,x,off}	K. Hughes
TH2892	MC243	*fla-2157* (Δ*flgG-L*) *fliC5050*::MudA *vh2*$^-$ *fljB*^{e,n,x,off}	*
TH2893	MC244	*fliA5059*::Tn*10d*Tc *fla-2157* (Δ*flgG-L*) *fliC5050*::MudA *vh2*$^-$ *fljB*^{e,n,x,off}	*
pTH721		pMS531 (*fliA*$^+$) / LT2	K. Hughes
TH2796	GC81	p*flhDC*$^+$/LT2	G. Chilcott
TH2251	SJW1448	*fliA2087 vh2*$^-$ *fljB*^{e,n,x,off}	S.Yamaguchi
TH2249	SJW1387	*flhC2035 vh2*$^-$ *fljB*^{e,n,x,off}	S.Yamaguchi
TH2250	SJW1400	*flhD2040 vh2*$^-$ *fljB*^{e,n,x,off}	S.Yamaguchi

Table 2.1 continued

TH strain	Original strain	Genotype	Source[a]
	MC119	*fdp*$^+$ *zge7057*::Tn*10d*Tc *leu414 supE attA*::[P22 *sieA44 16-amH1455 tpfr-49*] Fels$^-$	*
	MC115	*flgM5222*::Mud-Cm *fdp*$^+$ *leu414 supE attA*::[P22 *sieA44 16-amH1455 tpfr-49*] Fels$^-$	*
	MC121	p*flhDC*$^+$/ *fdp*$^+$ *zge7057*::Tn*10d*Tc *leu414 supE attA*::[P22 *sieA44 16-amH1455 tpfr-49*] Fels$^-$	*
	MC123	*flgM5222*::Mud-Cm *fdp*$^+$ *leu414 supE attA*::[P22 *sieA44 16-amH1455 tpfr-49*] Fels$^-$	*
	MC148	*pyrC691*::Tn*10d*Tc *fla-2157* (Δ*flgG-L*) *fdp*$^+$ *leu414 supE attA*::[P22 *sieA44 16-amH1455 tpfr49*] Fels$^-$	*
TH1901		*ataA*::[P22(Ap521)] *leuA414 supE hsdSB* Fels$^-$	K. Hughes
TH471	MS1868	*leu414 hsdSB* (r^-m^+) Fels$^-$	M. Susskind
TH2791	MC86	*flgM5222*::Mud-Cm	*
TH2788	KG1033	*fliY5221*:Tn*10d*Tc	K. Visick
TH2864	MC382	*flgM5222*::Mud-Cm *fla-2157* (Δ*flgG-L*) *fliC5050*::MudA *vh2*$^-$ *fljB*^{e,n,x,off}	*
TH2965	MC307	*fliA*5225* (H14D) *fla-2157* (Δ*flgG-L*) *fliC5050*::MudA *vh2*$^-$ *fljB*^{e,n,x,off}	*
TH2966	MC345	*fliA*5225* (H14D) *flgM5222*::Mud-Cm *fla-2157* (Δ*flgG-L*) *fliC5050*::MudA *vh2*$^-$ *fljB*^{e,n,x,off}	*
TH2967	MC385	*fliA*5226* (H14N) *fliY5221*::Tn*10d*Tc *fla-2157* (Δ*flgG-L*) *fliC5050*::MudA *vh2*$^-$ *fljB*^{e,n,x,off}	*
TH2968	MC386	*fliA*5226* (H14N) *fliY5221*::Tn*10d*Tc *flgM5222*::Mud-Cm *fla-2157* (Δ*flgG-L*) *fliC5050*::MudA *vh2*$^-$ *fljB*^{e,n,x,off}	*
TH2969	MC387	*fliA*5227* (H14Y) *fliY5221*::Tn*10d*Tc *fla-2157* (Δ*flgG-L*) *fliC5050*::MudA *vh2*$^-$ *fljB*^{e,n,x,off}	*
TH2970	MC388	*fliA*5227* (H14Y) *fliY5221*::Tn*10d*Tc *flgM5222*::Mud-Cm *fla-2157* (Δ*flgG-L*) *fliC5050*::MudA *vh2*$^-$ *fljB*^{e,n,x,off}	*
TH2971	MC303	*fliA*5228* (V33E) *fla-2157* (Δ*flgG-L*) *fliC5050*::MudA *vh2*$^-$ *fljB*^{e,n,x,off}	*
TH2972	MC341	*fliA*5228* (V33E) *flgM5222*::Mud-Cm *fla-2157* (Δ*flgG-L*) *fliC5050*::MudA *vh2*$^-$ *fljB*^{e,n,x,off}	*

Table 2.1 continued

TH strain	Original strain	Genotype	Source[a]
TH2973	MC298	*fliA*5229* (M1045) *fla-2157* (Δ*flgG-L*) *fliC5050*::MudA *vh2*⁻ *fljB*^{e,n,x,off}	*
TH2974	MC336	*fliA*5229* (M104T) *flgM5222*::Mud-Cm *fla-2157* (Δ*flgG-L*) *fliC5050*::MudA *vh2*⁻ *fljB*^{e,n,x,off}	*
TH2975	MC401	*fliA*5230* (N114K) *fliY5221*::Tn*10d*Tc *fla-2157* (Δ*flgG-L*) *fliC5050*::MudA *vh2*⁻ *fljB*^{e,n,x,off}	*
TH2976	MC408	*fliA*5230* (N114K) *fliY5221*::Tn*10d*Tc *flgM5222*::Mud-Cm *fla-2157* (Δ*flgG-L*) *fliC5050*::MudA *vh2*⁻ *fljB*^{e,n,x,off}	*
TH2977	MC302	*fliA*5231* (N114T) *fla-2157* (Δ*flgG-L*) *fliC5050*::MudA *vh2*⁻ *fljB*^{e,n,x,off}	*
TH2978	MC340	*fliA*5231* (N114T) *flgM5222*::Mud-Cm *fla-2157* (Δ*flgG-L*) *fliC5050*::MudA *vh2*⁻ *fljB*^{e,n,x,off}	*
TH2979	MC329	*fliA*5232* (L124F) *fla-2157* (Δ*flgG-L*) *fliC5050*::MudA *vh2*⁻ *fljB*^{e,n,x,off}	*
TH2980	MC369	*fliA*5232* (L124F) *flgM5222*::Mud-Cm *fla-2157* (Δ*flgG-L*) *fliC5050*::MudA *vh2*⁻ *fljB*^{e,n,x,off}	*
TH2981	MC328	*fliA*5233* (T138I) *fla-2157* (Δ*flgG-L*) *fliC5050*::MudA *vh2*⁻ *fljB*^{e,n,x,off}	*
TH2982	MC368	*fliA*5233* (T138I) *flgM5222*::Mud-Cm *fla-2157* (Δ*flgG-L*) *fliC5050*::MudA *vh2*⁻ *fljB*^{e,n,x,off}	*
TH2983	MC300	*fliA*5234* (N139I) *fla-2157* (Δ*flgG-L*) *fliC5050*::MudA *vh2*⁻ *fljB*^{e,n,x,off}	*
TH2984	MC338	*fliA*5234* (N139I) *flgM5222*::Mud-Cm *fla-2157* (Δ*flgG-L*) *fliC5050*::MudA *vh2*⁻ *fljB*^{e,n,x,off}	*
TH2985	MC310	*fliA*5235* (N139K) *fla-2157* (Δ*flgG-L*) *fliC5050*::MudA *vh2*⁻ *fljB*^{e,n,x,off}	*
TH2986	MC350	*fliA*5235* (N139K) *flgM5222*::Mud-Cm *fla-2157* (Δ*flgG-L*) *fliC5050*::MudA *vh2*⁻ *fljB*^{e,n,x,off}	*
TH2987	MC400	*fliA*5236* (P190Q) *fliY5221*::Tn*10d*Tc *fla-2157* (Δ*flgG-L*) *fliC5050*::MudA *vh2*⁻ *fljB*^{e,n,x,off}	*
TH2988	MC407	*fliA*5236* (P190Q) *fliY5221*::Tn*10d*Tc *flgM5222*::Mud-Cm *fla-2157* (Δ*flgG-L*) *fliC5050*::MudA *vh2*⁻ *fljB*^{e,n,x,off}	*

Table 2.1 continued

TH strain	Original strain	Genotype	Source[a]
TH2989	MC333	*fliA*5237* (P190S) *fla-2157* (Δ*flgG-L*) *fliC5050*::MudA *vh2*⁻ *fljB*^{e,n,x,off}	*
TH2990	MC372	*fliA*5237* (P190S) *flgM5222*::Mud-Cm *fla-2157* (Δ*flgG-L*) *fliC5050*::MudA *vh2*⁻ *fljB*^{e,n,x,off}	*
TH2991	MC399	*fliA*5238* (V196G) *fliY5221*::Tn*10d*Tc *fla-2157* (Δ*flgG-L*) *fliC5050*::MudA *vh2*⁻ *fljB*^{e,n,x,off}	*
TH2992	MC406	*fliA*5238* (V196G) *fliY5221*::Tn*10d*Tc *flgM5222*::Mud-Cm *fla-2157* (Δ*flgG-L*) *fliC5050*::MudA *vh2*⁻ *fljB*^{e,n,x,off}	*
TH2993	MC403	*fliA*5239* (T198K) *fliY5221*::Tn*10d*Tc *fla-2157* (Δ*flgG-L*) *fliC5050*::MudA *vh2*⁻ *fljB*^{e,n,x,off}	*
TH2994	MC410	*fliA*5239* (T198K) *fliY5221*::Tn*10d*Tc *flgM5222*::Mud-Cm *fla-2157* (Δ*flgG-L*) *fliC5050*::MudA *vh2*⁻ *fljB*^{e,n,x,off}	*
TH2995	MC402	*fliA*5240* (L199R) *fliY5221*::Tn*10d*Tc *fla-2157* (Δ*flgG-L*) *fliC5050*::MudA *vh2*⁻ *fljB*^{e,n,x,off}	*
TH2996	MC343	*fliA*5240* (L199R) *fliY5221*::Tn*10d*Tc *flgM5222*::Mud-Cm *fla-2157* (Δ*flgG-L*) *fliC5050*::MudA *vh2*⁻ *fljB*^{e,n,x,off}	*
TH2997	MC305	*fliA*5241* (L199Q) *flgM5222*::Mud-Cm *fla-2157* (Δ*flgG-L*) *fliC5050*::MudA *vh2*⁻ *fljB*^{e,n,x,off}	*
TH2998	MC409	*fliA*5241* (L199Q) *fla-2157* (Δ*flgG-L*) *fliC5050*::MudA *vh2*⁻ *fljB*^{e,n,x,off}	*
TH2999	MC313	*fliA*5242* (Q202L) *flgM5222*::Mud-Cm *fla-2157* (Δ*flgG-L*) *fliC5050*::MudA *vh2*⁻ *fljB*^{e,n,x,off}	*
TH3000	MC353	*fliA*5242* (Q202L) *fla-2157* (Δ*flgG-L*) *fliC5050*::MudA *vh2*⁻ *fljB*^{e,n,x,off}	*
TH3001	MC318	*fliA*5243* (Q202R) *flgM5222*::Mud-Cm *fla-2157* (Δ*flgG-L*) *fliC5050*::MudA *vh2*⁻ *fljB*^{e,n,x,off}	*
TH3002	MC358	*fliA*5243* (Q202R) *fla-2157* (Δ*flgG-L*) *fliC5050*::MudA *vh2*⁻ *fljB*^{e,n,x,off}	*
TH3003	MC383	*fliA*5244* (E203D) *fliY5221*::Tn*10d*Tc *fla-2157* (Δ*flgG-L*) *fliC5050*::MudA *vh2*⁻ *fljB*^{e,n,x,off}	*
TH3004	MC384	*fliA*5244* (E203D) *fliY5221*::Tn*10d*Tc *flgM5222*::Mud-Cm *fla-2157* (Δ*flgG-L*) *fliC5050*::MudA *vh2*⁻ *fljB*^{e,n,x,off}	*

Table 2.1 continued

TH strain	Original strain	Genotype	Source[a]
TH3005	MC306	*fliA*5245* (N206K) *flgM5222*::Mud-Cm *fla-2157* (Δ*flgG-L*) *fliC5050*::MudA *vh2*⁻ *fljB*^{e,n,x,off}	*
TH3006	MC344	*fliA*5245* (N206K) *fla-2157* (Δ*flgG-L*) *fliC5050*::MudA *vh2*⁻ *fljB*^{e,n,x,off}	*
TH3007	MC308	*fliA*5246* (E209D) *fla-2157* (Δ*flgG-L*) *fliC5050*::MudA *vh2*⁻ *fljB*^{e,n,x,off}	*
TH3008	MC347	*fliA*5246* (E209D) *flgM5222*::Mud-Cm *fla-2157* (Δ*flgG-L*) *fliC5050*::MudA *vh2*⁻ *fljB*^{e,n,x,off}	*
TH3009	MC404	*fliA*5247* (V213E) *fliY5221*::Tn*10d*Tc *fla-2157* (Δ*flgG-L*) *fliC5050*::MudA *vh2*⁻ *fljB*^{e,n,x,off}	*
TH3010	MC411	*fliA*5247* (V213E) *fliY5221*::Tn*10d*Tc *flgM5222*::Mud-Cm *fla-2157* (Δ*flgG-L*) *fliC5050*::MudA *vh2*⁻ *fljB*^{e,n,x,off}	*
TH3011	MC320	*fliA*5248* (V213G) *fla-2157* (Δ*flgG-L*) *fliC5050*::MudA *vh2*⁻ *fljB*^{e,n,x,off}	*
TH3012	MC380	*fliA*5248* (V213G) *flgM5222*::Mud-Cm *fla-2157* (Δ*flgG-L*) *fliC5050*::MudA *vh2*⁻ *fljB*^{e,n,x,off}	*
TH3013	MC319	*fliA*5249* (S226N) *fla-2157* (Δ*flgG-L*) *fliC5050*::MudA *vh2*⁻ *fljB*^{e,n,x,off}	*
TH3014	MC359	*fliA*5249* (S226N) *flgM5222*::Mud-Cm *fla-2157* (Δ*flgG-L*) *fliC5050*::MudA *vh2*⁻ *fljB*^{e,n,x,off}	*
TH3015	MC299	*fliA*5250* (S226R) *fla-2157* (Δ*flgG-L*) *fliC5050*::MudA *vh2*⁻ *fljB*^{e,n,x,off}	*
TH3016	MC337	*fliA*5250* (S226R) *flgM5222*::Mud-Cm *fla-2157* (Δ*flgG-L*) *fliC5050*::MudA *vh2*⁻ *fljB*^{e,n,x,off}	*
TH3017	MC322	*fliA*5251* (R231Q) *fla-2157* (Δ*flgG-L*) *fliC5050*::MudA *vh2*⁻ *fljB*^{e,n,x,off}	*
TH3018	MC362	*fliA*5251* (R231Q) *flgM5222*::Mud-Cm *fla-2157* (Δ*flgG-L*) *fliC5050*::MudA *vh2*⁻ *fljB*^{e,n,x,off}	*
	MC417	pMS531 (*fliA*⁺)/ *flgM5222*::Mud-Cm *fla-2157* (Δ*flgG-L*) *fliC5050*::MudJ *vh2*⁻ *fljB*^{e,n,x,off}	*
	MC183	*fliA*5465* (*fliA* UTR -15GtoA) *fla-2157* (Δ*flgG-L*) *fliC5050*::MudJ *vh2*⁻ *fljB*^{e,n,x,off}	*

Table 2.1 continued

TH strain	Original strain	Genotype	Source[a]
	MC1038	*flhD92*::Tn*10 fliA*5225* (H14D) *flgM5222*::Mud-Cm *fla-2157* (Δ*flgG-L*) *fliC5050*::MudA *vh2*$^-$ *fljB*^{e,n,x,off}	*
	MC1039	*flhD92*::Tn*10 fliA*5226* (H14N) *flgM5222*::Mud-Cm *fla-2157* (Δ*flgG-L*) *fliC5050*::MudA *vh2*$^-$ *fljB*^{e,n,x,off}	*
	MC1040	*flhD92*::Tn*10 fliA*5227* (H14Y) *flgM5222*::Mud-Cm *fla-2157* (Δ*flgG-L*) *fliC5050*::MudA *vh2*$^-$ *fljB*^{e,n,x,off}	*
	MC1041	*flhD92*::Tn*10 fliA*5228* (V33E) *flgM5222*::Mud-Cm *fla-2157* (Δ*flgG-L*) *fliC5050*::MudA *vh2*$^-$ *fljB*^{e,n,x,off}	*
	MC1042	*flhD92*::Tn*10 fliA*5229* (M104T) *flgM5222*::Mud-Cm *fla-2157* (Δ*flgG-L*) *fliC5050*::MudA *vh2*$^-$ *fljB*^{e,n,x,off}	*
	MC1043	*flhD92*::Tn*10 fliA*5230* (N114K) *flgM5222*::Mud-Cm *fla-2157* (Δ*flgG-L*) *fliC5050*::MudA *vh2*$^-$ *fljB*^{e,n,x,off}	*
	MC1044	*flhD92*::Tn*10 fliA*5231* (N114T) *flgM5222*::Mud-Cm *fla-2157* (Δ*flgG-L*) *fliC5050*::MudA *vh2*$^-$ *fljB*^{e,n,x,off}	*
	MC1045	*flhD92*::Tn*10 fliA*5232* (L124F) *flgM5222*::Mud-Cm *fla-2157* (Δ*flgG-L*) *fliC5050*::MudA *vh2*$^-$ *fljB*^{e,n,x,off}	*
	MC1046	*flhD92*::Tn*10 fliA*5233* (T138I) *flgM5222*::Mud-Cm *fla-2157* (Δ*flgG-L*) *fliC5050*::MudA *vh2*$^-$ *fljB*^{e,n,x,off}	*
	MC1047	*flhD92*::Tn*10 fliA*5234* (N139I) *flgM5222*::Mud-Cm *fla-2157* (Δ*flgG-L*) *fliC5050*::MudA *vh2*$^-$ *fljB*^{e,n,x,off}	*
	MC1048	*flhD92*::Tn*10 fliA*5235* (N139K) *flgM5222*::Mud-Cm *fla-2157* (Δ*flgG-L*) *fliC5050*::MudA *vh2*$^-$ *fljB*^{e,n,x,off}	*
	MC1049	*flhD92*::Tn*10 fliA*5236* (P190Q) *flgM5222*::Mud-Cm *fla-2157* (Δ*flgG-L*) *fliC5050*::MudA *vh2*$^-$ *fljB*^{e,n,x,off}	*

Table 2.1 continued

TH strain	Original strain	Genotype	Source[a]
	MC1050	*flhD92*::Tn*10 fliA*5237* (P190S) *flgM5222*::Mud-Cm *fla-2157* (Δ*flgG-L*) *fliC5050*::MudA *vh2*$^{-}$ *fljB*^{e,n,x,off}	*
	MC1051	*flhD92*::Tn*10 fliA*5238* (V196G) *flgM5222*::Mud-Cm *fla-2157* (Δ*flgG-L*) *fliC5050*::MudA *vh2*$^{-}$ *fljB*^{e,n,x,off}	*
	MC1052	*flhD92*::Tn*10 fliA*5239* (T198K) *flgM5222*::Mud-Cm *fla-2157* (Δ*flgG-L*) *fliC5050*::MudA *vh2*$^{-}$ *fljB*^{e,n,x,off}	*
	MC1054	*flhD92*::Tn*10 fliA*5241* (L199R) *flgM5222*::Mud-Cm *fla-2157* (Δ*flgG-L*) *fliC5050*::MudA *vh2*$^{-}$ *fljB*^{e,n,x,off}	*
	MC1055	*flhD92*::Tn*10 fliA*5242* (Q202L) *flgM5222*::Mud-Cm *fla-2157* (Δ*flgG-L*) *fliC5050*::MudA *vh2*$^{-}$ *fljB*^{e,n,x,off}	*
	MC1056	*flhD92*::Tn*10 fliA*5243* (Q202R) *flgM5222*::Mud-Cm *fla-2157* (Δ*flgG-L*) *fliC5050*::MudA *vh2*$^{-}$ *fljB*^{e,n,x,off}	*
	MC1057	*flhD92*::Tn*10 fliA*5244* (E203D) *flgM5222*::Mud-Cm *fla-2157* (Δ*flgG-L*) *fliC5050*::MudA *vh2*$^{-}$ *fljB*^{e,n,x,off}	*
	MC1058	*flhD92*::Tn*10 fliA*5245* (N206K) *flgM5222*::Mud-Cm *fla-2157* (Δ*flgG-L*) *fliC5050*::MudA *vh2*$^{-}$ *fljB*^{e,n,x,off}	*
	MC1059	*flhD92*::Tn*10 fliA*5246* (E209D) *flgM5222*::Mud-Cm *fla-2157* (Δ*flgG-L*) *fliC5050*::MudA *vh2*$^{-}$ *fljB*^{e,n,x,off}	*
	MC1060	*flhD92*::Tn*10 fliA*5247* (V213E) *flgM5222*::Mud-Cm *fla-2157* (Δ*flgG-L*) *fliC5050*::MudA *vh2*$^{-}$ *fljB*^{e,n,x,off}	*
	MC1061	*flhD92*::Tn*10 fliA*5248* (V213G) *flgM5222*::Mud-Cm *fla-2157* (Δ*flgG-L*) *fliC5050*::MudA *vh2*$^{-}$ *fljB*^{e,n,x,off}	*
	MC1062	*flhD92*::Tn*10 fliA*5249* (S226N) *flgM5222*::Mud-Cm *fla-2157* (Δ*flgG-L*) *fliC5050*::MudA *vh2*$^{-}$ *fljB*^{e,n,x,off}	*

Table 2.1 continued

TH strain	Original strain	Genotype	Source[a]
	MC1064	*flhD92*::Tn*10 fliA*5250* (S226R) *flgM5222*::Mud-Cm *fla-2157* (Δ*flgG-L*) *fliC5050*::MudA *vh2*$^-$ *fljB*^{e,n,x,off}	*
	MC1065	*flhD92*::Tn*10 fliA*5251* (R231Q) *flgM5222*::Mud-Cm *fla-2157* (Δ*flgG-L*) *fliC5050*::MudA *vh2*$^-$ *fljB*^{e,n,x,off}	*
	MC1066	*flhD92*::Tn*10 flgM5222*::Mud-Cm *fla-2157* (Δ*flgG-L*) *fliC5050*::MudA *vh2*$^-$ *fljB*^{e,n,x,off}	*
TH1367		*thiA541*::Tn*10* (linked to *rpoBC*)	J. Roth
TH3034	TN2757	*leuBCD485 pepT*::MudJ *zhb1624*::Tn*10d*Tc (50% linked to *rpoA*)	C. Miller
TH2782		*flgM*5223* (I58L) *flgM5208*::MudK	
TH3470		*flgM*5434* (58N59) *flgM5208*::MudK	
TH2781		*flgM*5224* (L66S) *flgM5208*::MudK	K. Visick
TH3476		*flgM*5439* (K76I, M77K) *flgM5208*::MudK	
TH3475		*flgM*5438* (ΔM77) DUP1114[(*flgM5208*)*MudK*(*purB1879*)	
TH3472		*flgM*5436* (I82T) *fla-2018* (Δ*flhA-cheA*) *fliC5050*::MudJ *vh2*$^-$ *fljB*^{e,n,x,off}	
TH3489		*flgM*5440* (S85stop;UCG to UAG) *fla-2018* (Δ*flhA-cheA*) *fliC5050*::MudJ *vh2*$^-$ *fljB*^{e,n,x,off}	*
TH3613	MC65	pMC64 (*flgM*$^+$)/ LT2	*
pTH818		pJK238 (*flgM* codons 42-97)/ LT2	J. Karlinsey
	MC971	pMC138 (*flgM* codons 42-87)/ LT2	*
	MC973	pMC135 (*flgM* codons 42-77)/ LT2	*
	MC974	pMC136 (*flgM* codons 42-81)/ LT2	*
	MC975	pMC137 (*flgM* codons 42-63)/ LT2	*
TH2780		*flgM5208*::MudK (Mot$^-$ Lac+)	K. Hughes
TH3225		*flgM5222*::MudJ *attA*::[P22 *sieA44* Kn-9 P_{fliC}(-438-->+6)-CAT *9*$^+$]	K. Hughes
TH3747	MC1008	DEL1140[(*flgA5211*)*MudJ*(*flgN5220*)]	*

Table 2.1 continued

TH strain	Original strain	Genotype	Source[a]
	MC1252	pMC64 (*flgM*$^+$)/ DEL1140 [(*flgA5211*)*MudJ*(*flgN5220*)]	*
	MC1253	pJK238 (*flgM* codons 42-97)/ DEL1140 [(*flgA5211*)*MudJ*(*flgN5220*)]	*
	MC1254	pMC138 (*flgM* codons 42-87)/ DEL1140 [(*flgA5211*)*MudJ*(*flgN5220*)]	*
	MC1255	pTrc99A/ DEL1140 [(*flgA5211*)*MudJ*(*flgN5220*)]	*
TH2822		DUP1114[(*flgM5208*)*MudB*(*pur1879*)]	K. Hughes
TH2825		DUP1116[(*flgM*5224* (L66S) *flgM5208*)*MudB*(*pur1879*)]	K. Hughes
TH3656	MST4109	*leuBCD485 trp*::[*spc*^{r} P_{lac}T7 RNAP *lacI*]	S. Maloy

[a]Strains constructed in the course of this work

Table 2.2. List of plasmids used or constructed in the course of this work

Plasmid	Relevant genotype	Source[a]
pMH71	*flgAMN*$^+$ (*S. typhimurium*); amp^r; *ori*(pBR322)	M. Carsiotis
pMS531	PCR amplified *fliA*$^+$ gene (*S. typhimurium*) (minimal promoter + coding sequence; -119 to +766 bp relative to first base of GTG start codon); in *Sma*I site of pBSII; amp^r	M. Starnbach
p*flhDC* (GC29)	*flhDC*$^+$ (*S. typhimurium*); amp^r	G. Chilcott
pMC16	P22'*sieA*::[Kn-9; (pBSIISK+ polylinker sequence *KpnI-EcoRI*)]::P22*arc*'; amp^r; kan^r; tet^s; *ori*(pBR322)	*
	pMS361 (M. Susskind) derivative constructed in several steps. *KpnI-BamHI*(blunt) fragment [containing PBSIISK+ polylinker sequence (*KpnI* to *EcoRI*) fused to 500 bp *EcoRI* to *BamHI* fragment from pPY190 (P. Youderian) containing first 160 bp of P22 *arc* gene] cloned into pMS361 derivative pMC7 [*PstI-KpnI-PstI* linker cloned into *PstI* site adjacent to P_{ant} sequence] digested with *KpnI* and *BamHI*. *EcoRI* site flanking P22 *sieA* sequence destroyed; 187 bp of *Tc* gene sequence between BamHI and SphI sites deleted.	
pMC17	P22'*sieA*::[Kn-9; $P_{fliC(-36\ to\ +6)}$]::P22*arc*'; amp^r; kan^r; tet^s; *ori*(pBR322)	*
	KpnI-EcoRI fragment from pJK127 (J. Karlinsey) containing -36 to +6 bp of P_{fliC} promoter inserted into pMC16 digested with *KpnI* and *EcoRI*.	
pMC56	PCR amplified *flgM*$^+$ gene (*S. typhimurium*) (from start codon (+53) to +371) with *BspHI* site introduced at start codon, cloned into *SmaI* site of pBSIIKS+; amp^r	*
pMC61	P_{trc}*fliA*$^+$ *lacI*^{Q}; amp^r; *ori*(pBR322)	*
	780 bp *EcoRI* fragment (blunted with Klenow) from pMS531 containing the entire *fliA* gene, cloned into pTrc99A (4.2 kb; Pharmacia) digested with *NcoI* and *XbaI* and blunted with Klenow	
pMC64	P_{trc}*flgM*$^+$ amp^r *lacI*^{Q}; amp^r; *ori*(pBR322)	*
	340 bp *BspHI-PstI* fragment from pMC56 containing the entire *flgM* gene, cloned into pTrc99A digested with *NcoI* and *HindIII*	

Table 2.2 continued

Plasmid	Relevant genotype	Source
pMC66	P22*'sieA*::[Kn-9; *fliA*$^+$ $P_{fliC(-36\ to\ +6)}$]::P22*arc'*; amp^r; kan^r; tet^s; *ori*(pBR322)	*
	1 kb *BssHII* fragment from pMS531 containing the *fliA* gene, cloned into pMC17 digested with *StuI*	
pMC74	P22*'sieA*::[Kn-9 *fliA*5244*(E203D)	*
	$P_{fliC(-36\ to\ +6)}$]::P22*arc'*; amp^r; kan^r; tet^s; *ori*(pBR322)	
	1 kb *BssHII* fragment from pMC68 (identical to pMS531, except that it contains the *fliA*5244*(E203D) allele), cloned into pMC17 digested with *StuI*	
pMC96	P_{trc}*fliA*$^+$ P_{trc}*flgM*$^+$ *lacI*^{Q}; amp^r; *ori*(pBR322)	*
	1.4 kb *SspI* fragement from pMC61 containing the P_{trc}*fliA*$^+$ cassette, cloned into pMC64 digested with *NsiI*	
pJK238	P_{trc}*'flgM* (codons 42-97); amp^r; *ori*(pBR322)	J. Karlinsey
	212 bp PCR amplified *'flgM* gene fragment (codons 42 -97), digested with *NcoI* and cloned into pTrc99A digested with *NcoI* and *SmaI*	
pMC135	P_{trc}*'flgM* (codons 42-77); amp^r; *ori*(pBR322)	*
	NcoI-HphI(blunted with Mung Bean exonuclease) fragment from pJK238 cloned into pTrc99A digested with *NcoI* and *SmaI*	
pMC136	P_{trc}*'flgM* (codons 42-81); amp^r; *ori*(pBR322)	*
	NcoI-PleI(blunted with Klenow) fragment from pJK238 cloned into pTrc99A digested with *NcoI* and *SmaI*	
pMC137	P_{trc}*'flgM* (codons 42-63); amp^r; *ori*(pBR322)	*
	NcoI-TaqI(blunted with Klenow) fragment from pJK238 cloned into pTrc99A digested with *NcoI* and *SmaI*	
pMC138	P_{trc}*'flgM* (codons 42-87); amp^r; *ori*(pBR322)	*
	pJK238 digested with *NruI* and *PstI*, treated with Klenow, and religated.	
pKH445	P_{T7}His$_6$-*fliA*$^+$ *lacI*^{Q}; amp^r	J. Karlinsey
pKH486	P_{tac}*gst-fliA*$^+$; amp^r	J. Karlinsey

Table 2.2 continued

Plasmid	Relevant genotype	Source
pGEX-3X	P_{tac}*gst*; amp^r	Pharmacia
pJK302	P_{T7}His$_6$-*flgM*$^+$ *lacI*^{Q}; kan^r	J. Karlinsey
pJK306	P_{T7}His$_6$-*flgM*5436*(I82T) *lacI*^{Q}; kan^r	J. Karlinsey
pJK314	P_{T7}His$_6$-*flgM*5224*(L66S) *lacI*^{Q}; kan^r	J. Karlinsey
pJK127	*fliC* promoter (-36 to +6 bp) in pBSII SK$^-$; amp^r	J. Karlinsey
pKK233-2	P_{trc} expression vector; amp^r; *ori*(pBR322)	Pharmacia
pJK128	*fliC* promoter (-36 to +6 bp) in pKK233-2 (replacing P_{trc}) amp^r; *ori*(pBR322)	J. Karlinsey
pQETσ^{70}	P_{T5}His$_6$-*rpoD*$^+$ (*S. typhimurium*)	A. Dombroski
pT7his$_6$flα	P_{T7}His$_6$-*rpoA*$^+$ (*S. typhimurium*)	R. Gourse
paii17	$(rrnBT_1T_2)_{4x}$ $P_{T7\ RNAP}$; *lacI*^{Q}; amp^r; *ori*(pBR322)	B. Jack; New England Biolabs
pMC180	$(rrnBT_1T_2)_{4x}$ $P_{T7\ RNAP}$-His$_6$; *lacI*^{Q}; amp^r; *ori*(pBR322) 119 bp *XbaI-BamHI* fragment from pET15b (Novagen) containing the His$_6$ sequence, cloned into paii17 digested with *XbaI* and *BamHI*	*
pMC195	$(rrnBT_1T_2)_{4x}$ $P_{T7\ RNAP}$-His$_6$; *PtrcflgM*$^+$; *lacI*^{Q}; amp^r; *ori*(pBR322) 0.9 kb *SspI* fragment from pMC64 containing the P_{trc}*flgM*$^+$ cassette, cloned into pMC180 digested with *NruI*	*
pMC204	$(rrnBT_1T_2)_{4x}$ $P_{T7\ RNAP}$-His$_6$-*fliA*$^+$; *PtrcflgM*$^+$; *lacI*^{Q}; amp^r; *ori*(pBR322) 0.8 kb PCR amplified *fliA*$^+$ gene (codons 2-231) preceded by 3 in-frame codons (ATG CTG GAG) and flanked by *NdeI* and *BamHI* sites, digested with *NdeI* and *BamHI*, and cloned into pMC180, digested with the same enzymes	*

Table 2.2 continued

Plasmid	Relevant genotype	Source
pMC208	$(rrnBT_1T_2)_{4x}$ $P_{T7\ RNAP}$ -His_6-*fliA*5225*(H14D); *PtrcflgM*$^+$; *lacI*^{Q}; amp^r; *ori*(pBR322)	* same construction as pMC204
pMC209	$(rrnBT_1T_2)_{4x}$ $P_{T7\ RNAP}$ -His_6-*fliA*5226*(H14N); *PtrcflgM*$^+$; *lacI*^{Q}; amp^r; *ori*(pBR322)	* same construction as pMC204
pMC210	$(rrnBT_1T_2)_{4x}$ $P_{T7\ RNAP}$ -His_6-*fliA*5228*(V33E); *PtrcflgM*$^+$; *lacI*^{Q}; amp^r; *ori*(pBR322)	* same construction as pMC204
pMC211	$(rrnBT_1T_2)_{4x}$ $P_{T7\ RNAP}$ -His_6-*fliA*5229*(M104T); *PtrcflgM*$^+$; *lacI*^{Q}; amp^r; *ori*(pBR322)	* same construction as pMC204
pMC212	$(rrnBT_1T_2)_{4x}$ $P_{T7\ RNAP}$ -His_6-*fliA*5230*(N114K); *PtrcflgM*$^+$; *lacI*^{Q}; amp^r; *ori*(pBR322)	* same construction as pMC204
pMC213	$(rrnBT_1T_2)_{4x}$ $P_{T7\ RNAP}$ -His_6-*fliA*5233*(T138I); *PtrcflgM*$^+$; *lacI*^{Q}; amp^r; *ori*(pBR322)	* same construction as pMC204
pMC215	$(rrnBT_1T_2)_{4x}$ $P_{T7\ RNAP}$ -His_6-*fliA*5240*(L199R); *PtrcflgM*$^+$; *lacI*^{Q}; amp^r; *ori*(pBR322)	* same construction as pMC204
pMC216	$(rrnBT_1T_2)_{4x}$ $P_{T7\ RNAP}$ -His_6-*fliA*5244*(E203D); *PtrcflgM*$^+$; *lacI*^{Q}; amp^r; *ori*(pBR322)	* same construction as pMC204
pMC218	$(rrnBT_1T_2)_{4x}$ $P_{T7\ RNAP}$ -His_6-*fliA*5247*(V213E); *PtrcflgM*$^+$; *lacI*^{Q}; amp^r; *ori*(pBR322)	* same construction as pMC204
pMC219	$(rrnBT_1T_2)_{4x}$ $P_{T7\ RNAP}$ -His_6-*fliA*5251*(R231Q); *PtrcflgM*$^+$; *lacI*^{Q}; amp^r; *ori*(pBR322)	* same construction as pMC204

[a]Plasmids constructed in the course of this work denoted by "*"

CHAPTER 3

Genetic Analysis of the σ^{28}/FlgM Interaction

INTRODUCTION

Salmonella typhimurium and *Escherichia coli* have served as model organisms for the study of flagellar biogenesis. These bacteria possess six to eight peritrichous flagella which are rotated to propel the cell through a liquid environment. The flagellar organelle is typically viewed as a three-part structure comprised of the membrane-associated basal body, a flexible linker called the hook, and the filament. Synthesis and assembly of the flagellum occurs in stages, beginning with the cytoplasmic face of the basal body and proceeding outward. The flagellum is hollow, and flagellar components are delivered as needed to the tip of the growing structure through the central channel.

The flagellar regulon of *S. typhimurium* includes over 50 genes organized in at least 15 operons (124), most of which map to three regions on the chromosome (Figure 3.1). The flagellar genes of *S. typhimurium* and their putative functions are listed in Table 3.1. These genes are organized into a transcriptional heirarchy of three classes: Class 1, Class 2 and Class 3 (Figure 3.2). Transcription of the Class 1 master operon, *flhDC*, is regulated by a variety of signals that relay information about the external environment, such as temperature and osmolarity (162, 163, 166), and by the nutritional status of the cell (93, 167, 191). FlhD and FlhC are positive regulatory proteins that act in concert with the primary sigma factor, σ^{70}, to transcribe the Class 2 genes(117). One of the Class 2 genes, *fliA*, encodes a flagellar-specific sigma factor, σ^{28} (141), which is required for transcription of the Class 3 genes (92, 104). The majority of the Class 2 genes encode the structural components of the hook and basal substructures (the HBB) and the proteins required for their assembly. The Class 3 genes encode all of the components of the filament substructure, and the motor force generator and chemotaxis proteins.

The transcriptional classes of the flagellar regulon in *S. typhimurium* and *E. coli* can be distinguished on the basis of their promoter structure. The promoter of the *flhDC* regulon is recognized by σ^{70}; regulatory elements responsive to the cyclic AMP/CAP complex and the osmoregulator OmpR also control transcription from this promoter, (163). The Class 2 and Class 3 genes are both preceded by a -10 consensus sequence, GCCGATAA, distinct from that of σ^{70}-dependent promoters. For most of the Class 2 operons (*fliA* being the exception in *S. typhimurium*), there is no -35 consensus sequence. Contact between the FlhD/FlhC complex, bound to a control element just upstream of the -35 position, and the α subunit of RNAP is believed to substitute for the contact normally made between the σ^{70} subunit and the -35 consensus at Class 2 promoters (115, 117). The promoters of the σ^{28}-dependent Class 3 genes and the *fliA* operon do share sequence homology 15 base pairs upstream of the -10 consensus; the σ^{28} promoter consensus sequence is TAAA-$N_{(15)}$-GCCGATAA.

Until recently, it was thought that transcription of the Class 2 operons was the exclusive domain of the FlhD/FlhC/Eσ^{70} complex, and that Eσ^{28} was only responsible for transcribing the Class 3 genes. The discovery that the *fliA* operon could be transcribed in the absence of FlhD and FlhC *in vivo* (102), and that at least two Class 2 operons could be transcribed *in vitro* by purified Eσ^{28} (116), suggests that the transcriptional regulatory network of the flagellar operon is more complex. The current model is that while initiation of flagellar transcription is absolutely dependent upon the *flhDC* operon, once a sufficient amount of σ^{28} has been synthesized, Eσ^{28} is able to upregulate Class 2 transcription as well as initiate Class 3 transcription. There is also evidence the σ^{28} and FlgM autogenously regulate the *flhDC* operon, perhaps as means of downregulating flagellar gene expression once the flagella are synthesized (100).

The heirarchical expression of the flagellar genes is coupled to the ordered biogenesis of the flagellar organelle (Figure 3.2). Synthesis and assembly of the

filament, motor force generators and chemotaxis proteins does not begin until assembly of the basal body/hook substructure is essentially complete. Although σ^{28} is expressed simultaneously with the HBB subunits, its activity is kept in check until HBB assembly is finished; mutation of any of the genes required for a functional HBB results in constitutive inhibition of σ^{28} activity. The gene responsible for this inhibition was disocovered when a transposon insertion mutant was isolated that restored Class 3 gene expression in mutants defective for Class 2 genes (known collectively as *fla* mutants) (51, 181). The transposon was mapped to a novel flagellar gene downstream of *flgA* at centisome 26 on the *Salmonella* chromosome (the term centisome has replaced minutes as the coordinate system for the *S. typhimurium* chromosomal map. One centisome is equivalent to 1% of the genome (155). Sequence analysis of the gene, called *flgM*, predicted a small (97 amino acid) basic protein; *in vitro* expression of *flgM* produced a protein with an apparent molecular weight of ~10 kDa (50). Transcriptional analysis of the *flgM* gene showed that while it was coexpressed with the Class 2 genes from the upstream *flgA* promoter, the majority of *flgM* transcription initiated at a Class 3 promoter directly upstream of the *flgM* gene (52, 74). The nature of the signal sent by a defective HBB which caused FlgM to inhibit σ^{28} activity was not immediately obvious, nor was it clear what effect that signal had on FlgM activity. Neither transcription nor translation of the *flgM* gene was increased in the presence of a *fla* mutation (52). Indeed, transcription of *flgM* was observed to decline in a *fla* mutant, a response that was consistent with its being transcribed from a Class 3 promoter, but which failed to suggest a mechanism for the activation of FlgM-mediated inhibition by a *fla* mutation. There was no evidence to suggest that FlgM was modified from an inactive to an active form in the presence of a *fla* mutation (Karlinsey and Hughes, unpublished observations).

FlgM did not appear to function as a classic negative transcriptional regulator; although purified FlgM could inhibit σ^{28}-dependent transcription *in vitro*, no promoter-specific DNA binding activity was demonstrated (Karlinsey and Hughes, unpublished data; 142). The observation that *in vitro* synthesized σ^{28} and FlgM could be cross-linked suggested that FlgM-mediated inhibition of σ^{28} activity could involve a direct interaction between the two proteins (142). The apparent redistribution of σ^{28} from a complex with core RNAP to a complex with FlgM when the purified proteins were combined and cross-linked led to the proposal that FlgM was acting as an "anti-sigma factor," binding free σ^{28} to sequester it from core RNAP (142). Unfortunately, the σ^{28} polyclonal antisera used to detect of σ^{28} in these assays also cross-reacted with FlgM, so the data were not definitive. This model was consistent with the observation that it was the relative amounts of σ^{28} and FlgM, not their absolute levels inside the cell, that determined the effect on Class 3 transcription. Introducing a plasmid containing the *flgM* gene into a strain which had no flagellar defect caused Class 3 transcription to decrease (50), while the presence of a plasmid containing the *fliA* gene was able to overcome Class 3 inhibition in a *fla* mutant background (74). A plasmid expressing both σ^{28} and FlgM from heterologous promoters does not inhibit Class 3 transcription (Chadsey and Chilcott, unpublished observations).

It was not clear how FlgM was able to sense completion of the HBB substructure until it was proposed that FlgM, like the structural components of the flagellum, was able to be exported through the central channel of the nascent organelle (74, 101). According to this model, FlgM would not be recognized by the flagellar-specific export apparatus on the cytoplasmic face of the basal body until hook assembly was complete. Thus, the intracellular concentration of FlgM would be maintained at a level sufficient to inhibit σ^{28} during assembly of the HBB substructure. Hook completion would trigger a switch in the specificity of the export apparatus from Class 2

to Class 3 gene products, enabling FlgM to be secreted into the extracellular medium. The resulting decrease in intracellular FlgM would relieve the inhibition of σ^{28}, and allow Class 3 transcription to proceed. Measurements of the amount of FlgM in the extracellular media of various flagellar mutants supported this model. FlgM was not detected outside the cells of *S. typhimurium* strains defective for basal body or hook formation. Class 3 mutants defective for both of the flagellin genes or for *fliD* (which encodes the flagellar cap protein required for the polymerization of flagellin at the distal tip of the filament), showed elevated levels of extracellular FlgM. The higher than normal rate of FlgM export in these mutant strains could have been due to a lack of competition for the flagellar export machinery, or to an increase in the flux of exported protein through the truncated flagella, or both. A translational fusion of the LacZ protein near the C-terminus of FlgM (residue 86) caused a dominant motility defect and a decrease in the amount of amount of exported flagellin in an otherwise normal strain. The result was interpreted to mean that the FlgM-LacZ fusion was too bulky to be exported through flagellar channel, causing it to accumulate inside the cell and inhibit Class 3 transcription (it also indicated that the C-terminal 10 amino acids of FlgM were not required for its anti-sigma activity).

While it appeared that the basic mechanism for the ability of FlgM to act as a structural sensor had been established, the mechanism by which FlgM was acting to inhibit σ^{28} activity was still unclear. Although its classification as an anti-sigma factor was not disputed (indeed, the discovery of FlgM heralded the general acceptance of the anti-sigma model for transcriptional regulation), the details of the FlgM/σ^{28} interaction, and the way in which that interaction was able to affect σ^{28} activity, were not well established. The goal of my thesis research was to characterize this interaction genetically, use that information to generate models for the mechanism of FlgM-mediated inhibition of σ^{28}, and to attempt to test those models *in vitro* using purified

proteins. The experiments presented in this chapter constitute the genetic analysis. Possible models for the anti-sigma activity of FlgM are outlined in the Discussion section at the end of this chapter.

RESULTS

Selections for Class 3^{ON} mutants. The model for negative regulation of σ^{28} by FlgM predicted a direct interaction between the two proteins. Characterization of *fliA* mutants defective for this interaction was expected to define the region(s) of σ^{28} that bound FlgM (although we recognized that mutation of residues outside an interaction domain could have an allosteric effect on FlgM binding). It was hoped that the nature and location of structural changes in σ^{28} that interfered with FlgM binding would suggest possible models for the mechanism of anti-sigma factor activity. For example, clustering of mutations in the putative core binding domain of σ^{28} would imply that FlgM prevented σ^{28}-dependent transcription by competing with core RNAP for σ^{28} binding. We reasoned that *fliA* mutants defective for FlgM binding (henceforth referred to as *fliA** mutants) might be isolated by selecting or screening for mutants capable of transcribing Class 3 genes in the presence of inhibitory levels of FlgM (Class 3^{ON} mutants). Other classes of mutants, such as those linked to *flgM* or to novel genes whose products mediate the σ^{28}/FlgM interaction were also predicted.

The first efforts to isolate *fliA** mutants employed a Mu*dJ* fusion to the chromosomal copy of the Class 3 flagellin gene *fliC* as the reporter for σ^{28}-dependent transcription. Mu*dJ* is a kanamycin resistant transposon containing a promoterless copy of the *lacZ* operon; when Mu*dJ* inserts into an operon in the correct orientation, transcription of *lacZ* becomes subject to regulation by the promoter of that operon (17). The *fliC*::MudJ is positively regulated by σ^{28} such that in a wild type *S. typhimurium* background, cells are Lac^{+}. However, in a *fla* mutant background, FlgM-mediated

inhibition of σ^{28}-dependent transcription leads to a Lac$^-$ phenotype (Table 3.2). Mutants defective for negative regulation by FlgM could therefore be selected by demanding *lacZ* expression in a *fla* mutant background This was done by selecting for growth on media containing lactose as the sole carbon source. Mutations responsible for the Lac$^+$ phenotype were then tested by cotransdution for linkage to the *fliC*::Mu*dJ* allele. An intermediate linkage suggested that the mutation was near, but not in the *fliC* locus (and therefore a potential *fliA** mutant); this class was saved for further analysis. 100% linkage of the Lac$^+$ phenotype to the *fliC*::Mu*dJ* was presumed to result from expression of LacZ from a cryptic σ^{70}-dependent promoter upstream of the *lacZ* operon; these mutants were discarded. The results of this selection are summarized in Table 3.3. The high frequency of unlinked mutations isolated in this selection for spontaneous mutants prompted us to employ localized mutagenesis of the *fliA* region of the chromosome in an effort to increase the relative frequency of *fliA** mutants. In these experiments, the donor chromosome, containing the *fliC*::Mu*dJ* mutation, was subjected to mutagenesis by hydroxylamine (HA) or diethylsulfate (DES) before being used to transduce a *fla* recipient to kanamycin resistance. Transductants were screened for a Lac$^+$ phenotype. The results of these experiments are summarized in Table 3.4. While localized mutagenesis did increase the relative frequency of *fliC*-linked linked mutations, the majority of these were 100% linked to the *fliC*::Mu*dJ*. The bias towards mutations in this locus could have been due to the larger size of the *fliC-lacZ* transcriptional fusion relative to that of the *fliA* gene, or to the possibility that the sequence upstream of *lacZ* might be more easily mutated to generate a cryptic σ^{70}-dependent promoter than *fliA* could be mutated to gain *fliA** activity.

Although these strategies for isolation of potential *fliA** mutants had produced two potential *fliA** mutants, MC3 and MC4, the high background of unlinked mutations and mutations 100% linked to the *fliC*::Mu*dJ* locus emphasized the need for a more

efficient selection process. A modified challenge phage-based system was identified as a potential solution to this problem. The principle advantage of this system was that the majority of mutants recovered in a challenge phage-based selection were expected to be in a phage-borne copy of the *fliA* gene, and that non-*fliA* mutants could be easily distinguished by a single genetic test.

The challenge phage system, originally developed as a genetic tool for the analysis of protein-DNA interactions (5), utilizes the control mechanism between lysis and lysogeny in phage P22. In the challenge phage, this decision is determined by the expression of antirepressor (Ant), a phage-encoded protein that antagonizes expression of the P22 lysogenic repressor c2. The c2 repressor functions to induce the formation of a lysogen; expression of Ant overrides this pathway, and causes the phage to grow lytically. In the challenge phage, the *ant* gene is placed under the control of the transcriptional regulatory system under study, such that it functions as a reporter gene. Overexpression of *ant* promotes lytic phage growth, and results in the formation of clear plaques on a lawn of susceptible host cells; repression of *ant* allows the phage to lysogenize the host cell (challenge phage unable to express Ant are still able to form plaques on a lawn of susceptible host cells, though the plaques in this case are turbid. This is because in the absence of Ant, the decision between lysis and lysogeny is determined by the second immunity region of P22, *immC*, which is regulated by c2 in an analogous manner to the regulation of phage λ by the c1 repressor (150). Mutant phage that overexpress Ant can be selected (rather than screened for among a background of turbid plaques) on host strains that express Ant from a chromosomal copy of the P22 *c2* gene. The presence of high levels of c2 during infection blocks the lytic pathway; the only phage capable of forming plaques on such a host are those that can counter by expressing a high level of Ant.

To permit the challenge phage to be used as a tool for the selection of *fliA** mutations, a copy of the *fliA* gene was introduced into the phage genome, and the *ant* gene was placed under the control of the *fliC* promoter, such that expression of Ant could be positively regulated by the phage-borne *fliA* gene. Thus, in the presence of FlgM, σ^{28}-dependent *ant* transcription would be shut off; if the non-permissive strain was also *c2*$^+$, the phage would be forced to lysogenize the host cell. Only phage able to express Ant from the *fliC* promoter in the presence of FlgM would be expected to grow lytically on a *c2*$^+$host (Figure 3.3). Any plaques arising on a lawn of such cells would therefore be the result of (1) mutation of the phage-borne copy of the *fliA* gene to *fliA** (while a modified challenge phage could also grow lytically in a *flgM* or *fliA** mutant host cell, these mutations would not be present in the adjacent cells in the lawn, and the plaque would not spread), or (2) expression of the *ant* gene from a novel σ^{70}-dependent promoter. Phage purified from these plaques would be tested for FlhD/FlhC-dependent plaque formation to screen against those mutants whose plaque phenotype was unlinked to *fliA*.

Several modified challenge phage were constructed to test the feasibility of this method. Different length *fliC* and *fliA* promoters were tested in an effort to optimize σ^{28}-dependent expression of Ant (a correlation between promoter size and promoter strength had been demonstrated for these promoters; data not shown). Ideally, the amount of σ^{28} expressed from the phage-borne *fliA* gene would be sufficient to induce the formation of plaques on a *c2*$^+$ host in the absence of negative regulation by FlgM, but not so high that FlgM could not be induced to inhibit plaque formation by a *fliA*$^+$ phage. A phage that met these criteria could be used to select for *fliA** phage mutants that were insensitive to FlgM. Unfortunately, expression of σ^{28} from the phage-borne *fliA* gene appeared to be inefficient; even when the strongest promoters were used to drive σ^{28} and Ant expression, FlgM-mediated inhibition could not be overcome on a *c2*$^+$

host. This fact made it necessary to identify a host background that would permit *fliA** mutant phage to be screened for (rather than selected) on the basis of their plaque phenotype.

Pilot experiments to identify a suitable *S. typhimurium* strain for the isolation of *fliA** mutant phage were carried out. The three phage used in these experiments are depicted in Figure 3.4. Φ17 (3.4A) carried only the minimal *fliC* promoter upstream of *ant* (-36 to +6 bp relative to the start of transcription ; Heather Bonifield, personal communication); it did not carry a copy of the *fliA* gene. The plaque phenotype of this phage was expected to be dependent on the σ^{28} activity of the host strain. Φ66 (3.4B) was identical to Φ17 except that it also carried a copy of the *fliA* gene, under the control of its own promoter (the 118 bp preceding the initiator GTG codon). Φ74 (3.4C) was identical to Φ66, except that it carried the mutant *fliA*5244* allele (during the construction of these phage, a *fliA** gene was cloned from a mutant isolated by Keith Compton (strain MC6; see Table 3.7A). As the prototype *fliA** mutant phage, comparison of Φ74 with Φ66 on various host strains was expected to identify host genetic backgrounds on which the plaque phenotype of *fliA** mutant phage could be distinguished from that of $fliA^+$ phage.

The plaque phenotypes of Φ17, Φ66 and Φ74 on various $c2^-$ host strains are presented in Table 3.5. Plaque phenotypes confirmed that Ant expression in these phage was σ^{28}-dependent, and that increasing the level of σ^{28} expression or activity enhanced Ant-dependent lytic growth (as evidence by the clear plaque phenotype of Φ66 and Φ74, and of Φ17 on the strains overexpressing σ^{28}, or FlhD and FlhC, from a plasmid). Restoration of the turbid plaque phenotype on a *fla* mutant host indicated that FlgM was able to regulate the transcription of *ant* from the *fliC* promoter just as it regulated the Lac phenotype of *S. typhimurium* strains containing a *fliC*::Mu*dJ*. Φ74 was expected to be less sensitive to FlgM-mediated inhibition of Ant expression than

Φ66, due to the presence of the *fliA** allele. The identical turbid phenotypes of these two phage on the *fla* mutant host did not support this prediction. Apparently, the *fliA** allele carried by Φ74 was not strong enough, or was not being expressed at high enough levels, to overcome FlgM-mediated inhibition in this context. Introducing a stronger *fliA* promoter upstream of the *fliA* genes of these phage did not alter the phenotypes of these phage on the *fla* background (data not shown). Thus, no suitable $c2^-$ host background was identified for the isolation of *fliA** mutant phage.

Φ17, Φ66 and Φ74 were also tested on a number of $c2^+$ mutant hosts, to determine whether Φ74 might form plaques distinct from those of Φ66 in these backgrounds. The results of these plaque assays are presented in Table 3.6. In the presence of c2 repressor, none of the phage could form plaques unless the *flgM* gene was disrupted (strain MC115), FlhD and FlhC were overexpressed from a plasmid (MC121), or rate of FlgM export was increase by a *fliD* mutation (MC143). The only $flgM^+$ strain on which Φ74 was able to form plaques distinct from those of Φ17 and Φ66 was the $c2^+$ *fliD* mutant. This result suggested that it might be possible to screen for *fliA** phage on the basis of their larger plaque size.

An attempt was made to isolate *fliA** mutants of Φ66 on MC143. To increase the frequency of potential *fliA** mutants, phage stocks was subjected to hydroxylamine mutagenesis prior to plating on the *fliD* host. Mutagenesis of Φ17 was also carried out to determine whether the larger plaque phenotype could arise in the absence of the *fliA* gene. Treatment with the mutagen led to a 4 to 5 log drop in phage titers; the appearance of virulent mutants ($c2^-$ mutants able to form clear plaques on a susceptible host) at a frequency of 3 to 5% indicated that the mutagenesis treatment was successful. When plated on MC143, both of the mutagenized phage stocks produced larger plaque mutants at a frequency of approximately 1 to 2%. Although the Φ66 plates had slightly more large plaque mutants than the Φ17 plates, the lack of a convenient genetic test to

distinguish potential *fliA** phage from the background of larger plaque mutants discouraged us from pursuing them. This screen offered no advantage over the mutant isolation schemes based on Lac phenotypes, and was therefore set aside.

Sequence analysis of potential fliA mutants.* In addition to the two mutants isolated in the Lac$^+$ selections (see Tables 3.2 and 3.3), members of the Hughes lab had isolated large sets of potential *fliA** mutants that could be screened by sequence analysis for mutations in the *fliA* locus. Seven mutants between 18 and 56% linked to the *fliC*::Mu*dJ* allele had been isolated by Keith Compton by selecting for Lac$^+$ revertants in a number of different *fla fliC*::Mu*dJ* mutant backgrounds (see Appendix, Table A.1). Karen Visick and Kit Brown had both isolated Lac$^+$ motile (Mot$^+$) revertants of nonmotile mutant strains expressing a FlgM-LacZ fusion protein. 19 mutants (17 KG and 2 KB strains) whose Mot$^+$ phenotype was between 12 and 94% linked to the *fliY5221*::Tn*10d*Tc allele (*fliA* is ~90% linked to this allele) were included in the sequence analysis. Finally, a set of 36 Lac$^+$ revertants of a *fla fliC*::Mu*dA* strain 100% linked to the *fliA* locus was generated by Kelly Hughes. The entire collection of 64 potential *fliA** mutants is presented in Table 3.7A.

fliA loci were sequenced by PCR amplification of the genes from the chromosome of the potential *fliA** mutants and sequencing the PCR products directly. The results of the sequence analysis of the potential *fliA** mutants is presented in Table 3.7A. (Note: the 65th and 66th *fliA** alleles presented in Table 3.8A, from MC1080 and MC1175 were isolated and sequenced at a later time. They do not appear in the subsequent *in vivo* analyses of the *fliA** mutants presented in this chapter). In every *fliA* gene in which a mutation was found, those single mutations were the only changes in the gene. In total, 29 different point mutations resulting in single amino acid substitutions, and 3 different point mutations in the region between the promoter and the

initiator codon of the *fliA* gene were identified (summarized in Table 3.7B). The lack of secondary mutations, and the repeated isolation of a number of the point mutations argues that these changes to the *fliA* gene were responsible for the *fliA** phenotype of the mutants. Based on their position in the *fliA* gene, the mutations could be grouped into three classes: those at the amino terminal end of the σ^{28} protein (region 2.1), those in the middle of the protein (region 3.1) and those near the carboxy-terminal end (region 4.1/4.2).

In vivo characterization of fliA mutants.* A single mutant representing each substitution mutation was selected for further characterization *in vivo*. To evaluate the ability of the *fliA** mutants to express Class 3 genes in the presence of inhibitory levels of FlgM, the *fliA** alleles were transduced into a *fla fliC*::Mu*dA* background, and the level of β-galactosidase activity in these strains was assayed. The results of these assays are reported in Table 3.8, columns 2 and 3, and displayed graphically in Figure 3.5 (where the height of the bar above each mutation reflects the β-galactosidase activity of each *fliA** mutant normalized to that of the *fliA*$^+$ strain, i.e. the data presented in Table 3.8, column 3). No obvious correlation existed between the location of a mutation and its strength. In each of the three conserved sigma domains 2.1, 3.1 and 4.1/4.2, there were substitutions that appeared to confer a high degree of insensitivity to FlgM (such as H14N, M104T, and L199R), and mutations that were only slightly more active than wild type σ^{28} in the presence of FlgM (such as V33E, L124F, and V196G).

Was the enhanced activity of the *fliA** mutants in the presence of FlgM due to a defect in FlgM binding or sensitivity to negative regulation by FlgM, or could the phenotype of the mutants be attributed to an increase in the steady state level of σ^{28}, or to a higher basal sigma factor activity? Mutants of the first type would be expected to behave similarly to wild type σ^{28} in the absence of FlgM (unless the substitution

mutation also affected basal sigma activity). Mutants of the second type would be expected to have higher than normal activity in the absence of FlgM. To evaluate σ^{28}-dependent gene expression in the absence of FlgM, a transposon insertion mutation was introduced into the *flgM* gene in each of the *fliA* fla* fliC::Mu*dA* strains, and the β-galactosidase assays repeated. These data are presented in Table 3.8, columns 4 and 5. None of the mutants appeared to be significantly more active than the *fliA*$^+$ strain in this experiment (one mutant, V196G, showed a decreased level of activity). However, the positive control for increased sigma factor activity (MC417, which contains additional copies of the *fliA* gene on a plasmid) also did not express higher levels of β-galactosidase than the *fliA*$^+$ parent strain. This result suggested that in the absence of FlgM, the level of σ^{28} in the *fliA*$^+$ strain was already in such excess that any further increase in the level or activity of σ^{28} would have no positive effect on transcription from the *fliC* promoter. To accurately measure the basal sigma factor activities of the *fliA** mutants, therefore, it would be necessary to identify a strain background in which σ^{28} was limiting.

It had been demonstrated that in the absence of the Class 1 master regulatory proteins FlhD and FlhC, *fliA* was still transcribed at a low level (102). We tested the level of σ^{28}-dependent β-galactosidase expression in an *flhD*::Tn*10 flgM fliC*::Mu*dA* mutant to determine whether this strain background might provide the required "σ^{28}-limiting" conditions. Though the β-galactosidase activity of this strain was severely reduced from that in an *flhDC*$^+$ strain, it was still at least seven-fold above that of a control strain lacking the *lacZ* gene (data not shown). It seemed possible, therefore, that a *fliA** mutation that increased the activity or level of σ^{28} would enhance transcription of *lacZ* from the *fliC* promoter in this background. The *flhD*::Tn*10* allele was introduced into the *fliA* flgM fla fliC*::Mu*dA* strains, and the β-galactosidase assays were repeated. These results are presented in Table 3.9, and depicted graphically in Figure 3.6. The

majority of the *fliA** mutants appeared to have equal or less activity than the *fliA*$^+$ strain. This outcome is consistent with their being defective for negative regulation by FlgM, and does not suggest that the σ^{28}* proteins are more efficient or more abundant than wild type σ^{28}. Only the three substitution mutants at residue 14, in the putative core RNAP binding domain of σ^{28}, displayed higher than normal levels of activity. The possibility that these mutant σ^{28}* proteins functioned more efficiently or accumulated to a higher level in the cell would be tested in a later stage of the research.

Screening class 3^{ON} mutations for linkage to the rpo loci. Selections for *S. typhimurium* mutants able to express Class 3 genes in the presence of inhibitory levels of FlgM invariably turned up mutants unlinked to *fliA*, *flgM*, or the reporter gene. These unlinked mutants could have been defective for additional genes involved, either directly or indirectly, in the repression of σ^{28} activity. Alternatively, the unlinked mutants might represent other loci that, like *fliA*, are positive regulators of Class 3 gene expression which are negatively regulated by FlgM. One model for FlgM inhibition of σ^{28} activity proposes that FlgM negatively regulates both free σ^{28} and σ^{28} that has associated with core RNAP to form holoenzyme ($E\sigma^{28}$). If FlgM were interacting with $E\sigma^{28}$, then core RNAP, like σ^{28}, might be capable of mutating to prevent FlgM from recognizing $E\sigma^{28}$, or interfering with $E\sigma^{28}$ activity. The isolation of such mutants would make a strong case for an "anti-holoenzyme" activity of FlgM.

The existing collection of unlinked mutants isolated by previous selections for the Class 3^{ON} phenotype (see Appendix, Table A.3) were screened for linkage to the *rpoBC* operon at 90.2 centisomes (Cs) (encoding the β and β' core subunits) and the *rpoA* locus at 74.5 Cs (encoding the α subunit) (155). The strategy used was to replace the *rpoBC* and *rpoA* regions of the chromosome in each of the candidate mutant strains (by cotransduction of a linked selectable marker), and screen for the disappearance of

the Class 3^{ON} phenotype. None of the 24 mutants isolated by Karen Visick showed any linkage to the *rpoBC* locus (the 50 mutants from Keith Compton's collection were not checked for linkage to *rpoBC*). The complete collection of 74 unlinked mutants were tested for linkage to the *rpoA*-linked transposon *zhb-1624*::Tn*10d*Tc. Only one mutant strain, KG1613, appeared to revert to Mot- upon transduction with the *rpoA*-linked transposon at the expected 50% frequency. To confirm linkage of the *zhb-1624*::Tn*10d*Tc to the mutation in KG1613, a tetracyline resistant Mot^+ transductant from the cross was purified and used to transduce the Mot- *flgM*::Mu*d*K strain KG1150 (the parent strain of KG1613) to tetracyline resistance. Surprisingly, the Mot^+ phenotype was not cotransduced with the transposon in this experiment (48/48 transductants were nonmotile). The same transducing lysate was also unable to cotransduce a Lac^- *fla fliC*::Mu*d*A mutant to Lac^+. If KG1613 contained an *rpoA** mutation that conferred an ability to express Class 3 flagellar genes in the presence of inhibitory levels of FlgM, then penetrance of that phenotype appeared to be dependent on the genetic background of the mutant strain. It is possible that KG1613 was a double mutant, and that the presence of both mutations was required for the Class 3^{ON} phenotype.

Analysis of flgM mutants defective for inhibition of σ^{28}. An analysis of *flgM** mutants defective for inhibition of σ^{28} activity (*flgM**)was carried out to genetically define the anti-sigma factor domain of FlgM. The selection for motile Lac^+ revertants of mutants expressing the FlgM-LacZ fusion protein performed by Karen Visick had yielded 8 *flgM*-linked mutants; sequence analysis of these mutants identified 5 different mutations that could relieve the motility defect of the parent strain: I58L, 58(N)59, K76IM77K, and ΔM77 (181). Two additional *flgM** mutants, I82T and S85stop, were obtained by Kelly Hughes (28). These 7 spontaneous *flgM** mutants are depicted in Figure 3.7A.

An N-terminally truncated FlgM protein, including only residues 42 through 97, was able to repress Class 3 gene expression when overexpressed from a plasmid. This result demonstrated that the C-terminal half of FlgM alone was sufficient to inhibit σ^{28} *in vivo*. A series of C-terminal deletion mutants were constructed further define the region of FlgM essential for anti-sigma activity. These plasmids are described in Figure 3.7B. The anti-σ^{28} activity of the truncated FlgM proteins expressed from these plasmids (as judged by their effect on motility when induced in LT2), and their ability to be detected by Western analysis are also shown. The FlgM proteins expressed by pMC135, pMC136 and pMC137 could not be detected, so their lack of activity *in vivo* cannot be attributed to loss of critical σ^{28} binding determinants. The minimum anti-sigma domain of FlgM defined by this analysis spanned residues 42 through 86.

The fact that most of the *flgM** substitution mutants were isolated in the context of the FlgM-LacZ fusion protein made quantitative *in vivo* analysis of their anti-sigma activity problematic (because *fliC*::Mu*d* insertions could not be used as a reporter gene for Class 3 gene expression). Only the *flgM*-5436*(I82T) allele, which was isolated in the native *flgM* gene, could be assayed for its ability to inhibit σ^{28}-dependent expression in the *fla fliC*::Mu*d*A background. The β-galactosidase activity in the presence of the I82T mutation was ~6-fold higher than that in the corresponding *flgM*$^+$ strain (data not shown). An attempt was made to quantify the anti-sigma activities of the truncated FlgM proteins expressed from plasmids pJK238 and pMC138 by assaying the level of chloramphenicol acetyl transferase (CAT) activity expressed from the *fliC* promoter. The reporter system used for these assays was a *fla flgM* mutant lysogenized with a derivative of the challenge phage in which the *ant* gene downstream of the *fliC* promoter had been replaced by the CAT gene. Although the truncated FlgM proteins expressed by pJK238 and pMC138 had a measurable defect in their ability to repress CAT expression from the lysogen (Table 3.10) their specific activity could not be

estimated (Western analysis had revealed the steady state levels of the FlgM proteins to be far lower than that of native FlgM). Accurate measurements of FlgM* activity would require purification and *in vitro* analysis of the mutant alleles.

Discussion

A number of selection schemes were employed to isolate *fliA** mutants. Both the selection for Mot$^+$ Lac$^+$ revertants of strains expressing a FlgM-LacZ fusion, and selections for Lac$^+$ revertants in *fla fliC*::Mu*d* mutant backgrounds were able to provide us with this class of mutants. The high background of non-*fliA* mutants that was a problem in the early Lac-based selections could be eliminated by screening pools of potential *fliA** mutants for their ability to restore Class 3 gene expression to a *fliA*::Tn*10d*Tc mutant (see Chapter 2), making this selection method a very powerful tool. The modified challenge phage-based selection was not productive. We were able to generate recombinant challenge phage that expressed Ant in a σ^{28}-dependent manner, but this expression was never sufficient to permit the selection of potential *fliA** mutants in a *c2*$^+$ host strain, or to distinguish them from *fliA*$^+$ phage in *c2*$^-$ host strains.

Almost all of the mutants that were linked to the *fliA* locus had mutations in the *fliA* coding sequence, or in the region between the promoter and the initiator codon (these mutations may increase the stability or translation of the *fliA* message). In addition to recovering seven of the eight substitution mutants published previously (103), we isolated an additional 21 mutations in the coding sequence of *fliA*. In a few instances, no changes were found; either these mutants contained mutations farther upstream in the *fliA* promoter, or their mutations were actually in genes near *fliA*. Downstream of *fliA* in the same operon are two genes, *fliZ* and *fliY*, that may negatively regulate *fliA* expression or activity (139). A number of sigma factor genes are directly followed by the gene for a negative regulator (reviewed in 75). Although the

fliY::Tn*10d*Tc used to map *fliA** alleles had no significant effect of σ^{28}-dependent expression, *fliZ* remains a candidate. The nearby *fliS* and *fliT* genes in the *fliD* operon may function as part of the flagellar-specific export pathway (189, 190). These genes have been implicated in flagellin export, but it is conceivable that they could also be mutated to recognize similar export signals in FlgM.

The distribution of *fliA** mutants identified three conserved sigma factor regions which could be mutated allow σ^{28} to escape inhibition by FlgM. Mutations conferring resistance to an anti-sigma factor have also been isolated in the sporulation specific sigma factor, σ^{F} of *Bacillus subtilis*, which is negatively regulated by the anti-sigma factor SpoIIAB (33). The distribution of mutations in σ^{F} is very similar to that obtained by us and elsewhere (103), with the majority mapping to the C-terminal region 4.1/4.2, and the rest mapping to regions 3.1 and 2.1. Although there is no homology between FlgM and SpoIIAB, this result argues that they are interacting with their respective sigma factors in an analogous fashion.

The strongest (i.e. most insensitive to FlgM) *fliA** mutations did not seem to be limited to just one sigma region. Substitutions in each region were able to effect a level of Class 3 transcription almost as high as that achieved by wild type σ^{28} in the absence of FlgM (Table 3.8). There was a strong correlation, however, between the activity in the absence of FlgM (the basal sigma factor activity), and the position mutated. Of all the σ^{28}* mutants assayed, only those with substitutions at residue 14 had higher-than-wild type activity (Table 3.9 and Figure 3.6). Two statements can be made about these data. First, it is unlikely that the Class 3^{ON} phenotype of the *fliA** mutants (with the exception of the residue 14 mutants) is due to an increase in either the level of σ^{28} protein or basal sigma activity (unless an increase in one is balanced by a concomitant decrease in the other). Most of the mutations probably affect the ability of FlgM to regulate σ^{28} in some way. Second, unless the mutations at residue 14 simply serve to

increase the steady state level of σ^{28}, they could be an extremely interesting class. Because residue 14 is contained within the putative core binding domain, it is tempting to speculate that the higher level of activity in these mutants is due to an enhanced affinity of the mutant σ^{28}* proteins for core RNAP. When aligned with the σ^{70} family sigma factors (118), residue 14 of σ^{28} lies very near to a seven residue motif, VEANLRL, that has been identified as being important for core binding (178). Although the homology between σ^{28} and σ^{70} in these positions is poor (Figure 3.8), it is possible that they share a tertiary structure.

Based on a genetic analysis of the ability of truncated σ^{28} proteins to interact with FlgM *in vivo*, the minimal FlgM binding domain was proposed to lie within residues 154 through 227 (comprising regions 3.1 through 4.2) (103). To reconcile this location with the apparent ability of FlgM to inhibit core RNAP binding by σ^{28} (142), the authors proposed that binding by FlgM at the C-terminal end of σ^{28} had an allosteric effect on the ability of σ^{28} to interact with core RNAP at its N-terminal domain. Although *fliA** mutants were also isolated in regions 2.1 and 3.1, outside of the proposed FlgM binding domain (103), no explanation was offered to explain their presence. Furthermore, the data suggested that σ^{28} residues N-terminal to 154 did contribute to FlgM binding (103). Similar to our genetic analysis of σ^{28}, an analysis of SpoIIAB binding by σ^{F} (33) also suggested that additional FlgM binding in regions 2.1 and 3.1 of σ^{28} might have been overlooked in the earlier study. *In vitro* assays of SpoIIAB binding by truncated σ^{F} proteins suggested that regions 2.1, 3.1 and 4.1/4.2 of σ^{F} each bound SpoIIAB independently. Perhaps similar interactions between regions 2.1 and 3.1 of σ^{28} and FlgM were not detected because of protein instability, because the large vector-derived peptides fused to the σ^{28} proteins interfered with FlgM binding *in vivo*, or because the affinity of regions 2.1 and 3.1 individually was below the limit of detection of the assay (103).

Our sequence analysis of *fliA** mutants suggested several mechanisms for FlgM-mediated inhibition of σ^{28}. The simplest hypothesis is that FlgM sterically prevents σ^{28} from associating with core RNAP by masking core binding determinants, most likely in region 2.1, but also possibly in region 3.1. In this case, the mutations in regions 2.1, 3.1 and 4.1/4.2 could each define FlgM binding domains. This hypothesis would be consistent with the analysis published previously (103) if it was assumed that the binding domain in region 4.1/4.2 had the highest affinity for FlgM, and was therefore the only significant interaction detected by his assay.

Another hypothesis predicts that regions 3.1 and 4.1/4.2 comprise the major FlgM binding domains; the mutations at residue 14 (and perhaps 13) in region 2.1 alter some other property of σ^{28} that enables it to function more efficiently in the presence of FlgM. One way this could be achieved is if the residue 14 mutations increased the affinity of σ^{28} for core RNAP. If FlgM inhibits σ^{28} activity by competing with core RNAP for free σ^{28}, then increasing the rate or stability of $E\sigma^{28}$ complex formation could tip the kinetics in favor of a productive interaction between σ^{28} and core RNAP. Alternatively, if FlgM were able to inhibit $E\sigma^{28}$ as well as free σ^{28}, then any mutation that increased the rate at which $E\sigma^{28}$ was able to initiate transcription would also shift the kinetics towards Class 3 gene expression (this hypothesis assumes that $E\sigma^{28}$ bound to DNA is resistant to FlgM). Perhaps the region 2.1 mutations enhanced the ability of σ^{28} to recognize the -10 consensus sequence common to Class 2 and Class 3 flagellar promoters via an allosteric effect on the nearby region 2.4 (the putative -10 promoter binding domain).

A third hypothesis is that FlgM binding occurs only in region 4.1/4.2, and that this binding causes an allosteric change in the N-terminal core binding domain(s) that prevents σ^{28} from associating with core RNAP. In this case, the region 3.1 *fliA** mutants might be defective for the propagation of the allosteric signal from the FlgM

binding domain to region 2.1. These mutants might bind FlgM normally, but be unaffected by its presence. Although it might be supposed that FlgM bound to $E\sigma^{28}$ would interfere with recognition of the -35 promoter sequence, there is precedence for RNAP holoenzyme being able to accommodate the other region 4.2-binding proteins (1, 14, 25, 69, 79). Conserved sigma region 4.1 is predicted to contain an amphipathic helix followed by a helix-turn-helix (HTH) DNA-binding motif in region 4.2 that is believed to mediate -35 promoter recognition (55, 62, 118). It is the second helix of the HTH that is thought to make specific contacts with DNA; the role of the first helix is to lie against the second and help position it in the major groove (7). Most of the region 4.1/4.2 residues affected by *fliA** mutations are located in the region preceding the second helix of the HTH, or at its very C-terminal end (Figure 3.9). Thus, FlgM binding may not obstruct the σ^{28} residues involved in making direct contacts with the DNA. It is also possible that FlgM *does* interact with residues in the second helix, but that mutations that disrupted those contacts were not isolated because they also destroyed promoter binding.

Selections for *fliA** mutants also yielded a class linked to the *flgM* gene. Sequence analysis of these *flgM** mutations identified residues in the C-terminal half of the protein that are likely to make specific contacts with σ^{28} (28, 181). An NMR analysis of free FlgM revealed that the entire protein lacks structure, but that upon σ^{28} binding, the C-terminal half becomes constrained (28). The region of FlgM that undergoes this conformational shift extends from residue 41 to the C-terminus; we propose that this entire region constitutes the σ^{28} binding domain. That portions of this domain can be deleted without abolishing anti-σ^{28} activity indicates that parts of this region are not essential. A deletion analysis of FlgM carried out by Kutsukake defined the minimal σ^{28} binding domain as lying between residues 64 and 88 (80). Our data argue that residues N-terminal of residue 55 are also essential.

Table 3.1 Genes involved in flagellation, motility and chemotaxis in *S. typhimurium*

Operon Class	Gene	Product function or structure
Region I (26.4 to 26.6 Cs)		
2,3	*flgN*	Initiation of flagellar filament assembly
2,3	*flgM*	Anti-sigma factor
2	*flgA*	P-ring assembly
2	*flgB*	Basal-body rod
2	*flgC*	Basal-body rod
2	*flgD*	Hook cap (scaffold)
2	*flgE*	Hook
2	*flgF*	Basal-body rod
2	*flgG*	Basal-body rod
2	*flgH*	Basal-body L ring
2	*flgI*	Basal-body P ring
2	*flgJ*	Unknown
2,3	*flgK*	Hook filament junction
2,3	*flgL*	Hook filament junction
Region II (41.7 to 42.1 Cs)		
2	*flhE*	Unknown
2	*flhA*	Export apparatus?
2	*flhB*	Assists *fliK* in hook length contol; export specificity?
3	*cheZ*	CheY phosphatase
3	*cheY*	Switch regulator (as CheY-P)
3	*cheB*	Chemoreceptor methylesterase
3	*cheR*	Chemoreceptor methyltransferase
3	*tar*	Aspartate chemoreceptor
3	*cheW*	Positive regulator of CheA
3	*cheA*	CheY and CheB kinase
3	*motA*	Motor force generators
3	*motB*	Motor force generators
1	*flhC*	Positive regulation of gene expression
1	*flhD*	Positive regulation of gene expression

Table 3.1 continued

Operon Class	Gene	Product function or structure
Region IIIa (42.4 to 42.6 Cs)		
2,3	*fliY*	Unknown; homology to extracellular solute-binding protein family[b]
2,3	*fliZ*	Unknown[b]
2,3	*fliA*	Flagellar specific sigma factor
?	*fliB*	N-methylation of flagellin
3	*fliC*	Flagellin (filament subunit)
2,3	*fliD*	Filament cap
2,3	*fliS*	Export of flagellin?[c]
2,3	*fliT*	Member of the axial family of structural proteins[c]
Region IIIb (42.7 to 42.9 Cs)		
2	*fliE*	Basal body
2	*fliF*	Basal body MS ring
2	*fliG*	Motor/switch
2	*fliH*	Export apparatus?
2	*fliI*	Export apparatus?
2	*fliJ*	Unknown
2	*fliK*	Hook length control
2	*fliL*	Unknown
2	*fliM*	Motor/switch
2	*fliN*	Motor/switch
2	*fliO*	Unknown
2	*fliQ*	Unknown
2	*fliR*	Unknown

Table 3.1 continued

Operon Class	Gene	Product function or structure
51.6 Cs		
?	*flk*	Sensor or P and L-ring assembly; regulator of FlgM levels?[d]
60.1 Cs		
3	*fljA*	Repressor of *fliC*
3	*fljB*	Flagellin
3	*hin*	Site-specific inversion of phase I flagellin DNA

[a]References for the information in this table can be found in (123) and (155), unless otherwise indicated.

[b](139)

[c](91, 189, 190)

[d](88; Karlinsey and Hughes (unpublished observations))

Table 3.2 Lac phenotypes of flagellar mutants in a *fliC*::Mu*d* mutant

Genotype	Lac Phenotype
fliC::Mu*d*	+
fliA fliC::Mu*d*	-
fla fliC::Mu*d*	-
flgM fla fliC::Mu*d*	+
fliA fla fliC*::Mu*d*	+

Table 3.3. Selection for spontaneous Lac$^+$ revertants of *fla fliC*::Mu*dJ* mutant[a]

Relative frequency of revertant class[b]	Revertant phenotype on minimal lactose	linkage to *fliC*::Mu*dJ*	strain
1/36	large colonies	30 to 40%	MC4
3/36	large and small	100%	not saved
32/36	large and small	unlinked (*flgM*?)	not saved

[a]TH2430

[b]16 independent experiments; 10^8 cells/plate; avg. 160 Lac$^+$ revertants/plate
At least 2 colonies/experiment (large & small) screened for linkage to *fliC*::Mu*dJ*

Table 3.4. Screen for mutagen-induced Lac$^+$ revertants of *fla*[a] *fliC*::Mu*dJ* mutant

Mutagen	Lac phenotype of transductants	Frequency[b]	linkage to *fliC*::Mu*dJ*	strain
none	Lac +/-	NA	NA	TH2430
DES	Lac++	5%	5/5 100%	not saved
	Lac+/-	95%	not mapped	
HA	Lac++	40%	1/16 19% 1/16 unlinked 14/16 100%	MC3 not saved not saved
	Lac+/-	60%	not mapped	

[a] *fla* = *fla-2157* Δ(*flgG-L*).

[b] DES experiment: 460 colonies screened; 22 more Lac$^+$ than parent
HA experiment: 650 colonies screened

Table 3.5. Plaque phenotypes of modified challenge phage on *c2*$^-$ hosts

Host strain	Host genotype	Φ17 plaque phenotype	Φ66 plaque phenotype	Φ74 plaque phenotype
LT2	wild type	turbid	small clear (0.5 mm)	small clear (2 mm)
pTH721	p*fliA*$^+$/LT2	clear	small clear	
GC81	p*flhDC*$^+$/LT2	clear	small clear	
TH2249	*flhC*	turbid		
TH2250	*flhD*	turbid		
TH2251	*fliA*	turbid		
TH1722	*fla*	turbid	turbid	turbid

Table 3.6. Plaque phenotypes of modified challenge phage on *c2*$^+$ hosts

Host strain	Host genotype	Φ17 plaque phenotype	Φ66 plaque phenotype	Φ74 plaque phenotype
MC119	*c2*$^+$	no plaques	no plaques	no plaques
MC115	*flgM c2*$^+$	small turbid (~0.75 mm)	pinpoint turbid (clearer than Φ17)	turbid (~1 mm)
MC121	p*flhDC*$^+$/c2$^+$	pinpoint turbid (1° streak only)	pinpoint turbid (1° streak only)	pinpoint turbid (1° streak only)
MC143	*fliD c2*$^+$	turbid (~0.5 mm)	turbid (~0.5 mm)	turbid (~2.0 mm)
MC123	*fliA flgM c2*$^+$	no plaques	no plaques	
MC148	*fla c2*$^+$	no plaques	no plaques	no plaques

Table 3.7A. Linkage and sequence data for potential *fliA** mutants

Original Isolate	MC strain	Genotype of parent strain	Original mutant phenotype	Linkage	Mutation[a]
g	3	Δ(*flgG-L*) *fliC*::Mu*dJ*	Lac+	20% (*fliC*)	*fliA* UTR[b] -15 GtoA
7.3	4	Δ(*flgG-L*) *fliC*::Mu*dJ*	Lac+	40%(*fliC*)	none found
1722-6	5	Δ(*flgG-L*) *fliC*::Mu*dJ*	Lac+[ts]	30% (*fliC*)	*fliA* UTR[b] -7 GtoA
1722-10	6	Δ(*flgG-L*) *fliC*::Mu*dJ*	Lac+	18% (*fliC*)	E203D
1723-14	7	Δ(*flhA-cheA*) *fliC*::Mu*dJ*	Lac+	50% (*fliC*)	H14Y
1726-1	8	Δ(*fliE-K*) *fliC*::Mu*dJ*	Lac+[ts]	56% (*fliC*)	none found
1726-7	9	Δ(*fliE-K*) *fliC*::Mu*dJ*	Lac+[ts]	37% (*fliC*)	H14Y
1726-10	10	Δ(*fliE-K*) *fliC*::Mu*dJ*	Lac+[ts]	35% (*fliC*)	H14D
2111-42	11	Δ(*flgHI*) *fliC*::Mu*dJ*	Lac+	50% (*fliC*)	none found
KG1714		*flgM*+ *flgM*::Mu*dK*	Mot+	94% (*fliY*)	V196G
KG1726		"	"	92% (*fliY*)	N206K
KG1727		"	"	93% (*fliY*)	Q202L
KG1729		"	"	86% (*fliY*)	H14N
KG1730		"	"	86% (*fliY*)	N206K
KG1731		"	"	12% (*fliY*)	none found
KG1732		"	"	85% (*fliY*)	Q202L
KG1733		"	"	84% (*fliY*)	T198K
KG1734		"	"	90% (*fliY*)	E209D
KG1735		"	"	91% (*fliY*)	E302D
KG1736		"	"	85% (*fliY*)	E203D
KG1740		"	"	?	P190Q
KG1741		*flgM*::Mu*dK*	"	93% (*fliY*)	Q202L
KG1742		"	"	91% (*fliY*)	E209D
KG1743		*flgM*+ *flgM*::Mu*dK*	Mot+	91% (*fliY*)	none found

Table 3.7A continued

Original Isolate	MC strain	Genotype of parent strain	Original mutant phenotype	Linkage	Mutation[a]
KG1744		"	"	92% (*fliY*)	Q202L
KG1745		"	"	88% (*fliY*)	N114K
KG1746		"	"	88% (*fliY*)	none found
KG1747		"	"	90% (*fliY*)	L199R
KG1752		"	"	86% (*fliY*)	T198K
KG1753		"	"	86% (*fliY*)	none found
KG1754		"	"	82% (*fliY*)	V213E
KB33		*flgM*::Mud*K*	"	? (*fliC*)	Q202L
KB46		*flgM*::Mud*K*	"	? (*fliC*)	Q202L
KTH1	298	Δ(*flgG-L*) *fliC*::Mud*A*	Lac+	100% (*fliA*)	M104T
KTH2	299	"	"	"	S226R
KTH3	300	"	"	"	N139I
KTH5	301	"	"	"	Q202L
KTH6	302	"	"	"	N114T
KTH8	303	"	"	"	V33G
KTH17	304	"	"	"	N114K
KTH18	305	"	"	"	L199Q
KTH20	306	"	"	"	N206K
KTH23	307	"	"	"	H14D
KTH30	308	"	"	"	E209D
KTH36	309	"	"	"	E209D
KTH39	310	"	"	"	N139K
KTH40	311	"	"	"	none found
KTH4.2	312	"	"	"	P190S
KTH7.1	313	"	"	"	Q202L
KTH9.1	314	"	"	"	*fliA* UTR -7 GtoA[b]
KTH10.1	315	"	"	"	Q202L
KTH11.2	316	"	"	"	none found
KTH12.2	317	"	"	"	none found

Table 3.7A continued

Original Isolate	MC strain	Genotype of parent strain	Original mutant phenotype	Linkage	Mutation[a]
KTH13.1	318	"	"	"	Q202R
KTH15.1	319	"	"	"	S226N
KTH16.1	320	"	"	"	V213G
KTH21.1	321	"	"	"	L124F
KTH22.1	322	"	"	"	R231Q
KTH24.1	323	"	"	"	*fliA* UTR[b] -14 CtoT
KTH25.1	324	"	"	"	T138I
KTH26.1	325	"	"	"	none found
KTH27.2	326	"	"	"	none found
KTH29.2	327	"	"	"	H14N
KTH31.1	328	"	"	"	T138I
KTH33.1	329	"	"	"	L124F
KTH34.2	331	"	"	"	P190S
KTH35.1	332	"	"	"	none found
KTH38.1	333	"	"	"	P190S
KTH28	334	"	"	"	N206K
KTH37	335	"	"	"	none found
C2	1080	Δ(*tar-flhD*) *fliC*::MudJ	"	"	K13E
C10	1175	"	"	"	A103V

[a] Region sequenced: from ~ 50 bp upstream of start codon through stop codon
[b] UTR is numbered relative to first base upstream of the start codon, designated -1

Table 3.7B. Summary of *fliA** mutant analysis

σ^{28} mutation	base change	Times isolated	*fla* mutation of parent strain
K13E	AAA to GAA	1	Δ(*tar-flhD*)
H14D	CAC to GAC	1	Δ(*flgG-L*)
H14N	CAC to AAC	3	Δ(*fliE-K*); Δ(*flgG-L*)
H14Y	CAC to TAC	2	Δ(*flhA-cheA*); Δ(*fliE-K*)
V33E	GTG to GAC	1	Δ(*flgG-L*)
A103E	GCG to GTG	1	Δ(*tar-flhD*)
M104T	ATG to ACG	1	Δ(*flgG-L*)
N114K	AAT to AAA	2	*flgM*::Mud*K*; Δ(*flgG-L*)
N114T	AAT to ACT	1	Δ(*flgG-L*)
L124F	CTT to TTT	2	Δ(*flgG-L*)
T138I	ACC to ATC	2	Δ(*flgG-L*)
N139I	ACC to ATC	1	Δ(*flgG-L*)
N139K	AAC to AAA	1	Δ(*flgG-L*)
P190Q	CCG to CAG	1	*flgM*::Mud*K*
P190S	CCG to TCG	3	Δ(*flgG-L*)
V196G	GTG to GGG	1	*flgM*::Mud*K*
T198K	ACG to AAG	2	*flgM*::Mud*K*
L199Q	CTG to CAG	1	Δ(*flgG-L*)
L199R	CTG to CGG	1	*flgM*::Mud*K*
Q202L	CAG to CTG	9	*flgM*::Mud*K*; Δ(*flgG-L*)
Q202R	CAG to CGG	1	Δ(*flgG-L*)
E203D	GAA to GAC	3	*flgM*::Mud*K*; Δ(*flgG-L*)
N206K	AAT to AAG	3	*flgM*::Mud*K*; Δ(*flgG-L*)
E209D	GAG to GAT	2	*flgM*::Mud*K*
V213E	GTA to GAA	1	Δ(*flgG-L*)
V213G	GTA to GGA	1	Δ(*flgG-L*)
S226N	AGT to AAT	1	Δ(*flgG-L*)
S226R	AGT to CGT	1	Δ(*flgG-L*)
R231Q	CGA to CAA	1	Δ(*flgG-L*)
fliA UTR	-15 G to A	1	Δ(*flgG-L*)
fliA UTR	-14 C to T	1	Δ(*flgG-L*)
fliA UTR	-7 G to A	2	Δ(*flgG-L*)

Table 3.8 σ^{28}*-dependent expression of β-galactosidase[a] +/- FlgM

σ^{28} allele	*flgM*$^+$		*flgM*$^+$ *fliA** / *flgM*$^+$ *fliA*$^+$	*flgM*$^-$		*flgM*$^-$ *fliA** / *flgM*$^-$ *fliA*$^+$
fliA$^+$	28	(4)	----	2800	(360)	----
H14D	850	(210)	**33**	3400	(440)	**1.3**
H14N	1100	(140)	**40**	3100	(1000)	**1.2**
H14Y	380	(120)	**12**	2300	(480)	**0.8**
V33E	240	(47)	**8**	3400	(170)	**1.1**
M104T	1400	(190)	**46**	2800	(130)	**1.0**
N114K	1400	(370)	**41**	2400	(280)	**0.9**
N114T	540	(63)	**19**	3200	(52)	**1.2**
L124F	260	(89)	**9**	2700	(930)	**1.0**
T138I	900	(110)	**31**	2600	(610)	**1.0**
T139I	1200	(320)	**42**	2900	(350)	**1.0**
N139K	1100	(290)	**38**	2600	(85)	**0.9**
P190Q	90	(11)	**2**	3100	(350)	**1.1**
P190S	160	(46)	**6**	3300	(330)	**1.2**
V196G	75	(19)	**2**	1400	(55)	**0.5**
T198K	400	(23)	**11**	2800	(720)	**1.0**
L199Q	960	(140)	**33**	2600	(470)	**0.9**
L199R	1400	(310)	**45**	2400	(280)	**0.9**
Q202L	290	(21)	**10**	3000	(940)	**1.1**
Q202R	550	(72)	**18**	2600	(630)	**0.9**
E203D	230	(29)	**7**	3300	(150)	**1.2**
N206K	210	(56)	**7**	3100	(480)	**1.1**
E209D	210	(51)	**7**	3200	(840)	**1.2**
V213E	1900	(110)	**53**	3000	(1100)	**1.1**
V213G	340	(71)	**12**	2800	(380)	**1.0**
S226N	1300	(260)	**43**	3000	(340)	**1.1**
S226R	360	(130)	**12**	2700	(650)	**1.0**
R231Q	1500	(91)	**52**	2800	(440)	**1.0**
p*fliA*$^+$/*fliA*$^+$	-----	-----	----	3000		**1.1**

[a] σ^{28}-dependent expression of β-galactosidase was assayed in a *fla-2157* (Δ*flgG-L*) *fliC5050*::MudA *vh2*$^-$ *fljB*^{e,n,x} mutant background. *flgM*$^-$ denotes the *flgM5222*::Mu*d*-Cm allele. β-galactosidase units are expressed in nmol/min/OD_{650}/ml. Values reported in colums 2 and 4 represent the averages from at least three independent assays; standard deviations are reported in parenthesis. The activity of each *fliA** mutant relative to that of the *fliA*$^+$ parent was calculated within each independent assay, and then averaged. The average relative activities (in bold) are reported in column 3 (*flgM*$^+$ background) and column 5 (*flgM*$^-$ background)

Table 3.9 σ^{28}*-dependent expression of β-galactosidase in absence of FlhDC and FlgM[a]

σ^{28} allele	β-galactosidase Activity
fliA$^+$	15 (1.4)
H14D	32 (1.2)
H14N	37 (8.7)
H14Y	33 (2.5)
V33E	10 (1.0)
M104T	12 (1.0)
N114K	16 (4.0)
N114T	15 (2.6)
L124F	6.5 (2.4)
T138I	11 (1.1)
T139I	12 (1.7)
N139K	13 (0.6)
P190Q	9.3 (1.5)
P190S	12 (3.1)
V196G	3.0 (1.0)
T198K	12 (0.0)
L199R	7.0 (1.0)
Q202L	11 (0.6)
Q202R	15 (2.5)
E203D	13 (2.1)
N206K	11 (1.5)
E209D	13 (3.8)
V213E	11 (1.2)
V213G	8.3 (1.5)
S226N	9.0 (1.0)
S226R	14 (1.2)
R231Q	10 (1.0)

[a] Assays performed in an *flhD flgM fliC*::Mu*dA* mutant background. β-galactosidase activities (nmol/min/OD_{650}/ml) represent an average of at least three independent assays. β-galactosidase activity of a *lac*$^-$ strain lacking the *fliC*::Mu*dA* allele was <2 units.

Table 3.10 Inhibition of σ^{28}-dependent CAT activity by truncated FlgM mutants

Strain	Genotype	Truncated FlgM protein	CAT activity[a]
MC1255	pTrc99A/*flgAMN*⁻	none	266 Units
MC1252	pMC64/*flgAMN*⁻	1-97 (full-length)	2 Units
MC1253	pJK238/*flgAMN*⁻	42-97	102 Units
MC1254	pMC138/*flgAMN*⁻	42-87	120 Units

[a] Units expressed as nmol chloramphenicol catalyzed $(min)^{-1}$ $(\mu g$ total soluble protein$)^{-1}$

Figure 3.1 Genes involved in flagellar biogenesis and function in *Salmonella typhimurium*. This figure was adapted from Macnab (123). Chromosomal map positions are indicated in centisomes (Cs), according to the new coordinate nomenclature proposed by Sanderson et al.(155). Most of the genes are clustered in three regions of the chromosome; region III has been further subdivided into IIIa and IIIb, due to the presence of non-flagellar genes between the *fliDST* operon and *fliE* (91). A new gene, *flk* , lies outside the three flagellar regions (88). Arrows indicate the extent and orientation of operons, where known; the double arrow over *hin* indicates that it alternates between two orientations due to phase variation. For a description of the functions of the gene products, see Table 3.1.

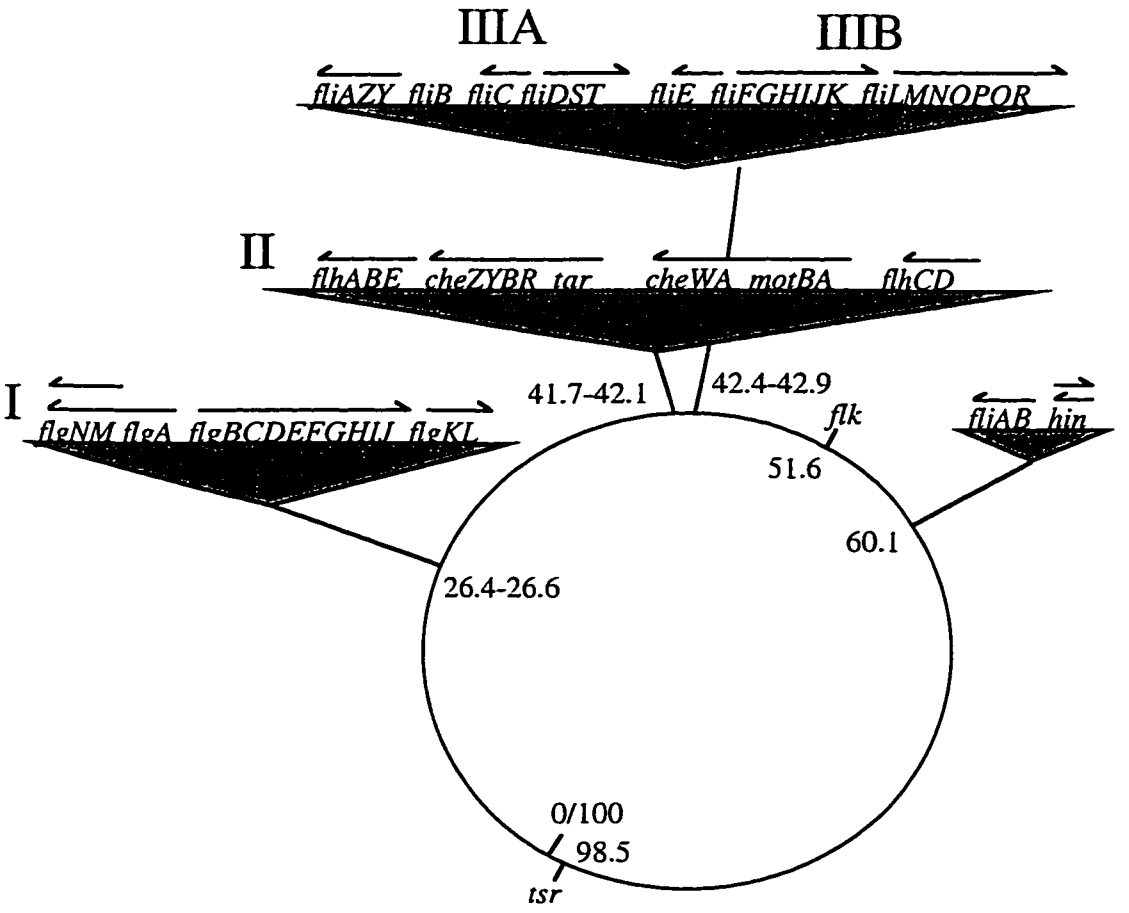
IIIA
IIIB
fliAZY fliB fliC fliDST
fliE fliFGHIJK fliLMNOPQR
II
flhABE cheZYBR tar
cheWA motBA
flhCD
I
fleNM fleA flgBCDEFGHIJ flgKL
41.7-42.1
42.4-42.9
flk
51.6
fliAB hin
60.1
26.4-26.6
0/100
98.5
tsr

Figure 3.2 Transcriptional organization of the flagellar operons is coupled to organelle assembly. The flagellar regulon of *S. typhimurium* is organized into a transcriptional heirarchy of three promoter classes (see text). Class 2 genes encode the hook and basal body (HBB) substructures as well as the *fliA* and *flgM* regulatory genes. Class 2 promoters require the positive transcriptional regulatory proteins FlhD and FlhC, encoded by the Class 1 operon. The Class 2 *fliA* gene encodes the flagellar specific sigma factor σ^{28}, which is required for transcription from Class 3 promoters. The HBB substructure penetrates the inner membrane (IM), peptidoglycan (PG) and outer membrane (OM), and is hollow, serving as a channel for the export of flagellar components to the distal tip of the growing structure. FlgM inhibits σ^{28} through a direct interaction prior to completion of the HBB. Completion of the HBB signals the flagellar specific export apparatus to begin exporting FlgM, releasing σ^{28} to transcribe the Class 3 genes, which encode the filament proteins and the components of the chemotaxis and motor force generator systems.

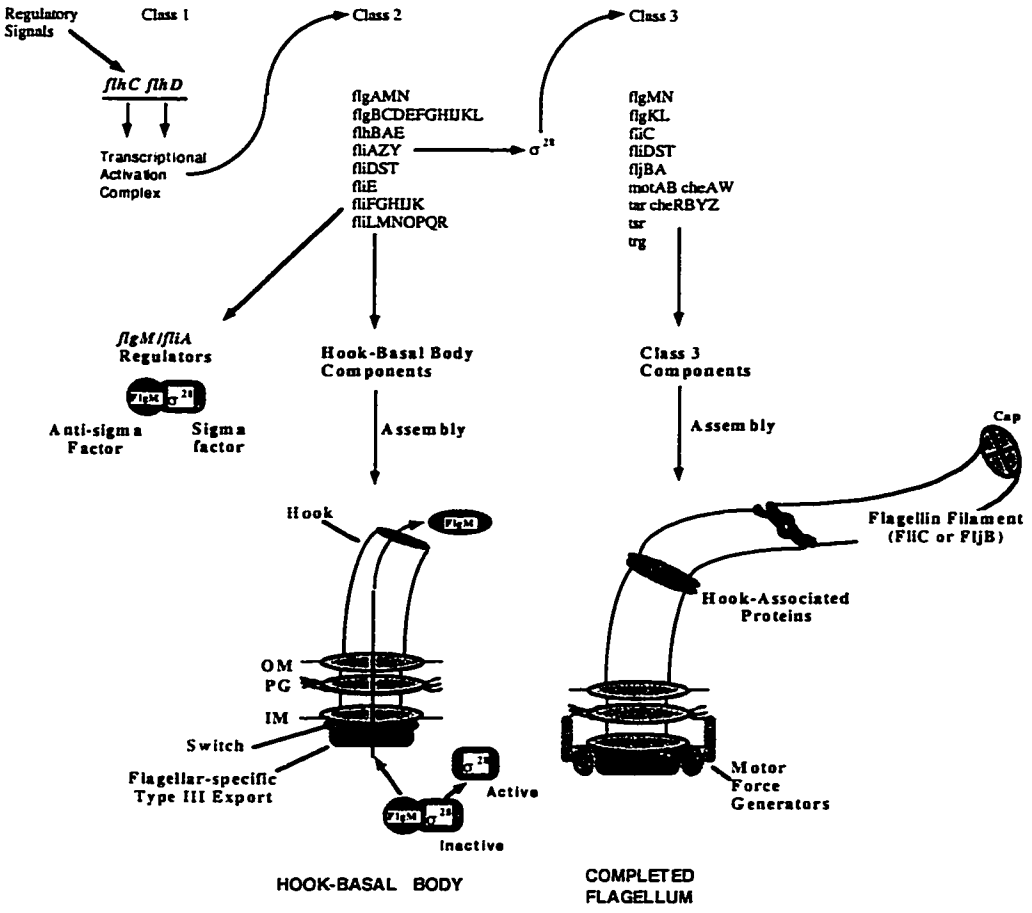
Regulatory Signals
Class 1
Class 2
Class 3
flhC flhD
Transcriptional Activation Complex
flgAMN
flgBCDEFGHIJKL
flhBAE
fliAZY
fliDST
fliE
fliFGHIJK
fliLMNOPQR
flgMN
flgKL
fliC
fliDST
fljBA
motAB cheAW
tar cheRBYZ
tsr
trg
flgM/fliA Regulators
Anti-sigma Factor
Sigma factor
Hook-Basal Body Components
Class 3 Components
Assembly
Assembly
Cap
Flagellin Filament (FliC or FljB)
Hook
Hook-Associated Proteins
OM
PG
IM
Switch
Flagellar-specific Type III Export
Active
Inactive
Motor Force Generators
HOOK-BASAL BODY
COMPLETED FLAGELLUM

Figure 3.3 Modified P22 challenge phage-based selection for *fliA** mutants. When a challenge phage infects a host cell, it can either enter the lytic pathway, which leads to propagation of the phage and lysis of the host cell, or it can integrate into the chromosome as a lysogen, a process that does not kill the host. In the challenge phage, the decision between the lytic pathway and lysogeny is determined by expression of the phage P22 antirepressor protein (Ant), which antagonizes the expression of the lysogenic repressor c2. In the modified challenge phage shown in this figure, Ant expression has been made dependent upon σ^{28}, by placing *ant* under the control of the Class 3 *fliC* promoter. If a phage carrying a *fliA*$^{+}$ allele infects a cell expressing high levels of FlgM, σ^{28}-dependent transcription will be inhibited, Ant will not be expressed, and the phage will lysogenize the host. If the copy of the *fliA* gene carried by the phage is *fliA**, then transcription of *ant* will proceed despite the presence of FlgM, and the phage will lyse the host.

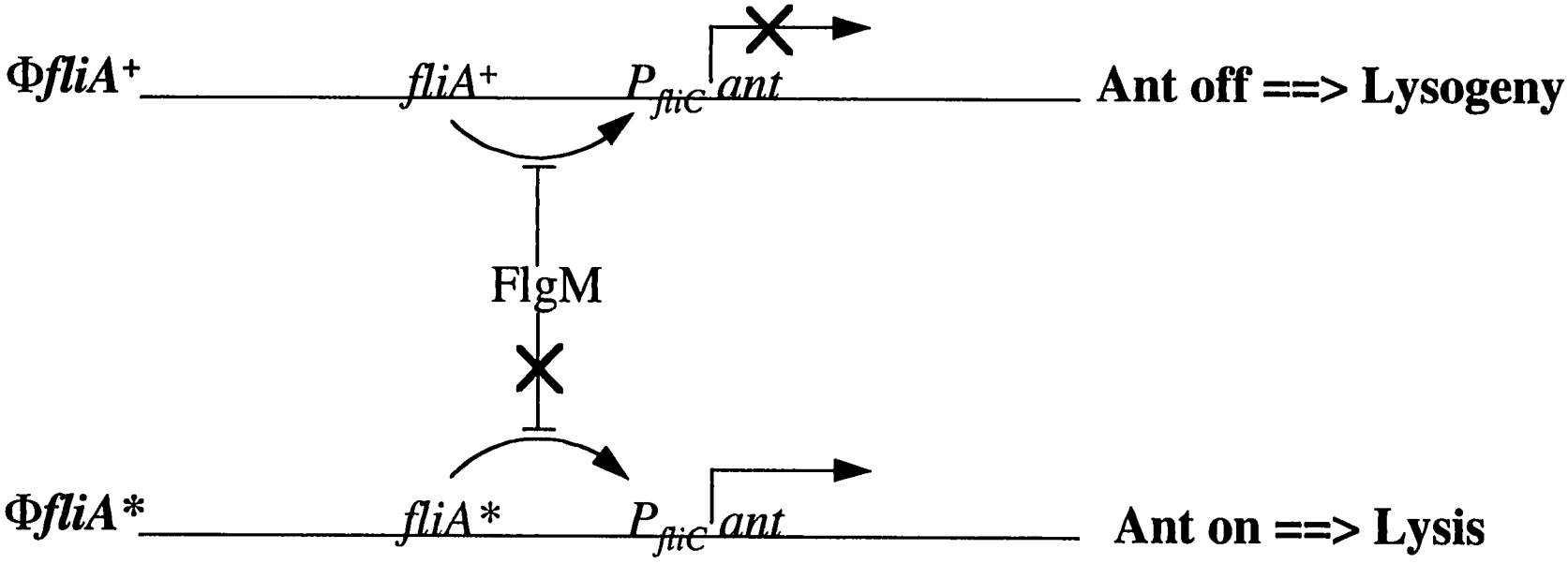
ΦfliA+
fliA+
P fliC
ant
Ant off ==> Lysogeny
FlgM
ΦfliA*
fliA*
P fliC
ant
Ant on ==> Lysis

Figure 3.4 Modified P22 challenge phage. The salient genetic features (left), and a simple diagram (right) of each phage is shown. The *mnt* gene of the phage has been replaced by a copy of the gene for kanamycin resistance (*kan*^{R}). This gene permits the selection and enumeration of lysogens, but was not important for the selection scheme outlined in Figure 3.3. [A] Φ17 contains the minimal *fliC* promoter (-36 to +6 bp relative to the transcription start site). [B] Φ66 is identical to Φ17, except that it also carries a wild type copy of the *fliA* gene under the control of its own promoter (the 118 bp preceding the initiator GTG codon of *fliA*). [C] Φ74 is identical to Φ66, except that it contains a copy of the *fliA*5244*(E203D) allele.

Phage Genotype	Phage Map
A Φ17 ΦP22 Δ*mnt sieA*::[*kan*^{R} $P_{fliC(-36\ to\ +6)}$]::*arc*	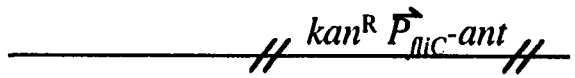
B Φ66 ΦP22 Δ*mnt sieA*::[*fliA*$^{+}$ *kan*^{R} $P_{fliC(-36\ to\ 6)}$]::*arc*	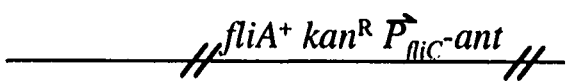
C Φ74 ΦP22 Δ*mnt sieA*::[*fliA**E203D *kan*^{R} $P_{fliC(-36\ to\ +6)}$]::*arc*	

Figure 3.5 Relative *in vivo* transcriptional activity of the σ^{28} * mutants in the presence of FlgM. To determine the levels of σ^{28}-dependent LacZ expression in the presence of FlgM, β-galactosidase assays were performed for each *fliA** mutant and *fliA*$^+$ in the *fla-2157*(Δ*flgG-L*) *fliC5050*::Mu*d*A mutant background. The activity of each mutant was normalized to that of the *fliA*$^+$ strain to derive the relative activity (values are reported in Table 3.8, column 3). σ^{28} is represented by a horitzontal line, with conserved sigma factor regions denoted by shaded boxes. The position of the *fliA** mutations is indicated, and the relative activity of each mutant is plotted above the mutation in bar graph form.

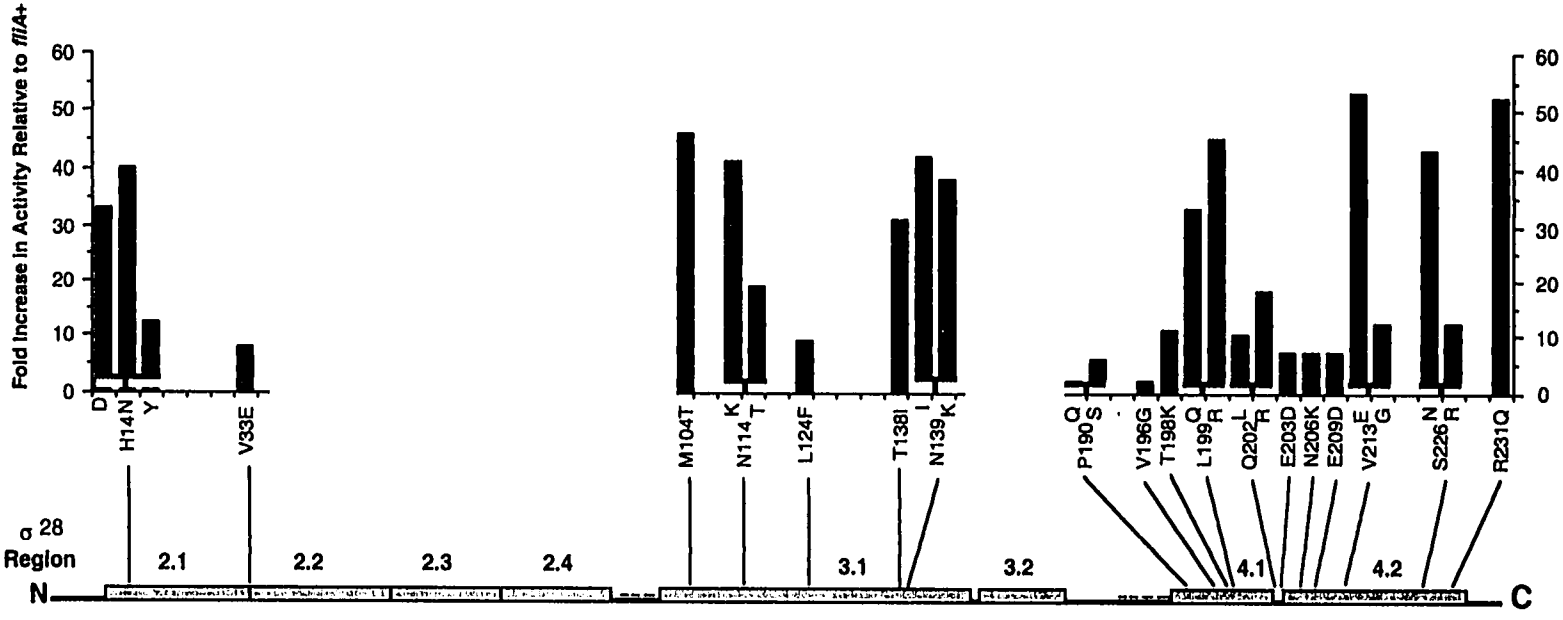
Fold Increase in Activity Relative to fliA+
60
50
40
30
20
10
0
D
H14N
Y
V33E
M104T
K
N114
T
L124F
T138I
I
N139
K
P190
Q
S
V196G
T198K
L199
Q
R
Q202
L
R
E203D
N206K
E209D
V213
E
G
S226
N
R
R231Q
σ 28
Region
2.1
2.2
2.3
2.4
3.1
3.2
4.1
4.2
N
C

Figure 3.6 *In vivo* transcriptional activity of the σ^{28}* mutants in the absence of FlgM. To determine the levels of σ^{28}-dependent LacZ expression in the absence of FlgM, β-galactosidase assays were performed for each *fliA** mutant and *fliA*$^{+}$ in the *flhD92*::Tn*10* *fla-2157*(Δ*flgG-L*) *flgM5222*::Mu*d*-Cm *fliC5050*::Mu*d*A mutant background. The β-galactosidase activity of each mutant (in nmol/min/OD_{650}/ml) is indicated above the protein in bar graph form (standard deviation is shown). The β-galactosidase activity of the *fliA*+ strain is indicated by the dashed line.

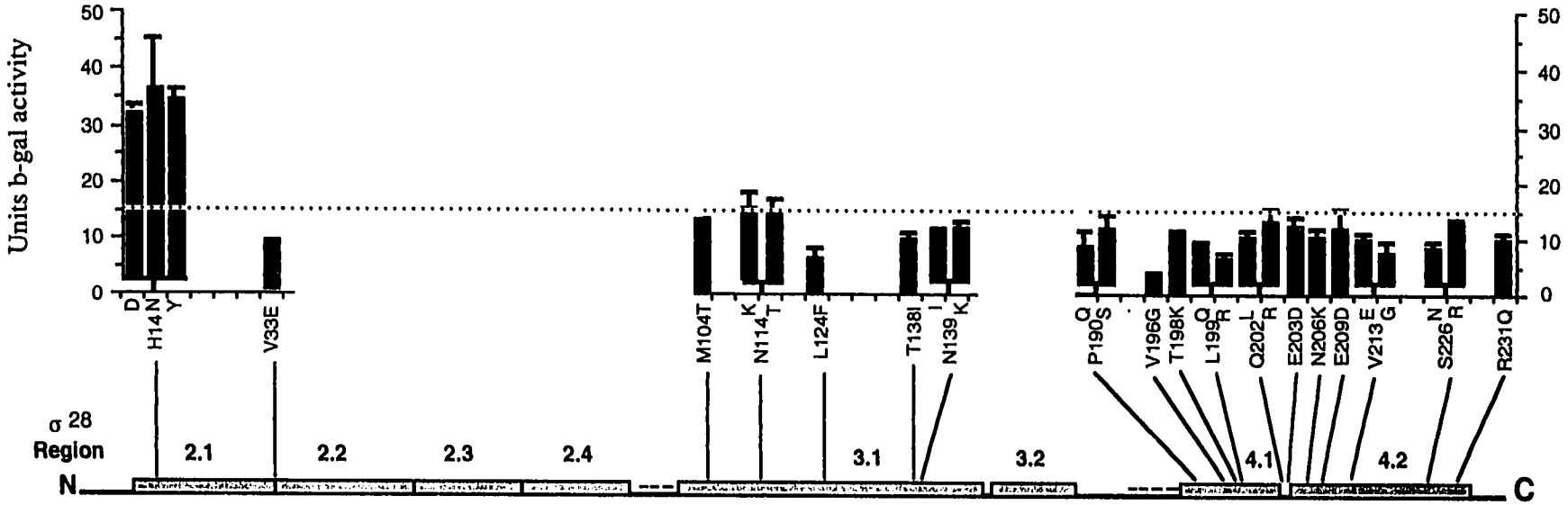
Units b-gal activity
50
40
30
20
10
0
H14D
H14N
H14Y
V33E
M104T
N114K
N114T
L124F
T138I
N139I
N139K
P190Q
P190S
V196G
T198K
L199Q
L199R
Q202L
Q202R
E203D
N206K
E209D
V213E
V213G
S226N
S226R
R231Q
σ 28
Region
2.1
2.2
2.3
2.4
3.1
3.2
4.1
4.2
N
C

Figure 3.7 [A] Summary of FlgM* mutants that define residues important for anti-σ^{28} activity. The isolation of *flgM**mutations is described elsewhere (28, 181). The 97 amino acid FlgM protein is represented as an open bar. Arrows denote amino acid substitutions resulting from point mutations in the *flgM* gene; the parenthesis around residues Lys 76 and Met 77 indicate that these substitutions occurred together in a double mutant. The caret marks the site of an in-frame three base pair insertion between docons 58 and 59 that introduces an Asn codon. ΔM represents a three base pair deletions that removes codon Met 77. The shaded box highlights the proposed σ^{28} binding domain (residues 41-97) as determined by NMR spectroscopy (28).

[B] *In vivo* activity of truncated FlgM mutants. Truncated FlgM proteins are denoted by open bars. Numbers in parentheses indicate the residues of FlgM included in each protein. i through vi. plasmids expressing truncated FlgM proteins. vii. the FlgM-LacZ fusion protein expressed from the *flgM*5208::Mu*d*K gene fusion; the shaded portion represents the LacZ protein. *In vivo* anti-σ^{28} activity, as judged by the ability of each protein to inhibit motility in LT2, and the ability of each protein to be detected by Western analysis, is indicated by a +,+/- or -.

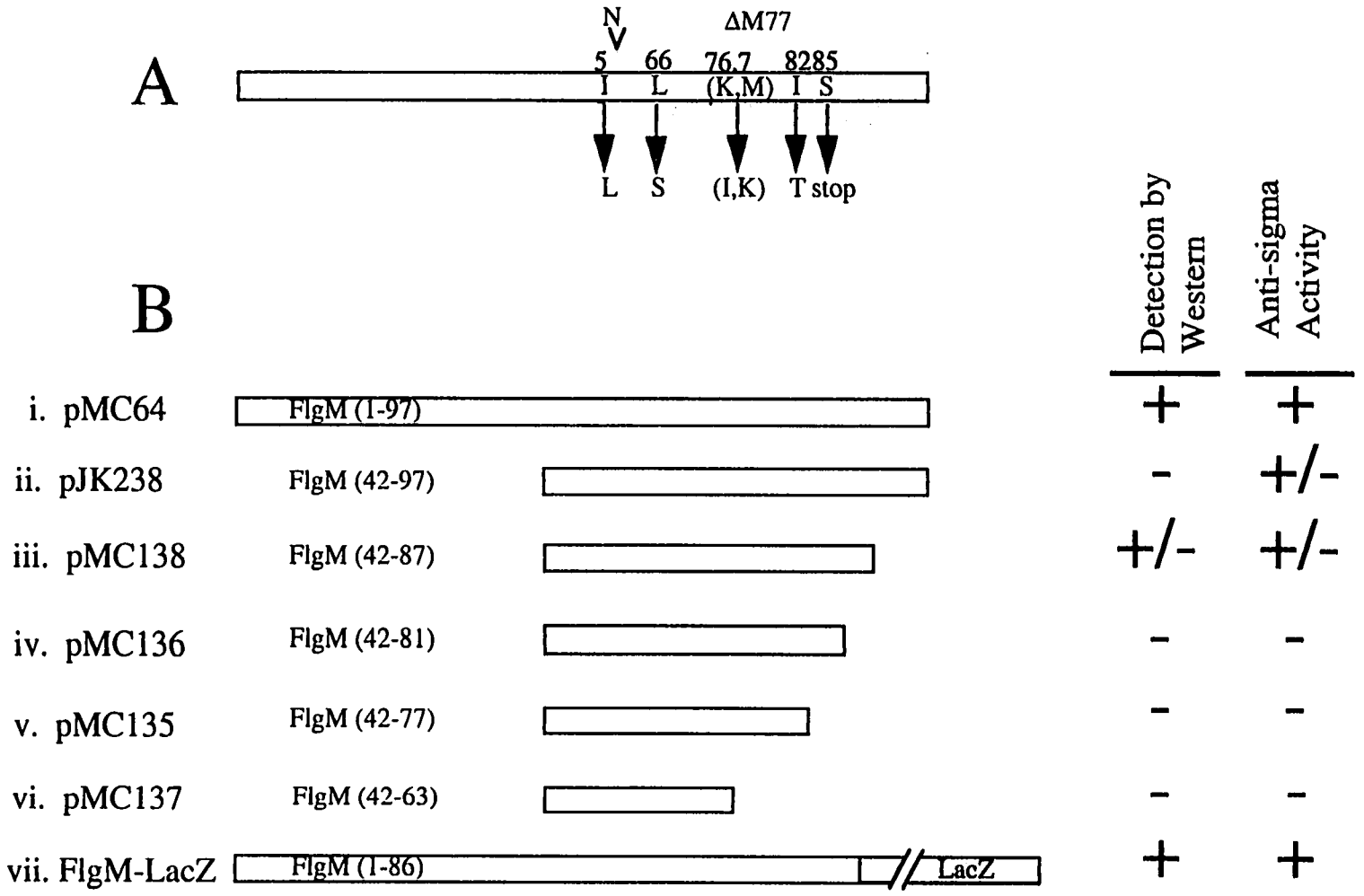
A
N
ΔM77
5 66 76,7 8285
I L (K,M) I S
L S (I,K) T stop
B
Detection by Western
Anti-sigma Activity
i. pMC64
FlgM (1-97)
+
+
ii. pJK238
FlgM (42-97)
-
+/-
iii. pMC138
FlgM (42-87)
+/-
+/-
iv. pMC136
FlgM (42-81)
-
-
v. pMC135
FlgM (42-77)
-
-
vi. pMC137
FlgM (42-63)
-
-
vii. FlgM-LacZ
FlgM (1-86)
LacZ
+
+

Figure 3.8 Alignment of conserved sigma region 2.1 from σ^{70} and σ^{28}. Residues 373 to 399 of σ^{70}, and residues 10 to 33 of σ^{28} are shown aligned according to Lonetto et al. (118). The conserved core binding motif of σ^{70} (178) is underlined. A potentially homologous region in σ^{28} is also underlined. Positions 13, 14 and 33 of σ^{28} (the sites of the region 2.1 *fliA** mutations) are indicated by "*".


σ70 373 K A R R A K E M V E A N L R I S I K K Y T N 399
σ28 10 -- -- V M D H S L W Q R Y V P R H E L R L Q V 33
* * *

Figure 3.9 [A] Distribution of σ^{28}* substitution mutations that confer decreased sensitivity to FlgM *in vivo*. The 239 amino acid σ^{28} protein is represented by a horitzontal bar; boxes denote conserved sigma factor domains. Regions Possible structural motifs and putative domain functions are indicated below the protein (118, 128).

[B] Region 4.2 of σ^{28} modeled as an amphipathic helix. Residues altered by *fliA** substitution mutations are indicated by black circles.

A

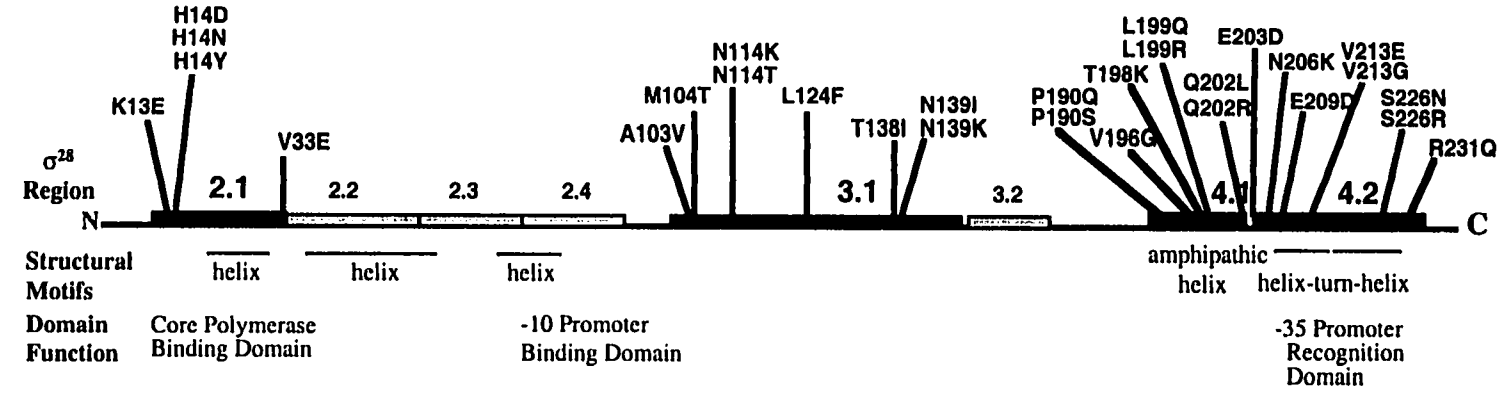

B

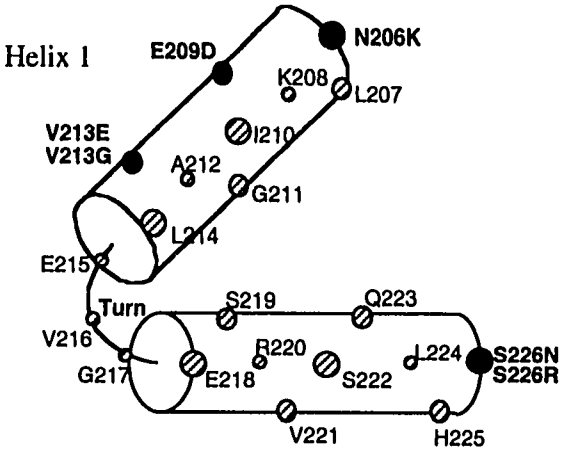

Helix 2
(-35 recognition helix)

Chapter 4

Biochemical Analysis of the Mechanism for FlgM-mediated Inhibition of σ^{28} Activity

Introduction

A preliminary biochemical analysis of FlgM led to the hypothesis that FlgM is an anti-sigma factor which binds σ^{28} and prevents it from interacting with core RNAP (142). Using purified σ^{28} and FlgM, the authors were able to demonstrate that FlgM inhibited $E\sigma^{28}$-dependent transcription, and that that inhibition was specific for $E\sigma^{28}$ ($E\sigma^{70}$-dependent transcription was not sensitive to FlgM). Based on the ability of σ^{28} and FlgM to be crosslinked *in vitro*, the authors concluded that FlgM interacts directly with free σ^{28}, and that that interaction somehow interferes with the ability of σ^{28} to form a stable complex with core RNAP. While their data was suggestive, it did not thoroughly test the competitive binding hypothesis for FlgM-mediated inhibition. Furthermore, alternative hypotheses for FlgM-mediated inhibition of σ^{28} activity were not adequately tested. We therefore re-examined this issue. The data summarized in this section (Figures 4.1 through 4.4) include experiments performed by Joyce Karlinsey (Hughes lab). This work provided the basis for the experiments presented in the results section of this chapter.

To demonstrate an interaction between σ^{28} and FlgM, a crosslinking reagent was added directly to an *in vitro* coupled transcription/translation system in which σ^{28} and FlgM were coexpressed from the same plasmid (142). Crosslinking, while sometimes necessary when the proteins being studied are of low abundance, can generate a false positive result when the protein concentration is high, as it would be in a reaction where σ^{28} and FlgM were overexpressed. Furthermore, both the *fliA* and *flgM* genes were preceded by their own promoters on the expression plasmid. Normal

protein/DNA interaction between σ^{28} and the Class 3 *flgM* promoter could have accounted for the proximity of σ^{28} and FlgM in this assay. FlgM binding as a repressor to the upstream region of the *fliA* gene, a possibility that had never been ruled out, could also have brought the two proteins close enough together to be crosslinked.

Coimmuneprecipitation experiments could not be done to demonstrate an interaction between σ^{28} and FlgM, because anti-FlgM antibodies cross-reacted with σ^{28} and anti-σ^{28} antibodies cross-reacted with FlgM (J. Karlinsey and K. Hughes, unpublished observations; 142). To test for a direct interaction between FlgM and σ^{28} without cross-linking, a glutathione-S-transferase (GST)-σ^{28} fusion was expressed by pKH486. When crude extracts of *S. typhimurium* cells expressing GST-σ^{28} were passed over a glutathione-Sepharose column, the GST-σ^{28} fusion protein, bands corresponding to the α (not visible by Coomassie staining), β and β' subunits of RNAP, and the FlgM protein were all retained (the presence of α, and the identity of FlgM were confirmed by Western analysis; data not shown) (Figure 4.1A, lane 2). Neither FlgM nor the RNAP subunits bound to the unfused GST protein (Figure 4.1A, lane 1). Copurification of core RNAP subunits with the GST-σ^{28} fusion was expected; the presence of these subunits served as an internal control for the activity of the GST-σ^{28} fusion. It was possible that FlgM and core RNAP were binding to the same GST-σ^{28} fusion molecule to form a ternary complex, but this could not be tested in this assay. That FlgM was capable of binding directly to σ^{28} was confirmed when we attempted to purify native σ^{28} from a *flgM*$^+$ strain of *S. typhimurium*. A peptide with an apparent molecular weight of 10 kDa copurified in stoichiometric amounts with σ^{28} under non-denaturing conditions; amino terminal sequencing confirmed its identity as FlgM (M. Chadsey and K. Hughes, unpublished observations). Taken together, these data supported the results obtained previously (142).

We took advantage of the GST-σ^{28} based assay for σ^{28}/FlgM complex formation to assess the relative affinities of a wild type and a mutant FlgM* peptide ("*" is used to designate mutants defective for σ^{28} inhibition) for GST-σ^{28}. The GST-σ^{28} expression vector (pKH486) was introduced into merodiploid *S. typhimurium* strains expressing FlgM-LacZ fusion peptides in addition to native FlgM (both expressed from the *flgAMN* operon, which was duplicated in these strains). Cell extracts from pKH486/TH2822 (expressing FlgM and FlgM-LacZ) and pKH486/TH2825 (expressing FlgM and FlgM*L66S-LacZ) were analyzed as above (Figure 4.1B). A comparison of lane 2 with lane 1 reveals that GST-σ^{28} bound significantly less of the FlgM*L66S-LacZ fusion (and consequently more of the competing native FlgM protein) than it did of the FlgM-LacZ fusion . This result can be attributed to a weaker affinity of the FlgM*L66S-LacZ fusion for GST-σ^{28}, as the intracellular level of the mutant LacZ fusion protein in TH2825 was determined by quantitative Western analysis to be equivalent to that of the wild type version in TH2822 (data not shown). These data suggested that the defect in the ability of FlgM*L66S-LacZ to inhibit σ^{28} was due to a decreased affinity of that mutant for σ^{28}.

The effect of FlgM on Eσ^{28}-dependent transcription *in vitro* had been examined previously by titrating FlgM into an *in vitro* transcription assay containing Eσ^{70} and a ten-fold excess of σ^{28} (142). Both a σ^{28}-dependent and a σ^{70}-dependent promoter substrate were provided. The data showed that at a one-to-one ratio of FlgM to σ^{28}, transcription from the *fliC* promoter was almost completely inhibited. However, the presence of a competing sigma factor in this assay meant that the stoichiometry of inhibition could not be accurately determined from the data. In addition, the non-denaturing method used to purify native σ^{28} for these assays probably allowed for contamination of his protein preparation with FlgM. SDS-PAGE analysis of the purified σ^{28} revealed the presence of a low MW band that could have been FlgM (142).

For our *in vitro* assays of FlgM anti-sigma activity, σ^{28} and FlgM preparations were free of cross-contaminants. σ^{28} was overexpressed as an N-terminally tagged histidine fusion protein, and purified by affinity chromatography under denaturing conditions to remove FlgM. The core RNAP used in these assays was free of contaminating sigma factors. Figure 4.2A illustrates the activity of His-σ^{28} protein purified in this manner. Maximal transcription from the linear *fliC* promoter substrate was achieved with a 5:1 molar excess of σ^{28} to core RNAP. Purified FlgM protein was added to transcription assays which included σ^{28} at a 5:1 molar ratio to core (Figure 4.2B). Contrary to published results (142) very little FlgM was required to have a significant effect on transcription. A 45% reduction in transcription was obtained at a 1:10 molar ratio of FlgM to σ^{28} (but at a 1:2 ratio of FlgM to core RNAP). One explanation for these results is that the specific activity of the His-σ^{28} preparation was only ~20%, so that the ratio of FlgM to active σ^{28} at 50% maximal transcription was actually 1:2. An alternative explanation might be that FlgM inhibition was occurring at the holoenzyme level.

We wished to know at what point in the transcription process FlgM was acting to inhibit σ^{28}-dependent transcription. The filter binding technique (67) was employed to test the effect of FlgM on promoter binding by Eσ^{28}. In these assays, specific binding of promoter DNA is tested by challenging protein/DNA complexes with nonspecific competitor DNA. Neither σ^{28} nor FlgM alone was able to bind DNA containing the *fliC* promoter in this assay (Figure 4.3A, lanes 2 and 8). Only RNAP containing σ^{28} bound specifically to the *fliC* promoter (compare Figure 4.3A, lanes 4 and 6 with Figure 4.3B, lanes 1 and 4). Specific binding of Eσ^{28} to the *fliC* promoter was inhibited by FlgM regardless of the order of addition of proteins to the reaction mixture (Figure 4.3B, lanes 2 and 3). In these two lanes, it appeared that σ^{28} that had first been incubated with core RNAP for a period of time sufficient to allow Eσ^{28}

formation (as evidenced by the data in Figure 4.3B, lane 1) was as susceptible to FlgM-mediated inhibition as free σ^{28}. However, once $E\sigma^{28}$ formed a complex with the promoter, subsequent incubation with FlgM could not reverse this process (data not shown), suggesting that FlgM was not able to displace $E\sigma^{28}$ from the promoter. The apparent susceptibility of $E\sigma^{28}$ to negative regulation by FlgM could have been due to competitive binding of FlgM to σ^{28} that was either spontaneously released from the $E\sigma^{28}$ complex, or was actively displaced from $E\sigma^{28}$ by FlgM. A third possibility was that FlgM was forming a stable ternary complex with $E\sigma^{28}$ that was unable to bind DNA.

Addition of FlgM to a mixture of σ^{28} and core RNAP led to a decrease in the amount of σ^{28} that could be crosslinked to core. σ^{28} was observed to redistribute into a complex with FlgM (142). These results were interpreted as evidence for competition between FlgM and core RNAP for σ^{28} binding (the first hypothesis). However, FlgM was present in such excess over core RNAP in these assays that the data should not have been used to draw any conclusion about the relative affinity of σ^{28} for core RNAP in the presence of FlgM. Furthermore, it could not be ruled out that the $E\sigma^{28}$ complex did not also contain FlgM (which would support the second or third hypothesis).

Resolution of protein complexes on native gels was employed to test for the existence of a ternary FlgM/$E\sigma^{28}$ complex. FlgM, σ^{28}, and core RNAP were electrophoresed either by themselves, or in different combinations on a native gel (Figure 4.4A, lanes 1-7). Protein complexes from the native gel were analyzed by SDS-PAGE to identify their constituents (Figure 4.4B, lanes 10-14). When σ^{28} and FlgM were mixed, a novel band appeared on the native gel (Figure 4.4A., lane 3) which proved to be a heterocomplex (Figure 4.4B, lane 14). The possibility that FlgM was comigrating with σ^{28} by virtue of a non-specific interaction was tested by mixing FlgM with bovine serum albumin (BSA) which has a predicted pI similar to that of σ^{28} (4.97

and 4.91 respectively). No FlgM was found associated with BSA (data not shown). When core RNAP was mixed with σ^{28}, FlgM, or both proteins together, no novel bands appeared, though the appearance of the RNAP complex in the presence of σ^{28} was changed, possibly due to the formation of $E\sigma^{28}$ (Figure 4.4A, lanes 4-7). SDS-PAGE analysis of the RNAP complex revealed the presence of comigrating proteins (Figure 4.4B, lanes 9-13). As expected, σ^{28} associated with core RNAP (Figure 4.4B, lane 11). Separation of the RNAP complex in Figure 4.4A, lane 6 (σ^{28} and FlgM added) revealed that a small amount of FlgM (visible by Coomassie staining), was found to comigrate with the σ^{28}/core RNAP complex (Figure 4.4B, lane 12). Changing the order in which the proteins were added to the reaction mixture did not alter the outcome of this experiment (Figure 4.4B, lane 13). These results supported the third hypothesis that invoked a stable ternary complex, though they would also be consistent with a transient interaction between FlgM and $E\sigma^{28}$.

While FlgM by itself did not appear to associate with core RNAP in the Coomassie-stained gel (Figure 4.4B, lane 10), its presence was detected by Western analysis of the complex using FlgM antisera (data not shown). Another unexpected result was that FlgM associated with $E\sigma^{70}$ (Figure 4.4C, lane 17) even though FlgM had been shown not to affect σ^{70}-dependent transcription *in vitro* (142). Still, less FlgM was associated with $E\sigma^{70}$ alone than if σ^{28} was also included to allow the formation of $E\sigma^{28}$ (compare Figure 4.4C lane 17, to 4.4C lanes 19 and 20). If these interactions were specific, then they implied two things: 1) that part of the interaction between FlgM and $E\sigma^{28}$ might involve direct contacts between FlgM and core RNAP, and 2) that FlgM-mediated inhibition at the holoenzyme level should be mediated through contacts unique to $E\sigma^{28}$. Of the three regions identified as potential FlgM binding domains (see Chapter 3, and 103), region 4.1/4.2 of σ^{28} is the least

homologous to σ^{70} (118). Given the importance of this region for promoter recognition, it would make an appropriate target for negative regulation by FlgM.

The comigration of FlgM with $E\sigma^{28}$ was the strongest evidence thus far for the existence of a ternary complex. An alternative explanation had to be considered, however. It was possible that FlgM, σ^{28} and core RNAP in that region of the gel were actually in dynamic equilibrium, with σ^{28} rapidly alternating between a complex with core RNAP and a complex with FlgM. While complexed to free σ^{28}, FlgM would migrate faster than core RNAP; once released, it would migrate more slowly. The net effect of this cycle would be to distribute FlgM throughout the zone in which core RNAP was migrating. To rule out this possibility, it would be necessary to develop an assay system in which the components were not able to come to equilibrium during the course of the experiment.

In summary, our evidence indicated that while the published hypothesis for the mechanism of inhibition of σ^{28} by FlgM (142) was not necessarily incorrect, it might be incomplete. We had provided evidence that FlgM, possibly in addition to binding free σ^{28} to sequester it from core RNAP, was able to regulate $E\sigma^{28}$ activity. However, because all of our assays were carried out under equilibrium conditions, we could not distinguish which of our three hypotheses for negative regulation of $E\sigma^{28}$ by FlgM could best account for our observations. The experiments presented in the next section were designed to resolve this issue.

Results

Mutations in the C-terminal half of FlgM disrupt anti-sigma factor activity. Our original protocol for *in vitro* transcription assays of σ^{28} activity had been based on a method published previously (141). These assays proved labor-intensive, requiring the products of transcription reactions to be analyzed by PAGE and quantified by

densitometry. We developed a new protocol based on the "spot transcription" method (122). In these assays, transcript production is measured by spotting the transcription reaction onto DEAE cellulose disks and quantifying incorporated label using a scintillation counter. Figure 4.5A depicts the results of a typical assay. Transcription of the σ^{28}-dependent *fliC* promoter was specific, and reached a near-maximal rate of synthesis at a 1:1 ratio of σ^{28} to core RNAP. The high specific activity of the native σ^{28} protein in this assay was characteristic of sigma prepared by the method of Hagar and Burgess (58), in which purified sigma factor proteins are rapidly renatured from 6 M Guanidine. In our hands, native σ^{28} reconstituted in this fashion had maximum activity immediately after renaturation; this activity declined rapidly after 12 to 24 hours, even at -80° C, stabilizing at around 10 to 20% of its original activity.

flgM mutants defective for inhibition of σ^{28} activity (*flgM** mutants) had been isolated during the course of the genetic analysis of FlgM-mediated inhibition of flagellin expression in export deficient mutant strains (see Chapter 3). Two of these, missense mutants with single amino acid substitutions in the C-terminal σ^{28}-binding domain of FlgM (28, 80), were chosen for further characterization *in vitro* to determine whether their *in vivo* phenotype was in fact due to a decrease in their ability to inhibit the σ^{28} transcription machinery (σ^{28} and/or $E\sigma^{28}$). The mutant *flgM** alleles were cloned into N-terminal histidine tag fusion vectors, overexpressed and purified by affinity chromatography The purified mutant proteins, His-FlgM*L66S and His-FlgM*I82T, were then compared with His-FlgM for their ability to inhibit σ^{28}-dependent transcription from the *fliC* promoter *in vitro*. When $E\sigma^{28}$ was challenged with increasing amounts of His-FlgM, transcription from this promoter rapidly declined, and reached background (σ^{28}-independent) levels at a 4:1 ratio of FlgM to σ^{28} (Figure 4.5B). Both FlgM* mutants demonstrated reduced ability to inhibit σ^{28}-dependent transcription; even at a 10:1 ratio of FlgM* to σ^{28}, transcription was not completely

abolished. The effect of the missense mutations on the ability of FlgM to inhibit σ^{28}-dependent transcription *in vitro*, while reproducible, was not as large as that seen *in vivo*. This is likely due to the fact that these*in vitro* assays had to be carried out at a protein concentration almost two orders of magnitude higher than the K_d of the σ^{28}/FlgM complex (see Table 4.1). At these concentrations, we would predict that the effect of a 4 to 10x decrease in the affinity of FlgM for σ^{28} on anti-sigma factor activity would be subtle. The simplest explanation for the effect of the missense mutations *in vivo* and *in vitro* is that they fail to bind to or inhibit the activity of σ^{28} and/or Eσ^{28} as efficiently as wild type FlgM.

Kinetic analysis of the FlgM/Eσ^{28}, FlgM/σ^{28}, and σ^{28}/Core RNAP interactions. The surface plasmon resonance (SPR)-based system (Biacore Inc.) was used to evaluate the interaction of FlgM with Eσ^{28} under non-equilibrium conditions. SPR enables the measurement of molecular interactions in real time by following the specific adsorption and desorption of a protein in solution (the analyte) to its binding partner (the ligand) immobilized on a sensor surface (90). The association rate constant (k_a) can be determined by analyzing a collection of binding curves in which the concentration of analyte flowing over a fixed concentration of ligand is varied. The dissociation rate constant (k_d) can likewise be calculated from the subsequent decrease in signal that occurs after the analyte pulse has ended, and the continuous flow of buffer removes analyte from the sensor surface as it dissociates from bound ligand.

This latter feature of the SPR system enabled us to test one hypothesis for FlgM inhibition of Eσ^{28} that was not easily evaluated by other methods, i.e. that FlgM binds to Eσ^{28} and increases the rate of dissociation of σ^{28} from core RNAP. We reasoned that if FlgM possessed the ability to destabilize Eσ^{28}, then the dissociation rate of the Eσ^{28} complex would increase in the presence of FlgM. If, however, the apparent

susceptibility of $E\sigma^{28}$ to FlgM demonstrated by the filter binding assays was simply due to the ability of FlgM to compete with core RNAP for spontaneously dissociated σ^{28}, then the dissociation rate of the $E\sigma^{28}$ complex would be unaffected by FlgM. For these experiments, σ^{28} (28 kDa) was used as the ligand and core RNAP (380 kDa) as the analyte, since this arrangement would result in the largest change in signal (which is directly proportional to MW) per molecule of analyte released. Controls to ensure that the measurements would not be skewed by analyte rebinding during the dissociation phase were performed (see Chapter 2).

The effect of FlgM on the rate of dissociation of $E\sigma^{28}$ is shown in Figure 4.6A. The results indicate that FlgM significantly increases the rate of $E\sigma^{28}$ dissociation, increasing the k_d of the complex approximately 4-fold. Reducing the FlgM concentration from 250 nM (used above) to 50 nM diminished this effect (such that the k_d was increased only 2.5-fold), and the effect was not completely abolished until the concentration of FlgM was decreased to 10 nM (data not shown). A FlgM-induced increase in the k_d of holoenzyme was not observed when His-σ^{70} was substituted as the ligand (Figure 4.6B), demonstrating specificity for $E\sigma^{28}$ (the sharp drop in signal immediately following the end of analyte injection was due to the difference in refractive index between the analyte buffer and the running buffer in this experiment, and did not affect interpretation of the data). The fact that FlgM did not appear to affect $E\sigma^{70}$ suggests that holoenzyme dissociation is mediated by contacts at least partially contained on σ^{28}. In a separate experiment, the ability of core RNAP to bind to FlgM was tested by injecting a 125 nM solution of core over a dense FlgM ligand surface; no specific binding was observed (data not shown).

SPR was used to compare σ^{28} binding by the FlgM*L66S and FlgM*I82T missense mutants with that of wild type FlgM. In these experiments, His-FlgM proteins were used as the ligand, and the analyte was native σ^{28}. The k_a and k_d for each

interaction, the calculated dissociation constant (K_d), and the relative affinity of the mutant FlgM* variants for σ^{28} are reported in Table 4.1. The ~3.6-fold weaker affinities of the mutant FlgM* proteins for σ^{28} was reproducible; an independent preparation of FlgM proteins and native σ^{28} gave similar results. The results obtained when the inverse experiment (His-σ^{28} as ligand, wild type and mutant His-FlgM proteins as analyte) was performed supported those of the first assay, though in these experiments, the σ^{28} binding defect of the mutants was more pronounced, mainly due to an increase in the k_d (this discrepancy might be attributed to the presence of the histidine tag on σ^{28}, or to the different ligand capture method used in these experiments). Also presented in Table 4.1 are the results of a kinetic analysis of core RNAP binding by σ^{28}. The calculated K_d for the Eσ^{28} complex is similar to the K_d of Eσ^{70}, 500 pM, as determined by fluorescent spectroscopy (49).

The mutant FlgM* proteins were tested to determine whether their σ^{28} binding defects also affected their ability to dissociate Eσ^{28}. Figure 4.6A shows that at 250 nM, neither of the FlgM* proteins was able to significantly increase the dissociation of Eσ^{28} above the rate in the control experiment, providing further evidence that destabilization of Eσ^{28} by FlgM appears to involve specific contacts between FlgM and σ^{28}.

Discussion

The experiments presented in this chapter demonstrate a direct interaction between FlgM and Eσ^{28}. The copurification of FlgM and RNAP subunits with GST-σ^{28} (Figure 4.1A), and the comigration of FlgM with Eσ^{28} in native gels (Figure 4.4) were consistent with hypotheses involving a ternary FlgM/Eσ^{28} complex. The negative effect of FlgM on promoter binding by Eσ^{28} (Figure 4.3) implied that this putative interaction disabled Eσ^{28} in some way. However, the filter binding assays could not distinguish between direct inhibition of Eσ^{28} promoter binding by FlgM and an equally

likely possibility, i.e. that in the presence of equimolar FlgM, σ^{28} spontaneously released from core RNAP was efficiently scavenged by the anti-σ factor, resulting in the redistribution of σ^{28} from a complex with $E\sigma^{28}$ to an inactive σ^{28}/FlgM complex. Any assay in which FlgM, σ^{28} and core RNAP had sufficient opportunity to come to equilibrium prior to sampling would complicate interpretation of the results obtained. This difficulty was solved by using the SPR-based system, which made it possible to test one mechanism for direct inhibition of $E\sigma^{28}$ by FlgM. SPR assays of the effect of FlgM on $E\sigma^{28}$ stability revealed that FlgM increased the rate of dissociation of the complex, presumably through an interaction with the σ^{28} subunit. Though this effect could have been caused by the ability of FlgM to interfere with rebinding of core RNAP to σ^{28} during dissociation, extensive controls indicated this was unlikely to be the case here (see Chapter 2). We term this novel regulatory activity of FlgM "holoenzyme destabilization."

Before the mechanism for holoenzyme destabilization can be discussed, it is important to consider how σ^{28} may be interacting with FlgM and core RNAP individually. The σ^{28}/FlgM complex may involve multiple contacts between FlgM and σ^{28} at regions 2.1, 3.1 and 4.1/4.2, analogous to the interaction between σ^{F} and SpoIIAB (see Chapter 3, and 33, 103). Multiple interactions between σ^{28} and FlgM could account for the extreme stability of the complex, as reflected in the K_d of ~200 pM. The size of the σ^{28} binding domain of FlgM, 25 to 57 contiguous residues (28, 80), is sufficiently large to contact several non-contiguous domains on σ^{28}. This entire region, normally unstructured, is known to undergo a conformational change when it binds σ^{28}, since upon complex formation it becomes constrained (28). The substitution at FlgM residue 66 is part of a contiguous 14 residue region that appears to adopt a helical structure upon σ^{28} binding (29). Unlike the I82T mutation, L66S appears to decrease the k_a of the σ^{28}/FlgM interaction, which may imply that substitution of a

polar residue for a hydrophobic one at this position perturbs the folding of FlgM that occurs upon binding of σ^{28}. The observation that the FlgM missense mutants which are defective for free σ^{28} binding are also defective for the interaction with $E\sigma^{28}$ suggests that the site(s) on free σ^{28} that contact the altered FlgM residues also mediate the interaction between FlgM and $E\sigma^{28}$.

If, as is likely, the emerging concept of the σ/core RNAP interaction can be generalized to σ^{28}, then both regions 2 and 3 of σ^{28} may participate in core RNAP binding. A multipartite interaction between σ^{28} and core RNAP means that the $E\sigma^{28}$ complex might breathe without completely dissociating. A breathing complex could be viewed as one in which σ regions 2 and 3 are alternately exposed as they temporarily lose contact with core RNAP (Figure 4.7A), making them available to competing binding partners such as FlgM. Alternatively, breathing could be imagined as an allosteric process in which the conformation of σ^{28} alternates between a tightly bound conformation and a weakly bound conformation (Figure 4.7B). This second scenario does not assume that σ regions normally buried in the σ^{28}/core RNAP interface are exposed by breathing.

We suggest two alternative models for destabilization of $E\sigma^{28}$ by FlgM (Figure 4.7). The first is called the "competitive displacement" model [A], where destabilization of $E\sigma^{28}$ results from the displacement of σ from core RNAP as FlgM competes for binding to σ regions 2 and 3 exposed by breathing. FlgM may initiate this process by interacting with its unique binding site in regions 4.1/4.2. Establishing contact at this site would increase the probability of subsequent interactions with regions 2.1 and 3.1. It is reasonable to expect regions 4.1/4.2 to be accessible on $E\sigma^{28}$, since they must be able to interact with the -35 promoter determinants. It is also possible that FlgM binds first to one of the domains it shares with core RNAP (these two possibilities are not differentiated in Figure 4.7). The second, called the "allosteric displacement" model

[B], predicts that FlgM can interact with $E\sigma^{28}$ at exposed σ regions 4.1/4.2, and that the interaction stabilizes a "FlgM-bound" conformation of σ^{28} that cannot interact efficiently with core RNAP. Additional contacts between FlgM and σ^{28} are proposed to form after dissociation of the σ subunit from $E\sigma^{28}$.

Both models invoke a ternary complex between FlgM and $E\sigma^{28}$. Attempts to demonstrate similar complexes in other anti-σ/σ factors systems have been largely unsuccessful, with the exception of the copurification of the phage T4 protein AsiA with $E\sigma^{70}$ (143, 173). The relative stability of the AsiA/$E\sigma^{70}$ complex is probably due to the fact that AsiA, in conjunction with the phage T4 protein MotA, is also required to promote $E\sigma^{70}$-directed transcription at middle phage promoters (146). Often, the conclusion drawn from these negative results is that core RNAP binding and anti-σ factor binding are mutually exclusive. We submit that, at least in the case of $E\sigma^{28}$ and FlgM, it is only the unstable nature of the ternary complex that has prevented its isolation. The presence of the complex in the native gel assays was probably due to the extremely high concentration (> 1 μM σ^{28} and FlgM; 100 nM core RNAP) of the proteins in the samples.

The SPR experiments revealed that in the presence of FlgM, the half life of the $E\sigma^{28}$ complex decreased approximately 4-fold to 4 minutes. However, because the signal generated by FlgM binding to $E\sigma^{28}$ was insignificant compared to the drop in signal caused by $E\sigma^{28}$ dissociation, we were unable estimate the half life of the putative FlgM-$E\sigma^{28}$ complex itself. It is possible that the half life of this complex is significant on the time scale required for $E\sigma^{28}$ to initiate transcription at a promoter (the kinetics of closed complex formation have been measured to be in the range of 2 x 108 M-1 sec-1; 153) If this is the case, then the primary mechanism of $E\sigma^{28}$ inhibition by FlgM may be steric interference with promoter recognition by the -35 promoter binding domain in

regions 4.1/4.2, analogous to the proposed action of AsiA at phage T4 early promoters (1, 159, 160).

In the SPR experiments, the concentration of FlgM had to be greater than 10 nM in order to have an effect on the dissociation rate of $E\sigma^{28}$. This level is much higher than the K_d of the σ^{28}/FlgM complex (~200 pM). This observation is consistent with our proposal that some of the potential contacts between FlgM and σ^{28} may be masked in the $E\sigma^{28}$ complex. The apparent preference of FlgM for $E\sigma^{28}$ over free σ^{28} in the transcription assay using His-σ^{28} (Figure 4.2B) was thus probably due to low specific activity of the His-σ^{28} protein. At the protein concentrations used in that assay, the dominant interaction should have been between FlgM and free His-σ^{28}. FlgM had no effect on $E\sigma^{70}$ stability at the concentration used in the experiment in Figure 4.5B. If the association of FlgM with $E\sigma^{70}$ in the native gel assay (Figure 4.4C) was specific, then the K_d of that interaction must be even higher than that of the FlgM/$E\sigma^{28}$ complex. This would be predicted, since at least some the contacts recognized by FlgM on σ^{28} would not be present on σ^{70}. Alternatively, the failure to detect an interaction between FlgM and $E\sigma^{70}$ or with core RNAP in the SPR assays could indicate that the weak affinity of FlgM for these complexes in the native gel assays was nonspecific.

Preliminary measurements of FlgM in exponentially growing *S. typhimurium* indicate that the concentration of FlgM is approximately 400 nM in wild type cells, and is at least twice that in a mutant strain defective for FlgM export (assuming a cell size of 0.5 μm x 2 μm; data not shown). Two predictions can be made based on these measurements. First, at these concentrations of FlgM, there should be essentially no free σ^{28} in the cell; all σ^{28} should either be involved in a potentially active complex with core RNAP, or sequestered by FlgM (the K_d of the σ^{28}/FlgM interaction is on the same order of magnitude as that estimated for σ^{28}/core RNAP (Table 4.1). Second, relatively small changes in the concentration of FlgM when it is already ~3 orders of magnitude

over the K_d of the σ^{28}/FlgM complex will not affect the efficiency with which that interaction occurs, but they could affect the ability of FlgM to interact with $E\sigma^{28}$. Therefore, at least while FlgM levels are high, as they are believed to be prior to the completion of the hook/basal body substructure (HBB) (74, 101), FlgM-mediated inhibition of $E\sigma^{28}$ may be an important regulatory mechanism. There is a 10 to 15 minute interval between the onset of σ^{28} and FlgM expression, and the appearance of σ^{28}-dependent gene products inside the cell (J. Karlinsey and K. Hughes, unpublished observations). Assuming a 4 minute half-life of $E\sigma^{28}$ in the presence of a high concentration of FlgM (>250 nM), this interval is sufficient for $E\sigma^{28}$ levels to be significantly affected by FlgM.

It appears that small changes in the affinity or concentration of FlgM are sufficient to have a meaningful effect on σ^{28} activity *in vivo*. *S. typhimurium* mutants expressing FlgM* proteins with only an 4 to 10-fold higher K_d for the interaction with σ^{28} could be easily distinguished from their *flgM*$^+$ parent strain on the basis of σ^{28}-dependent gene expression (28). In the SPR experiments, the effect of these mutations on the ability of FlgM to destabilize $E\sigma^{28}$ was significant. The level of FlgM in a *S. typhimurium* basal body mutant that is unable to export FlgM (and therefore does not express σ^{28}-dependent genes) is only 2-fold higher than that of an export competent strain that expresses σ^{28}-dependent genes normally (89). These observations are consistent with intracellular FlgM levels being close to the threshold concentration for σ^{28} inhibition.

Our data suggest that in addition to simply sequestering free σ^{28} from core RNAP, FlgM is capable of negatively regulating $E\sigma^{28}$ itself. We propose that regulation at the level of $E\sigma^{28}$ serves to enhance the sensitivity of the cell to changes in FlgM levels during biogenesis of the flagellar organelle. The ability to finely tune the expression of σ^{28}-dependent genes should maximize efficiency during assembly.

Recent work in our lab suggests that the level of FlgM prior to HBB completion may be more dynamic and responsive to intermediate stages in HBB development than was previously thought . Our current hypothesis is that FlgM levels are highest while the basal body substructure is being assembled, then decrease slightly during hook assembly as a prelude to dropping to their lowest level once the hook is completed and the HBB becomes competent for export (89). One purpose of the slight decrease in FlgM levels could be to ease FlgM inhibition of $E\sigma^{28}$ activity just prior to completion of the HBB. A low level of σ^{28}-dependent expression at this stage would enable the cell to synthesize a small pool of filament subunits for polymerization the moment the HBB was completed. This strategy would prevent there being a lag in flagellar biogenesis while maximal expression of flagellin was getting underway. Once export of FlgM through the completed HBB had commenced, the level of intracellular FlgM might reach a point where even sequestration of free σ^{28} from core RNAP is no longer efficient; during maturation of the filament, σ^{28}-dependent expression of flagellin is expected to reach its highest rate.

It has been proposed that as the flagella increase in length, export of FlgM should become increasingly difficult (74). This, together with the fact that *flgM* transcription is positively regulated by $E\sigma^{28}$ (52) and therefore is expected to be maximal during filament polymerization, could mean that the intracellular concentration of FlgM gradually returns to a high level as the flagella reach their mature length. FlgM inhibition of $E\sigma^{28}$ may play a homeostatic role once flagellar biogenesis is complete. Presumably at this stage there would be a large pool of active $E\sigma^{28}$. Dismantling of these complexes might play an important role in shifting the focus of cellular transcription away from flagellar promoters.

Table 4.1. Analysis of binding of FlgM proteins[a] and core RNAP to σ^{28}

Ligand	Analyte	k_a (10^5 M^{-1} sec^{-1})	k_d (10^{-4} sec^{-1})	K_d (pM)	Relative Affinity K_d*/K_d WT
His-FlgM	σ^{28}	8.9	1.6	180	---
		(5.0)	(1.0)	(200)	---
His-FlgM*L66S	σ^{28}	2.4	1.5	630	3.5x
		(2.3)	(1.6)	(720)	(3.6x)
His-FlgM*I82T	σ^{28}	5.6	3.7	660	3.7x
		(3.4)	(2.5)	(740)	(3.7x)
His-σ^{28}	His-FlgM	5.5	1.6	290	---
His-σ^{28}	His-FlgM*L66S	2.1	8.5	4000	13.8x
His-σ^{28}	His-FlgM*I82T	5.5	16	3000	10.3x
His-σ^{28}	core RNAP	4.8	3.9	800	

[a] His-FlgM proteins (wild type and mutant) were prepared in parallel. Data set in parentheses was generated with an independently purified series of His-FlgM proteins and native σ^{28}.

Figure 4.1 [A] FlgM associates with GST-σ^{28}. Crude cell extracts from *S. typhimurium* strain LT2 expressing either GST alone or a GST-σ^{28} fusion were passed over glutathione-Sepharose affinity columns. Proteins that remained on the column following washing were eluted, separated by SDS-PAGE, and stained with Coomassie blue. [lane 1] GST alone; [lane 2] GST-σ^{28} fusion.

[B] FlgM*L66S mutant is defective for the interaction with GST-σ^{28}. Assays were performed as above except that crude cell extracts were prepared from strains expressing FlgM-LacZ (Lane 1), and FlgM*L66S-LacZ (Lane 2).

A

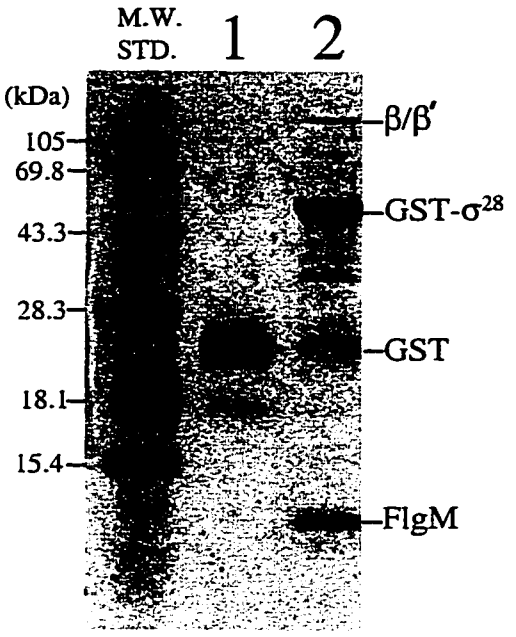
M.W.
STD.
1
2
(kDa)
105
69.8
43.3
28.3
18.1
15.4
β/β′
GST-σ28
GST
FlgM

B

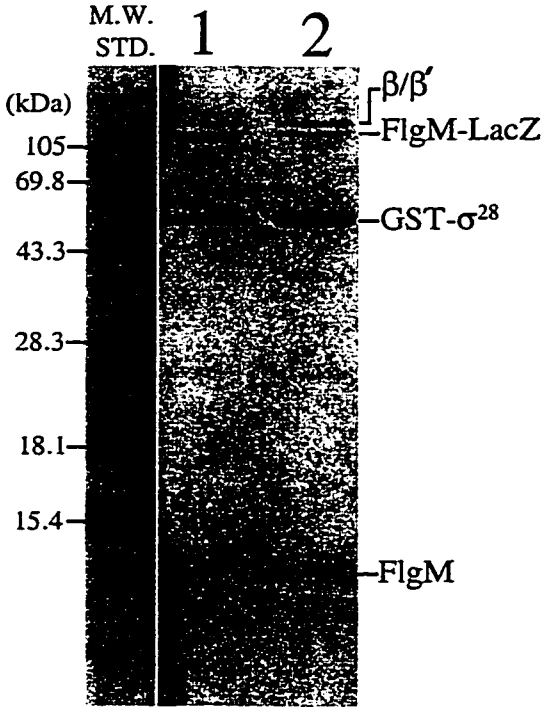
M.W.
STD.
1
2
(kDa)
105
69.8
43.3
28.3
18.1
15.4
β/β′
FlgM-LacZ
GST-σ28
FlgM

Figure 4.2 [A] Transcription from a σ^{28}-dependent promoter by reconstituted Eσ^{28}. *In vitro* transcription reactions contained 14 nM core RNAP (E) and 3 nM *fliC* promoter template. The molar ratio of His-σ^{28} to core RNAP in each reaction is indicated on the X-axis.

[B] Inhibition of σ^{28}-dependent transcription by FlgM. *In vitro* transcription assays were performed as above. The molar ratio of His-σ^{28} to core RNAP was 5:1. The molar ratio of FlgM to His-σ^{28} in each reaction is indicated on the X-axis.

A

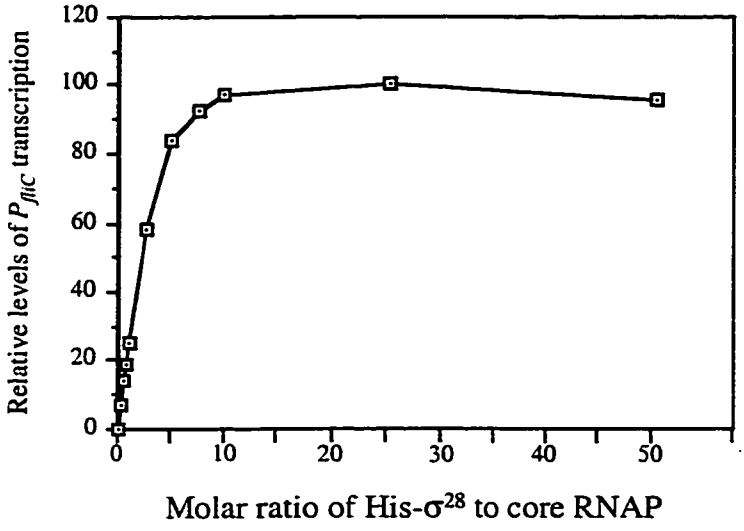
Relative levels of P_{fliC} transcription
120
100
80
60
40
20
0
0
10
20
30
40
50
Molar ratio of His-σ28 to core RNAP

B

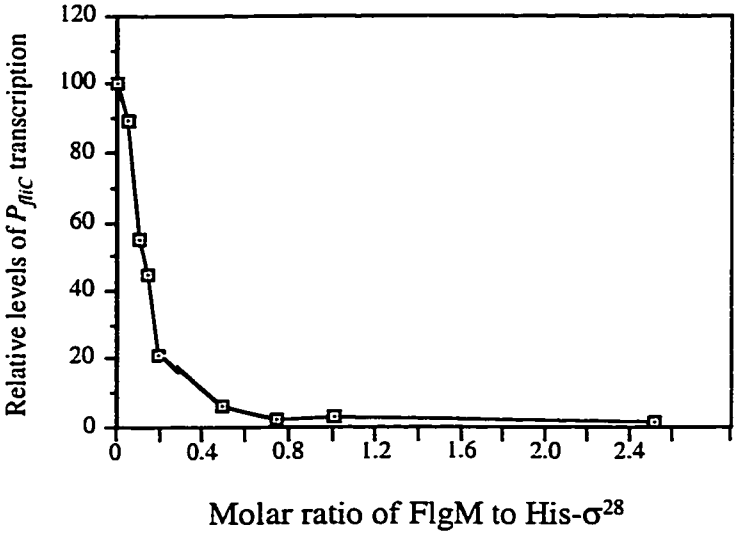
Relative levels of P_{fliC} transcription
120
100
80
60
40
20
0
0
0.4
0.8
1.2
1.6
2.0
2.4
Molar ratio of FlgM to His-σ28

Figure 4.3 FlgM interferes with specific binding of $E\sigma^{28}$ to the *fliC* promoter. Filter binding assays were used to evaluate the effect of FlgM on promoter binding by $E\sigma^{28}$. Proteins indicated above each lane were incubated together for 10 minutes prior to the addition of labeled promoter DNA. In [A] lane 5, and [B] lanes 2 and 3, proteins enclosed in brackets were pre-incubated for 10 minutes before the addition of the third protein; reactions were incubated a further 5 minutes before DNA was added. The hatched bars indicate the standard deviation (assays performed in triplicate). [A] Non-competed binding of the *fliC* promoter by σ^{28}, core RNAP (E), and FlgM. [B] Competed binding of the *fliC* promoter by σ^{28}, core RNAP (E), and FlgM. Samples were chased with unlabeled sheared salmon sperm DNA (a competitor for non-specific DNA binding) prior to sampling, so promoter DNA retained on filters represents only that bound specifically by protein.

A

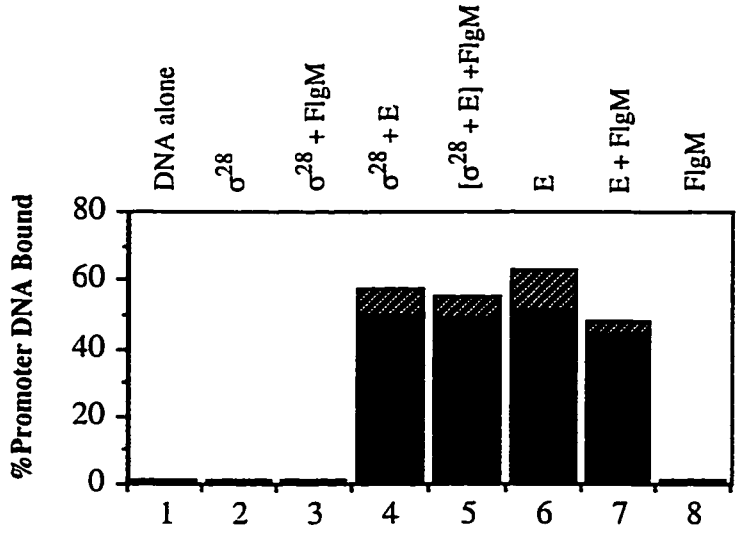
DNA alone
σ28
σ28 + FlgM
σ28 + E
[σ28 + E] +FlgM
E
E + FlgM
FlgM
% Promoter DNA Bound
80
60
40
20
0
1
2
3
4
5
6
7
8

B

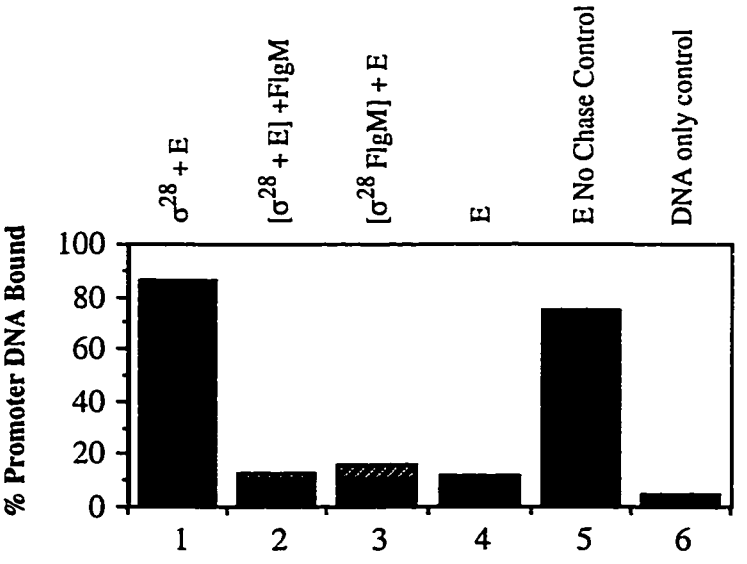
σ28 + E
[σ28 + E] +FlgM
[σ28 FlgM] + E
E
E No Chase Control
DNA only control
% Promoter DNA Bound
100
80
60
40
20
0
1
2
3
4
5
6

Figure 4.4 FlgM associates with holoenzyme *in vitro*. A combination of native PAGE [A], and denaturing SDS-PAGE [B], was used to detect complexes formed by FlgM, σ^{28}, and core RNAP. [A] Proteins shown at the top of the panel were incubated together for 15 minutes, then electrophoresed on a native polyacrylamide gel. In lane 6, proteins enclosed in brackets were pre-incubated for 10 minutes before the addition of the third protein and a further 5 minute incubation. Protein complexes were visualized by staining with Coomassie blue. [B] Bands corresponding to core RNAP or the σ^{28}/FlgM complex in [A] were excised and separated by SDS-PAGE to identify the proteins contained within them. Lane 8, σ^{28} and FlgM standards; lanes 9 through 12, the core RNA polymerase bands from lanes 4, 7, 5 and 6, respectively; lane 13, the core RNA polymerase band from a separate native gel in which the order of protein addition was as indicated at the top of the gel; lane 14, the σ^{28}/FlgM band from lane 3. [C] Denaturing gel analysis of proteins associated with $E\sigma^{70}$. A native gel (not shown) was electrophoresed with the mixture of proteins indicated at the top of lanes 16 through 20; incubations were performed as in [A]; analysis of core RNAP complex bands was performed as in [B]. Lane 15, σ^{28} and FlgM standards; lanes 16 through 20, the core RNAP-associated proteins from the mixtures indicated at the top of the lane.

A

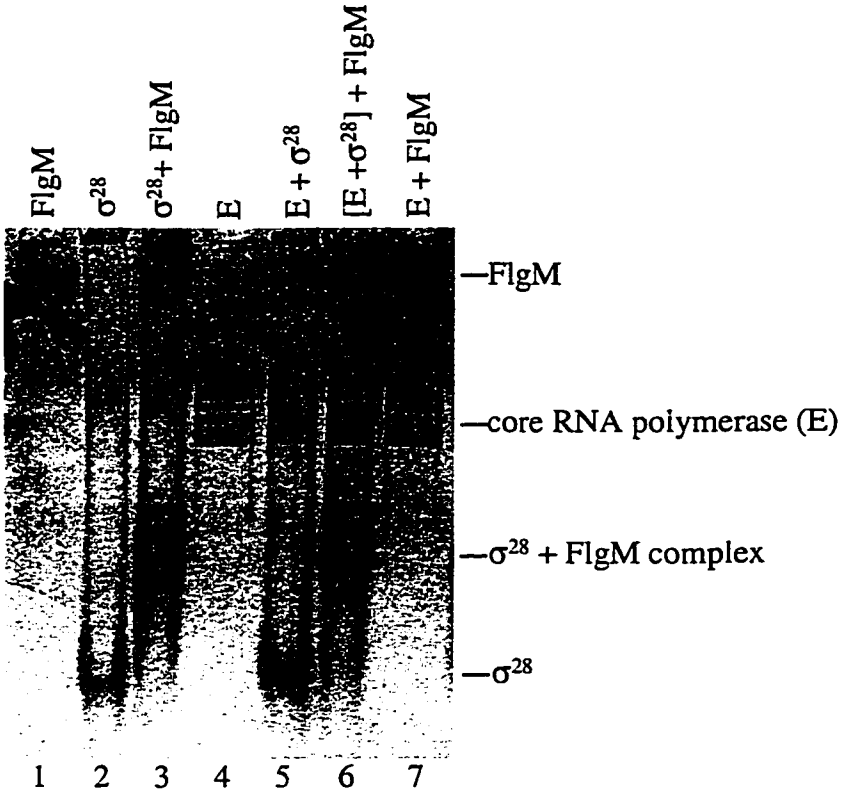
FlgM
σ28
σ28+ FlgM
E
E + σ28
[E +σ28] + FlgM
E + FlgM
—FlgM
—core RNA polymerase (E)
—σ28 + FlgM complex
—σ28
1
2
3
4
5
6
7

B

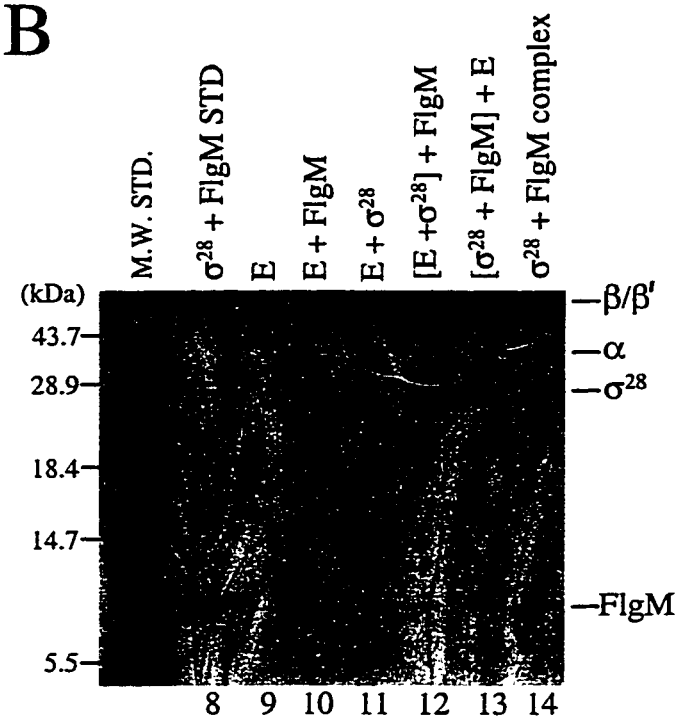
M.W. STD.
σ28 + FlgM STD
E
E + FlgM
E + σ28
[E +σ28] + FlgM
[σ28 + FlgM] + E
σ28 + FlgM complex
(kDa)
43.7
28.9
18.4
14.7
5.5
β/β′
α
σ28
FlgM
8 9 10 11 12 13 14

C

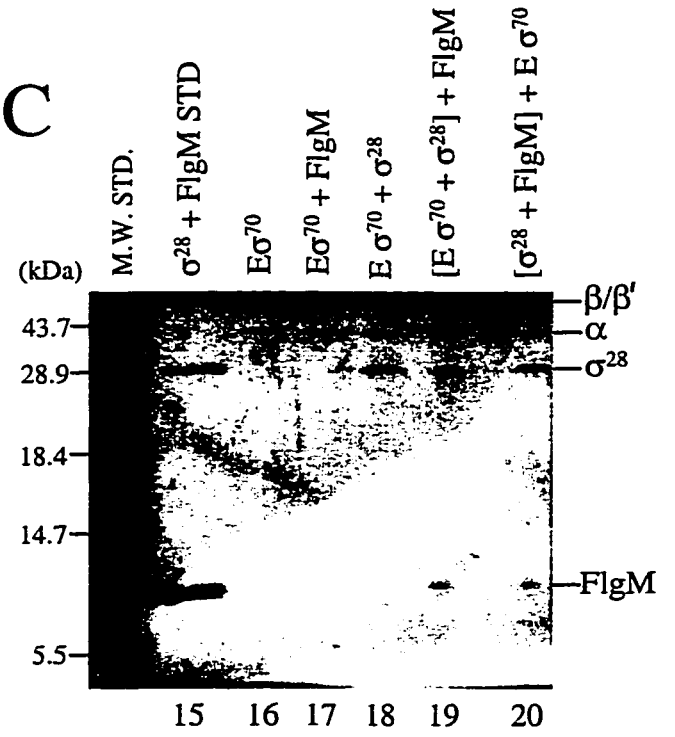
M.W. STD.
σ28 + FlgM STD
Eσ70
Eσ70 + FlgM
E σ70 + σ28
[E σ70 + σ28] + FlgM
[σ28 + FlgM] + E σ70
(kDa)
43.7
28.9
18.4
14.7
5.5
β/β′
α
σ28
FlgM
15 16 17 18 19 20

Figure 4.5 [A] Transcription from a σ^{28}-dependent promoter by reconstituted Eσ^{28}. Reaction mixtures contained 30 nM His-core RNAP (E) and 3 nM template DNA (either the σ^{28}-dependent *fliC* promoter [O], or the σ^{70}-dependent *tac* promoter [●]). The molar ratio of native σ^{28} to core RNAP in each reaction is indicated on the X-axis. The amount of ^{3}H-UTP incorporated during 10 minute RNA synthesis reactions is indicated on the Y-axis. Error bars indicate the standard deviation (assays performed in triplicate).

[B] Inhibition of σ^{28}-dependent transcription by FlgM and mutant FlgM* proteins. Purified His-FlgM proteins were incubated with native σ^{28} and core RNAP prior to the initiation of transcription. Reaction mixtures contained 30 nM core RNAP and 15 nM σ^{28}. FlgM [O]; FlgM*L66S [Δ]; FlgM*I82T [▲]. The molar ratio of His-FlgM to σ^{28} in each reaction is indicated on the X-axis. The level of RNA synthesis during each 10 minute transcription reactions is expressed in terms of the percent maximal transcription (in the absence of His-FlgM protein). Error bars indicate the standard deviation (assays performed in triplicate).

A

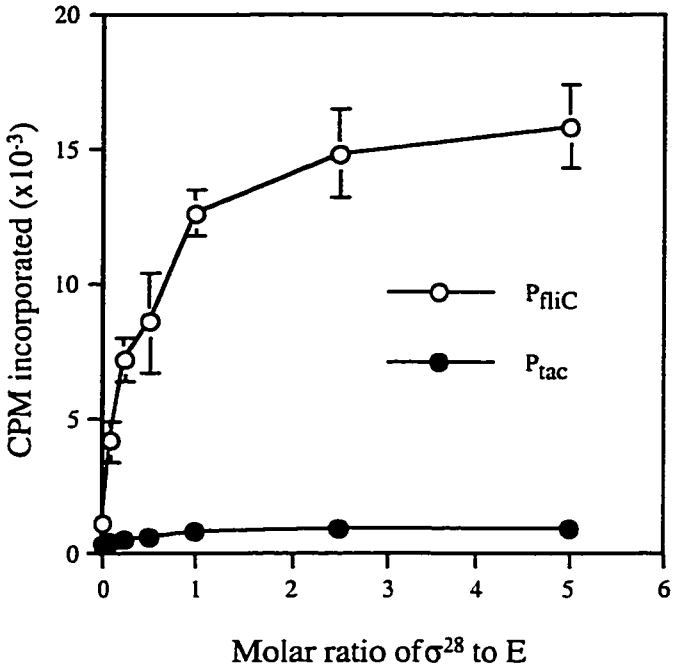
20
15
10
5
0
CPM incorporated (x10-3)
PfliC
Ptac
0
1
2
3
4
5
6
Molar ratio of σ28 to E

B

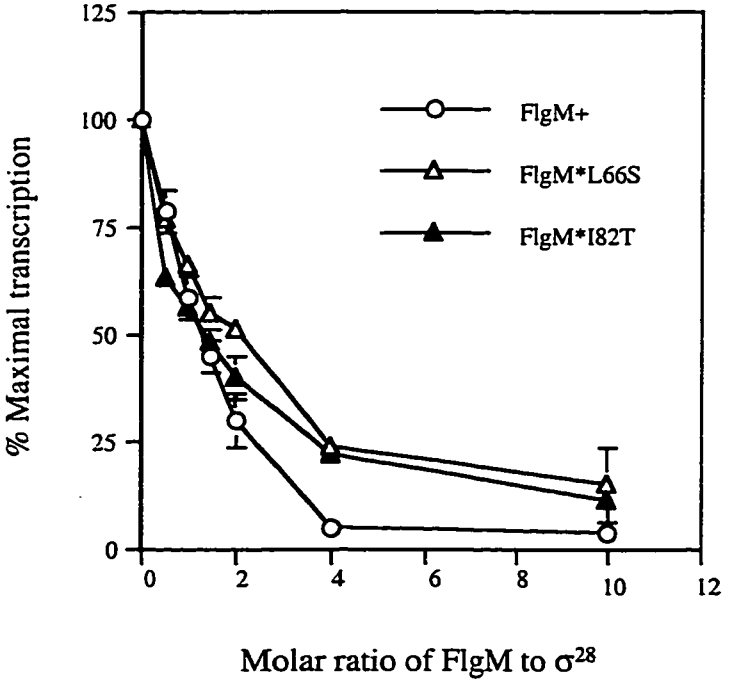
125
100
75
50
25
0
% Maximal transcription
FlgM+
FlgM*L66S
FlgM*I82T
0
2
4
6
8
10
12
Molar ratio of FlgM to σ28

Figure 4.6 SPR analysis of the effect of FlgM proteins on the rate of dissociation of RNAP holoenzyme. An SPR-based assay was used to evaluate the effect of FlgM on the stability of $E\sigma^{28}$. The amount of core RNAP bound to sigma immobilized on the chip surface was measured in resonance units (RU); the change in RU during the course of the experiments are plotted as a function of time (seconds). All curves have been normalized relative to the start of analyte injection. The horizontal bar at the top of each panel defines the period during which core RNAP (the analyte) was injected (association phase). The dissociation rate constant (k_d) for RNAP holoenzyme in the presence of the FlgM proteins or in HBS buffer are displayed next to the curves. [A] FlgM increases the rate of $E\sigma^{28}$ dissociation, and FlgM* mutants are defective for this activity. A 50 nM solution of purified core RNAP in HBS buffer was injected over a surface of immobilized σ^{28} to generate a layer of $E\sigma^{28}$. Dissociation of $E\sigma^{28}$ was carried out in HBS buffer, or in HBS buffer containing 250 nM His-FlgM, 250 nM His-FlgM*L66S, or 250 nM His-FlgM*I82T. [B] $E\sigma^{70}$ is not destabilized by FlgM. These experiments were carried out in the same manner as above, except that His-σ^{70} instead of σ^{28} served as the immobilized ligand, and the amount of His-FlgM during dissociation was 50 nM.

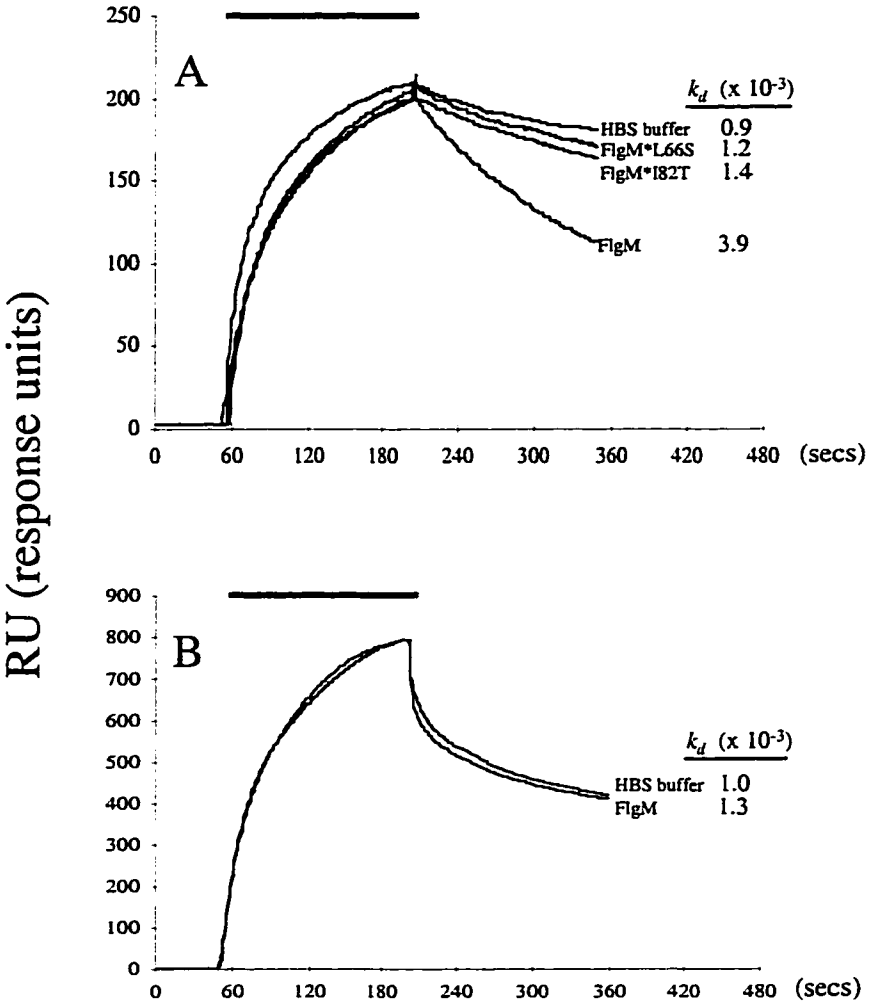
RU (response units)
A
B
k_d (x 10^{-3})
HBS buffer 0.9
FlgM*L66S 1.2
FlgM*I82T 1.4
FlgM 3.9
k_d (x 10^{-3})
HBS buffer 1.0
FlgM 1.3
(secs)
(secs)

Figure 4.7 Models for the mechanism of FlgM-mediated holoenzyme destabilization. Conserved σ regions 2, 3 and 4 are numbered. σ^{28} regions interacting with core RNAP (E) are shaded dark gray; σ^{28} regions interacting with FlgM are shaded light gray. Free FlgM is depicted as an unstructured molecule; σ^{28}-bound FlgM is depicted in a constrained conformation. For simplicity, only the C-terminal σ^{28}-binding domain of FlgM is shown participating in the interaction with σ^{28}. [A] Competitive Displacement model. $E\sigma^{28}$ breathing alternately exposes σ regions 2 and 3. FlgM partially bound to σ^{28} can compete with E for rebinding to regions 2 and 3 to effect dissociation. For simplicity, FlgM is only shown interacting with one of the two partially bound forms of σ^{28}. [B] Allosteric Displacement model. Binding of FlgM to exposed region 4 stabilizes a σ^{28} conformation that is incompatible with E, resulting in the release of the σ^{28}/FlgM complex.

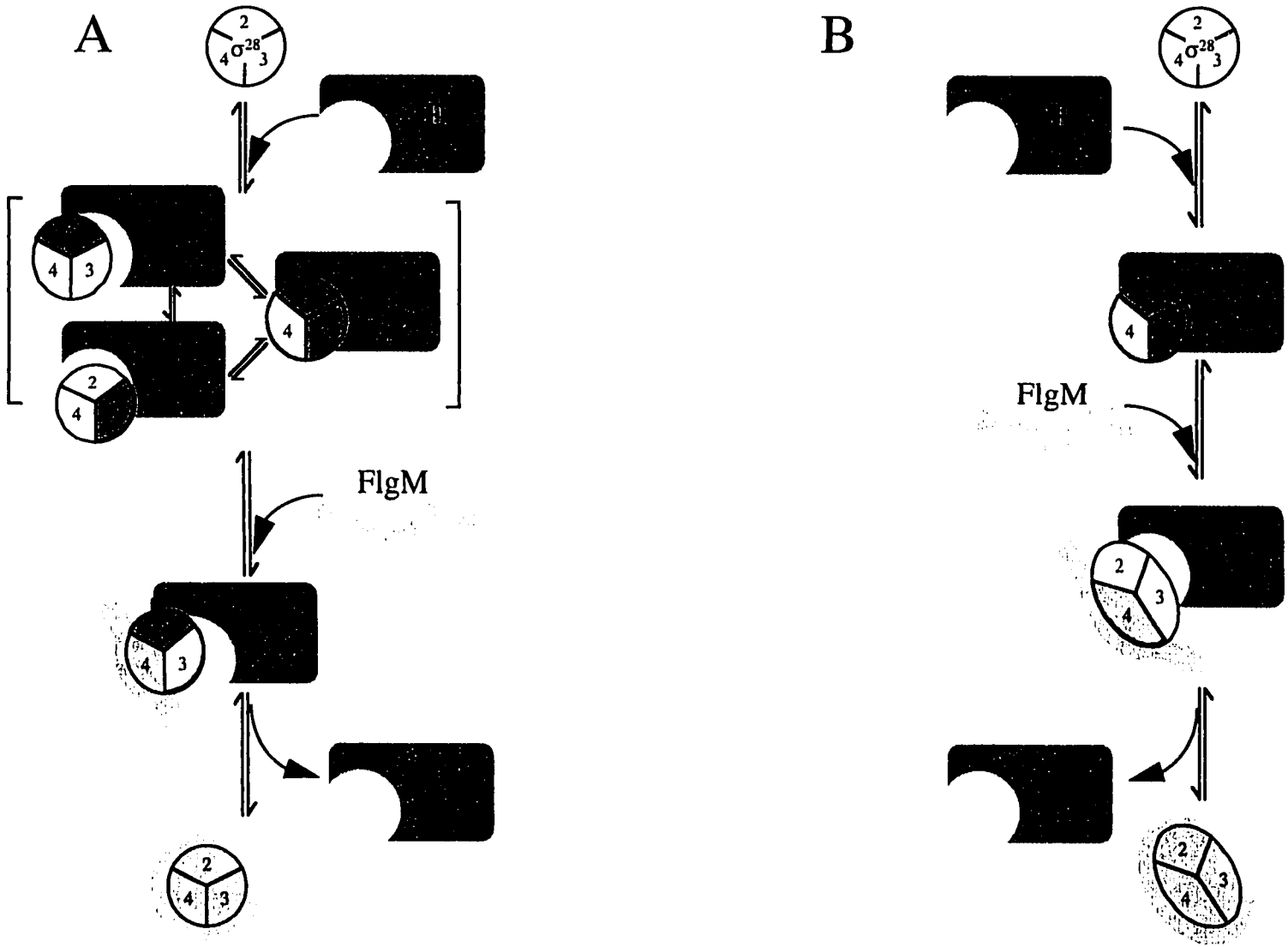
A
2
4 σ28 3
4 3
4
2
4
FlgM
4 3
2
4 3
B
2
4 σ28 3
4
FlgM
2
3
4
2
3
4

CHAPTER 5

In Vitro Characterization of σ^{28}* Mutants

INTRODUCTION

Our investigation into the mechanism of FlgM inhibition of σ^{28} activity began with a genetic analysis of mutants defective for negative regulation of Class 3 gene expression. This analysis generated a collection of *fliA* mutants able to transcribe Class 3 promoters in the presence of FlgM (*fliA** mutants). *In vivo* assays of *fliA** activity suggested that most of these mutants were defective in some aspect of their interaction with FlgM (the possible exceptions were the mutants altered at residues 14 in the putative core RNAP binding domain). Models for the mechanism of FlgM-mediated inhibition based on the distribution of *fliA** mutations predicted three potential classes of *fliA** mutants: those that had a decreased affinity for FlgM, those that bound FlgM normally, but were unaffected by its presence, and those that bound core RNAP with a higher affinity.

The experiments described in this chapter were intended to test these models by characterizing the interactions between the mutant σ^{28} proteins (σ^{28}*) and FlgM, and between the σ^{28}* mutants and core RNAP. SPR-based assays of the affinities of the σ^{28}* mutants for FlgM were expected to reveal which regions of σ^{28} were involved in FlgM binding. A decreased affinity for FlgM would indicate that the mutated residue normally contributed to complex formation. A σ^{28}* mutant that bound FlgM normally might belong to the second predicted class of *fliA** mutants, i.e. those defective for a FlgM-induced allosteric shift that presumed to disrupt core RNAP binding. An increased affinity for core RNAP would support the idea that FlgM and core RNAP are in direct competition for σ^{28} binding (as well as provide evidence for domain-specific contact between a sigma factor and core RNAP).

In vitro transcription assays of the activities of the σ^{28}* mutants in the presence of FlgM would reveal whether a decreased affinity for FlgM correlated with decreased sensitivity to inhibition by FlgM (this result would be predicted, based on the *in vitro* behavior of the FlgM* mutants (see Chapter 4). Any σ^{28}* mutants that had normal FlgM binding activity would be assayed to determine whether they could also function more efficiently than wild type σ^{28} in the presence of FlgM. If these mutants displayed a decreased sensitivity to negative regulation by FlgM, it would support the allosteric model for anti-σ^{28} activity (see Chapter 3 and 103).

The previous chapter described our efforts to determine the form(s) of σ^{28} (free σ^{28} vs. Eσ^{28}) inhibited by FlgM. In addition to demonstrating a high affinity complex between FlgM and free σ^{28}, we were able to show that FlgM is capable of interacting with Eσ^{28}, and that the effect of that interaction is to destabilize the holoenzyme complex. Our models for the mechanism of holoenzyme destabilization invoked a multipartite interaction between FlgM and σ^{28}, involving conserved sigma domains 2.1, 3.1 and 4.1/4.2 (based on the distribution of fliA* mutants obtained in the genetic analysis, and by analogy to another sigma/anti-sigma factor interaction; 33). The following analysis of the affinities of the σ^{28}* mutants for FlgM would provide evidence for or against these models. We also proposed that FlgM and core RNAP both recognize regions 2.1 and 3.1 of σ^{28}; the competitive displacement model for holoenzyme destabilization predicted that FlgM must bind to these regions to effect the release of σ^{28} from holoenzyme. By repeating the SPR-based assays for holoenzyme destabilization using σ^{28}* mutants, the involvement of regions 2.1, 3.1 and 4.1/4.2 in this process might be determined.

A number of σ^{28}* mutants from each region were chosen for the *in vitro* analysis. The major criterion in the selection of these mutants was their degree of FlgM-insensitivity *in vivo*. The biochemical analysis of FlgM* mutants had demonstrated that

an easily distinguishable *in vivo* phenotype could be relatively subtle *in vitro*. We reasoned that the σ^{28}* mutants with the strongest *fliA** phenotypes would be more likely to have detectable differences in their *in vitro* activity. The mutants chosen on this basis were: H14D and H14N (region 2.1); M104T, N114K and T138I (region 3.1); L199R (region 4.1), V213E and R231Q (region 4.2). Two additional mutants were also chosen: V33E (region 2.1), because it appeared to confer insensitivity to FlgM by a different mechanism than the other region 2.1 mutants at residue 14, and E203D (region 4.1) because we were interested in the effect this conservative substitution mutation could have on FlgM binding or inhibition.

RESULTS

Purification of σ^{28} mutants.* The toxicity of high levels of σ^{28}* protein required that the σ^{28}* mutants be overexpressed in the presence of FlgM. Consequently, it was necessary to purify the σ^{28}* proteins under denaturing conditions to remove contaminating FlgM. σ^{70} recovered 100% of its original activity when renatured from 6 M Guanidine (58), and native σ^{28} also appeared to recover a high level of activity when renatured according to this protocol (see Chapter 4). Denaturing purification of histidine tagged proteins by nickel affinity chromatography was used successfully to purify His-σ^{28} protein (see Chapter 4). N-terminally tagged His-σ^{28} and native σ^{28}* regained equivalent levels of activity when renatured from 6 M guanidine; in *in vitro* transcription assays, the rate of transcription approached its maximum at a one-to-one ratio of either σ^{28} or His-σ^{28} to core RNAP (data not shown). Accordingly, the σ^{28}* mutants were purified as N-terminal His-tag fusion proteins. That the purified renatured His-σ^{28}* proteins eluted as monomers from a sizing column (see Chapter 2) indicated that none of the substitution mutations caused gross defects in refolding leading to protein aggregation.

Kinetic analysis of σ^{28}/FlgM and σ^{28}*/core RNAP interactions.*_SPR-based assays of the σ^{28}*/FlgM interactions were carried out as described in Chapter 4, except the His-FlgM ligand was covalently linked via a lysine residue to the sensor surface (the nickel affinity sensor chip to which His-FlgM was non-covalently attached in the previous experiments could not be used here because it would also non-specifically capture the His-σ^{28}* analyte). The k_a and k_d, the calculated dissociation constant, and the relative affinities of each σ^{28}*/FlgM pair are reported in Table 5.1 (a complete kinetic analysis was not performed for the H14D and H14N mutants. Preliminary binding assays indicated that their affinity for His-FlgM was identical to that of wild type σ^{28}). With the exception of H14D and H14N, all of the σ^{28}* mutants exhibited a decreased affinity for FlgM, with the most drastic binding defects caused by the substitutions at positions L199R and V213E. To test whether the severe FlgM binding defects of these two mutants was due to a low specific activity rather than to disruption of critical contact residues, we performed the inverse assay, using His-σ^{28} proteins as the ligand, and measuring binding of soluble His-FlgM. In these assays, the covalently immobilized σ^{28} was regenerated by a pulse of 6 M Guanidine buffer and renatured on the sensor surface immediately prior to each round of FlgM binding. Previous assays of core RNAP binding by a σ^{28} surface treated in this manner indicated that the specific activity of the σ^{28} was completely restored following each regeneration cycle. For comparison, wild type σ^{28} and two σ^{28}* mutants moderately defective for FlgM binding, E203D and R231Q, were also analyzed in this fashion. The k_a and k_d, the calculated dissociation constant, and relative binding affinities of these σ^{28}*/FlgM pairs are reported in Table 5.1B. FlgM binding by the wild type σ^{28} and the E203D and R231Q mutants was quantifiable; the rate constants obtained from these data were on the same order as those obtained in the first set of assays. Neither L199R nor V213E

bound a significant level of FlgM in these assays. This behavior was consistent with the substitution mutations at residues 199 and 213 disrupting important FlgM contacts.

The His-σ^{28}*/core RNAP interactions were measured using the same protocol developed for assaying core RNAP binding by wild type σ^{28}. The current Biacore technology allows three different ligand surfaces and a blank reference surface to be assayed simultaneously. The data summarized in Table 5.2 are therefore grouped in sets of three σ^{28} alleles, with the relative affinities of two σ^{28}* mutants for core RNAP derived by comparison to an internal wild type σ^{28} control in each set. Two conclusions were drawn from these data. First, the high affinities of each of the mutant σ^{28}* alleles for core RNAP indicated that none of the substitution mutations caused any gross structural defects that could account for the FlgM binding defects measured by SPR above. Second, although there were some differences between the K_d values obtained for some of the σ^{28}*/core RNAP interactions and the K_d of the wild type σ^{28}/core RNAP measured in parallel, this variability was not greater than that observed among independent assays of the wild type σ^{28}/core RNAP interaction. In assays such as these, where the comparison being made is between the different ligand surfaces for the same analyte (as opposed previous assays measuring the ability of various σ^{28}* mutants to bind to the same FlgM surface), variation within one order of magnitude cannot be considered significant, especially when the k_a and k_d approach the limits of the system's sensitivity, as they do here. Therefore, we conclude from these assays that all of the σ^{28}* mutants bind core with approximately equal affinity.

We wondered whether mutations that decreased the affinity of FlgM for free σ^{28}* would also interfere with the ability of FlgM to dissociate the Eσ^{28}* complex. The rates of holoenzyme dissociation in the presence and in the absence of FlgM was compared for four σ^{28}* mutants with moderate to strong defects for FlgM binding (Table 5.3). Two region 3.1 mutants, N114K and T138I, behaved similarly to wild

type σ^{28} in these assays, dissociating from core RNAP approximately 5x faster in the presence of FlgM. These results suggested that FlgM binding to region 3.1 was not involved in the process of holoenzyme dissociation. In contrast, the region 4.1 mutants L199R and E203D both dissociated from core RNAP at the same rate regardless of whether FlgM was present during the dissociation phase. The insensitivity of these mutant $E\sigma^{28}$* complexes to FlgM indicated that contacts with region 4.1 were critical for holoenzyme destabilization. Although the H14D and H14N mutants had not demonstrated altered binding kinetics for either core or FlgM, the possibility that the mutations interfered with the ability of FlgM to dissociate $E\sigma^{28}$* was tested. The presence of FlgM did not increase the rate of $E\sigma^{28}$* dissociation in these assays above that of wild type $E\sigma^{28}$. Thus, the *in vivo* phenotype of the H14D and H14N mutants did not seem to be due to an increased resistance to negative regulation by FlgM.

In vitro transcription activities of the σ^{28} mutants*. We had predicted that the σ^{28}* mutants with a decreased affinity for FlgM would be able to transcribe more efficiently in the presence of FlgM. *In vitro* transcription assays were carried out to test this prediction. Having ruled out the possibility that the *fliA** phenotype of the residue 14 mutants was due to a higher affinity for core RNAP, we were interested to know whether they retained their "enhanced basal activity" phenotype *in vitro*. σ^{28}* mutants from each region were assayed in parallel, both alone and in the presence of FlgM. Because the specific activity of the σ^{28} preparations was less than 100% by the time the transcription assays were performed, these experiments are interpreted qualitatively.

Figure 5.1A illustrates the basal sigma activities of the region 2.1 σ^{28}* mutants relative to wild type σ^{28}. As expected, the σ^{28}* mutants H14D and H14N had a very similar profile to wild type σ^{28}. Unexpectedly, V33E demonstrated a higher than wild type activity. An independent preparation of σ^{28}* proteins gave essentially identical

results (data not shown). Despite a 9-fold decrease in its affinity for FlgM, the V33E mutant was as sensitive to FlgM-mediated inhibition as wild type σ^{28} in these assays (Figure 5.2A). H14D and H14N actually appeared to be slightly more sensitive to FlgM than wild type σ^{28}.

The basal sigma activities of the region 3.1 mutants are shown in Figure 5.1B. Again, one of the mutants, T138I, had a higher activity than wild type σ^{28}. The other two mutants, M104T and N114K, appeared to function less efficiently than wild type σ^{28}. All of these mutants displayed a higher tolerance for FlgM than wild type σ^{28} (Figure 5.2B), consistent with their decreased affinity for FlgM. The sensitivity of these *in vitro* transcription assays may have been such that a greater than 10-fold increase in the K_d of the σ^{28}*/FlgM interaction was required to have a detectable effect on transcription in the presence of FlgM.

The variation in the basal sigma activities of the region 4.1/4.2 σ^{28}* mutants (Figures 5.1C and 5.1D) reflects the importance of this region in the interaction between Eσ^{28} and the promoter. V213E and R231Q appeared to be less active than wild type σ^{28}. L199R was barely able to stimulate specific transcription at the same molar ratio of σ^{28} to core RNAP that produced a 30-fold increase in the wild type σ^{28} assay. The core RNAP binding activity of the σ^{28}*(L199R) protein used in this assay appeared to be low, however, since transcription could be partially rescued by increasing the amount of σ^{28} protein in the reaction. Our SPR assays had demonstrated that L199R is capable of binding core RNAP with normal affinity when assayed immediately after renaturation out of 6 M Guanidine buffer; the low basal sigma activity demonstrated by this mutant in the transcription assays suggests that the activity of purified σ^{28}*(L199R) protein is unstable. Figure 5.2C illustrates the effect of FlgM on the ability of the σ^{28}* mutants E203D, V213E and R231Q to carry out transcription. E203D and R231Q, whose FlgM binding defects were of the same magnitude as those of the region 3.1 σ^{28}* mutants,

also exhibited a similar degree of sensitivity to FlgM in these assays. V213E, which exhibited a 55 to 70-fold weaker affinity for FlgM, was not inhibited by a level of FlgM sufficient to completely abolish promoter-specific transcription by wild type σ^{28}. In the presence of a 50-fold excess of FlgM, V213E was able to transcribe at 80% of its maximal level, and at a 250-fold excess of FlgM (the highest level tested), transcription was only reduced 50% (data not shown). The ability of L199R to direct transcription in the presence of FlgM was assayed at a 30-fold excess of σ^{28} factor relative to core RNAP. Even at a concentration of σ^{28}* several times higher than the K_d of the σ^{28}*L199R/FlgM interaction (120 nM), a 25-fold molar excess of FlgM to σ^{28}*L199R did not abolish transcription (the level was still 10-fold above background; data not shown), consistent with the severe FlgM binding defect of this mutant.

Western analysis of the relative levels of σ^{28} and FlgM in vivo. The above experiments had provided evidence for direct contacts between FlgM and all three regions of σ^{28}, and demonstrated that those contacts were important for FlgM-mediated inhibition of σ^{28} activity. No explanation had been found, however, for the enhanced activity of the H14D and H14N mutants seen *in vivo*, both in the presence and in the absence of FlgM. A quantitative analysis of the intracellular levels of the σ^{28}* proteins had never been done, so the possibility remained that substitutions at residue 14 merely increased the steady state level of σ^{28} in these *fliA** mutants. Efforts to develop a quantitative assay to measure the absolute levels of σ^{28} and FlgM had not been successful (the cross-reactivity of our anti-σ^{28} and anti-FlgM antibodies prevented us from employing straightforward quantitative immunoprecipitation assays).

In order to address the issue of steady state levels of σ^{28} and FlgM in the *fliA** mutants, we performed qualitative Western analyses comparing the amounts σ^{28} and FlgM protein in each mutant strain to those in a wild type strain. An example of one of

these experiments is shown in Figure 5.3. Of all of the *fliA** mutants tested, only the H14D and H14N expressed a significantly higher level of σ^{28} than the wild type strain. The Class 3^{ON} phenotype of these *fliA** mutants might be explained by a higher than normal ratio of σ^{28} to FlgM protein in the cell. To determine if this was the case, total cell protein from wild type σ^{28} and the σ^{28}* H14D aned H14N mutants was serially diluted, separated by SDS-PAGE, and probed with anti-σ^{28} and anti-FlgM antibodies. By comparing the rates at which the σ^{28} and FlgM signals diminished with increasing dilution in the wild type strain and the mutant strains, we hoped to be able to detect any differences in the relative levels of the two proteins. The results of this experiment are shown in Figure 5.4. In the wild type strain, the intensity of the σ^{28} and FlgM signals was similar, such that they both appeared to be on the verge of fading out at the highest dilution (shorter exposures of this chemiluminescent Western confirmed this observation). In the two mutants strains, however, the σ^{28} signal seemed to persist longer than the FlgM signal. This effect was more noticeable in H14N than in H14D. Thus, the higher level of Class 3 transcription in these mutants could be attributed to a higher ratio of σ^{28} to FlgM.

Discussion

Our interpretation of the genetic analysis of *fliA** mutants described in Chapter 3 was that there are three distinct FlgM binding domains on σ^{28}, in regions 2.1, 3.1 and 4.1/4.2. This is a different conclusion than the one reached previously (103), but it agrees with work carried out in an analogous sigma factor/anti-sigma factor system in *B. subtilis*, σ^{F}/SpoIIAB (33). The location of FlgM binding determinants in the potential core binding regions 2.1 and 3.1 is consistent with our observation that the concentration of FlgM required to see an effect on Eσ^{28} stability is much higher than the K_d of the σ^{28}/FlgM complex. Our evidence for a direct interaction between FlgM and

regions 2.1 and 3.1 makes it unnecessary to invoke an allosteric mechanism to explain the ability of FlgM to interfere with core binding by free σ^{28}; simple steric inhibition of the core binding determinants could account for this activity. The *fliA** phenotypes of the two region 2.1 mutants that failed to demonstrate either a decreased affinity for, or sensitivity to, FlgM *in vitro* could be explained by their higher than normal *in vivo* levels relative to FlgM. Thus, characterization of σ^{28}* mutants isolated by selecting for a Class 3^{on} phenotype has resulted in a clearer picture of the mechanism of FlgM-mediated inhibition.

The severity of the FlgM binding defects caused by mutations in region 4.1/4.2 suggests that this region contains the dominant FlgM binding determinants. This hypothesis is consistent with the observation that, *in vivo*, only σ^{28} polypeptides containing region 4.1/4.2 had significant FlgM binding activity (103). A σ^{28}/FlgM interaction that was initiated at region 4.1/4.2 would rapidly progress to form a multipartite complex, as the local concentration of FlgM would then be sufficient to promote the presumably weaker interactions between FlgM and σ^{28} regions 2.1 and 3.1. Requiring that complex formation occur stepwise, beginning with the least well-conserved σ^{28} region 4.1/4.2, would explain how FlgM is able to target the highly conserved core RNAP binding domains while simultaneously maintaining specificity for σ^{28}.

The ability of FlgM to increase the rate of dissociation of holoenzyme containing region 3.1 σ^{28}* mutants, but not region 4.1 σ^{28}* mutants, suggests that region 3.1 of core RNAP-bound σ^{28} is not accessible to FlgM. We proposed in Chapter 4 that region 3.1 of σ^{28}* may participate in the σ^{28}/core RNAP interaction. Masking of region 3.1 by core would explain why region 3.1 σ^{28}* mutations that decrease the affinity of FlgM for free σ^{28} had no effect on FlgM-mediated Eσ^{28}* dissociation. This result is also consistent with the allosteric displacement mechanism for holoenzyme destabilization,

which does not require FlgM to interact with σ^{28} regions involved in core RNAP binding to achieve holoenzyme destabilization.

The *in vitro* transcription assays revealed differences in the basal sigma activity of the σ^{28}* mutants. Certain mutants, V33E and T138I, exhibited a higher-than-normal level of activity. Because these mutants are only moderately defective for FlgM binding, their strong *fliA** phenotype *in vivo* may in part be due to this enhanced basal activity. Other mutants were impaired in their basal sigma activity. These were (in order of severity), L199R, V213E and R231Q, and N114K and M104T. It is worth noting that the basal sigma activity of E203D, the most conservative substitution mutation included in the *in vitro* analysis, was identical to that of wild type. Aspartic acid differs from glutamic acid only in that its side chain is shorter by one methylene group; it is not surprising that this substitution should not introduce any gross structural defects that would compromise sigma factor activity. That so subtle a change should have a significant effect on FlgM binding argues that this residue makes a positive energetic contribution to the interaction.

Because the specific activity of the σ^{28}* proteins used in these transcription assays was low, we did not determine at what concentration of each σ^{28}* mutant maximal transcription was reached. It is not possible from our data to distinguish between σ^{28}* mutants that were simply required at a higher or lower concentration in order to achieve the same maximal level of transcription as wild type σ^{28}, and mutants whose maximal level of transcription was different from that of wild type σ^{28}. The importance of this distinction is illustrated in Figure 5.5. For simplicity, the complex process of transcription is represented as involving only two basic steps: promoter binding, and promoter clearance (Figure 5.5A). In this model, all of the steps involved in the formation of a Eσ/promoter complex (E + σ, Eσ + promoter, and closed complex formation) are considered together as a process characterized by the equilibrium constant

K_1. Similarly, the forward rates of all of the steps between closed complex formation and elongation have been condensed into a single rate constant, k_2. Figures 5.5B and 5.5C illustrate the different transcription curves that would result should either K_1 or k_2 become less efficient. A σ^{28}* mutant defective for holoenzyme formation or promoter binding, but normal for isomerization, transcription initiation and clearance would produce the curve in (B). A σ^{28}* mutant that occupied the promoter with normal efficiency, but was impaired at a subsequent step would produce the curve in (C). Both curves appear similar when sigma is limiting, as it was in the transcription assays performed on the σ^{28}* mutants. Information about the maximal level of transcription supported by the σ^{28}* mutants would have allowed us to go further in our analysis, and class the mutants according to the stage of transcription affected by their substitution mutation.

What might the effects of the various substitution mutations on basal sigma activity be? Both of the mutations that enhanced σ^{28} activity, V33E and T138I, occurred in sigma domains that are thought to be important to the σ/core RNAP interaction. Despite our failure to detect a significant difference between the ability of these mutants and wild type σ^{28} to form holoenzyme, it is still possible that the mutations affect the interaction between σ^{28} and core RNAP at a later point in the transcription process. The sigma/core interface is where information about the state of the promoter is communicated to the core enzyme. Leonetti has proposed that the interactions and points of contact between the sigma subunit and core RNAP are likely to evolve during the progression from closed complex to the elongation phase (108). Depending on how region 2.1 of σ^{28} is aligned with σ^{70}, two possible effects of the substitution at V33 can be imagined. The alignment of Lonetto et al. (118), shown in Figure 5.6, positions V33 on the kink between helices 12b and 13, as defined by the crystal structure of σ^{70} (128), very near to the DNA binding helix (helix 14) in region

2.4. It is conceivable that the substitution at this position has a positive effect on the ability of region 2.4 to interact with the -10 determinants of the promoter. Alternatively, if region 2.1 is aligned on the basis of homology between the core binding motif VEANLRL of σ^{70} and the EA-LRL sequence of σ^{28}, V33, which closely follows that sequence, aligns with a conserved hydrophobic residue proposed to form part of the core binding surface (128). Substitution of a charged residue for a hydrophobic one at a protein/protein interface might destabilize that interaction. Perhaps a weakened interaction facilitates the dissociation of core from sigma bound at the promoter during the elongation phase of transcription. The Lonetto alignment also positions T138I very near to a stretch of residues that has been demonstrated to contribute to core binding in σ^{32} (85, 193). Little is known about the structure and function of region 3.1, so it is difficult to theorize about the effect of this substitution other than to suggest that, like V33E, it may enhance a sigma/core interaction occurring at the promoter.

In keeping with the importance of region 4.1/4.2 for promoter recognition, the substitutions in this domain had the greatest impact on basal sigma factor activity. The introduction of a positive charge at position L199 appeared to destabilize the purified σ^{28}*(L199R) protein. L199 is a conserved aliphatic residue in a region that can be modeled as an amphipathic helix. Based on the similarity of region 4.1/4.2 to other DNA binding proteins, it has been proposed that this putative amphipathic helix stabilizes the HTH motif in the adjacent -35 promoter binding domain by packing against the first helix of that motif (118). The substitution of a positively charged residue at L199R may disrupt this stabilizing interaction. When σ^{28} region 4.2 is modeled as a helix-turn-helix, V213 lies along the hydrophobic face of the first helix (see Figure 3.9). Introduction of a negative charge at this position may interfere with packing of this helix against the second helix of the HTH, or with the upstream amphipathic helix. R231 lies at the very C-terminal end of region 4.2; there is no

evidence for contacts between analogous residues in other sigma factors and DNA at this position. However, recent evidence supports a role for this region in the sigma/core interaction. Substitution of a tryptophan at residue L278 of σ^{32} (analogous to residue L232 in σ^{28}) caused a strong transcriptional defect (85). A 20-fold higher concentration of this mutant σ^{32} protein was required to achieve the wild type maximal transcription level (85). Glycerol gradient sedimentation experiments revealed that L278W was defective for core RNAP binding (85). We did not detect a significant decrease in the ability of σ^{28}* R231Q to form holoenzyme in our SPR-based assay. Therefore, we propose that if this residue is involved in the σ^{28}/core interaction, its influence is felt at a later step in the transcription process.

Figure 5.6 shows regions 2.1, 3.1 and 4.1/4.2 of *E. coli* σ^{70}, *S. typhimurium* σ^{28}, and *B. subtilis* σ^{F} aligned according to Lonetto et al. (118). The positions at which anti-sigma factor insensitive mutations were obtained in σ^{28} and in σ^{F} (33) are indicated. In both cases, mutations that disrupted the sigma factor/anti-sigma factor interaction clustered in regions 2.1, 3.1 and 4.1/4.2, implying that the two sigma factor/anti-sigma factor pairs interact in a topologically similar manner. Substitution of alanine at σ^{F} positions V48, V137, E149, E156 and L213 revealed that the residues likely to be making important positive contributions to the σ^{F}/SpoIIAB interaction were hydrophobic. By analogy, V33, A103, M104, L124, V196, L199 and V213 of σ^{28} may play a similar role in the σ^{28}/FlgM interaction. The isolation of *flgM** mutations in hydrophobic residues (L66S and I82T) is also suggestive of a hydrophobic interface between σ^{28} and FlgM. Positions at which substitution of an alanine restored the ability of a σ^{F} mutant to interact with SpoIIAB were interpreted as being near enough to important hydrophobic contacts that substitution of a bulky or charged residue could interfere with SpoIIAB binding. A number of the non-conservative σ^{28}* mutations also

occurred at positions adjacent to hydrophobic residues (M104T, N114K, T138I, T198K, N206K and R231Q).

While it is likely that the interactions between σ^{28}/FlgM and σ^{F}/SpoIIAB are mechanistically similar, they may differ in the degree to which the three sigma domains contribute to complex formation. *In vivo*, the most SpoIIAB-insensitive *sigF* mutants were those with substitutions in region 3.1. Though a comparison of purified σ^{F} mutant proteins has not been done to confirm that these region 3.1 mutants also have the strongest effect *in vitro*, this result suggests that the most important determinants for SpoIIAB binding may be located in this region. Our results indicate that region 4.1/.4.2 of σ^{28} is the dominant FlgM binding domain. We have proposed that the interaction with region 4.1/4.2 is critical for the holoenzyme destabilization activity of FlgM. Whether SpoIIAB is also able to regulate $E\sigma^{F}$ activity remains to be determined.

Although the σ^{28}* mutants chosen for biochemical analysis included those with the strongest *in vivo fliA** phenotypes, the activities of the purified σ^{28}* proteins by themselves and in the presence of FlgM did not always reflect this fact. It is likely that a combination of factors in addition to basal sigma activity and affinity for FlgM combine to determine the strength of the *in vivo* phenotypes of *fliA** mutants. One of these factors is the ratio of σ^{28} to FlgM. The relative amount of σ^{28} was slightly elevated in the H14D and H14N *fliA** mutant strains. Given that the σ^{28}* proteins purified from these strains did not display any *in vitro* activity that could account for their apparent insensitivity to FlgM *in vivo*, this shift in the ratio of σ^{28} to FlgM may be the basis for the *fliA** phenotype of these mutants. It is not clear how this imbalance is achieved, since FlgM expression is positively regulated by σ^{28}. The possibility that the H14 mutants might transcribe the *fliA* promoter more efficiently, or the *flgA* and *flgM* promoters less efficiently, than wild type σ^{28} was tested *in vitro*. The data do not support this hypothesis, however (data not shown). A quantitative analysis of σ^{28} and

FlgM steady state levels and turnover rates in these mutants *in vivo* may resolve this issue.

Table 5.1A Kinetic Analysis of FlgM/σ^{28}* Interactions[a]

σ^{28} Allele	k_a (M^{-1} sec^{-1})	k_d (sec^{-1})	K_d (M)	Relative Affinity for FlgM
+	$1.7x10^5$	$1.0x10^{-4}$	$5.6x10^{-10}$	----------
H14D	ND	ND	ND	same as wild type σ^{28}
H14N	ND	ND	ND	same as wild type σ^{28}
V33E	$1.5x10^5$	$9.0x10^{-4}$	$5.0x10^{-9}$	9-fold weaker
+	$1.7x10^4$	$7.0x10^{-5}$	$2.5x10^{-10}$	----------
M104T	$2.0x10^5$	$6.8x10^{-4}$	$3.6x10^{-9}$	14-fold weaker
N114K	$1.8x10^5$	$7.2x10^{-4}$	$4.0x10^{-9}$	16-fold weaker
T138I	$1.6x10^5$	$6.0x10^{-4}$	$3.8x10^{-9}$	15-fold weaker
+	$2.6x10^5$	$5.4x10^{-5}$	$2.0x10^{-10}$	----------
L199R	$1.1x10^4$	$1.3x10^{-3}$	$1.2x10^{-7}$	600-fold weaker
E203D	$1.8x10^5$	$4.7x10^{-4}$	$2.6x10^{-9}$	13-fold weaker
V213E	$5.0x10^4$	$7.0x10^{-4}$	$1.4x10^{-8}$	70-fold weaker
R231Q	$2.6x10^5$	$9.0x10^{-4}$	$3.5x10^{-9}$	18-fold weaker

[a]Ligand is His-FlgM; Analyte is His-σ^{28} protein

Table 5.1B Kinetic Analysis of σ^{28}*/FlgM Interactions[a]

σ^{28} Allele	k_a (M^{-1} sec^{-1})	k_d (sec^{-1})	K_d (M)	Relative Affinity for FlgM
L199R	No significant binding of HT-FlgM analyte			
E203D	$1.7x10^5$	$2.3x10^{-3}$	$1.2x10^{-8}$	13-fold weaker
+	$2.3x10^5$	$2.1x10^{-4}$	$9.1x10^{-10}$	----------
V213E	No significant binding of HT-FlgM analyte			
R231Q	$2.7x10^5$	$3.7x10^{-4}$	$1.4x10^{-9}$	8-fold weaker
+	$2.3x10^5$	$4.2x10^{-5}$	$1.8x10^{-10}$	----------

[a]Ligand is His-σ^{28} protein; Analyte is His-FlgM

Table 5.2 Kinetic Analysis of σ^{28}*/core RNAP Interactions[a]

σ^{28} Allele	k_a	k_d	K_d	Relative Affinity for FlgM
+	1.2×10^{6}	7.7×10^{-4}	6.4×10^{-10}	----------
H14D	5.4×10^{5}	1.0×10^{-3}	2.0×10^{-9}	3-fold weaker
H14N	3.6×10^{5}	8.8×10^{-4}	2.0×10^{-9}	3-fold weaker
V33E	3.8×10^{5}	3.1×10^{-4}	6.5×10^{-10}	3-fold tighter
H14N	4.8×10^{5}	5.9×10^{-4}	1.4×10^{-9}	same as wild type σ^{28}
+	3.1×10^{5}	5.2×10^{-4}	1.7×10^{-9}	----------
M104T	1.4×10^{6}	7.1×10^{-4}	5.0×10^{-10}	same as wild type σ^{28}
+	7.9×10^{5}	6.8×10^{-4}	8.6×10^{-10}	----------
T138I	7.5×10^{5}	4.2×10^{-4}	5.6×10^{-10}	same as wild type σ^{28}
N114K	6.8×10^{5}	5.2×10^{-4}	7.6×10^{-10}	same as wild type σ^{28}
T138I	2.1×10^{6}	3.8×10^{-4}	1.8×10^{-10}	same as wild type σ^{28}
+	1.2×10^{6}	4.4×10^{-4}	3.7×10^{-10}	----------
L199R	5.2×10^{5}	6.0×10^{-4}	1.2×10^{-9}	same as wild type σ^{28}
E203D	4.6×10^{5}	6.5×10^{-4}	1.4×10^{-9}	same as wild type σ^{28}
+	5.4×10^{5}	5.3×10^{-4}	1.0×10^{-9}	----------
V213E	5.6×10^{5}	4.0×10^{-4}	7.3×10^{-10}	same as wild type σ^{28}
R231Q	4.5×10^{5}	6.3×10^{-4}	1.4×10^{-9}	same as wild type σ^{28}
+	4.8×10^{5}	3.9×10^{-4}	8.0×10^{-10}	----------

[a]Ligand is His-σ^{28} protein; Analyte is core RNAP

Table 5.3 Dissociation of $E\sigma^{28+}$ and $E\sigma^{28}*$ in the absence and presence of FlgM[a]

	k_d of $E\sigma^{28}$ (x 10^{-3} sec^{-1})[b]	
σ^{28} protein	- FlgM	+ FlgM
+	0.6	3.0
H14D	0.7	3.2
H14N	0.6	2.5
+	3.5	6.8
N114K	2.0	16
T138I	1.8	11
+	3.4	21
L199R	8.0	4.7
E203D	3.6	3.5

[a]Ligand is His-σ^{28}; Analyte is core RNAP

[b]Dissociation of $E\sigma^{28}$ was measured in HBS buffer (-FlgM), or in the presence of His-$FlgM^+$ (100 nM His-$FlgM^+$ nM for experiments involving region 2.1 σ^{28} mutants, 250 nM for those involving region 3.1 and 4.1/4.2 σ^{28} mutants).

Figure 5.1 Transcription from a σ^{28}-dependent promoter by reconstituted Eσ^{28*}. Reaction mixtures contained 15 nM RNAP (E) (except in [A], where core was present at 30 nM) and 3 nM *fliC* promoter template DNA. The molar ratio of native σ^{28} to core RNAP in each reaction is indicated on the X-axis. The amount of ^{3}H-UTP incorporated during 10 minute RNA synthesis reactions is indicated on the Y-axis. Error bars in indicate the standard deviation (assays performed in triplicate). [A] Basal sigma activities of region 2.1 σ^{28*} mutants. [B] Basal sigma activities of region 3.1 σ^{28*} mutants. [C] and [D] Basal sigma activities of region 4.1/4.2 σ^{28*} mutants.

A

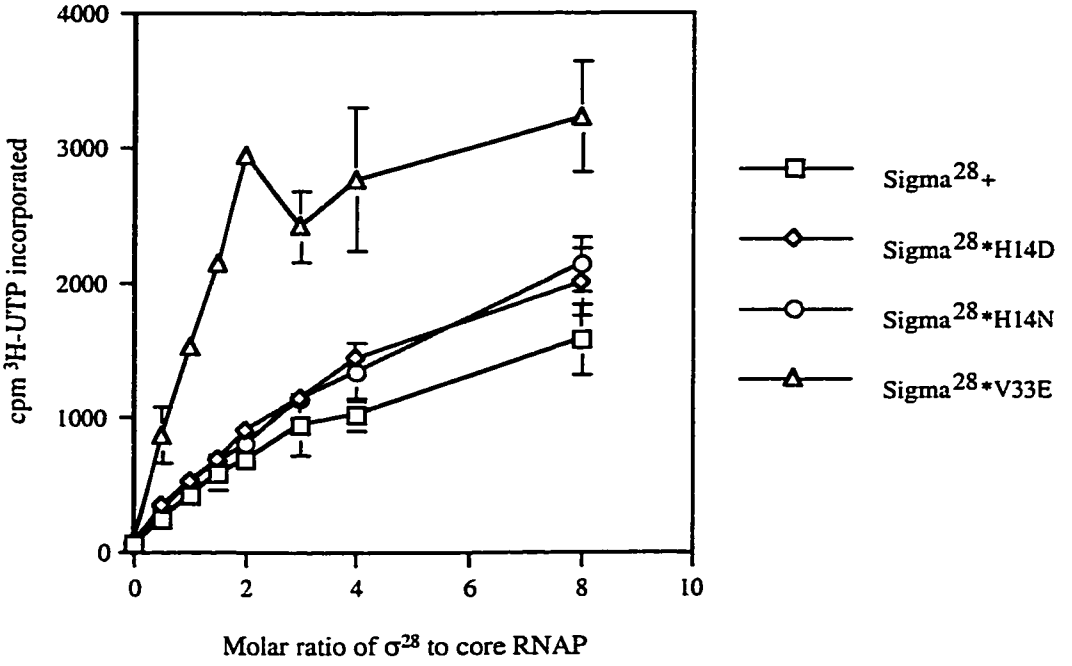
4000
3000
2000
1000
0
cpm ³H-UTP incorporated
0
2
4
6
8
10
Molar ratio of σ²⁸ to core RNAP
Sigma²⁸+
Sigma²⁸*H14D
Sigma²⁸*H14N
Sigma²⁸*V33E

B

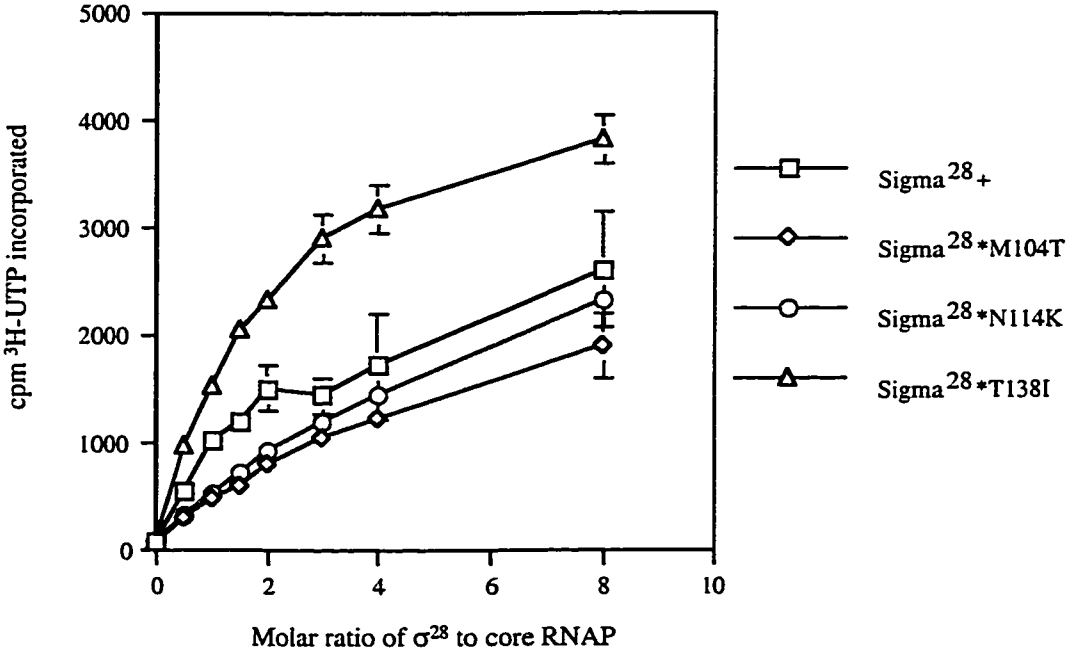
5000
4000
3000
2000
1000
0
cpm ³H-UTP incorporated
0
2
4
6
8
10
Molar ratio of σ²⁸ to core RNAP
Sigma²⁸+
Sigma²⁸*M104T
Sigma²⁸*N114K
Sigma²⁸*T138I

C

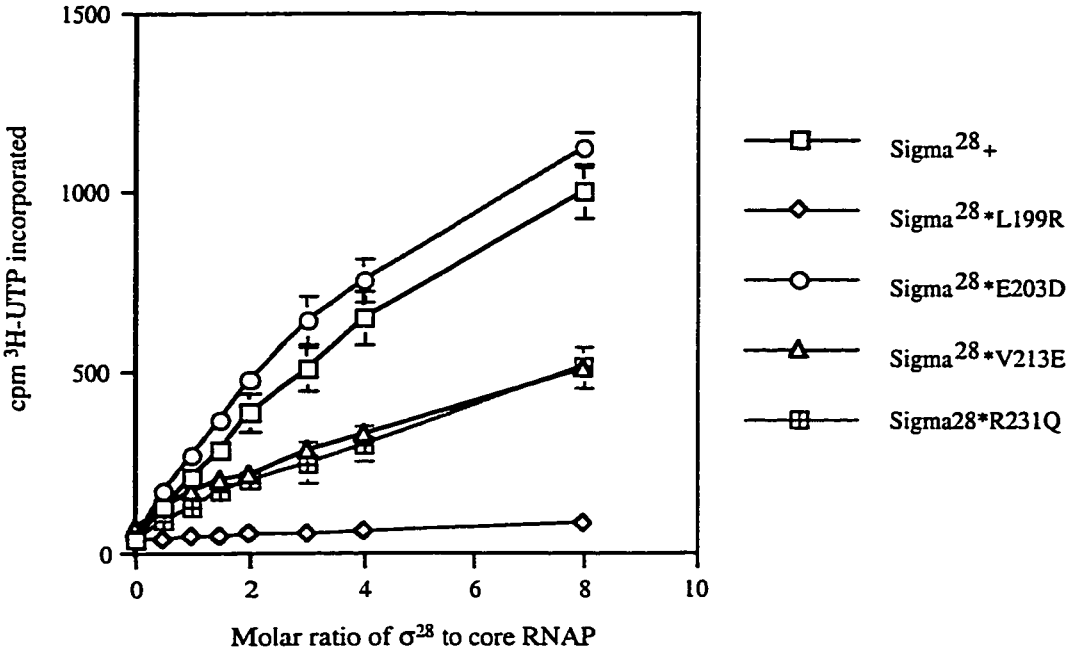
1500
1000
500
0
cpm ^{3}H-UTP incorporated
0
2
4
6
8
10
Molar ratio of σ^{28} to core RNAP
Sigma^{28}+
Sigma^{28}*L199R
Sigma^{28}*E203D
Sigma^{28}*V213E
Sigma28*R231Q

D

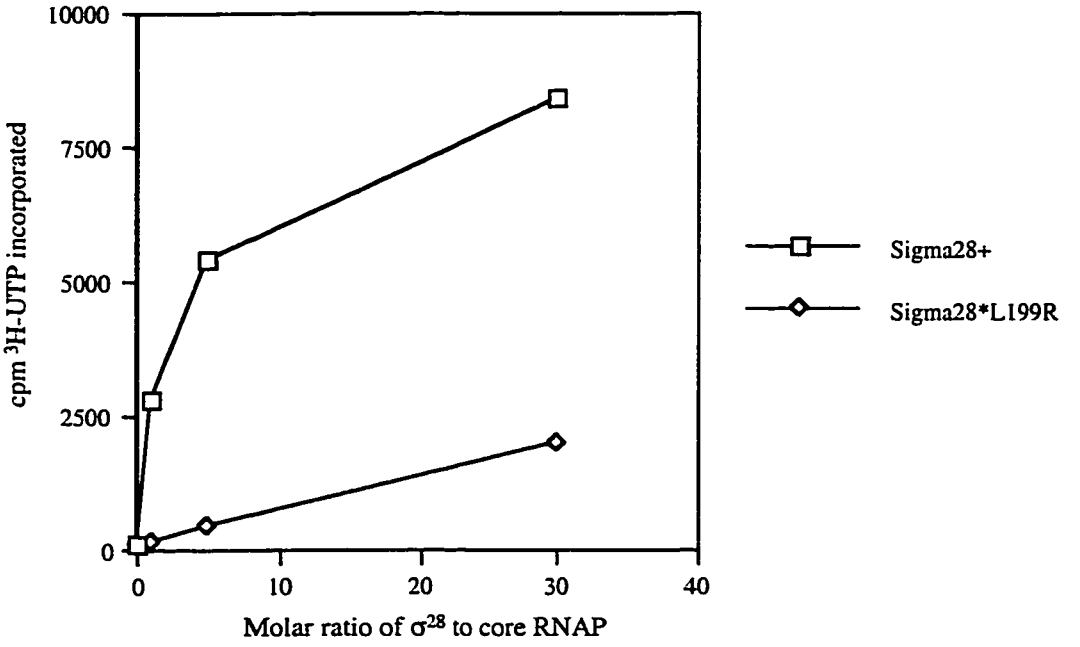
10000
7500
5000
2500
0
cpm ^{3}H-UTP incorporated
0
10
20
30
40
Molar ratio of σ^{28} to core RNAP
Sigma28+
Sigma28*L199R

Figure 5.2 Inhibition of σ^{28}*-dependent transcription by FlgM. Purified His-FlgM$^+$ was incubated with His-σ^{28+} and His-σ^{28}* proteins, and core RNAP, prior to the initiation of transcription. Reaction mixtures contained 15 nM core RNAP, 15 nM σ^{28}* and 3 nM *fliC* promoter template DNA. The molar ratio of FlgM to σ^{28} in each reaction is indicated on the X-axis. The level of RNA synthesis during each 10 minute transcription reactions is expressed in terms of the percent maximal transcription (in the absence of His-FlgM). [A] FlgM inhibition of region 2.1 σ^{28}* mutants. [B] FlgM inhibition of region 3.1 σ^{28}* mutants. [C] FlgM inhibition of region 4.1/4.2 σ^{28}* mutants.

A

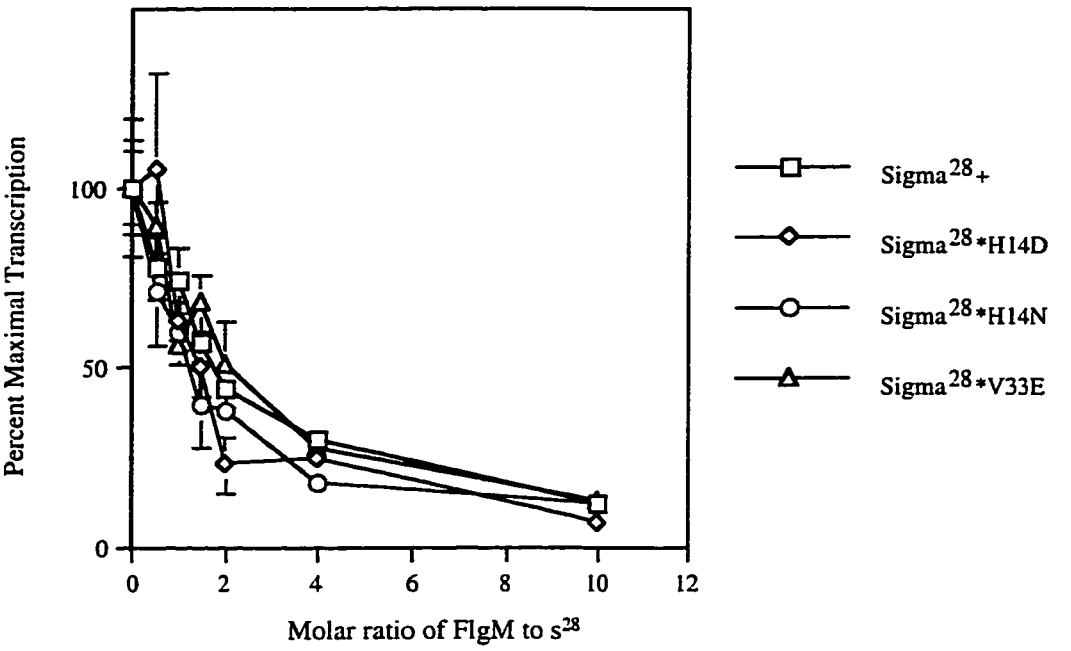
Percent Maximal Transcription
100
50
0
0
2
4
6
8
10
12
Molar ratio of FlgM to s28
Sigma28+
Sigma28*H14D
Sigma28*H14N
Sigma28*V33E

B

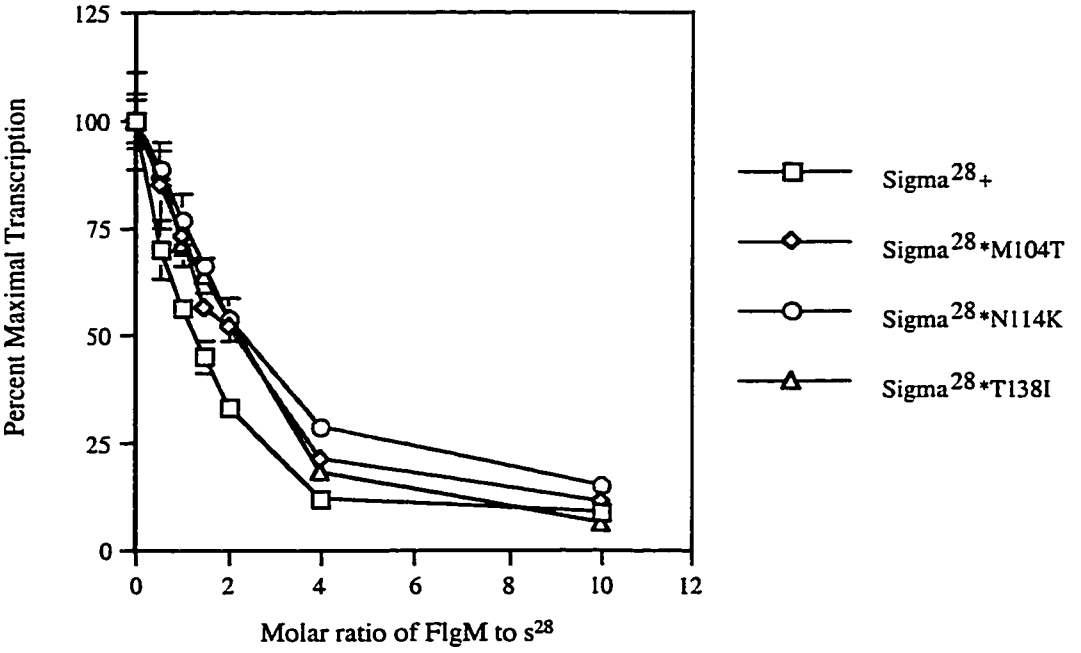
Percent Maximal Transcription
125
100
75
50
25
0
0
2
4
6
8
10
12
Molar ratio of FlgM to s28
Sigma28+
Sigma28*M104T
Sigma28*N114K
Sigma28*T138I

C

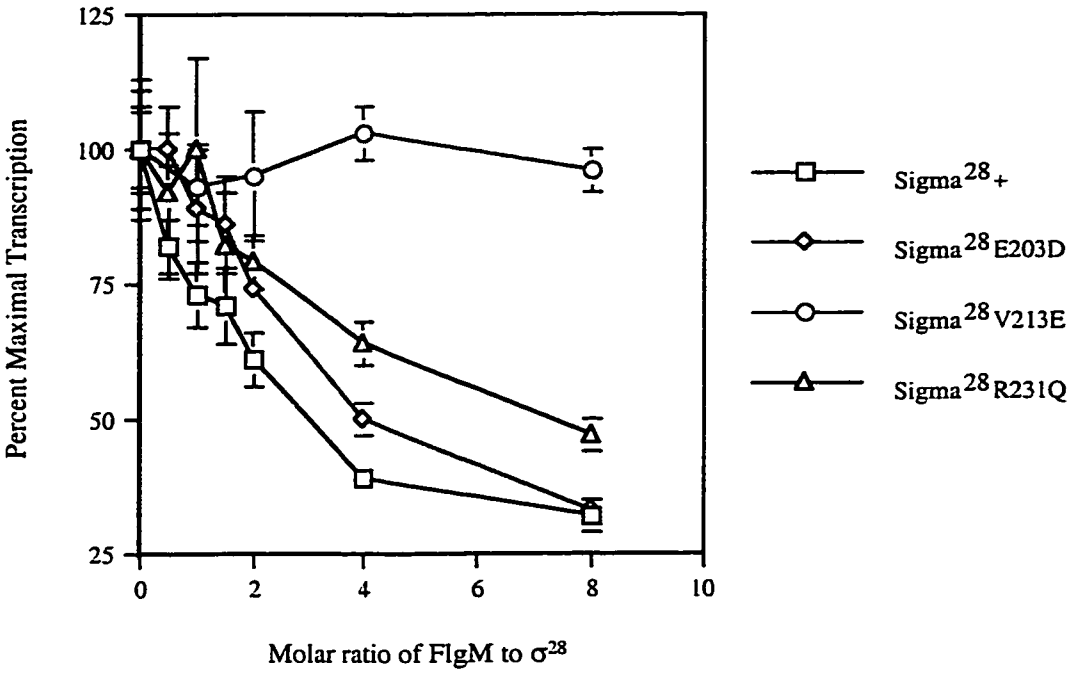
125
100
75
50
25
0
2
4
6
8
10
Percent Maximal Transcription
Molar ratio of FlgM to σ28
Sigma28+
Sigma28E203D
Sigma28V213E
Sigma28R231Q

Figure 5.3 Steady state levels of σ^{28*} and FlgM proteins *in vivo*. Western analysis of cellular protein levels in the *fliA** mutants chosen for biochemical analysis (and one *fliA** mutant with a point mutation in the 5' UTR of the *fliA* transcript). 25 μg of total cell protein from each *fliA** mutant was electrophoresed on 16.5% SDS-polyacrylamide gels, and transferred to a nylon membrane. The top half of each membrane was probed with affinity purified anti-σ^{28} antisera; the bottom half was probed with anti-FlgM antisera. The amount of σ^{28} and FlgM in the *fliA*$^{+}$ control strain is arbitrarily designated as "+" for both proteins. The amount of σ^{28*} and FlgM in each mutant strain is estimated to be equal to (+), more than (++), or less than (+/- to +/=) that of wild type based on the relative intensity of the σ^{28*} and FlgM bands compared to those of wild type in the adjacent lanes. The amount of σ^{28} and FlgM in the standard lane (far right on each gel) is 12. 5 and 2.5 μg, respectively.

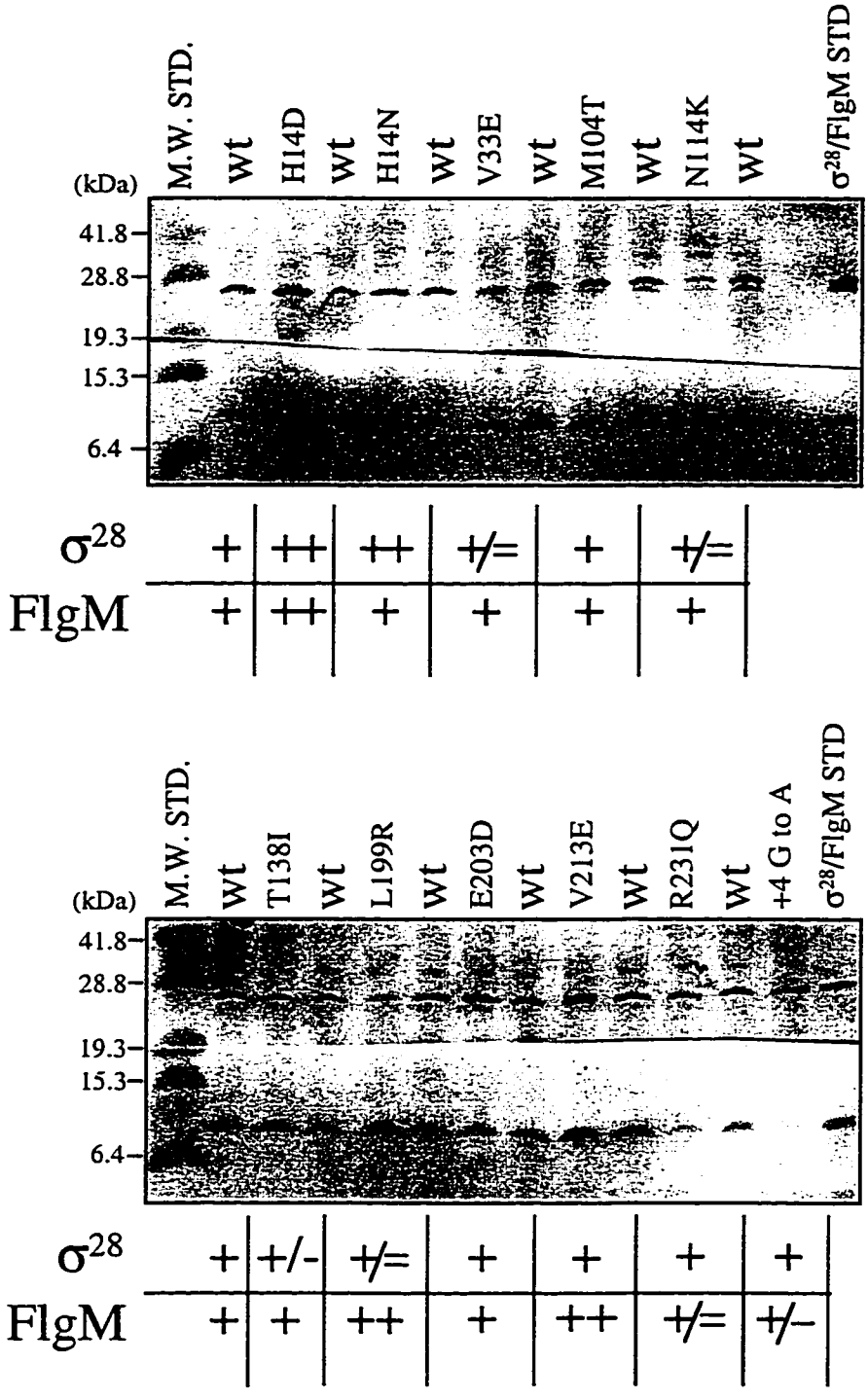
M.W. STD.
Wt
H14D
Wt
H14N
Wt
V33E
Wt
M104T
Wt
N114K
Wt
σ28/FlgM STD
(kDa)
41.8
28.8
19.3
15.3
6.4
σ28
FlgM
+
++
++
+/=
+
+/=
+
++
+
+
+
+
M.W. STD.
Wt
T138I
Wt
L199R
Wt
E203D
Wt
V213E
Wt
R231Q
Wt
+4 G to A
σ28/FlgM STD
(kDa)
41.8
28.8
19.3
15.3
6.4
σ28
FlgM
+
+/-
+/=
+
+
+
+
+
+
++
+
++
+/=
+/-

Figure 5.4 *fliA** mutants H14D and H14N have a higher ratio of σ^{28} to FlgM than *fliA*$^+$. The relative levels of σ^{28} and FlgM in the *fliA** mutants H14D and H14N were compared to that of an isogenic *fliA*$^+$ strain using Western analysis. Samples from serial 2-fold dilution series of total cell protein were electrophoresed on 16.5% SDS-polyacrylamide gels and transferred to a nylon membrane. Protein is loaded in decreasing amounts from left to right (from 50 to 1.56 μg for the *fliA*$^+$ strain, and from 12.5 to 0.1 μg for the *fliA** mutants). The top half of each membrane was probed with σ^{28} antisera; the bottom half was probed with FlgM antisera.

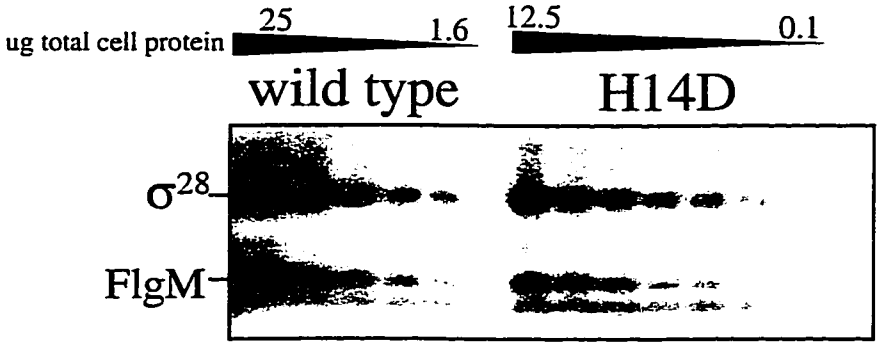
ug total cell protein
25
1.6
12.5
0.1
wild type
H14D
σ28
FlgM

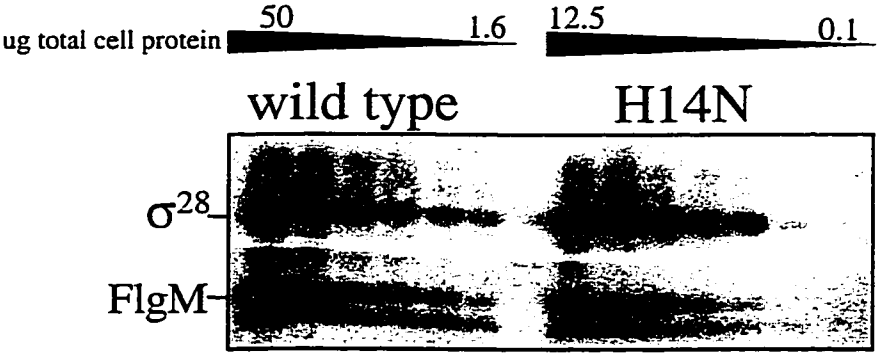
ug total cell protein
50
1.6
12.5
0.1
wild type
H14N
σ28
FlgM

Figure 5.5 The effect of two types of defects on σ^{28}-dependent transcription. [A] A simplified cartoon of transcription process as a two-step mechanism. The first step, characterized by the equilibrium constant K_1, includes the independent processes of holoenzyme formation, promoter recognition and closed complex formation. The second step, characterized by the forward rate constant k_2, includes the processes of isomerization and transcript initiation leading to promoter clearance. [B] and [C] Graphic representations of how σ^{28}* mutants defective for core binding or promoter recognition (a higher K_1) [B] or for isomerization, initiation or clearance (a slower k_2) [C] affects the rate of transcription.

A

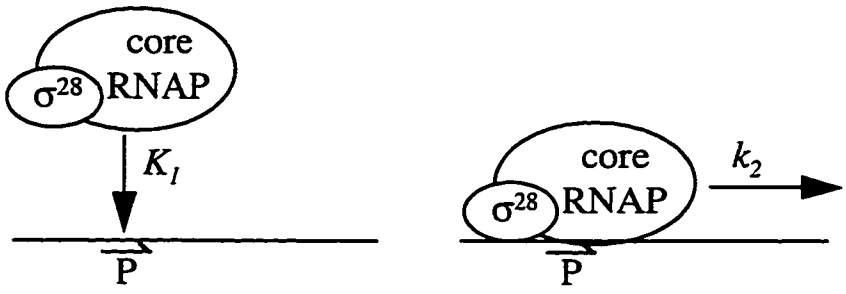
core
σ28 RNAP
K1
P
core
σ28 RNAP
k2
P

B

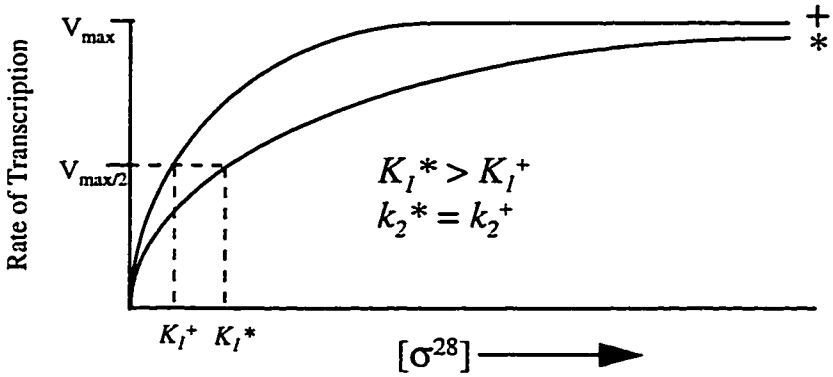
Vmax
Vmax/2
Rate of Transcription
+
*
K1* > K1+
k2* = k2+
K1+ K1*
[σ28]

C

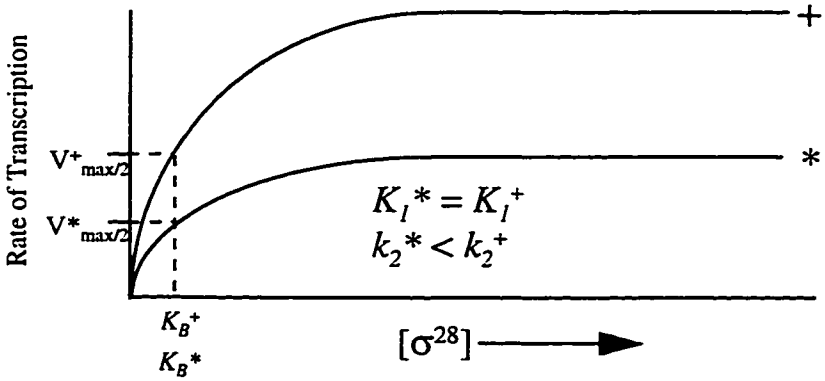
V+max/2
V*max/2
Rate of Transcription
+
*
K1* = K1+
k2* < k2+
KB+
KB*
[σ28]

Figure 5.6 An alignment of *E. coli* σ^{70}, *S. typhimurium* σ^{28}, and *B. subtilis* σ^{F}. Regions 2.1, 3.1 and 4.1/4.2 of the sigma factors are aligned according to Lonetto et al. (118). Amino acid similarity between the alternative sigma factors σ^{28} and σ^{F}, and σ^{70} is indicated by highlighting; gaps are indicated by dashed lines. The groups of residues considered identical are as follows: ST; RK; DE; NQ; FYW; ILVM. Positions altered by substitution mutations in *fliA** and *sigF* mutants insensitive to regulation by their respective anti-sigma factors are indicated by the presence of an asterix (σ^{28}*) or a caret (σ^{F}) [σ^{F} mutations published in \(33). The region 2.1 core binding motif (178) is underlined in the σ^{70} sequence; a possible homologue to this motif in σ^{28} is also underlined.

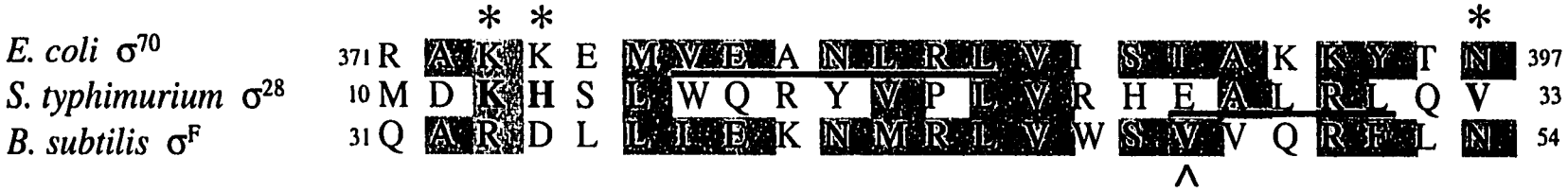

Region 2.1

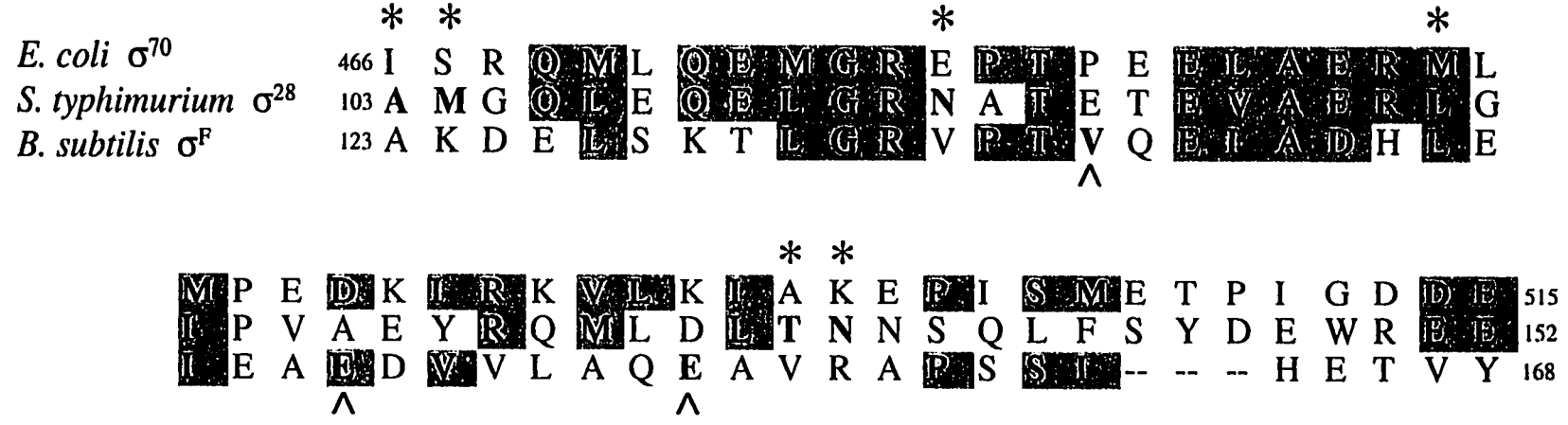

Region 3.1

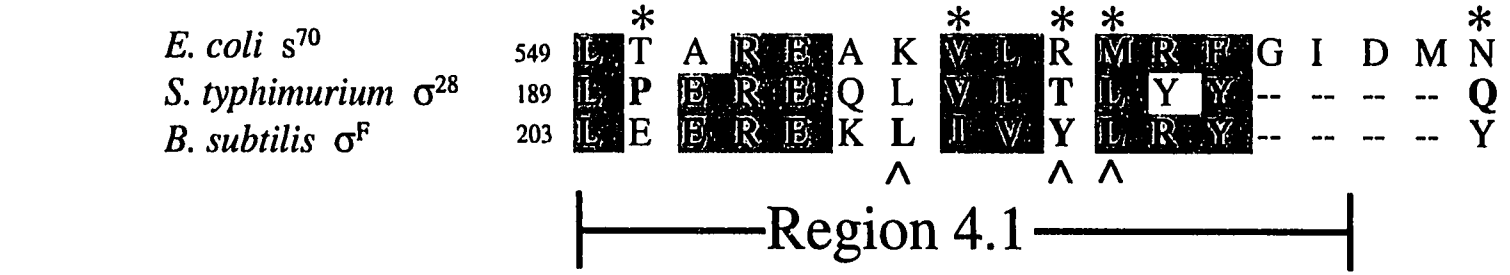
E. coli σ70
S. typhimurium σ28
B. subtilis σF
549 L T A R E A K V L R M R F G I D M N
189 L P E R E Q L V L T L Y Y -- -- -- -- Q
203 L E E R E K L I V Y L R Y -- -- -- -- Y
Region 4.1

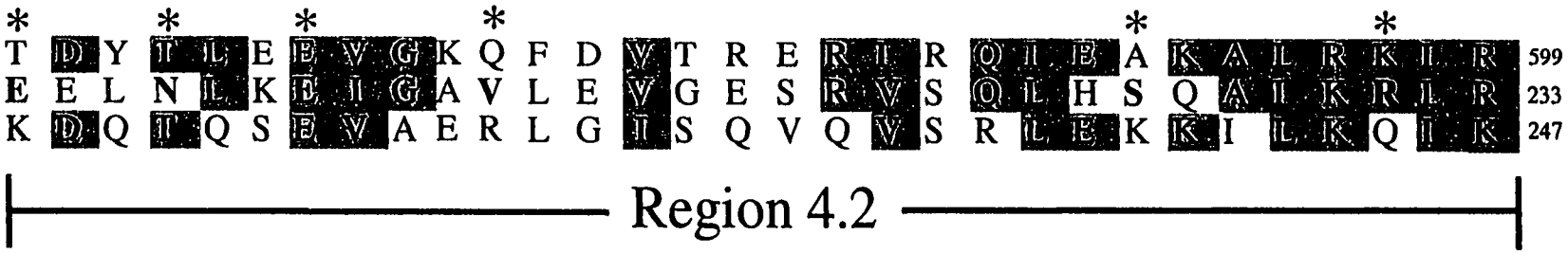
T D Y I L E E V G K Q F D V T R E R I R Q I E A K A L R K I R 599
E E L N L K E I G A V L E V G E S R V S Q L H S Q A I K R L R 233
K D Q T Q S E V A E R L G I S Q V Q V S R L E K K I L K Q I K 247
Region 4.2

Chapter 6

Discussion and Perspectives

SUMMARY

The research detailed in this dissertation focused on characterizing the mechanism by which the anti-sigma factor FlgM inhibits the flagellar specific sigma factor, σ^{28}. A collection of σ^{28} mutants defective for negative regulation by FlgM was generated to carry out this investigation. The distribution and *in vivo* phenotypes of these mutants suggested several possible models for the mechanism of FlgM-mediated inhibition. An *in vitro* analysis of the behavior of wild type and mutant σ^{28} proteins was performed to test these models. A summary of this research is provided below. This section is followed by a discussion of some of the questions raised by the research, and possible ways to address those questions.

Chapter 3 described the isolation and *in vivo* characterization of a collection of FlgM-insensitive *fliA* mutants (*fliA** mutants). These mutants were isolated on the basis of their ability to transcribe Class 3 genes in the presence of inhibitory levels of FlgM. This phenotype suggested that the mutant σ^{28} proteins (σ^{28}*) were insensitive to FlgM inhibition. Given that FlgM binds directly to σ^{28}, it was possible that sequence analysis of the *fliA** mutants might identify the σ^{28} domain(s) contacting FlgM. This information would be used to generate models for the mechanism of FlgM-mediated inhibition of sigma factor activity. Sequence analysis of the *fliA* locus of 64 *fliA** mutants identified 29 substitution mutations at 20 residues that conferred insensitivity to FlgM *in vivo*. These mutations mapped to three conserved σ factor regions, region 2.1, region 3.1 and region 4.1/4.2, identifying three possible points of contact between σ^{28} and FlgM. Genetic and biochemical analyses of related σ^{70} family sigma factors had

implicated these regions in core RNAP binding (regions 2.1, 3.1 and 4.1/4.2) and -35 promoter recognition (region 4.1/4.2).

Several models were proposed to explain the effect of FlgM on σ^{28} activity. The simplest model predicted that FlgM binds all three regions of σ^{28}, and prevents the formation of a transcriptionally active complex with core RNAP through direct steric inhibition of the putative core RNAP binding domain(s). Other models invoked an allosteric mechanism to explain the ability of FlgM to interfere with σ^{28}-holoenzyme ($E\sigma^{28}$) formation. These models proposed that FlgM indirectly interferes with holoenzyme formation by binding to region 4.1/4.2, or to regions 4.1/4.2 and 3.1. In these models, the mutations in regions 2.1 and 3.1 were proposed to increase the affinity of the competing σ^{28}/core RNAP interaction, or to block the transmission of an allosteric signal propagating from the C-terminal FlgM binding domain(s). Of particular interest were the substitution mutations at residue 14 within region 2.1, which, by analogy to σ^{70}, lay very near a core binding motif. Of all the σ^{28}* mutants, only H14D and H14N appeared to be more active that wild type σ^{28} *in vivo*. These results suggested that the mutations at residue 14 might bypass negative regulation by FlgM by increasing the affinity of σ^{28} for core RNAP.

Chapter 4 described our efforts to identify the stage or stages of transcription negatively regulated by FlgM. A published model for the mechanism of FlgM-mediated inhibition of σ^{28} (142) stated that the only role of FlgM was to sequester free σ^{28} from core RNAP. However, studies carried out in our lab indicated that free σ^{28} might not be the only target of FlgM. Promoter binding assays had demonstrated that in addition to sequestering free σ^{28}, FlgM could block promoter recognition by $E\sigma^{28}$. Moreover, a small amount of FlgM was found to comigrate with $E\sigma^{28}$ under non-denaturing conditions. These data suggested that FlgM was also capable of interacting with $E\sigma^{28}$ to inhibit σ^{28}-dependent transcription. Because of the apparent instability of the ternary

$E\sigma^{28}$ complex, it was proposed that the effect of FlgM binding was to destabilize the transcription complex and effect the premature release of the sigma factor. None of the previously published methods used to investigate potential anti-sigma factor/holoenzyme interactions could be employed to test this model, since they would not be able to distinguish between holoenzyme destabilization, and an equally likely possibility, i.e. that FlgM was simply able to compete efficiently with core RNAP for rebinding to σ^{28} spontaneously released from $E\sigma^{28}$. To address this issue, we developed an SPR-based assay to monitor the stability of the σ^{28}/core RNAP complex in the presence of FlgM. In addition to providing the first direct measurements of the kinetic rate constants for a sigma factor/core RNAP interaction, this assay revealed that FlgM was indeed able to induce the release of σ^{28} from core. FlgM had no effect on the stability of $E\sigma^{70}$. FlgM mutants defective for binding to free σ^{28} (as determined by SPR-based assays) were also defective for holoenzyme destabilization. We concluded that this novel activity was specific for $E\sigma^{28}$, and it was mediated at least partially by FlgM binding determinants on σ^{28}.

Chapter 5 describes our analysis of the σ^{28}* mutant activities *in vitro*. The affinities of the σ^{28}* mutants for FlgM and for core RNAP were determined by SPR. The results of the σ^{28}*/FlgM assays supported our model for a tripartite interaction between σ^{28} and FlgM; substitution mutations in regions 2.1, 3.1 and 4.1/4.2 were found to decrease the affinity of the interaction. None of the σ^{28}* mutants appeared to bind to core RNAP with a higher affinity, which had been proposed as another way that σ^{28} could overcome FlgM-mediated inhibition *in vivo*. The decreased affinity of the σ^{28}* mutants for FlgM enabled us to begin to examine our models for holoenzyme destabilization. We reasoned that σ^{28}* mutants that demonstrated a decreased affinity for FlgM as free sigma factors would also be less sensitive to FlgM as part of holoenzyme, unless the substitution mutation occurred in a region of σ^{28} that was

inaccessible to FlgM in this context. We found that holoenzyme containing region 4.1/4.2 mutants was more stable than wild type $E\sigma^{28}$ in the presence of FlgM, but that substitution mutations in region 3.1 did not affect the ability of FlgM to destabilize $E\sigma^{28}$*. We interpreted this result as evidence for the allosteric displacement model for holoenzyme destabilization, since this model did not invoke an interaction between FlgM and regions 2.1 or 3.1. *In vitro* transcription assays were consistent with the SPR data; σ^{28}* mutants with a decreased affinity for FlgM were less sensitive to FlgM-mediated inhibition. Only the residue 14 substitution mutants were not explained by the SPR and transcription assays; they had wild type activity in every assay. Western analysis of the relative levels of σ^{28} and FlgM in the H14D and H14N *fliA** mutants revealed that ratio of σ^{28} to FlgM was higher in these strains. This observation could account for their *in vivo* phenotype; the basis for this skewed ratio was not resolved.

HOLOENZYME DESTABILIZATION *IN VIVO*

The observation that FlgM is able to interact with σ^{28} bound to core to destabilize the holoenzyme complex, and the evidence that this interaction may only involve a subset of the FlgM binding domains on σ^{28}, has provided new insights about the manner in which σ^{28} binds to core RNAP. Whether holoenzyme destablization is simply an interesting *in vitro* phenomenon, or whether it plays a role in the regulation of σ^{28} activity *in vivo* has not yet been resolved. At present, we can only argue why such a regulatory mechanism might be useful to the process of flagellar biogenesis.

Because FlgM and core RNAP have an approximately equal affinity for free σ^{28} (see Chapter 5) FlgM would have to be present at many times the concentration of core RNAP (which is estimated to be ~3000 molecules/cell; 77), in order to prevent holoenzyme formation by a competitive binding mechanism. However, the ability of FlgM to negatively regulate $E\sigma^{28}$ means that the level of FlgM need only be equivalent to

that of σ^{28}, which is estimated to be ~350 molecules/cell (83). The autoregulatory network that controls expression of the *fliA* and *flgM* genes seems to be designed to achieve a balanced protein level rather than an excess of FlgM.

We measured the intracellular concentration of FlgM in exponentially growing *S. typhimurium* to be approximately 400 nM, three orders of magnitude above the K_d of the σ^{28}/FlgM interaction *in vitro*. Yet small changes in the level of FlgM *in vivo* have been observed to have a significant effect on Class 3 gene expression (74), suggesting that FlgM levels are actually near a threshold for regulation of σ^{28}-dependent transcription, i.e. the threshold for holoenzyme destabilization.

It must be noted that the 400 nM estimate for FlgM represents the average FlgM concentration of a population of cells that were not synchronized for flagellar synthesis. The recent isolation of a tetracyline-inducible promoter insertion upstream of the *flhDC* operon has made it possible to synchronize flagellar gene expression (V. Bettenworth and K. Hughes, unpublished results). Once a reliable method for quantitative analysis of σ^{28} and FlgM levels is developed, the absolute and relative amounts of these proteins over the course of flagellar biogenesis can be monitored. If the concentration of FlgM is found to be at least as high as that of σ^{28}, *and* above 10 nM (the *in vitro* estimate of the threshold for holoenzyme destabilization) prior to HBB completion, then the case for holoenzyme destabilization as a valid regulatory mechanism will be strengthened.

It will be very interesting to learn what happens to the levels of σ^{28} and FlgM as the cycle of flagellar biogenesis reaches completion. We have proposed that FlgM may also play a role in shifting the focus of the transcription machinery away from flagellar gene expression once flagella have reached their mature length (see Chapter 4). If $E\sigma^{28}$ activity is downregulated by FlgM following a round of flagellar biogenesis, then the levels of σ^{28} and FlgM would be predicted to fall as a result of decreased $E\sigma^{28}$-dependent transcription. What happens as the cell volume increases in preparation for

cell division is still a matter of speculation. One possibility is that a new cycle of Class 2 and Class 3 gene expression is initiated each time the concentration of FlgM falls below the threshold for inhibition of σ^{28}-dependent transcription. This scenario predicts that flagellar biogenesis, once initiated by the Class 1 genes *flhDC*, is self-sustaining until environmental signals communicate that motility is no longer necessary. The result would be continuous synthesis of new flagella throughout the cell cycle, such that the ratio of flagella to cell volume remained roughly constant (provided that the length of time required to synthesize flagella was shorter than the cell cycle).

Another possibility is that each new round of flagellar biogenesis requires renewed activation of Class 1 expression. The signals for this activation could be tied into the cell cycle, or they could come from the environment. Use of the tetracycline-inducible *flhDC* operon may be able to distinguish between these two possibilities. If the tetracycline used to induce the synchronous expression of the flagellar operon is washed away after *flhDC* expression is stimulated, then it should be possible to observe the number and rate of cycles of flagellar biogenesis that ensue in the absence of further Class 1 activation.

Protein interactions between FlgM, σ^{28} and core RNAP

Our models for the mechanism of holoenzyme destabilization make a number of assumptions about the nature of the σ^{28}/core RNAP complex, and about the σ^{28} domains targeted by FlgM. For example, the involvement of σ^{28} regions 2.1 and 3.1 in core binding is only predicted by analogy with other sigma factors. Direct evidence for these interactions is needed to substantiate the model that FlgM interferes with stable holoenzyme formation by competing with core RNAP for σ^{28} binding. The presence of FlgM binding determinants in each of the σ^{28} regions 2.1, 3.1 and 4.1/4.2 (suggested by our analysis of σ^{28}* mutants) should also be confirmed biochemically. Finally,

there is the unresolved matter of how FlgM binding to $E\sigma^{28}$ affects the stability of that complex.

The SPR-based assay for σ^{28}/core RNAP interaction can also be used to determine the contribution of individual σ^{28} domains to holoenzyme formation. The same protocol used to evaluate the binding of core RNAP to intact σ^{28} could be employed to test for specific binding of core RNAP to truncated σ^{28} proteins or proteolytic fragments containing either region 2.1 or 3.1. The tertiary structure of sigma is thought to consist of independent domains connected by flexible linker regions (22, 159). Conserved sigma regions 2 and 4 retain their individual activities when independently expressed (33, 36, 38, 154, 159). Thus, it is likely that regions 2, 3 and 4 of σ^{28} could be examined separately in SPR assays. The sensitivity of the SPR-based detection method could reveal sigma/core RNAP interactions that have been missed by other assays, such as glycerol gradient centrifugation and affinity chromatography. For example, these assays have failed to demonstrate a direct interaction between conserved sigma region 3 and core RNAP, though genetic and biochemical evidence has suggested that this region does participate in core binding (85, 147, 193).

SPR could also be employed to measure the independent binding affinities of FlgM for σ^{28} regions 2.1, 3.1 and 4.1/4.2, using a His-FlgM ligand surface to capture soluble truncated σ^{28} proteins. To obtain stable proteins, it might be necessary to express the individual σ^{28} domains as protein fusions with a large stable protein such as maltose binding protein, as was done to the study the interaction of σ^{F} regions with SpoIIAB (33). In addition to testing the tripartite binding model proposed for the σ^{28}/FlgM complex, this type of analysis could provide information about the relative importance of the three domains to σ^{28}/FlgM complex formation. Evidence presented in this thesis and by others (103) suggests that region 4.1/4.2 is the dominant FlgM

binding domain; SPR analysis should determine if this is the case. Such information is relevant to the models we have proposed for the interaction of FlgM with E σ^{28}.

Finally, SPR could be used to further investigate the mechanism of FlgM-mediated holoenzyme destabilization. The insensitivity of holoenzyme containing σ^{28}* region 3.1 mutants to FlgM was interpreted as evidence for the allosteric displacement model proposed in Chapter 4. This model predicts that only region 4.1/4.2 of σ^{28} should be required to see an effect of FlgM on the rate of holoenzyme dissociation in the SPR-based assay. The involvement of each of the σ^{28} regions in this process could be tested by analyzing the effect of FlgM on holoenzyme containing hybrid σ^{70}/ σ^{28} subunits. A hybrid sigma factor has been used successfully to demonstrate the specificity of sigma factor regions for particular promoter sequence determinants (96) By substituting various σ^{28} regions for σ^{70} regions, and then measuring the ability of FlgM to destabilize holoenzyme containing these recombinant sigma factors, it may be possible to distinguish between the competitive displacement mechanism, which requires FlgM to interact with all three σ^{28} regions to destabilize holoenzyme, and the allosteric displacement mechanism. A more complete analysis of the sensitivity of holoenzyme containing the various σ^{28}* mutants to FlgM may also help to distinguish these two models.

Although a specific interaction between FlgM and core RNAP was never observed in our SPR assays, under the high protein concentration conditions used in the native gel assays, a small amount of FlgM was detected with the core RNAP complex (see Chapter 4). A short stretch of sequence homology between FlgM and the region 2.1 core binding motif (VEANLRL) (178) suggests a possible basis for this association. The C-terminal σ^{28} binding domain of FlgM contains the sequence VEALK, which aligns reasonably well with the core binding motif if a gap is introduced between the Asn65 and Leu66 (Figure 6.1). The conserved hydrophobic residues that follow this

motif in σ^{70} (see Figure 1.4) are also present in FlgM. Leu66 has been shown to be important for σ^{28} inhibition *in vivo* (181) and *in vitro* (see Chapter 4). Interestingly, this region of FlgM also has significant homology to the DnaK chaperone of *B. subtilis* (Figure 6.1). DnaK negatively regulates σ^{32} by binding to it and presenting it to the FtsH protease (179); it is also thought to interact with $E\sigma^{32}$, and may possess holoenzyme destabilization activity (111, 170). Whether the VEALK sequence in FlgM mediates a low affinity interaction with core RNAP remains to be determined. Perhaps when FlgM is brought into close proximity with holoenzyme through contacts with σ^{28}, it uses this core binding motif-like sequence to displace σ^{28} from core through a competitive binding mechanism.

HIGH RESOLUTION CHARACTERIZATION OF THE σ^{28}/FlgM INTERACTION

NMR analysis of the σ^{28}/FlgM complex revealed that the entire C-terminal half of FlgM becomes constrained upon σ^{28} binding (28, 29). It is possible that contacts with σ^{28} occur along the length of this 54 amino acid region. The genetic analysis of *flgM** mutants defective for σ^{28} inhibition has not been carried out to saturation; the isolation and characterization of additional *flgM** mutants would almost certainly identify more FlgM residues that either directly contact σ^{28} or stabilize the σ^{28}/FlgM complex. To carry the analysis of the σ^{28}/FlgM interaction to the next level, however, genetic or biochemical experiments to identify specific contacts between σ^{28} and FlgM residues should be performed.

Although initial attempts to obtain *flgM*-linked extragenic suppressors of the *fliA** mutants were not successful (see Chapter 3), a modified approach could succeed. Targeted mutagenesis of the C-terminal half of *flgM* would preclude the isolation of non-*flgM* mutants and promoter mutants that suppressed the *fliA** phenotype by overexpressing FlgM, and should increase the relative frequency of the desired class of

flgM^{S} mutants. One way in which this could be accomplished is by PCR amplification of the C-terminal half of the *flgM* gene using mutagenic conditions. A library created by cloning the amplified product into expression vectors could be first screened in a *fliA*$^{+}$ strain for clones that were unable to suppress wild type σ^{28}. These mutants could then be pooled and tested for the presence of clones that were able to inhibit σ^{28}-dependent gene expression when introduced into the various *fliA** backgrounds.

A technically demanding, but potentially informative approach to the characterization of the σ^{28}/FlgM complex is X-ray crystallography. A complex of full-length proteins has proven recalcitrant to crystallization (G. Daughdrill, personal communication), probably because the unstructured N-terminal half of FlgM interferes with an ordered arrangement of the molecules. Attempts to crystallize complex that has been digested with proteases to remove unstructured portions of FlgM and σ^{28} have been unsuccessful (R. Strong and K. Hughes, personal communication). A more effective strategy to generate the starting material for crystallization might be to purify a complex of σ^{28} and a truncated FlgM peptide coexpressed *in vivo*. A C-terminal FlgM protein (residues 42 through 97) expressed *in vivo* has σ^{28} binding activity, although it could not be detected by Western analysis (see Chapter 3), indicating that it is significantly less stable than full length FlgM. Coexpression of σ^{28} with this protein might stabilize it sufficiently to allow the purification of σ^{28}/FlgM(42-97) complex.

REGULATION OF FlgM ACTIVITY

Our measurements of the dissociation rate of the σ^{28}/FlgM complex revealed a extremely long half-life *in vitro* (> one hour). However, temporal analysis of flagellar gene expression indicates that FlgM inhibition of σ^{28}-dependent Class 3 expression is lifted only minutes after the hook basal body (HBB) becomes competent for FlgM export (V. Bettenworth and K. Hughes, unpublished observations). How can these

two observations be reconciled? One possibility is that σ^{28} bound by FlgM is never released. The σ^{28}/FlgM complex may be targeted for degradation, similar to the way in the chaperones DnaK, DnaJ and GrpE regulate σ^{32} levels (see Chapter 1). In this case, transcription of the Class 3 genes would be carried out by σ^{28} synthesized after the onset of FlgM export. This model is inconsistent with one role we have proposed for FlgM, i.e. that it functions to allow σ^{28} to accumulate in preparation for high-level Class 3 gene expression following HBB completion. Perhaps it is important for the cell to be able to express *fliA* from a Class 2 rather than a Class 3 promoter, even though σ^{28} activity is not required until the HBB is complete. By coexpressing FlgM with σ^{28} at Class 2 times, σ^{28} accumulation would be avoided.

Another possibility is that the half-life of the complex *in vivo* is much shorter than the half-life *in vitro*. Destabilization of the σ^{28}/FlgM complex *in vivo* could be induced by interaction with a third, as yet unidentified, regulatory protein. Anti-anti-sigma factors that interact with sigma/anti-sigma factor complexes to effect the release of the sigma factor have been identified in a number of other bacteria (reviewed in75). Whether *S. typhimurium* possesses a dedicated anti-FlgM protein whose only function is to destabilize the σ^{28}/FlgM complex, or whether this putative regulator of FlgM turns out to be a component of the export apparatus that is also required for export of other flagellar proteins remains to be determined. In bacteria where anti-anti-sigma factors have been identified, they are typically coexpressed from the same operon that contains the genes for the sigma factor and the anti-sigma factor (reviewed in75). There is some evidence that the genes downstream of *fliA*, *fliZY* regulate the activity of σ^{28}, but the data suggests that their function may be as negative regulators of σ^{28}, not as antagonists of FlgM (139). The gene downstream of *flgM*, *flgN*, is required for wild type motility in *Salmonella* and *Proteus mirabilis*. The FlgN protein appears to play a role in the polymerization of flagellin (57, 105). It has also been observed that in a *flgN* mutant,

transcription of the *flgM* gene is decreased 10-fold, suggesting an additional role for FlgN in the regulation of Class 3 gene expression (K. Brown and K. Hughes, unpublished observations).

As a negative regulator of a negative regulator, null mutations in the putative anti-FlgM gene would be expected to have a constitutive Class 3^{OFF} phenotype. Selections for this phenotype would be complicated, since any Class 1 or Class 2 mutant could satisfy this criterion. Gain-of-function mutations in the putative anti-FlgM protein that strengthened its interaction with FlgM or that increased its steady state level would be expected to interfere with the ability of FlgM to inhibit σ^{28}. These mutants should have the Class 3^{ON} phenotype characteristic of *fliA** and *flgM** mutants. Both of the selections used to isolate *fliA** and *flgM** mutants produced classes of mutants unlinked to either of these loci (see Appendix, Table A.3). These chromosomal location of these mutants has yet to be determined. Characterization of these mutants may lead to the discovery of additional factors that influence expression of the genes of the flagellar regulon.

Figure 6.1 The σ^{28} binding domain of FlgM contains homology to σ^{70} in addition to σ^{32}. An alignment of *S. typhimurium* FlgM (residues 46 through 75) with *B. subtilis* DnaK (residues 523 through 551) is shown (from 8). Darkly shaded residues are identical; lightly shaded residues are similar (residues considered similar are: DE, RK, LVIS, ST, NQ). The region of FlgM that shows similarity to the core RNAP binding motif of σ^{70} (178) is underlined; the σ^{70} sequence is provided for comparison above the alignment.

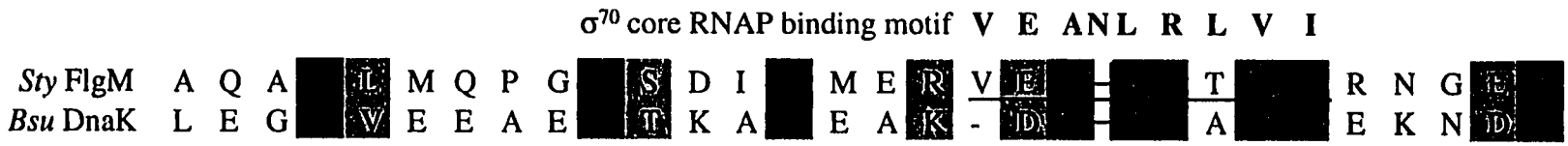
σ70 core RNAP binding motif V E ANL R L V I
Sty FlgM A Q A L M Q P G S D I M E R V E T R N G E
Bsu DnaK L E G V E E A E T K A E A K - D A E K N D

List of References

1. **Adelman, K., G. Orsini, A. Kolb, L. Graziani, and E. N. Brody.** 1997. The interaction between the AsiA protein of bacteriophage T4 and the σ^{70} subunit of *Escherichia coli* RNA polymerase. J. Biol. Chem. **272:**27435-27443.

2. **Alper, S., L. Duncan, and R. Losick.** 1994. An adenosine nucleotide switch controlling the activity of a cell type-specific transcription factor in B. subtilis. Cell. **77:**195-205.

3. **Artsimovitch, I., K. Murakami, A. Ishihama, and M. M. Howe.** 1996. Transcription activation by the bacteriophage Mu Mor protein requires the C-terminal regions of both alpha and sigma70 subunits of Escherichia coli RNA polymerase. J. Biol. Chem. **271:**32343-8.

4. **Barne, K. A., J. A. Bown, S. J. Busby, and S. D. Minchin.** 1997. Region 2.5 of the Escherichia coli RNA polymerase sigma70 subunit is responsible for the recognition of the 'extended-10' motif at promoters. Embo J. **16:**4034-40.

5. **Benson, N., P. Sugiono, S. Bass, L. Mendelman, and P. Youderian.** 1986. General selection for specific DNA-binding activities. Genetics. **114:**1-14.

6. **Bradford, M. M.** 1976. A rapid and sensitive method for the quantitation of microgram quantities of protein utilizing the principle of protein-dye binding. Anal. Biochem. **72:**248-254.

7. **Brennan, R., and B. Matthews.** 1989. The helix-turn-helix DNA binding motif. J. Biol. Chem. **264:**1903-1906.

8. **Brown, K. L., and K. T. Hughes.** 1995. The role of anti-sigma factors in gene regulation. Mol. Microbiol. **16:**397-404.

9. **Brun, Y. V., and L. Shapiro.** 1992. A temporally controlled σ factor is required for polar morphogenesis and normal cell division in *Caulobacter*. Genes & Dev. **6:**2395-2408.

10. **Buckle, M., A. Geiselmann, A. Kolb, and H. Buc.** 1991. Protein-DNA crosslinking at the *lac* promoter. Nucleic Acids Res. **19:**833-40.

11. **Burgess, R. R., and A. A. Travers.** 1970. *Escherichia coli* RNA polymerase: purification, subunit structure, and factor requirements. Fed. Proc. **29:**1164-1169.

12. **Burgess, R. R., A. A. Travers, J. J. Dunn, and E. K. Bautz.** 1969. Factor stimulating transcription by RNA polymerase. Nature. **221:**43-6.

13. **Burkholder, W. F., X. Zhao, X. Zhu, W. A. Hendrickson, A. Gragerov, and M. E. Gottesman.** 1996. Mutations in the C-terminal fragment of DnaK affecting peptide binding. Proc. Natl. Acad. Sci. USA. **93:**10632-7.

14. **Busby, S., and R. H. Ebright.** 1994. Promoter structure, promoter recognition, and transcription activation in prokaryotes. Cell. **79:**643-46.

15. **Callaci, S., and T. Heyduk.** 1998. Conformation and DNA binding properties of a single-stranded DNA binding region of sigma 70 subunit from Escherichia coli RNA polymerase are modulated by an interaction with the core enzyme. Biochem. **37:**3312-20.

16. **Casadaban, M. J., and J. Chou.** 1984. *In vivo* formation of gene fusions encoding hybrid β-galactosidase proteins in one step with a transposable Mu-*lac* transducing phage. Proc. Natl. Acad. Sci. USA. **81:**535-39.

17. **Casadaban, M. J., and S. N. Cohen.** 1979. Lactose genes fused to exogenous promoter in one step using a Mu-*lac* bacteriophage: *in vivo* probe for transpositional control sequences. Proc. Natl. Acad. Sci. USA. **76:**4530-33.

18. **Casanova, J.-L., C. Pannetier, C. Jaulin, and P. Kourilsky.** 1990. Optimal conditions for directly sequencing double-stranded PCR products with sequenase. Nucleic Acids Res. **18:**4028.

19. **Castilho, B. A., P. Olfson, and M. J. Casadaban.** 1984. Plasmid insertion mutagenesis and *lac* gene fusion with mini-Mu bacteriophage transposons. J. Bacteriol. **158:**488-495.

20. **Chamberlin, M. J.** 1974. The selectivity of transcription. Annual Reviiew of Biochemistry. **43:**721-75.

21. **Chan, R. K., D. Botstein, T. Watanabe, and Y. Ogata.** 1972. Specialized transduction of tetracycline resistance by phage P22 in *Salmonella typhimurium*. II. Properties of a high frequency transducing lysate. Virology. **50:**883-898.

22. **Chen, Y. F., and J. D. Helmann.** 1995. The Bacillus subtilis flagellar regulatory protein sigma D: overproduction, domain analysis and DNA-binding properties. J. Mol. Biol. **249:**743-53.

23. **Cliften, P. F., J. Y. Park, B. P. Davis, S. H. Jang, and J. A. Jaehning.** 1997. Identification of three regions essential for interaction between a σ-like factor and core RNA polymerase. Genes & Dev. **11:**2897-2909.

24. **Coggins, J. R., J. Lumsden, and A. D. Malcolm.** 1977. A study of the quaternary structure of Escherichia coli RNA polymerase using bis(imido esters). Biochem. **16:**1111-6.

25. **Colland, F., G. Orsini, E. N. Brody, H. Buc, and A. Kolb.** 1998. The bacteriophage T4 AsiA protein: a molecular switch for sigma 70-dependent promoters. Mol. Microbiol. **27:**819-829.

26. **Craig, E., B. Gambill, and R. Nelson.** 1993. Heat shock proteins: molecular chaperones of protein biogenesis. Microbiol. Rev. **57:**402-14.

27. **Daniels, D., P. Zuber, and R. Losick.** 1990. Two amino acids in an RNA polymerase sigma factor involved in the recognition of adjacent base pairs in the -10 region of a cognate promoter. Proc. Natl. Acad. Sci. USA. **87:**8075-9.

28. **Daughdrill, G. W., M. S. Chadsey, J. E. Karlinsey, K. T. Hughes, and F. W. Dahlquist.** 1997. The C-terminal half of the anti-sigma factor, FlgM, becomes structured when bound to its target, σ^{28}. Nat. Struct. Biol. **4:**285-291.

29. **Daughdrill, G. W., L. J. Hanely, and F. W. Dahlquist.** 1998. The C-terminal half of the anti-sigma factor FlgM contains a dynamic equilibrium solution structure favoring helical conformations. Biochem. **37:**1076-1082.

30. **Davis, R. W., D. Botstein, and J. R. Roth.** 1980. A manual for genetic engineering: advanced bacterial genetics. Cold Spring Harbor Laboratory Press, Cold Spring Harbor, N.Y.

31. **De Las Penas, A., L. Connolly, and C. A. Gross.** 1997. The sigmaE-mediated response to extracytoplasmic stress in Escherichia coli is transduced by RseA and RseB, two negative regulators of sigmaE. Mol. Microbiol. **24:**373-85.

32. **de Wet, J. R., H. Fukushima, N. N. Dewji, E. Wilcox, J. S. O'Brien, and Helinski.** 1984. Chromogenic immunodetection of human serum albumin and alpha-L-fucosidase clones in a human hepatoma cDNA expression library. DNA. **3:**437-446.

33. **Decatur, A. L., and R. Losick.** 1996. Three sites of contact between the *Bacillus subtilis* transcription factor σ^F and its antisigma factor SpoIIAB. Genes & Dev. **10:**2348-2358.

34. **deHaseth, P. L., and J. D. Helmann.** 1995. Open complex formation by *Escherichia coli* RNA polymerase: the mechanism of polymerase-induced strand separation of double helical DNA. Mol. Microbiol. **16:**817-824.

35. **Diederich, B., J. F. Wilkinson, T. Magnin, M. Najafi, J. Erringston, and M. D. Yudkin.** 1994. Role of interactions between SpoIIAA and SpoIIAB in regulating cell-specific transcription factor sigma F of Bacillus subtilis. Genes & Dev. **8:**2653-2663.

36. **Dombroski, A. J., W. A. Walter, and C. A. Gross.** 1993. Amino-terminal amino acids modulate sigma-factor DNA-binding activity. Genes & Dev. **7:**2446-2455.

37. **Dombroski, A. J., W. A. Walter, and C. A. Gross.** 1993. The role of the sigma subunit in promoter recognition by RNA polymerase. Cell. Mol. Biol. Res. **39:**311-7.

38. **Dombroski, A. J., W. A. Walter, M. T. Record, Jr., D. A. Siegele, and C. A. Gross.** 1992. Polypeptides containing highly conserved regions of transcription initiation factor sigma 70 exhibit specificity of binding to promoter DNA. Cell. **70:**501-12.

39. **Duncan, L., S. Alper, and R. Losick.** 1996. SpoIIAA governs the release of the cell-type specific transcription factor sigma F from its anti-sigma factor SpoIIAB. Methods Mol. Biol. **260:**147-64.

40. **Duncan, L., and R. Losick.** 1993. SpoIIAB is an anti-sigma factor that binds to and inhibits transcription by regulatory protein sigma F from Bacillus subtilis. Proc. Natl. Acad. Sci. USA. **90:**2325-9.

41. **Elliot, T.** 1993. Transport of 5-aminolevulinic acid by the dipeptide permease in *Salmonella typhimurium*. J. Bacteriol. **175:**325-31.

42. **Errington, J.** 1993. *Bacillus subtilis* sporulation: regulation of Gene expression and control of morphogenesis. Microbiol. Rev. **57:**1-33.

43. **Gamer, J., G. Multhaup, T. Tomoyasu, J. S. McCarty, S. Rudiger, H. J. Schonfeld, C. Schirra, H. Bujard, and B. Bukau.** 1996. A cycle of binding and release of the DnaK, DnaJ and GrpE chaperones regulates activity of the *Escherichia coli* heat shock transcription factor σ^{32}. Embo J. **15:**607-617.

44. **Gardella, T., H. Moyle, and M. M. Susskind.** 1989. A mutant Escherichia coli sigma 70 subunit of RNA polymerase with altered promoter specificity. J. Mol. Biol. **206:**579-90.

45. **Gaston, K., A. Bell, A. Kolb, H. Buc, and S. Busby.** 1990. Stringent spacing requirements for transcription activation by CRP. Cell. **62:**733-43.

46. **Geiduschek, E. P.** 1991. Regulation of expression of the late genes of bacteriophage T4. Annu. Rev. Genet. **25:**437-60.

47. **Gilbert, W.** 1976. , p. 193-205. *In* R. Losick and M. Chamberlin (ed.), RNA Polymerase. Cold Spring Harbor Laboratories, Cold Spring Harbor, NY.

48. **Gill, S. C., and P. H. von Hippel.** 1989. Calculation of protein extinction coefficients from amino acid sequence data. Anal. Biochem. **182:**319-326.

49. **Gill, S. C., S. E. Weitzel, and H.-P. H. von.** 1991. *Escherichia coli* σ^{70} and NusA proteins. I. Binding interactions with core RNA polymerase in solution and within the transcription complex. J. Mol. Biol. **220:**307-324.

50. **Gillen, K. L., and K. T. Hughes.** 1991. Molecular characterization of flgM, a gene encoding a negative regulator of flagellin synthesis in Salmonella typhimurium. J. Bacteriol. **173:**6453-9.

51. **Gillen, K. L., and K. T. Hughes.** 1991. Negative regulatory loci coupling flagellin synthesis to flagellar assembly in *Salmonella typhiumurium*. J. Bacteriol. **173:**2301-2310.

52. **Gillen, K. L., and K. T. Hughes.** 1993. Transcription from two promoters and autoregulation contribute to the control of expression of the Salmonella typhimurium flagellar regulatory gene flgM. J. Bacteriol. **175:**7006-15.

53. **Greiner, D. P., K. A. Hughes, A. H. Gunasekera, and C. F. Meares.** 1996. Binding of the sigma 70 protein to the core subunits of Escherichia coli RNA polymerase, studied by iron-EDTA protein footprinting. Proc. Natl. Acad. Sci. USA. **93:**71-5.

54. **Gribskov, M., and R. R. Burgess.** 1986. Sigma factors from E. coli, B. subtilis, phage SP01, and phage T4 are homologous proteins. Nucleic Acids Res. **14:**6745-63.

55. **Gribskov, M., and R. R. Burgess.** 1986. Sigma factors from *E. coli*, *B. subtilis*, phage SPO1, and phage T4 are homologous proteins. Nucleic Acids Res. **16:**6745-6763.

56. **Gross, C. A., D. B. Straus, J. W. Erickson, and T. Yura.** 1990. The function and regulation of heat shock proteins in *Escherichia coli*, p. 167-189. *In* R. Morimoto, A. Tissieres, and C. Georgopoulos (ed.), Stress proteins in biology and medicine. Cold Spring Harbor Laboratory Press, Cold Spring Harbor, N. Y.

57. **Gygi, D., G. Fraser, A. Dufour, and C. Hughes.** 1997. A motile but non-swarming mutant of Proteus mirabilis lacks FlgN, a facilitator of flagella filament assembly. Mol. Microbiol. **25:**597-604.

58. **Hagar, D. A., and R. R. Burgess.** 1980. Elution of proteins from sodium dodecyl sulfate-polyacrylamide gels, removal of sodium dodecyl sulfate, and renaturation of enzymatic activity: results with sigma subunit of *Escherichia coli* RNA polymerase, wheat germ DNA topoisomerase, and other enzymes. Anal. Biochem. **109:**76-86.

59. **Haldenwang, W. G.** 1995. The sigma factors of Bacillus subtilis. Microbiol. Rev. **59:**1-30.

60. **Harlow, E., and D. Lane.** 1988. Antibodies, a laboratory manual. Cold Spring Harbor Laboratories, Cold Spring Harbor, NY.

61. **Hawley, D. K., and W. R. McClure.** 1982. Mechanism of activation of transcription initiation from the lambda PRM promoter. J. Mol. Biol. **157:**493-525.

62. **Helmann, J. D., and M. J. Chamberlin.** 1988. Structure and function of bacterial sigma factors. Annu. Rev. Biochem. **57:**839-72.

63. **Herendeen, D. R., K. P. Williams, G. A. Kassavetis, and E. P. Geiduschek.** 1990. An RNA polymerase-binding protein that is required for communication between an enhancer and a promoter. Science. **248:**573-8.

64. **Herman, C., D. Thevenet, R. D'Ari, and P. Bouloc.** 1995. Degradation of σ^{32}, the heat shock regulator in *Escherichia coli*, is governed by HflB. Proc. Natl. Acad. Sci. USA. **92:**3516-20.

65. **Hernandez, V. J., L. M. Hsu, and M. Cashel.** 1996. Conserved region 3 of Escherichia coli final sigma70 is implicated in the process of abortive transcription. J. Biol. Chem. **271:**18775-9.

66. **Hillel, Z., and C. W. Wu.** 1977. Subunit topography of RNA polymerase from Escherichia coli. A cross- linking study with bifunctional reagents. Biochem. **16:**3334-42.

67. **Hinkle, D. C., and M. J. Chamberlin.** 1972. Studies of the binding of *Escherichia coli* RNA polymerase to DNA. I. The role of sigma subunit in site selection. J. Mol. Biol. **70:**157-195.

68. **Hinton, D. M.** 1991. Transcription from a bacteriophage T4 middle promoter using T4 MotA protein and phage-modified RNA polymerase. J. Biol. Chem. **266:**18034-44.

69. **Hinton, D. M., A.-R. March, J. S. Gerber, and M. Sharma.** 1996. Characterization of pre-transcription complexes made at a bacteriophage T4 middle promoter: involvement of the T4 MotA activator and the T4 AsiA protein, a sigma 70 binding protein, in the formation of the open complex. J. Mol. Biol. **256:**235-248.

70. **Hochschild, A., and S. L. Dove.** 1998. Protein-protein contacts that activate and repress prokaryotic transcription. Cell. **92:**597-600.

71. **Holmes, D. S., and Quigley.** 1981. A rapid boiling method for the preparation of bacterial plasmids. Anal. Biochem. **114:**193-97.

72. **Hsu, L. M.** 1996. Quantitative parameters for promoter clearance. Meth. Enzymol. **273:**59-71.

73. **Huang, X., d.-S. -. F. J. Lopez, and J. D. Helmann.** 1997. sigma factor mutations affecting the sequence-selective interaction of RNA polymerase with -10 region single-stranded DNA. Nucleic Acids Res. **25:**2603-2609.

74. **Hughes, K. T., K. L. Gillen, M. J. Semon, and J. E. Karlinsey.** 1993. Sensing structural intermediates in bacterial flagellar assembly by export of a negative regulator. Science. **262:**1277-1280.

75. **Hughes, K. T., and K. Matthai.** 1998. The Anti-sigma factors. Ann. Rev. Microbiol. **52.**

76. **Hughes, K. T., and J. R. Roth.** 1984. Conditionally transposition-defective derivative of Mu d1(Amp Lac). J. Bacteriol. **159:**130-7.

77. **Ishihama, A.** 1991. Global control of gene expression in bacteria., p. 121-140. *In* A. Ishihama and H. Yoshikawa (ed.), Control of cell growth and division. Springer, New York.

78. **Ishihama, A.** 1997. Promoter selectivity control of RNA polymerase, p. 53-70. *In* F. Eckstein and D. M. J. Lilley (ed.), Nuclei Acids and Molecular Biology, vol. 11. Springer-Verlag, Berlin.

79. **Ishihama, A.** 1993. Protein-protein communication within the transcription apparatus. J. Bacteriol. **175:**2483-9.

80. **Iyoda, S., and K. Kutsukake.** 1995. Molecular dissection of the flagellum-specific anti-sigma factor, FlgM, of Salmonella typhimurium. Mol. Gen. Genet. **249:**417-24.

81. **Jacob, T., and J. Monod.** 1961. Genetic regulatory mechanisms in the synthesis of proteins. J. Mol. Biol. **3:**318-356.

82. **Jishage, M., and A. Ishihama.** 1998. A stationary phase protein in Escherichia coli with binding activity to the major sigma subunit of RNA polymerase. Proc. Natl. Acad. Sci. USA. **95:**4953-8.

83. **Jishage, M., A. Iwata, S. Ueda, and A. Ishihama.** 1996. Regulation of RNA polymerase sigma subunit synthesis in *Escherichia coli*: intracellular levels of four species of sigma subunit under various growth conditions. J. Bacteriol. **178:**5447-5451.

84. **Joo, D. M., N. Ng, and R. Calendar.** 1997. A σ^{32} mutant with a single amino acid change in the highly conserved region 2.2 exhibits reduced core RNA polymerase affinity. Proc. Natl. Acad. Sci. USA. **94:**4907-4912.

85. **Joo, D. M., A. Nolte, R. Calendar, Y. N. Zhou, and D. J. Jun.** 1998. Multiple regions on the *Escherichia coli* heat shock transcription factor σ^{32} determine core RNA polymerase binding specificity. J. Bacteriol. **180:**1095-1102.

86. **Juang, Y. L., and J. D. Helmann.** 1995. Pathway of promoter melting by Bacillus subtilis RNA polymerase at a stable RNA promoter: effects of temperature, delta protein, and sigma factor mutations [published erratum appears in Biochemistry 1995 Oct 31;34(43):14270]. Biochem. **34:**8465-73.

87. **Juang, Y. L., and J. D. Helmann.** 1994. A promoter melting region in the primary sigma factor of Bacillus subtilis. Identification of functionally important aromatic amino acids. J. Mol. Biol. **235:**1470-88.

88. **Karlinsey, J. E., A. J. Pease, M. E. Winkler, J. L. Bailey, and K. T. Hughes.** 1997. The flk gene of Salmonella typhimurium couples flagellar P- and L-ring assembly to flagellar morphogenesis. J. Bacteriol. **179:**2389-400.

89. **Karlinsey, J. E., H.-C. T. Tsui, M. E. Winkler, and K. T. Hughes.** 1998. Flk couples *flgM* translation to flagellar ring assembly in *Salmonella typhimurium*. J. Bacteriol. **in press.**

90. **Karlsson, R., A. Michaelsson, and L. Mattsson.** 1991. Kinetic analysis of monoclonal antibody-antigen interactions with a new biosensor based analytical system. J. Immun. Meth. **145:**229-240.

91. **Kawagishi, I., V. Muller, A. W. Williams, V. M. Irikura, and R. M. Macnab.** 1992. Subdivision of flagellar region III on the *Escherichia coli* and *Salmonella typhimurium* chromosomes and identification of two additional flagellar genes. J. Gen. Microbiol. **138:**1051-65.

92. **Komeda, Y.** 1982. Fusions of flagellar operons to lactose genes on a Mu *lac* bacteriophage. J. Bacteriol. **150:**16-26.

93. **Komeda, Y., H. Suzuki, J.-I. Ishidsu, and T. Iino.** 1975. The role of cAMP in flagellation of *Salmonella typhimuium*. Mol. Gen. Genet. **142:**289-98.

94. **Krummel, B., and M. J. Chamberlin.** 1989. RNA chain initiation by Escherichia coli RNA polymerase. Structural transitions of the enzyme in early ternary complexes. Biochem. **28:**7829-42.

95. **Kumar, A., B. Grimes, N. Fujita, K. Makino, R. A. Malloch, R. S. Hayward, and A. Ishihama.** 1994. Role of the sigma 70 subunit of Escherichia coli RNA polymerase in transcription activation. J. Mol. Biol. **235:**405-413.

96. **Kumar, A., B. Grimes, M. Logan, S. Wedgwood, H. Williamson, and R. S. Hayward.** 1995. A hybrid sigma subunit directs RNA polymerase to a hybrid promoter in *Escherichia coli*. J. Mol. Biol. **246:**563-71.

97. **Kumar, A., H. S. Williamson, N. Fujita, A. Ishihama, and R. S. Hayward.** 1995. A partially functional 245-amino-acid internal deletion derivative of Escherichia coli sigma 70. J. Bacteriol. **177:**5193-5196.

98. **Kumar, S. A.** 1981. The structure and mechanism of action of bacterial DNA-dependent RNA polymerase. Prog. Biophys. Mol. Biol. **38:**165-210.

99. **Kundu, T. K., S. Kusano, and A. Ishihama.** 1997. Promoter selectivity of *Escherichia coli* RNA polymerase σ^F holoenzyme involved in transcription of flagellar and chemotaxis genes. J. Bacteriol. **179:**4264-4269.

100. **Kutsukake, K.** 1997. Autogenous and global control of the flagellar master operon, flhD, in Salmonella typhimurium. Mol. Gen. Genet. **254:**440-448.

101. **Kutsukake, K.** 1994. Excretion of the anti-sigma factor through a flagellar substructure couples flagellar gene expression with flagellar assembly in Salmonella typhimurium. Mol. Gen. Genet. **243:**605-12.

102. **Kutsukake, K., and T. Iino.** 1994. Role of the FliA-FlgM regulatory system on the transcriptional control of the flagellar regulon and flagellar formation in *Salmonella typhimurium*. J. Bacteriol. **176:**3598-3605.

103. **Kutsukake, K., S. Iyoda, K. Ohnishi, and T. Iino.** 1994. Genetic and molecular analyses of the interaction between the flagellum-specific sigma and anti-sigma factors in *Salmonella typhimurium*. Embo J. **13:**4568-4576.

104. **Kutsukake, K., Y. Ohya, and T. Iino.** 1990. Transcriptional analysis of the flagellar regulon of *Salmonella typhimurium*. J. Bacteriol. **172:**741-747.

105. **Kutsukake, K., T. Okada, T. Yokoseki, and T. Iino.** 1994. Sequence analysis of the *flgA* gene and its adjacent region in *Salmonella typhimurium*, and identification of another flagellar gene, *flgN*. Gene. **143:**49-54.

106. **Laemmli, U. K., and M. Favre.** 1973. Maturation of the head of bacteriophage T4. I. DNA packaging events. J. Mol. Biol. **80:**575-599.

107. **Lederber, J.** 1948. Detection of fermentation variants with tetrazolium. J. Bacteriol. **56:**695.

108. **Leonetti, J. P., K. Wong, and E. P. Geiduschek.** 1998. Core-sigma interaction: probing the interaction of the bacteriophage T4 gene 55 promoter recognition protein with E.coli RNA polymerase core. Embo J. **17:**1467-75.

109. **Lesley, S. A., and R. R. Burgess.** 1989. Characterization of the *Escherichia coli* transcription factor σ^{70}: localization of a region involved in the interaction with core RNA polymerase. Biochem. **28:**7728-2234.

110. **Li, M., H. Moyle, and M. M. Susskind.** 1994. Target of the transcriptional activation function of phage lambda cI protein. Science. **263:**75-7.

111. **Liberek, K., and C. Georgopoulos.** 1993. Autoregulation of the Escherichia coli heat shock response by the DnaK and DnaJ heat shock proteins. Proc. Natl. Acad. Sci. USA. **90:**11019-23.

112. **Liberek, K., J. Marszalek, D. Ang, C. Georgopoulos, and M. Zylicz.** 1991. Escherichia coli DnaJ and GrpE heat shock proteins jointly stimulate ATPase activity of DnaK. Proc. Natl. Acad. Sci. USA. **88:**2874-8.

113. **Liberek, K., D. Skowyra, M. Zylicz, C. Johnson, and C. Georgopoulos.** 1991. The Escherichia coli DnaK chaperone, the 70-kDa heat shock protein eukaryotic equivalent, changes conformation upon ATP hydrolysis, thus triggering its dissociation from a bound target protein. J. Biol. Chem. **266:**14491-6.

114. **Liberek, K., D. Wall, and C. Georgopoulos.** 1995. The DnaJ chaperone catalytically activates the DnaK chaperone to preferentially bind the sigma 32 heat shock transcriptional regulator. Proc. Natl. Acad. Sci. USA. **92:**6224-8.

115. **Liu, X., N. Fujita, A. Ishihama, and P. Matsumura.** 1995. The C-terminal region of the alpha subunit of Escherichia coli RNA polymerase is required for transcriptional activation of the flagellar level II operons by the FlhD/FlhC complex. J. Bacteriol. **177:**5186-8.

116. **Liu, X., and P. Matsumura.** 1996. Differential regulation of multiple overlapping promoters in flagellar class II operons in *Escherichia coli.* Mol. Microbiol. **21:**613-620.

117. **Liu, X., and P. Matsumura.** 1994. The FlhD/FlhC complex, a transcriptional activator of the Escherichia coli flagellar class II operons. J. Bacteriol. **176:**7345-7351.

118. **Lonetto, M., M. Gribskov, and C. A. Gross.** 1992. The σ^{70} family: sequence conservation and evolutionary relationships. J. Bacteriol. **174:**3843-3849.

119. **Lonetto, M. A., K. L. Brown, K. E. Rudd, and M. J. Buttner.** 1994. Analysis of the *Streptomyces coelicolor sigE* gene reveals the existence of a subfamily of eubacterial RNA polymerase sigma factorws involved in the regulation of extracytoplasmic functions. Proc. Natl. Acad. Sci. USA. **91:**7573-77.

120. **Lord, M., T. Magnin, and M. D. Yudkin.** 1996. Protein conformational change and nucleotide binding involved in regulation of sigmaF in Bacillus subtilis. J. Bacteriol. **178:**6730-6735.

121. **Losick, R., and J. Pero.** 1981. Cascades of sigma factors. Cell. **25:**582-84.

122. **Lowe, P. A., D. A. Hagar, and R. R. Burgess.** 1979. Purification and properties of the σ subunit of *Escherichia coli* DNA-dependent RNA polymerase. Biochem. **18:**1344-1352.

123. **Macnab, R. M.** 1996. Flagella and motility, p. 123-145. *In* F. C. Neidhardt (ed.), *Escherichia coli* and *Salmonella typhimurium*, vol. 1. ASM Press, Washington D. C.

124. **Macnab, R. M.** 1992. Genetics and biogenesis of bacterial flagella. Annu. Rev. Genet. **26:**131-58.

125. **Magnin, T., M. Lord, J. Errington, and M. D. Yudkin.** 1996. Establishing differential gene expression in sporulating Bacillus subtilis: phosphorylation of SpoIIAA (anti-anti-sigmaF) alters its conformation and prevents formation of a SpoIIAA/SpoIIAB/ADP complex. Mol. Microbiol. **19:**901-7.

126. **Magnin, T., M. Lord, and M. D. Yudkin.** 1997. Contribution of partner switching and SpoIIAA cycling to regulation of sigmaF activity in sporulating Bacillus subtilis. J. Bacteriol. **179:**3922-7.

127. **Makino, K., M. Amemura, S. K. Kim, A. Nakata, and H. Shinagawa.** 1993. Role of the sigma 70 subunit of RNA polymerase in transcriptional activation by activator protein PhoB in Escherichia coli. Genes & Dev. **7:**149-60.

128. **Malhotra, A., E. Severinova, and S. A. Darst.** 1996. Crystal structure of a σ^{70} subunit fragment from *E. coli* RNA polymerase. Cell. **87:**127-136.

129. **Maloy, S.** 1990. Experimental techniques in bacterial genetics. Jones and Bartlett publishers, Boston, MA.

130. **Maloy, S., and J. Roth.** 1983. Regulation of proline utilization in *Salmonella typhimurium*: characterization of *put*::Mu*d*(Ap, *lac*) operon fusions. J. Bacteriol. **154:**561-568.

131. **Marr, M. T., and J. W. Roberts.** 1997. Promoter recognition as measured by binding of polymerase to nontemplate strand oligonucleotide. Science. **276:**1258-1260.

132. **Masson, D., and J. Tscopp.** 1987. A family of serine esterases in lytic granules of cytolytic T lymphocytes. Cell. **49:**679.

133. **McCarty, J. S., S. Rudiger, H. J. Schonfeld, M.-J. Schneider, K. Nakahigashi, T. Yura, and B. Bukau.** 1996. Regulatory region C of the E. coli heat shock transcription factor, sigma32, constitutes a DnaK binding site and is conserved among eubacteria. J. Mol. Biol. **256:**829-837.

134. **McClure, W. R.** 1985. Mechanism and control of transcription initiation in prokaryotes. Annu. Rev. Biochem. **54:**171-204.

135. **McMahan, S. A., and R. R. Burgess.** 1994. Use of aryl azide cross-linkers to investigate protein-protein interactions: an optimization of important conditions as applied to Escherichia coli RNA polymerase and localization of a sigma 70-alpha cross-link to the C-terminal region of alpha. Biochem. **33:**12092-9.

136. **Merrick, M. J.** 1993. In a class of its own--the RNA polymerase sigma factor sigma 54 (sigma N). Mol. Microbiol. **10:**903-9.

137. **Min, K. T., C. M. Hilditch, B. Diederich, J. Errington, and M. D. Yudkin.** 1993. Sigma F, the first compartment-specific transcription factor of B. subtilis, is regulated by an anti-sigma factor that is also a protein kinase. Cell. **74:**735-742.

138. **Missiakas, D., M. P. Mayer, M. Lemaire, C. Georgopoulos, and S. Raina.** 1997. Modulation of the Escherichia coli sigmaE (RpoE) heat-shock transcription-factor activity by the RseA, RseB and RseC proteins. Mol. Microbiol. **24:**355-71.

139. **Mytelka, D., and M. Chamberlin.** 1996. *Escherichia coli fliAZY* operon. J. Bacteriol. **178:**24-34.

140. **Nagai, H., H. Yuzawa, M. Kanemori, and T. Yura.** 1994. A distinct segment of the sigma 32 polypeptide is involved in DnaK-mediated negative control of the heat shock response in Escherichia coli. Proc. Natl. Acad. Sci. USA. **91:**10280-10284.

141. **Ohnishi, K., K. Kutsukake, H. Suzuki, and T. Iino.** 1990. Gene fliA encodes an alternative sigma factor specific for flagellar operons in Salmonella typhimurium. Mol. Gen. Genet. **221:**139-47.

142. **Ohnishi, K., K. Kutsukake, H. Suzuki, and T. Lino.** 1992. A novel transcriptional regulation mechanism in the flagellar regulon of *Salmonella typhimurium*: an antisigma factor inhibits the activity of the flagellum-specific sigma factor, σ^F. Mol. Microbiol. **6:**3149-3157.

143. **Orsini, G., M. Ouhammouch, C.-J. P. Le, and E. N. Brody.** 1993. The *asiA* gene of bacteriophage T4 codes for the anti-σ^{70} protein. J. Bacteriol. **175:**85-93.

144. **Osawa, T., and T. Yura.** 1981. Effects of reduced amount of RNA polymerase sigma factor on gene expression and growth of *Escherichia coli*: studies of the *rpoD40* (amber) mutation. Mol. Gen. Genet. **184:**166-173.

145. **Ouhammouch, M., K. Adelman, S. R. Harvey, G. Orsini, and E. N. Brody.** 1995. Bacteriophage T4 MotA and AsiA proteins suffice to direct Escherichia coli RNA polymerase to initiate transcription at T4 middle promoters. Proc. Natl. Acad. Sci. USA. **92:**1451-5.

146. **Ouhammouch, M., G. Orsini, and E. N. Brody.** 1994. The *asiA* gene product of bacteriophage T4 is required for middle mode RNA synthesis. J. Bacteriol. **176:**3956-3965.

147. **Owens, J. T., R. Miyake, K. Murakami, A. J. Chmura, N. Fujita, A. Ishihama, and C. F. Meares.** 1998. Mapping the sigma70 subunit contact sites on escherichia coli RNA polymerase with a sigma70-conjugated chemical protease [In Process Citation]. Proc. Natl. Acad. Sci. USA. **95:**6021-6.

148. **Pabo, C. O., and R. T. Sauer.** 1984. Protein-DNA recognition. Annu. Rev. Biochem. **53:**293-321.

149. **Pinkney, M., and J. G. Hoggett.** 1988. Binding of the cyclic AMP receptor protein of Escherichia coli to RNA polymerase. Biochem. J. **250:**897-902.

150. **Ptashne, M.** 1992. A genetic switch: phage λ and higher organisms, 2 ed. Cell Press, Cambridge, MA.

151. **Ptashne, M.** 1967. Specific binding of the lambda phage repressor to lambda DNA. Nature. **214:**232-4.

152. **Raina, S., D. Missiakas, and C. Georgopoulos.** 1995. *The* rpoE gene encoding the σ^E (σ^{24}) heat shock sigma factor of *Escherichia coli*. Embo J. **14:**1043-1055.

153. **Record, T.** 1996. *Escherichia coli* RNA polymerase ($E\sigma^{70}$), promoters, and the kinetics of the steps of transcription intitiation, p. 792-821. *In* F. C. Neidhardt (ed.), *Escherichia coli* and *Salmonella typhimurium*, 2nd ed, vol. 1. ASM Press, Washington D. C.

154. **Roberts, C. W., and J. W. Roberts.** 1996. Base-specific recognition of the nontemplate strand of promoter DNA by E. coli RNA polymerase. Cell. **86:**495-501.

155. **Sanderson, K. E., A. Hessel, and K. E. Rudd.** 1995. Genetic map of *Salmonella typhimurium*, edition VIII. Microbiol. Rev. **59:**241-303.

156. **Sanderson, K. E., and J. R. Roth.** 1983. Linkage map of *Salmonella typhimurium*, edition VI. Microbiol. Rev. **47:**410-53.

157. **Schagger, H., and G. Jagow.** 1987. Tricine-sodium dodecyl sulfate-polyacrylamide gel electorphoresis for the separation of proteins in the range from 1 to 100 kDa. Anal. Biochem. **166:**368-379.

158. **Severinov, K., D. Fenyo, E. Severinova, A. Mustaev, B. T. Chait, A. Goldfarb, and S. A. Darst.** 1994. The sigma subunit conserved region 3 is part of "5'-face" of active center of Escherichia coli RNA polymerase. J. Biol. Chem. **269:**20826-8.

159. **Severinova, E., K. Severinov, D. Fenyo, M. Marr, E. N. Brody, J. W. Roberts, B. T. Chait, and S. A. Darst.** 1996. Domain organization of the *Escherichia coli* RNA polymerase σ70 subunit. J. Mol. Biol. **263:**637-647.

160. **Severinova, E. K., K. Severinov, and S. A. Darst.** 1998. Inhibition of *Escherichia coli* RNA polymerase by bacteriophage T4 AsiA. J. Mol. Biol. **279:**9-18.

161. **Shaw, W. V.** 1975. Chloramphenicol acetyltransferase from chloramphenicol-resistant bacteria. Meth. Enzymol. **43:**737-51.

162. **Shi, W., Y. Zhou, J. Wild, J. Adler, and C. A. Gross.** 1992. DnaK, DnaJ, and GrpE are required for flagellum synthesis in Escherichia coli. J. Bacteriol. **174:**6256-6263.

163. **Shin, S., and C. Park.** 1995. Modulation of flagellar expression in *Escherichia coli* by acetyl phosphate and the osmoregulator OmpR. J. Bacteriol. **177:**4696-4702.

164. **Shuler, M. F., K. M. Tatti, K. H. Wade, and C. P. Moran, Jr.** 1995. A single amino acid substitution in σ^E affects its ability to bind core RNA polymerase. J. Bacteriol. **177:**3687-3694.

165. **Siegele, D. A., J. C. Hu, W. A. Walter, and C. A. Gross.** 1989. Altered promoter recognition by mutant forms of the sigma 70 subunit of Escherichia coli RNA polymerase. J. Mol. Biol. **206:**591-603.

166. **Silverman, M., and M. Simon.** 1977. Bacterial flagella. Ann. Rev. Microbiol. **31:**379-419.

167. **Silverman, M., and M. Simon.** 1974. Chacterization of *Escherichia coli* flagellar mutants that are insensitive to catabolite repression. J. Bacteriol. **120:**1196-1203.

168. **Simpson, R. B.** 1979. Molecular topography of RNA polymerase interaction. Cell. **18:**277-85.

169. **Skelly, S., T. Coleman, C.-F. Fu, N. Brot, and H. Weissbach.** 1987. Correlation between the 32-kDa σ factor levels and *in vitro* expression of *Escherichia coli* heat shock genes. Proc. Natl. Acad. Sci. USA. **84:**8365-69.

170. **Skelly, S., C. F. Fu, B. Dalie, B. Redfield, T. Coleman, N. Brot, and H. Weissbach.** 1988. Antibody to sigma 32 cross-reacts with DnaK: association of DnaK protein with Escherichia coli RNA polymerase. Proc. Natl. Acad. Sci. USA. **85:**5497-501.

171. **Smith, D. B., and K. S. Johnson.** 1988. Single step purification of polypeptides expressed in *Escherichia coli* as fusions with glutathione-S transferase. Gene. **67:**31-40.

172. **Starnbach, M. N., and S. Lory.** 1988. The *fliA* (*rpoF*) gene of *Pseudomonas aeruginosa* encodes an alternative sigma factor required for flagellin synthesis. Mol. Microbiol. **6:**459-469.

173. **Stevens, A.** 1976. A salt-promoted inhibitor of RNA polymerase isolated from T4 phage-infected *E. coli*, p. 617-627. *In* R. Losick and M. Chamberlin (ed.), RNA polymerase. Cold Spring Harbor Laboratory Press, Cold Spring Harbor, N. Y.

174. **Stragier, P., and R. Losick.** 1990. Cascades of sigma factors revisited. Mol. Microbiol. **4:**1801-1806.

175. **Summers, W. C., and R. B. Siegel.** 1969. Control of template specificity of E. coli RNA polymerase by a phage- coded protein. Nature. **223:**1111-3.

176. **Tatti, K. M., M. F. Shuler, and C. P. Moran, Jr.** 1995. Sequence-specific interactions between promoter DNA and the RNA polymerase sigma factor E. J. Mol. Biol. **253:**8-16.

177. **Thompson, N. E., D. A. Hager, and R. R. Burgess.** 1992. Isolation and characterization of a polyol-responsive monoclonal antibody useful for gentle purification of *Escherichia coli* RNA polymerase. Biochem. **31:**7003-7008.

178. **Tintut, Y., and J. D. Gralla.** 1995. PCR mutagenesis identifies a polymerase-binding sequence of sigma 54 that includes a sigma 70 homology region. J. Bacteriol. **177:**5818-25.

179. **Tomoyasu, T., J. Gamer, B. Bukau, M. Kanemori, H. Mori, A. J. Rutman, A. B. Oppenheim, T. Yura, K. Yamanaka, H. Niki, and et al.** 1995. Escherichia coli FtsH is a membrane-bound, ATP-dependent protease which degrades the heat-shock transcription factor sigma 32. Embo J. **14:**2551-60.

180. **Travers, A. A.** 1969. Bacteriophage sigma factor for RNA polymerase. Nature. **223:**1107-10.

181. **Visick, K. G.** 1993. University of Washington, Seattle, WA.

182. **Vogel, H. J., and D. M. Bonner.** 1956. Acetylornithase of *Escherichia coli*: partial purification and some properties. J. Biol. Chem. **218:**97-106.

183. **Waldburger, C., T. Gardella, R. Wong, and M. M. Susskind.** 1990. Changes in conserved region 2 of Escherichia coli sigma 70 affecting promoter recognition. J. Mol. Biol. **215:**267-76.

184. **Way, J. C., M. A. Davis, D. Morisato, D. E. Roberts, and N. Kleckner.** 1984. New Tn*10* derivatives for transposon mutagenesis and for construction of *lacZ* operon fusions by transposition. Gene. **32:**369-79.

185. **White, B. A. (ed.).** 1993. PCR protocols: current methods and applications, vol. 14. Humana Press, Totowa, N.J.

186. **Williams, K. P., G. A. Kassavetis, and E. P. Geiduschek.** 1987. Interactions of the bacteriophage T4 gene 55 product with Escherichia coli RNA

polymerase. Competition with Escherichia coli sigma 70 and release from late T4 transcription complexes following initiation. J. Biol. Chem. **262:**12365-71.

187. **Wilson, C., and A. J. Dombroski.** 1997. Region 1 of σ^{70} is required for efficient isomerization and initiation of transcription by *Escherichia coli* RNA polymerase. J. Mol. Biol. **267:**60-74.

188. **Winkelman, J. W., and D. P. Clark.** 1984. Proton suicide: general method for direct selection of sugar transport- and fermentation-defective mutants. J. Bacteriol. **160:**687-690.

189. **Yokoseki, T., T. Iino, and K. Kutsukake.** 1996. Negative regulation by fliD, fliS, and fliT of the export of the flagellum-specific anti-sigma factor, FlgM, in Salmonella typhimurium. J. Bacteriol. **178:**899-901.

190. **Yokoseki, T., K. Kutsukake, K. Ohnishi, and T. Iino.** 1995. Functional analysis of the flagellar genes in the fliD operon of Salmonella typhimurium. Microbiol. **141:**1715-1722.

191. **Yokota, T., and J. S. Gots.** 1970. Requirement of adenosine 3',5'-cyclic phosphate for flagella formation in *Escherichia coli* and *Salmonella typhimurium.* J. Bacteriol. **103:**513-516.

192. **Youderian, P., A. Vershon, S. Bouvier, R. Sauer, and M. Susskind.** 1983. Changing the DNA-binding specificity of a repressor. Cell. **35:**777-783.

193. **Zhou, Y. N., W. A. Walter, and C. A. Gross.** 1992. A mutant σ^{32} with a small deletion in conserved region 3 of sigma has reduced affinity for core RNA polymerase. J. Bacteriol. **174:**5005-5012.

194. **Zhu, X., X. Zhao, W. F. Burkholder, A. Gragerov, C. M. Ogata, M. E. Gottesman, and W. A. Hendrickson.** 1996. Structural analysis of substrate binding by the molecular chaperone DnaK. Science. **272:**1606-14.

195. **Zuber, P., J. Healy, H. L. Carter, S. Cutting, C. P. Moran, Jr., and R. Losick.** 1989. Mutation changing the specificity of an RNA polymerase sigma factor. J. Mol. Biol. **206:**605-14.

Appendix

Class 3^{ON} mutants isolated by others

Table A.1 Linkage of Lac$^+$ revertants (isolated by Keith Compton) to *fliC* locus

Parent strain	Linkage of Lac$^+$ phenotype to *fliC*::Mu*dJ*					
	selection at 37°C			selection at 42°C (ts)		
	partial	100%	unlinked	partial	100%	unlinked
TH1722 Δ(*flgG-L*) *fliC*::Mu*dJ*	**2/13** #10 (18%) #? (88%)	**1/13**	**10/13**	**1/17** #6 (30%)	**3/17**	**13/17**
TH1723 Δ(*flhA-cheA*) *fliC*::Mu*dJ*	**1/20** #4 (85%) #8 (80%) #14 (50%)	**16/20**	**1/20**		**20/20**	
TH1724 Δ(*flhAB*) *fliC*::Mu*dJ*		**2/20**	**18/20**		**1/20**	**19/20**
TH1726 Δ(*fliE-K*) *fliC*::Mu*dJ*		**1/20**	**19/20**	**3/20** #1 (56%) #7 (37%) #10 (35%)		**17/20**
TH1727 Δ(*flgL-R*) *fliC*::Mu*dJ*	**4/20** #1 (56%) #6 (40%) #9 (45%) #14 (61%)		**16/20**		**1/20**	**19/20**
TH2111 Δ(*flgHI*) *fliC*::Mu*dJ*	**1/41** #42 (50%)		**40/41**	**1/49** #43 (10%)	**8/49**	**40/49**

Table A.2 Linkage of Lac$^+$ revertants (isolated by Keith Compton) to *flgM* locus

Parent strain	Linkage of Lac$^+$ phenotype to *pyrC*::Tn10			
	selection at 37°C		selection at 42°C (ts)	
	~50%	unlinked	~50%	unlinked
TH1722 Δ(*flgG-L*) *fliC*::MudJ	6/13	7/13	2/17	15/17
TH1723 Δ(*flhA-cheA*) *fliC*::MudJ	0/20	20/20	0/20	20/20
TH1724 Δ(*flhAB*) *fliC*::MudJ	0/20	20/20	4/20	16/20
TH1726 Δ(*fliE-K*) *fliC*::MudJ	3/20	17/20	0/20	20/20
TH1727 Δ(*flgL-R*) *fliC*::MudJ	4/20	16/20	1/20	19/20
TH2111 Δ(*flgHI*) *fliC*::MudJ	ND	ND	ND	ND

Table A.3 Class 3^{ON} mutants unlinked to either *fliA or flgM*

Lac$^+$ mutants isolated by Keith Compton			Mot$^+$ Lac$^+$ revertants isolated by Karen Gillen
fla background	37°C	ts	KG1582, 1585, 1594, 1596, 1611, 1612, 1613, 1614, 1615, 1621, 1622, 1624, 1627, 1629, 1635, 1639, 1641, 1642, 1644, 1645, 1655, 1656, 1662
TH1722 Δ(*flgG-L*) *fliC*::Mud*J*	#6,7,8,9,13, 16,17,19		
TH1723 Δ(*flhA-cheA*) *fliC*::Mud*J*	#15		
TH1724 Δ(*flhAB*) *fliC*::Mud*J*	#8,14	#1,3,4,5,6, 7,8,10	
TH1726 Δ(*fliE-K*) *fliC*::Mud*J*	#1,2,4,5,8, 9,10,11	#2,3,4,5,6, 8,9,11	
TH1727 Δ(*flgL-R*) *fliC*::Mud*J*	#1,2,3,4,5, 6,7,8	#2,3,4,5,7, 8,10,12	

Vita

Meggen Shepherd Chadsey

Education

University of Washington Seattle, WA	Ph.D. in Microbiology December, 1998
Cornell University Ithaca, NY	B.A. in Genetics May, 1989

Publications

Chadsey, M.S., Karlinsey, J.E. and K.T. Hughes. The flagellar anti-sigma factor FlgM actively dissociates *Salmonella typhimurium* σ^{28} RNA polymerase holoenzyme. Genes and Development, in press 9/98.

Daughdrill, G.W., Chadsey,. M.S., Karlinsey, J.E., Hughes, K.T. and F.W. Dahlquist. (1997) The C-terminal half of the anti-sigma factor, FlgM, becomes structured when bound to its target, σ^{28}. Nature Struct. Biol. **4**: 285-291.

Humbert, R., Withington, A., Richter, R., Chadsey, M., McEwan, N., Gray, J., Lara, J., Staley, J., Harrington, M., Thomas, L., Li, W.-F., Costa, L., Herrington, R., Sayles, G., Haynes J. and C. Furlong. (1995) Specific Approaches to Bioremediation. in *Advances in Hazardous Waste Management Technologies* eds. Robert Irwin and Subhas Sikdar. Technomic Publishing Co., Lancaster, PA.

IMAGE EVALUATION TEST TARGET (QA-3)

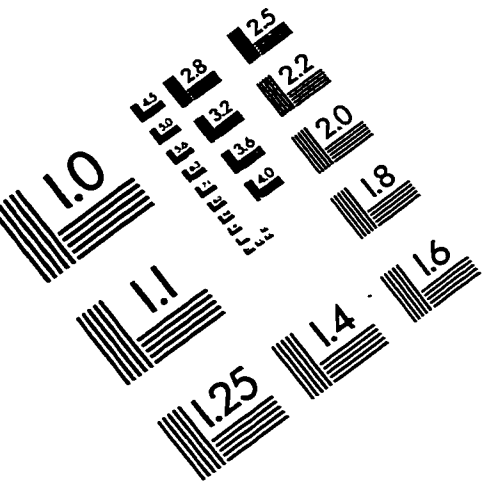

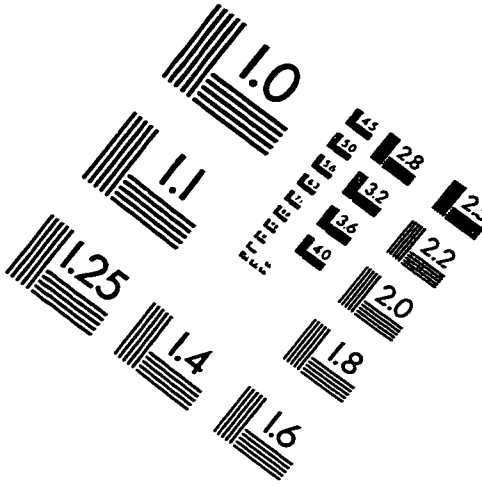

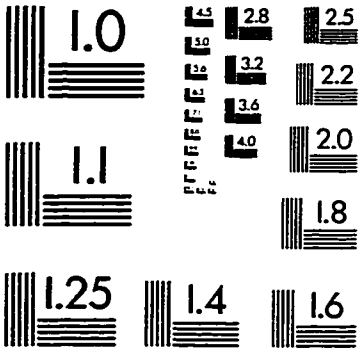

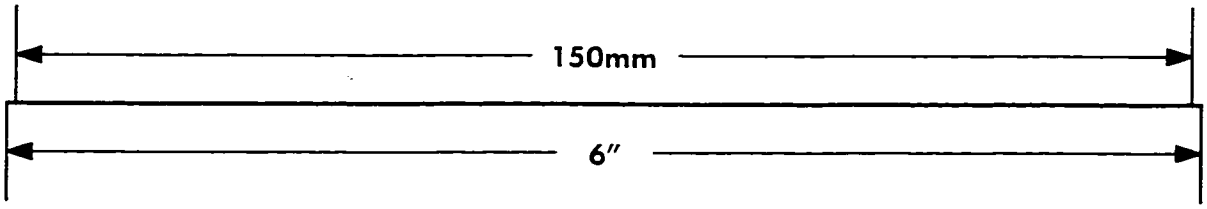

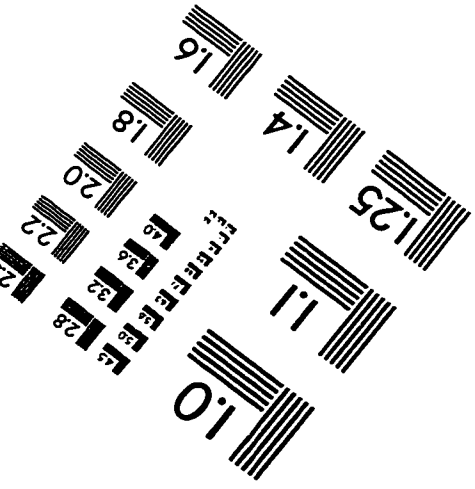

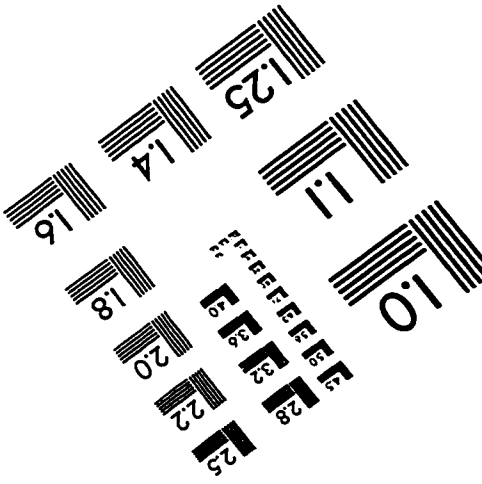

APPLIED IMAGE, Inc
1653 East Main Street
Rochester, NY 14609 USA
Phone: 716/482-0300
Fax: 716/288-5989